Presence, abundance and effects of microplastics on the Great Barrier Reef

PhD thesis by

Marina F. M. Santana

Master of Science, University of São Paulo 2015
Bachelor of Oceanography, University of São Paulo 2013

November 2021

For the degree of Doctor of Philosophy

College of Science and Engineering, James Cook University
Australian Institute of Marine Science
AIMS@JCU

The hardest decisions in life is whether to “walk away” or “try harder”

Ziad K. Abdelnour

Acknowledgements

The four years of a PhD journey can sometimes seem lonely, but it definitely is not. Science is not done by one person but by multiple people, either directly or indirectly. Therefore, I thank the organizations and people who have assisted me with my PhD research.

Specially, I acknowledge the funding bodies that financially supported this research project: James Cook University, the Australian Institute of Marine Science, and AIMS@JCU, for the PhD scholarship and internal funding opportunities, as well as the Australian Museum, the National Environmental Science Program, and the Great Barrier Reef Marine Park Authority for the research grants. I also acknowledge the immense contribution of my supervisors, Frederieke Kroon, Cherie Motti, Lynne van Herwerden and George Vanvounis, who have taught me valuable concepts and the practicalities of conducting science and helped me to hone my research skills. Similarly, I thank Björn Illing, Amanda Dawson and Richard Edmunds for mentoring me during these years, in the lab and with the writing, as well as by sharing with me lessons learnt throughout their research careers. To Carine Lefevre, thank you for guiding me through the process of planning for and executing a field trip to deliver experimental science of excellence.

Even so, if it wasn't for the input of many others this thesis would still not exist. Small challenges in research frequently occur, and sometimes all at once. From having the proper equipment and materials to perform the experiment, to quickly double checking technical information, to having enough hands to conduct complex and comprehensive studies, one person cannot do everything. I acknowledge Peter Thomas-Hall, Niall Jeeves and Michael Kebben from AIMS for the great technical support with setting up field and experimental gears, including the design and fabrication of new ones. I thank Anne Hoggett and Lyle Vail at the Lizard Island Research Station for the logistical support while conducting the experiments that are described in Chapters 3 and 4, and for opportunity to explore Lizard Island and surrounding reefs. I would also like to thank the whole AIMS SeaSIM team for the logistical and technical support throughout my Chapter 5 experiment, and for maintaining such a high standard aquarium facility. Specifically, I thank Andrea Severatti, Tom Barker and Tristan Lever for the

technical guidance and support on the development of the automated microplastic dosing system. For all their efforts in helping me to improve my statistical skills and knowledge in general, I thank Diego Barneche, Patricia Menendez and Murray Logan. Finally, I specially thank the dear friends and work colleagues who were at some point throughout these years part of the microplastic team at AIMS, and who helped me in one way or another: Merle Schlawinsky, Vilde Snekkevik, Michaela Miller, Dávid Kulcsár, Madeline Carsique, Kelley Meehan and Hope Sexton.

To my family and personal friends, I appreciate all the emotional support provided, including the shared excitement at my progress and the empathy shown when I struggled. I specially thank my husband and best friend, Caiuá Mani Peres, my parents, Berenice Ferreira Santana and Antonio Luiz Mourão Santana, and my brother, Otávio Santana.

Table of Contents

List of Tables

List of Figures

Publications associated with this thesis

Chapter 2: Santana, M.F.M.; Kroon, F. J.; Herwerden, L.V.; Vamvounis, G.; Motti, C.A. An assessment workflow to recover microplastics from complex biological matrices. under review Environmental Science and Technology.

Chapter 3: Santana, M.F.M.; Motti, C.A.; Vamvounis, G.; Herwerden, L.V.; Kroon, F. J. Distribution and compartmentalisation of microplastic contamination in abiotic and biotic matrices of Lizard Island coral reef, Australia. in prep.

Chapter 4: Santana, M.F.M.; Dawson, A. L.; Motti, C.A.; Herwerden, L.V.; Lefevre, C.; Kroon, F.J. Ingestion and depuration of microplastics by a planktivorous coral reef fish, *Pomacentrus amboinensis*. Frontiers in Environmental Science, 6, 1-6.

Chapter 5: Santana, M.F.M.; Snekkevik, V.; Severatti, A.; Barker, T.; Dawson, A.; Motti, C.A.; Herwerden, L.V.; Illing, B.; Kroon, F. J. Elevated seasonal temperatures increase the risk profile of microplastic fibres for juvenile *Acanthochromis polyacanthus*. in prep.

Other publications during PhD candidature

Dawson, A. L.; **Santana, M.F.M.**; Miller, M.E.; Kroon, F.J. 2021. Relevance and reliability of evidence for microplastic contamination in seafood: a critical review using Australian consumption patterns as a case study. Environmental Pollution, 276, 1-11.

Agostini, L.; Moreira, J.C.F.; Bendia, A.G.; Kmit, M.C.P.; Waters, L.G.; **Santana, M.F.M.**; Sumida, P.Y.G.; Turra, A.; Pellizari, V.H. 2021. Deep-sea plastisphere: long term experimental colonization of plastic-associated bacterial and archaeal communities in the Southwest Atlantic Ocean. Science of the Total Environment, 793, 1-12.

Santana, M.F.M.; Moreira, F.T.; Pereira, C.D.S.; Abessa, D.M.S; Turra, A. 2018. Continuous exposure to microplastic does not cause physiological effects in the cultivated mussel *Perna perna*. Arch. Environ. Contamination & Toxicoly, 74, 594-604.

Oliveira, A.L.; Barbosa, L.; Camargo, R.M.; **Santana**, **M.F.M.**; Moreira, F.; Turra, A. 2018. Integrating geotechnology in marine litter on beaches – a citizen science approach. Sustainability, Agri, Food and Environmental Research, 6, 50-62.

Santana, M.F.M.; Turra, A. 2020. Toxicity of microplastics in the marine environment. In: A handbook of environmental toxicology. 1st Ed. Edinburgh, UK: CAB International, 436-453.

Turra, A.; **Santana, M.F.M**.; Oliveira, A.L.; Barbosa, L.; Camargo, R.M; Moreira, F.; Denadai, M.R. Lixo nos mares: do entendimento à solução. 1st Ed. São Paulo, Brazil: IOUSP. 2020. 142 p. - publication in Portuguese

Publication plan and author contribution associated with this thesis

Chapter Number	Publication details	Extent of the intellectual input of each author, including the candidate
2	Santana, M.F.M.; Kroon, F. J.; Herwerden, L.V.; Vamvounis, G.; Motti, C.A. An assessment workflow to recover microplastics from complex biological matrices. under review Environmental Science and Technology.	MS obtained funding, conceptualized the study, conducted laboratory work, analysed the data, wrote the original draft, and reviewed and edited further versions of the manuscript. FK obtained funding, conducted field work, and contributed to study design and to reviewing and editing the manuscript. LH and GV both contributed to reviewing and editing the manuscript. CM contributed to study design, data analysis and reviewing and editing the manuscript. All authors contributed to the article and approved the submitted version.
3	Santana, M.F.M.; Motti, C.A.; Vamvounis, G.; Herwerden, L.V.; Kroon, F. J. Distribution and compartmentalisation of microplastic contamination in abiotic and biotic matrices of Lizard Island coral reef, Australia. in prep.	MS obtained funding, conceptualized the study, conducted field and laboratory work, analyzed the data, wrote the original draft, and reviewed and edited further versions of the manuscript. CM and GV contributed to reviewing and editing the manuscript. LH contributed to developing field relevant experimental research at the outset and to reviewing and editing the final manuscript. FK obtained funding, contributed to study design, as well as reviewing and editing the manuscript.
4	Santana, M.F.M.; Dawson, A. L.; Motti, C.A.; Herwerden, L.V.; Lefevre, C.; Kroon, F.J. Ingestion and depuration of microplastics by a planktivorous coral reef fish, *Pomacentrus amboinensis*. Frontiers in Environmental Science, 6, 1-6.	MS obtained funding, conceptualized the study, conducted field and laboratory work, analyzed the data, wrote the original draft, and reviewed and edited further versions of the manuscript. AD contributed to study design, analyzed the data, and contributed to reviewing and editing the manuscript. CM contributed to study design and reviewing and editing the manuscript. LH contributed to developing field relevant experimental research at the outset and to reviewing and editing the final manuscript. CL conducted field and laboratory work. FK obtained funding, contributed to study design, conducted field work, and contributed to reviewing and editing the manuscript. All authors contributed to the article and approved the submitted version.
5	Santana, M.F.M.; Snekkevik, V.; Severatti, A.; Barker, T.; Dawson, A.; Motti, C.A.; Herwerden, L.V.; Illing, B.; Kroon, F. J. Stress levels, not fitness parameters, change when juvenile coral reef fish are synergistically exposed to microplastic fibres and seasonal warming. in prep.	MS obtained funding, conceptualized the study, conducted experimental exposure and laboratory work, analyzed the data, wrote the original draft, and reviewed and edited further versions of the manuscript. VS conducted experimental exposure and laboratory work, and contributed to reviewing and editing the manuscript. AS and TB contributed to experimental design, specifically to the development of the microplastic automated dosing system. AD contributed to reviewing and editing the manuscript. CM and LH contributed to study design, and reviewing and editing the manuscript. BI obtained funding, contributed to study design, data analysis, as well as reviewing and editing the manuscript. FK obtained funding, contributed to study design, data analysis, as well as reviewing and editing the manuscript.

Statement of Contribution

Supervision

Adjunct Senior Lecturer **Lynne van Herwerden**, James Cook University

Adjunct Associate Professor **Frederieke Kroon**, Australian Institute of Marine Science and James Cook University

Associate Professor **George Vamvounis**, James Cook University

Adjunct Senior Lecturer **Cherie Motti**, Australian Institute of Marine Science and James Cook University

Other contributions

Financial Support	Stipend, research costs, and communication awards	Australian Institute of Marine Science James Cook University AIMS@JCU Australian Museum National Environmental Science Program (NESP) Great Barrier Reef Marine Park Authority (GBRMPA)
Field data collection	Technical assistance for trip preparation and/or sample collection	Carine Lefevre Joy Smith
Laboratory experimental conduction and data collection	Technical assistance for experimental setup, and maintenance and/or sample collection	Andrea Severatti Tom Barker Tristan Lever Carine Lefevre Kelley Meehan Samantha Jaworski
Intellectual Support	Statistical support	Patricia Menendez – Chapter 2 Diego Barneche – Chapters 3, 4, 5
	Laboratory procedures support	Amanda Dawson Björn Illing Peter Thomas-Hall
	Experimental design and/or writing support	Amanda Dawson Björn Illing Richard Edmunds
Volunteers	Sample collection in the field, animal husbandry in laboratory experiments, and/or sample processing	Caiuá Mani Peres Madeline Carsique Vilde Snekkevik Michaela Miller

Permit approvals and ethics statement

All necessary permits and approvals to conduct this work. Sample collections described in Chapters 3 and 4 were undertaken under the Great Barrier Reef Marine Park Authority permit number G12/35236.1. Sample collections supporting Chapter 3 and 4, as well as the experimental procedures of Chapters 4 and 5, were carried out in accordance with Animal Ethics protocol approved by the Animal Ethics Committee of James Cook University (approval numbers: A2506, A2635, and A2678 respectively). Priority was given to animal care at all stages of this study.

General Abstract

Marine debris represents a worldwide problem for oceans. Of the marine debris found, microplastics (< 5mm in size) are of particular concern due to their small size, persistence in the environment and uptake by marine organisms. A review of the microplastics literature revealed the threat microplastics pose to the water quality of coral reef ecosystems and found much of the data unsuited to an Ecological Risk Assessment in the Australian context. Therefore, this thesis examines (1) the extent and (2) effects of microplastic contamination on coral reef ecosystems of the Great Barrier Reef (GBR) using the principles of an Ecological Risk Assessment framework for hypothesis development and experimental design.

There are a multitude of methods designed to liberate microplastics from complex environmental samples and, to date, a universal method suited to all samples does not yet exist. This thesis explores the current methods available and, as an alternative, presents a criteria-guided workflow to tailor microplastic separation methods to specific sample types (e.g., abiotic [seawater, sediment], and biotic [various organisms]), here tested with coral, sponge, sea squirt and sea cucumber (Chapter 2). Differences in sample composition and morphology rendered some methods ineffective, and the sensitivity of rayon to most methods highlighted the importance of validating methods for specific microplastic polymers.

In Chapter 3, tailored methods revealed prevalent, albeit low, microplastic contamination in the water and sediment of a remote area of the GBR (Lizard Island), with this reflected in the inhabitant organisms. Microplastic profiles revealed there was a high risk of uptake of fibres and/or microplastics < 500 μm from the immediate surroundings. However, microplastic distributions in organisms did differ between the taxa with respect to shape, size, colour, or polymer type, confirming that while microplastic bioavailability is dependent on the levels of abiotic contamination, microplastic uptake is determined by taxa-specific factors.

To better understand risks associated with microplastic uptake by coral reef organisms, this project also measured microplastic ingestion and depuration kinetics in damselfish (Chapter 4). A positive relationship was observed between microplastic exposure concentration, quantity in organisms and depuration rates. The amount of microplastics in fish and microplastics depuration kinetics were found to be dose-dependent, with fibres resident in the gut for longer

than fragments. Despite of that, both microplastic fibres and fragments were almost fully depurated within 8 hours. Overall, this suggests that chronic exposure to higher concentrations of microplastic, and microplastic fibres, could pose health risks to fish.

To explore the effects of microplastic uptake on the health of reef organisms under a changing climate (Chapter 5), the baseline microplastic concentration (< 1 microplastic L^{-1}) established in Chapter 3 was used as the starting point for an environmentally realistic exposure study (Chapter 5). Fish were exposed to doses spanning from pre-plastic (0 microplastics L^{-1}), to future predicted (1 microplastic L^{-1} and 11 microplastics L^{-1}) marine microplastic contamination levels, in combination with forecasted increases in seawater temperatures (ambient + 1.5 and 3˚C). Results revealed that the cumulative impact of microplastic ingestion and elevated winter seawater temperatures altered cortisol levels in juvenile damselfish, a hormone linked to stress and other primary biological functions such as growth.

In summary, this thesis advances the technical approaches available to the field of microplastics research and establishes, through field surveys and realistic experimental exposures, current levels of marine microplastic contamination on the GBR as well as potential risks of such contamination to marine organisms, in particular fish, and in a warming climate.

Key words: marine debris, ecological risk assessment, tropical coral reef, impact, uptake

Chapter 1: Introduction to issues and concerns regarding microplastics in marine environments

1.1. Marine microplastic contamination and environmental impacts

Solid waste resulting in marine pollution is one of many modern anthropogenic impacts on natural systems (Galgani, 2010). Such marine debris, consisting of manufactured solid materials that have been used and subsequently lost or intentionally disposed of by humans, into marine environments (Galgani, 2010). Marine debris was first recognized as one of the major pollutants of marine environments in the 1970s by the Protocol of the International Convention for the Prevention of Pollution from Ships (MARPOL; Santos et al., 2008). In the same decade, microplastics (plastic particles < 5mm in length; Arthur et al., 2009), were first reported in the marine environment (Carpenter et al., 1972; Carpenter and Smith, 1972; Colton et al., 1974). Since then, plastic production has increased substantially (Europe, 2020) and is reflected in the cumulative amount of plastics and microplastics observed in the environment. In 2010, 4.8 to 12.7 million metric tons of plastic waste was estimated to have entered the oceans (Jambeck et al., 2015a) and by 2015, estimates of up to 51 trillion floating microplastics were reported globally (van Sebille et al., 2015). Heavily contaminated marine environments, such as the Mediterranean and Yellow Seas, already exhibit an unacceptable level of risk associated with microplastics (Everaert et al., 2020) and current estimates suggest up to 150 microplastics m^{-2} in surface seawaters (Everaert et al., 2020); https://rshiny.lifewatch.be/ng-ocean-plastic-challenge/). Given predictions of a 400% increase in plastic production by 2100 (Everaert et al., 2020) and that plastics persist in the marine environment for centuries (Andrady, 2011), a concomitant increase in marine microplastic contamination is also expected assuming an "as per usual" scenario (Jambeck et al., 2015b). Consequently, marine ecosystems are likely to be continuously (and increasingly) exposed to microplastic contamination over decadal timeframes, hence the potential for adverse effects to these ecosystems needs robust evaluation (Horton, 2021).

Microplastics are composed of a complex variety of plastic particulates - either manufactured in this size range for commercial use (i.e., primary microplastics), or resulting from the fragmentation of larger plastic products within the environment (i.e., secondary

microplastics) (Cole et al., 2011). The sources of both primary and secondary microplastics in the global marine environment are diverse, ranging from land-based activities such as industry (Rochman et al, 2015, Karlsson et al., 2018, Zeng, 2018), urbanism (Horton, 2021; Özkan and Gündoğdu, 2020; Kole et al, 2017), and agriculture (Ragoobur et al., 2021; Rehm et al., 2021) to sea-based activities such as commercial fishing (Karbalaei et al., 2020; Kurniawan et al., 2021; Pan et al., 2021) and leisure (Kumar and Varghese, 2021; Wu et al., 2021). Consequently, microplastics occur in a multitude of sizes, shapes, colours and chemical compositions (Rochman et al., 2019), which, in the marine environment, can influence their distribution, bioavailability, and potential adverse effects on organisms.

A number of studies have demonstrated the pervasive presence of microplastics in the global marine environment, including in marine waters (Frere et al., 2017; Kroon et al., 2018a; Obbard et al., 2014), sediments (Martin et al., 2017; Thompson et al., 2004; Van Cauwenberghe et al., 2013) and shorelines (Turra et al., 2014; Yu et al., 2016). Consequently, inhabitant species of contaminated environments are susceptible to microplastic contamination. Microplastic uptake, especially ingestion, is considered one of the main pathways for organismal contamination (GESAMP, 2016), although other uptake routes such as translocation of water through the gills (e.g., in fish) (Bour et al., 2020b; Zitouni et al., 2021) and tissue overgrowth (e.g., in corals) (Martin et al., 2019; Reichert et al., 2018) are also possible. The small size of microplastics makes them available to a wide range of organisms across different trophic levels and feeding strategies (Miller et al., 2020). Microplastic uptake has been confirmed for marine organisms in benthic and nektonic habitats, ranging from plankton to megafauna, including species harvested for human consumption (Germanov et al., 2018; Kroon et al., 2018b; Lusher, 2015; Santillo et al., 2017). Adverse physical impacts of microplastics on individual marine organisms have also been reported, including retention in digestive tracts (Lu et al., 2016) and internal tissue alterations due to particle abrasion (von Moos et al., 2012). Also concerning are the potentially adverse chemical impacts that may result from leached additives, monomers, or other chemical pollutants (e.g., polyaromatic hydrocarbons) adsorbed onto the relatively large surface areas of microplastics (Browne et al., 2013; Gambardella et al., 2017; Karami et al., 2016). Laboratory studies investigating the controlled exposure of model marine organisms, such as zooplankton, bivalves and fish, to both microplastics and/or associated additives and absorbed pollutants have revealed negative

impacts, including elevated cellular stress (Avio et al., 2015a; Lu et al., 2016), increased inflammation (Lu et al., 2016; von Moos et al., 2012), altered feeding patterns (Cole et al., 2015), shifted energy balance (Lo and Chan, 2018; Welden and Cowie, 2016), hindered reproduction (Cole et al., 2015; Sussarellu et al., 2016) and perturbed development (Sussarellu et al., 2016).

1.2. Marine microplastic contamination and ecological risk assessment

Despite growing global interest (Adam et al., 2021; Everaert et al., 2020; Jung et al., 2021), the full extent of the ecological risks microplastic contamination poses for marine ecosystems are still uncertain (GESAMP, 2016), and this prevents informed environmental policy decision making. Ecological risk is defined as the likelihood of adverse ecological effects to occur as a result of exposure to one or more stressors (USEPA, 1992). Ecological risk assessment (ERA) is a management tool used to systematically evaluate and organize scientific information to examine relationships between stressor exposure and adverse ecological effects (USEPA, 1998). As such, ERAs are important to identify and resolve environmental problems by establishing mitigation priorities and providing a scientific basis for regulatory actions (GESAMP, 2016; Landis and Yu, 2004; USEPA, 1998).

Based on the ERA framework developed by the United States Environmental Protection Agency (USEPA, 1992, 1998), the characterization of both exposure and resultant ecological effects determined during the ERA risk analysis phase (Figure 1.1) provides relevant information to evaluate the likelihood that any given stressor adversely affects ecological entities (USEPA, 1998). As such, data quality and quantity are of critical importance (USEPA, 1998). Characterization of exposure evaluates potential or actual co-occurrence or contact of the stressor with one or more ecological entities, and generally includes observations and measures of stressor exposure in relation to the ecosystem and ecological entity at risk. This information can be derived from, and iteratively improved by, field data and numerical models that describe sources, transport, and fate (van Sebille et al., 2015). In turn, characterization of ecological effects evaluates the ability of a stressor to have adverse effects on one or more ecological entities and includes examining environmentally relevant exposures, the effect(s) it has on ecological entities, and how these effects may change with varying stressor levels or act

synergistically with other stressors. Characterization of ecological effects of exposure can involve field and laboratory exposures to stressors as well as endpoints spanning different levels of biological organization as long as the ecological consequences of the observed responses are clearly elucidated (EPA, 1992). Considering this, organism level endpoints (e.g., reproduction, development, survival, and behaviour) are useful tools for ERAs because they can be directly associated with ecological features and are relatively straightforward to assess as ecological endpoints (Galloway et al., 2017).

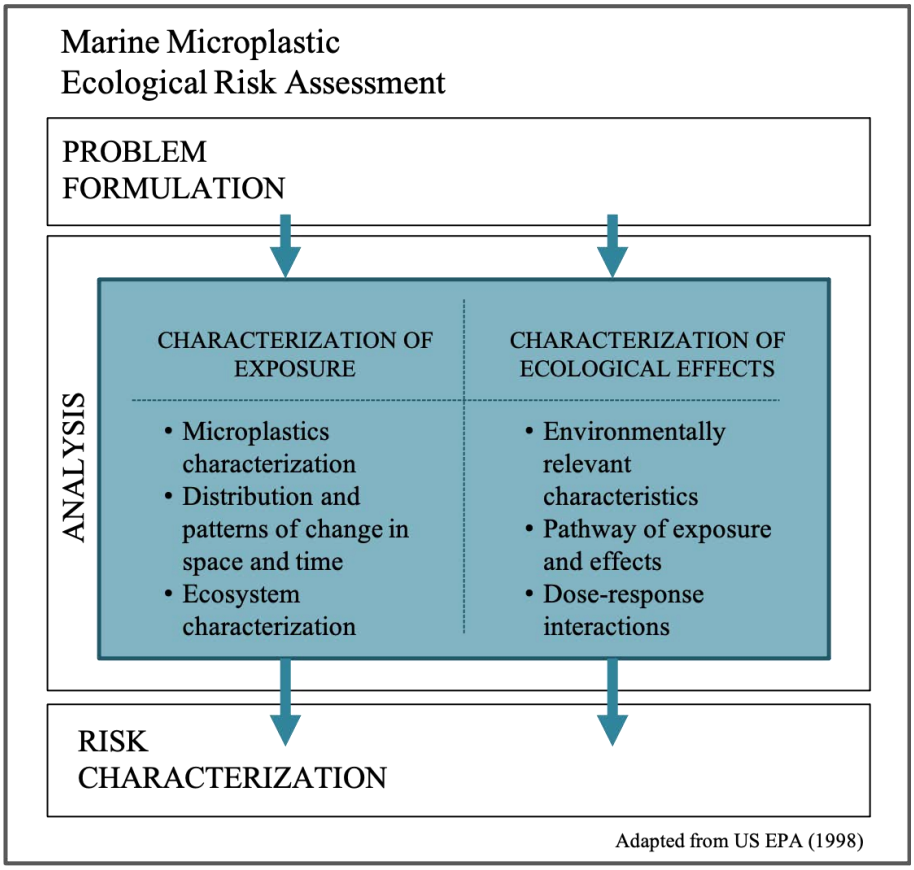

Figure 1.1: Workflow of an ecological risk assessment (ERA) based on the framework developed by the United States Environmental Protection Agency (USEPA, 1992; USEPA, 1998) and adapted for microplastic contamination.

Characterisation of microplastic exposure for an ERA requires information on abundance and composition of microplastics in water, sediment, and organisms based on the unique physical properties (e.g., shape, size, colour) and chemical composition of environmental

microplastics in the study system. This heterogeneous range of physicochemical characteristics also influences the spatial (Everaert et al., 2020) and temporal (Balthazar-Silva et al., 2020) distribution of microplastics within different compartments of the abiotic marine environment. As a result, organisms within a marine ecosystem are likely to experience variable exposure to microplastic contamination, which can lead to complex biological responses across different levels of organization (Ivar do Sul and Costa, 2014; Phuong et al., 2016; Syberg et al., 2015; Wright et al., 2013). Establishing environmentally relevant conditions of microplastic exposure coupled with multiple stressors (Everaert et al., 2020), and rigorous validation of the observed responses, is critical for characterising microplastic ecological effects. In addition, assessment of potential ecological consequences using multiple endpoints from different levels of biological organization (Prokić et al., 2019) provides comprehensive information on how a wide range of microplastic types and concentrations can uniquely affect a diverse range of organisms and life history stages (e.g., embryonic). Together this information can determine sensitivity to microplastics and whether this is exacerbated by other stressors such as climate change (Horton, 2021).

Information relevant to characterizing exposure and ecological effects thereof is reported in the current microplastic literature, but not comprehensively and/or consistently across studies (Hartmann et al., 2019; Lusher et al., 2020; Prata et al., 2020; Provencher et al., 2020; Rochman et al., 2019). Unfortunately, this diminishes the suitability of many studies to develop microplastic-specific ERAs.

For characterization of exposure, regardless of the ecosystem of interest, field-based studies do not follow standardized methods, definitions or categories, aside from the generally accepted maximum microplastics size of < 5 mm (Hartmann et al., 2019; Rochman et al., 2019). Often, microplastic concentration units are not harmonized across abiotic and biotic studies (Dawson et al., 2021; Miller et al., 2021) and concentration estimates are not validated or adjusted following quality assurance and quality control (QA/QC) practices (Lusher et al., 2020; Prata et al., 2020; Provencher et al., 2020). Furthermore, while microplastic presence and distribution has been examined in many marine ecosystems it has not been uniformly studied across hemispheres and latitudinal zones, and most ecosystems (e.g., tropical coral reefs) are understudied (Huang et al., 2021). Similarly, across the globe, only a few select taxa

have been assessed for microplastic contamination with teleost fish and bivalves being most common (Aragaw and Mekonnen, 2021; Miller et al., 2020).

For characterization of ecological effects there are several large-scale limitations. The use of polymer types, sizes, shapes, colours, and exposure concentrations within laboratory studies are often not aligned with field-based observations (Rochman et al., 2019). Studies detailing acute exposure far outnumber chronic exposure, despite the consistent presence of microplastic in the environment (Horton, 2021) and studies basing their hypotheses on ingestion of particles often lack confirmation that uptake is indeed responsible for the observed effects (Gambardella et al., 2017; Kaposi et al., 2014; Santana et al., 2021). Furthermore, sub-individual and individual endpoints are rarely linked to potential ecological consequences (Bour et al., 2018b; Cole and Galloway, 2015; McCormick et al., 2020) and concurrent use of multiple endpoints from differing organisational levels are rarely applied (Prokić et al., 2019). Additionally, very few studies have investigated effects of microplastics in combination with other stressors (Ferreira et al., 2016; Iwalaye et al., 2021; McCormick et al., 2020), despite ecosystems typically encountering multiple stressors concurrently, such as exposure to climate change associated temperature stress in combination with increased pollution of marine environments. Although many of these limitations are commonly associated with time and financial constraints of research projects, when feasible these should be addressed for refinement and continuous improvement of scientific information for environmental management.

1.3. Marine microplastic contamination in the Great Barrier Reef

The Great Barrier Reef (GBR) World Heritage Area (WHA) is the largest coral reef ecosystem in the world and has far-reaching ecological, economic, cultural, and social significance (GBRMPA, 2014). However, despite being protected as a marine park, the GBR WHA has key habitats and species that are currently deteriorating from the effects of many, often synergistic, anthropogenic pressures, including reduced water quality condition and global climate change (GBRMPA, 2014). Moreover, despite microplastics being a relatively well researched topic globally, there is a paucity of studies detailing contamination of the GBR WHA (Table 1.1a). However, recent studies have reported the presence of microplastics in GBR waters (Hall et al., 2015; Reisser et al., 2013a) and organisms (Caron et al., 2018; Jensen

et al., 2019; Kroon et al., 2018b; Santana et al., 2021; Wootton et al., 2021). Similarly, there are very few studies detailing effects of environmental microplastic contamination on GBR coral reef organisms (n = 7; Table 1.1b). Still, most of these studies demonstrated negative effects of microplastic exposure (McCormick et al., 2020; Reichert et al., 2018; Syakti et al., 2019), influenced or exacerbated by microplastic exposure conditions (Berry et al., 2019; Critchell and Hoogenboom, 2018), and also other stressors such as seawater temperature (Mendrik et al., 2021). This limited body of work suggests that key habitat forming species of the GBR such as corals, and significant contributors of nutrients to coral reef ecosystems such as fish (Critchell and Hoogenboom, 2018; McCormick et al., 2020), might be at risk from microplastic contamination, but the dearth of studies precludes a comprehensive understanding of associated ecological risks.

Table 1.1: Summary of microplastic (mp) exposure studies conducted in the Great Barrier Reef World Heritage Area (GBR WHA).

Area of study	Matrix	Concentration of microplastics found	Reference
Central GBR WHA (Orpheus Island)	surface seawater	up to 0.18 mp m^{-3}	(Hall et al., 2015)
Central GBR WHA	surface seawater	0.04 to 0.48 mp m^{-3}	(Jensen et al., 2019)*
Northern GBR (Cairns region)	turtle (Chelonia mydas)	3.5 mp $individual^{-1}$	(Caron et al., 2018)
Northern, Central and Southern GBR (Lizard Island, Orpheus Island, Heron Island and One Tree Island)	fish (Plectropomus spp.)	5.8 ± 0.8 (average ± standard error) mp $individual^{-1}$	(Kroon et al., 2018b)
Central GBR WHA	fish (Pomacentrus amboinensis)	0 to 131 mp $individual^{-1}$	(Jensen et al., 2019)*
Northern GBR (Lizard Island)	fish (Pomacentrus amboinensis)	Average of 2.25 mp $individual^{-1}$	(Santana et al., 2021)
Commercial fishing areas in Queensland	fish (common coral trout, paddletail, sea mullet, and other species from Family Mullidae)	1.58 ± 0.23 (average ± standard deviation) mp $individual^{-1}$	(Wootton et al., 2021)

*Study that assessed microplastic contamination in more than one matrix type.

Table 1.2: Summary of microplastic (mp) effect studies conducted on organisms inhabiting the Great Barrier Reef World Heritage Area.

Organism (taxon and species)	Endpoint measured	Observed responses	Reference
fish (Acanthochromis polyacanthus)	body condition and behaviour	negative effect on the growth and body condition only when food was replaced by plastic	(Critchell and Hoogenboom, 2018)
coral (Acropora humilis, Acropora millepora, Pocillopora verrucosa, Pocillopora damicornis, Porites lutea, Porites cylindrica)	bleaching and tissue necrosis	bleaching and tissue necrosis in five of six studied species	(Reichert et al., 2018)
coral (Acropora tenuis)	gamete fertilisation, embryo development and larval settlement	Fertilisation only negatively affected by the largest weathered microplastics	(Berry et al., 2019)
coral (Acropora formosa)	bleaching and necrosis	Both bleaching and necrosis were observed	(Syakti et al., 2019)
fish (Pomacentrus amboinensis)	behaviour and survival	Mp exposure had a greater effect on behaviour and survival than degraded habitat, with no evidence of synergistic effects.	(McCormick et al., 2020)
coral (Acropora sp., Seriatopora hystrix)	photosynthetic ability	Observed disruption to coral photosynthetic ability, varying according to microplastic type, seawater temperature and coral species	(Mendrik et al., 2021)
fish (Pomacentrus amboinensis)	body burden and depuration kinetics	Increased body burden and lower depuration rates for fibres over particles, and with increasing mp concentration	(Santana et al., 2021)

1.4. Thesis aim and structure

This PhD thesis aims to examine the extent and effects of microplastic contamination on coral reef ecosystems of the GBR WHA. Hypothesis development and experimental designs are based on the principles of ERA frameworks. Specifically, this project aims to understand: (1) microplastic presence, type, abundance, unique characteristics, and relationships between coral reef abiotic and biotic compartments; (2) microplastic uptake and depuration kinetics by coral reef organisms; and (3) ultimate effects of microplastic uptake at present and projected

future concentrations, on coral reef organisms exposed to various naturally encountered temperatures.

Field surveys of reefs at Lizard Island, whereby abiotic and biotic compartments are sampled and assessed for microplastic contamination, will be described providing baseline data for the design of environmentally relevant experimental laboratory studies. These exposure studies will establish environmentally relevant dose response curves (Critchell and Hoogenboom, 2018) spanning from present to future predicted (i.e., beyond 2100) microplastic concentrations to elucidate the impacts of marine microplastic contamination on coral reef organisms (Everaert et al., 2020).

This thesis is organized into six chapters, including this general introduction to the context of the study (Chapter 1), four data chapters, and a general discussion. Each data chapter addresses a clearly defined research question prepared in manuscript format; hence each chapter includes a topic-focussed introduction, a descriptive materials and methods section, followed by results, discussion and conclusion sections. The main objective and associated hypothesis (H_o) for each of the four data chapters are as follows:

1. Establish reproducible methods for isolating microplastics from reef organisms representing four physiologically different taxa

H_0: Methods for isolating microplastic from biological samples do not vary according to biological sample types

2. Examine exposure to microplastic contamination in the abiotic and biotic compartments of coral reefs around Lizard Island, including sea water, sediment and representative organisms of the four physiologically different taxa studied in Chapter 2.

H_0: microplastic contamination does not differ within nor between the abiotic and biotic compartments of Lizard Island coral reefs).

3. Investigate microplastic uptake, quantity in organisms and depuration kinetics by a model coral reef fish, *Pomacentrus amboinensis*, under current and future environmentally relevant conditions.

H_0: Microplastic uptake, quantity in organisms and depuration kinetics by *Pomacentrus amboinensis* do not differ among different plastics, regardless of amounts present in either the present or projected future environment.

4. Assess the ultimate effects of both microplastic uptake and sea water temperature on *Acanthochromis polyacanthus* under current and future environmentally relevant conditions.

H_0: Microplastic uptake in combination with different sea water temperatures does not affect levels of cortisol and total lipids, neither growth and condition factor of *Acanthochromis polyacanthus*, at environmentally relevant conditions of present or future exposures.

The general discussion provides a synthesis of the four data chapters and elucidates the ecological risks posed by microplastics contaminating coral reef ecosystems. Furthermore, recommendations for methodological improvements in and standardization of microplastic research associated with field and experimental procedures, for use in ERAs are provided.

Chapter 2: An assessment workflow to recover microplastics from complex biological matrices

Abstract

An assessment workflow was designed to systematically evaluate effectiveness and validate use of popular microplastic separation methods on various complex biological matrices. Efficacies of alkaline (potassium hydroxide; KOH) and acid (nitric acid; HNO_3) digestions, and density [sodium chloride; NaCl, potassium iodide; KI] flotation were evaluated against anatomically diverse marine taxa (scleractinia, porifera, tunicate, holothurians) and environmentally prevalent microplastics (polyethylene, polystyrene, polyester, polyvinylchloride, rayon). Criteria assessed included matrix clarification efficiency; impacts on microplastics; and microplastic recovery rates. Clarification efficiency was best for HNO_3-treated corals, sponges and ascidians; and KI-treated holothurian gut contents. KOH clarification efficiency was low, thus unsuitable for all taxa. PET discoloured regardless of reagent. All reagents unravelled rayon threads into constituent monofilaments, with discolouration also occurring post HNO_3. Recovery rates were high for microplastic fragments but low for rayon monofilaments; only KI yielded high rayon recovery efficiency. Following recovery from spiked tissues, all polymers were accurately assigned, with subtle spectral profile changes observed. Variability in recovery efficacy, resulting from matrix and polymer type, highlights the importance of early assessment to inform method choice. This workflow proved effective in establishing the soundest method, returning accurate microplastic contamination reports, and identifying method-specific limitations that may yield inaccurate microplastic estimations.

Key words: marine environment, clearance efficiency, microplastic characterization, recovery rates, invertebrates

2.1. Introduction

Microplastics (plastics from 1µm to 5mm in length) are commonly reported contaminating marine organisms across all trophic levels (Aragaw and Mekonnen, 2021; Miller et al., 2020). However, field studies on microplastic contamination have mainly targeted a few key marine taxa with specific focus on species for human consumption(Dawson et al., 2021), primarily teleost fish and bivalve species(Aragaw and Mekonnen, 2021; Miller et al., 2020). For ecological risk assessments, it is essential to also include taxa that are critical in marine ecological processes (e.g., habitat-forming and nutrient cycling) and uniquely susceptible to microplastic uptake but which may also require tailored sample processing techniques. The high variability in microplastic sizes, polymer types, shapes and colours found in environmental and biological matrices adds an additional level of complexity(Rochman et al., 2019). Combined, these make assessment of microplastic contamination in the marine environment a substantial methodological challenge, the most prominent aspect being the separation of microplastics from complex high-organic matrices (Lusher et al., 2020).

To quantify microplastic contamination in biological samples, effective and reproducible protocols are required for microplastic separation, identification and characterization. Marine organisms have highly diverse anatomies and body compositions, for which a variety of physical and chemical methods have been developed to liberate microplastics from their tissues (Lusher et al., 2020). The most common separation methods include visual sorting(Markic et al., 2019), digestions using acidic (e.g. nitric acid [HNO_3], either concentrated or in combination with perchloric acid or hydrochloric acid) (Devriese et al., 2015; Karami et al., 2017a; Naidoo et al., 2017), alkaline (e.g. potassium hydroxide [KOH] and sodium hydroxide [NaOH]) (Karami et al., 2017b; Roch and Brinker, 2017) and oxidative (e.g. hydrogen peroxide) (Donohue et al., 2019) reagents, and density flotation with sodium chloride (NaCl) (Avio et al., 2015b; Li et al., 2015). The effectiveness of the chemical separation method is often a function of the concentration of the active reagent, processing time, sample weight to volume ratio, and physical parameters (e.g. heat or agitation) (Lusher et al., 2020; Pfeiffer and Fischer, 2020; Yan et al., 2020; Zhang et al., 2020b). However, many studies neglect to validate their separation method specifically for use on their study organism(s) or report on the method's sensitivity, accuracy and precision.

The use of different separation methods can influence the clarification (or clearance) efficiency of biological tissue. A high level of clarification efficiency is desirable (Lusher et al., 2020) to significantly reduce sample processing time, increase the likelihood of recovering microplastics, especially from complex biological matrices (Dawson et al., 2020), and facilitate the accurate visual and chemical characterization of microplastics. Reagents and their application in separation methods can influence the physical and chemical characteristics of microplastics, as well as their recovery rates. Reagents have been implicated in changes to microplastic size, shape, colour, and chemical integrity (Enders et al., 2017; Hurley et al., 2018; Li et al., 2016), potentially resulting in inaccurate identification, estimation or characterization of microplastic contamination (Lusher et al., 2020). Such changes in microplastic characteristics are often associated with chemical alteration of the polymer structure itself (Prata et al., 2019; Roch and Brinker, 2017), or adsorption of residual tissue or digestion reagent on the microplastic's surface (Miller et al., 2021). Spike-recovery tests, ideally producing high and accurate recovery rates from the target organism, are critical to validate separation methods and provide confidence in the reported microplastic concentrations (Lusher et al., 2017a; Rochman et al., 2019). Although high clarification efficiency, minimal impact on microplastics and high recovery rates are all critical for efficient and accurate quantification of microplastic contamination (Lusher et al., 2020; Miller et al., 2017), these factors are not always considered or reported in microplastic field studies (Alfaro-Nunez et al., 2021; Fathoniah and Patria, 2021; Wang et al., 2021a).

This study assesses common separation methods to recover microplastics from complex biological matrices, and reports on their accuracy and precision, both of which are crucial data quality characteristics in ecological risk assessments. Specifically, an iterative workflow was designed and applied to systematically evaluate the efficacy of microplastic separation methods on four complex biological matrices, the scleractinia (hard coral) *Acropora millepora*, the porifera (sponge) *Rhopaloeides odorabile*, the tunicate (sea squirt) *Polycarpa aurata* and the holothurian (sea cucumber) *Holothuria atra*. These representative taxa perform critical ecological functions (Astudillo-Garcia et al., 2020; Knowlton, 2001(Mohsen et al., 2019), have diverse anatomies and body compositions, and are susceptible to microplastic uptake (Girard et al., 2021; Mohsen et al., 2019; Vered et al., 2019). Five microplastic polymer types, namely polyethylene (PE), polystyrene (PS), polyester (PET), polyvinylchloride (PVC), and rayon,

having various shapes, sizes and colours, were selected based on their reported prevalence in marine environments (Rochman et al., 2019), including in habitats where the target species are found, such as coral reefs (Hall et al., 2015; Jensen et al., 2019; Ripken et al., 2021). Finally, four different stepwise separation methods (KOH digestion, HNO_3 digestion, and NaCl and potassium iodide [KI] density flotation) were individually evaluated based on their routine use in microplastic studies (Lusher et al., 2020), their mode of action and the compatibility between the method and sample matrix. The efficacy of each separation method was assessed against the three key criteria: (i) clarification efficiency of the biological matrix; (ii) potential effects of separation method on physical and/or chemical microplastic characteristics, and (iii) microplastic recovery rates from different biological matrices. The challenges of selecting the superior microplastic separation method to recover and accurately identify microplastics from complex biological matrices are discussed and recommendations provided for future studies.

2.2.Methods

2.2.1. Study species

Specimens of hard corals (*A. millepora*), sponges (*R. odorabile*), sea squirts (*P. aurata*) and sea cucumbers (*H. atra*) were opportunistically collected on SCUBA from five separate reefs (Rib, Taylor, Feather, John Brewer and Farquharson) in the central region of the Great Barrier Reef (GBR), Australia, in 2017 and 2019. *Holothuria atra* were sampled by hand. Fragments of *A. millepora* and *R. odorabile* were sampled from larger colonies using bone cutters. Whole P. aurata were sampled using hammer and chisel. Immediately following collection, individual samples were placed into sealed bags, transported to the research vessel and frozen at -20˚C. Frozen samples were transported to the Australian Institute of Marine Science, Townsville, for processing and analysis. Coral and sponge samples were thawed and processed whole, as their anatomies are such that dissection is not efficient and/or possible. Sea cucumbers and sea squirts were dissected prior to processing, to eliminate non-target tissues and reduce the complexity of the sample matrix to process (Fu et al., 2020; Lusher et al., 2020). Sea cucumbers were longitudinally crosscut, their gastro-intestinal tracts (GIT) removed, contents scraped out

and processed. For sea squirts, the outer tunic was removed and the remainder of the body (including the pharynx) processed.

2.2.2. Microplastics tested

Secondary microplastics (GESAMP, 2019) of PE, PS, PET, PVC and rayon, of differing size, shape, and colour (Appendix A - Table S1) were prepared in the laboratory from commercially available plastic products. Microplastics of: PE were produced from yellow lids of single-use sterile containers (SARSTEDT Australia); PS from white transparent PS beads (Sigma Aldrich); PET from 2 L white transparent drinking water bottles (no identified brand); and PVC from grey rigid sheets (no identified brand). Microplastics of rayon were prepared from a black textile thread (Güttermann). Irregular fragments of PE, PS, PET and PVC were produced separately from each other by milling the source products in either a food blender with extractor blade attachment (Magic Bullet; used for PE and PS) or a Connoisseur 825 blender (Blendtec Australia; used for PET and PVC). After use for each polymer, blenders were cleaned with white cotton tissues and tap water to avoid cross-contamination.

To determine potential effects of separation method on microplastic characteristics, plastic size ranges were obtained by dry sieving the irregular fragments through z-stacked stainless steel laboratory test sieves (4.5, 3.5, 2.5, 1.5 mm aperture, Endecotts). PE, PS, PET and PVC microplastic fragments of similar size were then manually selected to ensure size consistency, enabling assessment of observed impacts of different separation methods on microplastic sizes. Average ± SD size of the microplastic fragments was 2.7 ± 0.6 mm all together. Minimum and maximum sizes per polymer type if found are presented in Appendix A – Table S1. Rayon microplastics approximately 4 mm in length were produced by cutting sections of thread with a surgical blade (Paramount, BS EN 27740), guided by a calliper (Kincrome, 1/1000 in). Maximum lengths of individual fragments and fibres were measured by stereomicroscopy and microphotography (Leica MZ16A, Leica DFC 500, Leica Application Suite LAS 4.4.0) using Fiji (ImageJ, 2.0.0-rc-69/1.52p). Microplastics used to determine potential effects of separation method were deliberately chosen within the larger range of microplastics particle sizes, to support accuracy of analytical procedures, including by reducing the chance of item loss during experimental procedures (e.g., filtration).

To determine recovery rates of microplastics from tissues of the four species studied, irregular microplastic fragments < 500 µm were obtained for PE, PS, PET and PVC by dry sieving (500 µm aperture, Endecotts) and manual selection (Appendix A - Table S1). Rayon microplastics (~ 2 mm) were obtained as detailed above. Microplastics used to determine recovery rates were deliberately chosen smaller to better represent the size classes likely to be found in test organisms (Girard et al., 2021; Huang et al., 2021; Mohsen et al., 2019; Vered et al., 2019).

Shape and colour of all microplastics were recorded using stereomicroscopy and microphotography and determined using customised shape and colour charts described in Supplementary Information (Appendix A - Figures S1 and S2). Prior to use, each polymer type was analysed using Attenuated Total Reflection Fourier transform infrared spectroscopy (ATR-FTIR; PerkinElmer Spectrum 100 FTIR spectrometer) and confirmed by screening against the NICDOCOM IR spectral library for polymers and related materials (NICODOM Ltd., Czech Republic) (Appendix A - Table S2), following Kroon et al.(Kroon et al., 2018a).

2.2.3. Choice of microplastic separation methods

The chemical reagents assessed included (i) acid digestion with nitric acid (70% HNO_3), (ii) alkaline digestion with potassium hydroxide (1 M - equivalent to 5.6% KOH - and 1.8 M - equivalent to 10% KOH), and density flotation with either (iii) sodium chloride (1.2 g cm^{-3} NaCl) or (iv) potassium iodide (1.7 g cm^{-3} KI). These reagents were chosen based on their properties (i.e., NaCl and KI are IR transparent and thus unlikely to interfere with the IR profiles of recovered microplastics(Thomas, 1997)) and prior reported use in microplastic environmental studies(Aslam et al., 2020; Lusher et al., 2020). The nature of reagents used and their mode of action (i.e., chemical digestion vs density flotation) were considered, along with compatibility between separation method and sample matrix (e.g., chemical digestion conditions suited to species with calcified skeletons). Therefore, an a priori decision was made that certain methods (but not others) were most compatible with particular matrices. Briefly, alkaline and acid digestions were tested on all four taxa, while density flotation was only applied to sea cucumber GIT contents. Technical information and procedural descriptions for

each separation method is detailed in Table S3 (Appendix A). Solutions of KOH, NaCl and KI were prepared prior to use, up to one week in advance. 70% HNO_3 was used as provided.

2.2.4. Processing parameters

Processing parameters for each separation method (i.e., duration of processing, reagent concentration, and laboratory temperature; Appendix A - Table S3) were selected based on discussions in the literature (Lusher et al., 2017b; Miller et al., 2017), and/or logistical concerns (e.g. duration of procedure, minimizing hazards). The amount of reagent required (ratio of reagent:sample, ml:g) was based on average reported volumes of reagent used to process 1 g of biological tissue (Van Cauwenberghe and Janssen, 2014), (Vandermeersch et al., 2015), (Kuhn et al., 2017). Maximum processing time was initially set to 24 hr (Cole et al., 2014) for all four separation methods evaluated and all examined biological matrices to simplify sample-handling logistics. Time was either increased (48 hr) if observed clarification efficiency was poor or decreased (12, 6 and 3 hr) if impacts on microplastics were observed (see below). All methods were conducted at room temperature (22 ± 1˚C); heating was strictly avoided to reduce detrimental impacts on microplastics such as morphological alteration, degradation or loss (Munno et al., 2018; Pfeiffer and Fischer, 2020).

2.2.5. Workflow to validate microplastic separation methods

Design of the iterative assessment workflow (Figure 2.1) incorporated three key assessment criteria identified from the literature (reviewed in Miller et al.(Miller et al., 2017), and examples of application provided in Yan et al.(Yan et al., 2020) and Miller et al.(Miller et al., 2021)): (i) clarification efficiency of each biological matrix examined; (ii) potential effects on physical and/or chemical characteristics of microplastic type, and (iii) microplastic recovery rates from each biological matrix. These criteria were tested in sequence, i.e., methods should first be successful in criterion 1 to then be assessed for criterion 2, similarly for criterion 3. When all three criteria were met, the separation method was considered validated for any particular biological matrix and microplastic polymer type, and thus suitable for experimental

use. Conversely, the separation method was excluded for use on a particular biological matrix if one or more criteria were not met.

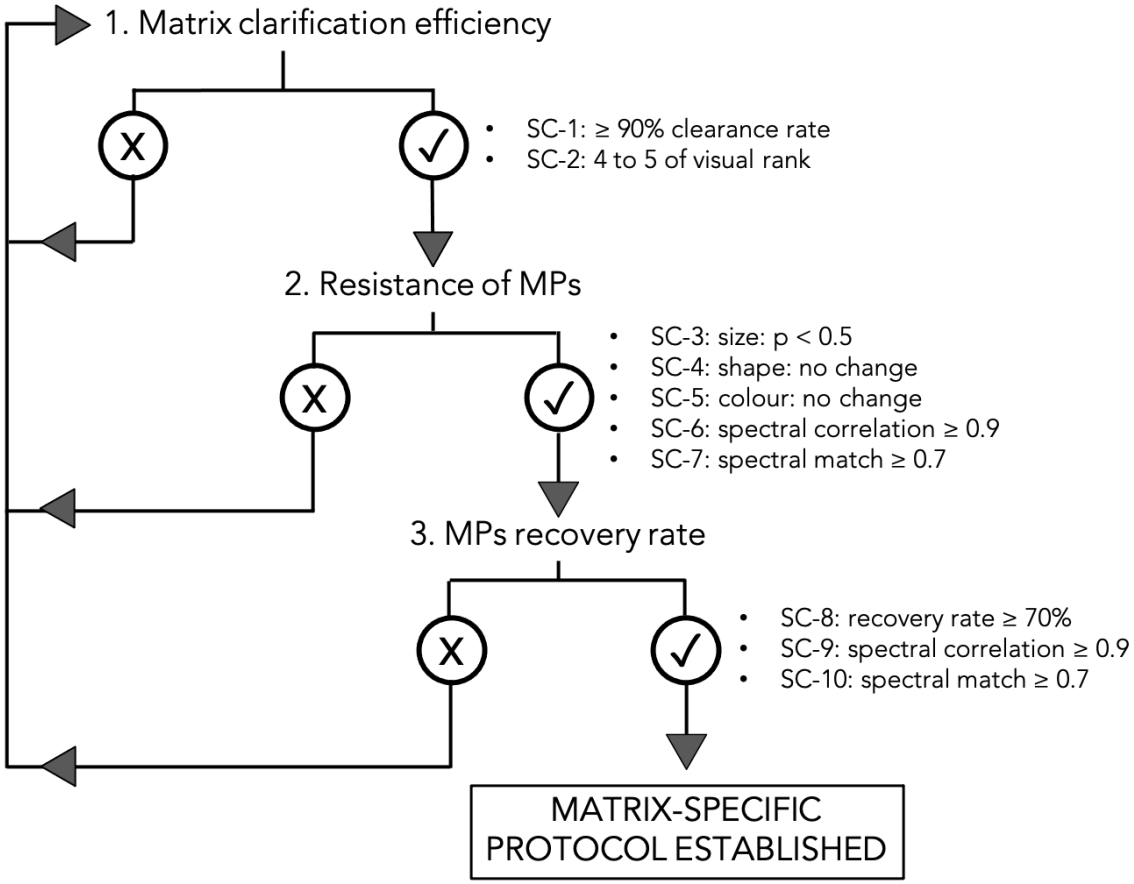

Figure 2.1: Systematic and interactive workflow to assess efficacy of separation methods to recover microplastics from complex biological matrices based on three key criteria (1, 2, 3). Sub-criteria (SC-1 to SC-9) were used as decision points for halting, refining, or proceeding with the respective separation method.

2.2.5.1.Criterion 1: Matrix clarification efficiency

To determine clarification efficiency, the four biological matrices were individually exposed to different separation methods in triplicates (4:1 ml of reagent to dry tissue of biological material, Appendix A - Table S3) and thereafter filtered for the criterion analysis described below. Initially, alkaline and acid digestion methods were applied to all four taxa for 24 hr (Appendix A - Table S3b). The two density flotation methods, also tested for 24 hr, were

only applied to sea cucumber GIT contents given they mainly contained inorganic material, i.e., sediments. Prior to exposure, each matrix was air dried for 48 hr in a fume hood in a semi-closed glass petri dish and weighed (Sartorius CP2245, max 220g d 0.1 mg).

Clarification efficiency of each method was evaluated based on the degree of elimination of hard and soft tissues and quantified based on two sub-criteria (SC): clarification rate (SC-1) and visual ranking (SC-2) (Appendix A - Figure S3). After filtration through pre-weighed stainless-steel filter discs (547 and/or 263 and/or 26 µm aperture; custom designed in-house, details to be published elsewhere), the retentate was air dried for 48 hr and the sample containing filter was weighed again. The clarification rate (%) was determined based on the difference in weight of the biological material pre- and post-treatment:

$$(\text{final weight}/\text{initial weight}) \times 100 \qquad \text{(Eq. 1)}$$

The retentate was also ranked visually using stereomicroscopy (Leica MZ16A) based on the following scoring: 1 = intact (i.e., no tissue digestion occurred), 2 = partially intact (i.e., some tissue digestion occurred but most organismal structure remained intact), 3 = partially digested (i.e., most tissue digested but retentate hampers either accurate microscopy and/or spectroscopy), 4 = mostly digested (i.e., most tissue digested and retentate does not hamper accurate microscopy and/or spectroscopy), and 5 = digested (i.e., retentate is almost or totally clear of organismal material) (see Appendix A - Figure S3 for illustration of rank scores). Clarification was determined in triplicate for each combination of separation method and taxon examined and considered efficient when mean clarification rate (SC-1) was ≥ 90% and mean visual rank (SC-2) was ≥ 4.

Efficient clarification was not always immediately achieved by all separation methods (see results). In these instances, exposure time was increased to 48 hr and clarification rate and visual ranking re-assessed. If no clarification efficiency improvement was observed, the concentration of the chemical reagent was increased and retested at both 24 and 48 hrs. Only when efficient clarification was achieved for a specific combination of separation method and biological matrix did the workflow progress to the second key criterion. If efficient clarification

could not be achieved, the specific combination of separation method and biological matrix was deemed inefficient and not further considered.

2.2.5.2. Criterion 2: Impacts on physical and chemical characteristics

To determine the impacts on physical and chemical characteristics, PE, PS, PET and PVC irregular fragments and rayon fibres were exposed, in isolation, to all separation methods having met criterion 1 and therefore advanced to the next step in the workflow. Pre-treatment, the physical and chemical characteristics of all five microplastics, including size, shape, colour and polymer type, were determined (described in section 5.2).

For each separation method tested (see results), five replicates of 10 items per microplastic type were exposed to 1 ml of the separation reagent for 24 hr. In addition, five replicates of 10 items per microplastic type were exposed for 24 hr to 1 ml of Milli-Q water as a positive control. Following recovery on 26 and 263 µm stainless steel discs, microplastics were photographed by microphotography and physically characterized (described in section 5.2). Chemical integrity of microplastics was assessed on a sub-sample (n = 5) of all recovered items from each replicate using ATR-FTIR (described in section 5.2).

Changes in physical characteristics, namely size (SC-3), shape (SC-4) and colour (SC-5) (Figure 2.1), were assessed by comparison with pre-treated control microplastics. Changes in microplastic size were assessed using RStudio (version 1.2.5042) by applying general linear models (glm) with Gamma distribution and pairwise hypothesis testing (p-value < 0.05), as per Miller et al. (2021). Changes in microplastic shape and colour were assessed against customised shape and colour charts based on descriptors commonly used in the literature (Hartmann et al., 2019; Rochman et al., 2019) (Appendix A – Figures S1 and S2). Impacts of separation methods on the physical characteristics were considered negligible when changes in size were not statistically significant, and shape and colour remained within the same category before and after treatment.

Changes in chemical characteristics caused by exposure to the chemical reagents were assessed based on spectral similarity to controls (PerkinElmer Spectrum 100 COMPARE function; SC-6) and the final polymer assignment (PerkinElmer SEARCH function using the NICDOCOM IR spectral library for polymers; SC-7) (Figure 2.1), as per Kroon et al.(Kroon

et al., 2018a). Correlation factors of ≥ 0.9 indicated high similarity between treated and control microplastics and therefore "no-change"(Dawson et al., 2020; Miller et al., 2021). Confidence in assignment to the original polymer type (i.e., PE, PS, PET, PVC, and rayon) was considered acceptable when a match of ≥ 70% was returned for the treated microplastic (Kroon et al., 2018a; Su et al., 2020; Yang et al., 2015).

Changes in physical and chemical characteristics, however, were not always negligible (see results). In these instances, the initial 24-hr exposure time was sequentially reduced to 12, 6 or 3 hr and microplastic physical and chemical properties assessed until impacts were no longer observed. Only once this was achieved for a specific combination of separation method and microplastic polymer type did the workflow progress to the third and final step, criterion 3. If negligible impacts could not be achieved, the specific combination of separation method and microplastic polymer type was deemed unsuitable and was only further considered if no viable alternative was available. Where FTIR profiles were changed, the carbonyl index (CI; ratio of carbonyl peak intensity before and after treatment; Supplementary Information) was calculated to provide insight into the extent of degradation, and whether this factor could support the pre-treatment polymer assignment.

2.2.5.3.Criterion 3: Microplastics recovery rate from biological material

To determine recovery rates of microplastics from the four biological matrices, recovery rates were calculated from three replicates of biological material (~ 3 g per replicate) per taxon, each spiked with five pieces of four polymers (PE, PS, PET and PVC). Based on the unravelling of rayon upon exposure to all four chemical reagents (see results), one replicate from each taxon was spiked with five rayon threads, while the other two replicates were spiked with five rayon monofilaments. Spiked coral, sponge and sea squirt tissues were treated, at room temperature, with 70% HNO_3 for 3, 6 and 24 hr, respectively, while sea cucumber GIT content was treated with both 1.2 g/cm3 NaCl and 1.7 g/cm3 KI for 24 hr (as previously determined by the workflow). Ratios of reagent per gram of tissue were the same ratio as that used when assessing against criterion 1. Following retention on the 26 µm mesh filter, the number of recovered microplastics was visually determined by stereomicroscopy and their polymer type confirmed by ATR-FTIR.

Overall recovery rate resulting from each combination of biological material, microplastic polymer type and separation method was evaluated according to the percent recovery rate (SC-8), the percent similarity to the initial polymer type (SC-9), and the confidence of the chemical assignment based on percent match to the spectral reference library (SC-10) (Figure 2.1). The percent recovery rate was calculated based on the difference in number recovered versus the number spiked:

$$(\text{No. of microplastics recovered}/\text{No. of microplastics initially spiked}) \times 100 \qquad \text{(Eq. 2)}$$

For rayon, only replicates with five monofilaments were used for the SC-8 calculation. Changes in chemical characteristics and confidence in the polymer assignment were assessed as per above (SC-6 and 7). Recovery rates were considered acceptable when the microplastic percent recovery rate (SC-8) was ≥ 70% (Cashman et al., 2020), the spectral similarity to untreated microplastics returned a correlation factor ≥ 0.9 (SC-9), and the match to the original polymer type in the spectral reference library was ≥ 70% (Kroon et al., 2018a; Lusher et al., 2013) (SC-10) confirming polymer assignment.

For those combinations of separation method, biological matrix and microplastic polymer type where acceptable recovery rates could not be achieved (see results), no further change in methodology was tested and the specific combination was deemed unsuitable for application.

2.3. Results and Discussion

2.3.1. Criterion 1: Matrix clarification efficiency

2.3.1.1. Efficiency of chemical (KOH, HNO3) digestions

Clarification of all four taxa with acid digestion, using 70% HNO_3 for 24 hr, was efficient with mean clarification rates > 95% for each taxon and mean visual ranking scores of ‘mostly digested’ (score 4; sponge and sea squirt) and ‘digested’ (score 5; coral and sea cucumber GIT content) (Table 2.1). Thus, HNO_3 digestions were effective in clarifying calcium carbonate in coral skeleton, spongin and silica spicules in sponge skeleton, protein rich tissue in sea squirts,

and inorganic sediment in sea cucumber GIT content. A shorter exposure time of 3 hr, to reduce the impacts of HNO_3 on the physical and/or chemical integrity of some microplastics (see section 6.2), resulted in an equally high clarification rate for coral (mean rate: 99.8% ± 0 SE; mean score 5) and sponge (mean rate: 95.1% ± 0.2 SE) tissues. However, the visual rank for sponge was low (mean score 3), whereas a slightly longer (6 hr) digestion of sponge resulted in an overall high clarification efficiency (mean rate: 97.7 ± 0.6 SE; score 3 - 4). In contrast, visual observations during digestions revealed that shorter exposure times of 70% HNO_3 were ineffective for sea squirts (data not reported). Thus, acid digestion with 70% HNO_3 resulted in effective clarification after 24 hr for all four taxa, and after 3 and 6 hr for coral and sponge, respectively. This method was progressed to the next stage of the workflow.

Table 2.1: Matrix clarification efficiency (criterion 1), as determined by clarification rate (CR, %, ± S.E., sub-criterion 1) and visual ranking (VR, score 1 to 5, sub-criterion 2), of coral (*Acropora millepora),* sponge (*Rhopaloeides odorabile*), sea squirt (*Polycarpa aurata*), and sea cucumber (*Holothuria atra*) samples treated with potassium hydroxide (1 M and 10% KOH), nitric acid (70% HNO_3), sodium chloride (1.2 g cm^{-3} NaCl) and potassium iodide (1.7 g cm^{-3} KI), at various concentrations and times of exposure (n = 3 replicates per treatment). Clarification rates ≥ 90% and visual ranking score ≥ 4 met the sub-criteria and are in bold font. Superscript numbers (1, 2,3,4) represent the iteration number: (1) first assessment of treatment, (2,3,4) second, third and four iteration using modified parameters of time and concentration. nd = not done, GIT = gastro-intestinal tract.

Method		Mean percentage (± SD) of material eliminated from samples							
Reagent	Time	Coral		Sponge		Sea squirt (minus tunic)		Sea cucumber (GIT contents)	
	(h)	CR	VR	CR	VR	CR	VR	CR	VR
1 M KOH	24	17 ± 6.6[1]	2	16.5 ± 1[1]	2	98.8 ± 0.4[1]	3	20.5 ± 3.77[1]	2
	48	20 ± 6.7[2]	2	18.8 ± 0.8[2]	2	71 ± 4[2]	3	22.5 ± 6.1[2]	2
10% KOH	24	16 ± 1.1[3]	2	19.3 ± 4.1[3]	2	74.3 ± 5.4[3]	3	nd	nd
	48	17.2 ± 1.4[4]	2	20.8 ± 4[4]	2	80 ± 0.4[4]	3	nd	nd
70% HNO_3	24	99.6 ± 0.2[1]	5	97.8 ± 0.6[1]	4	99.2 ± 0.1[1]	4	98.3 ± 0.1[1]	5
	3	99.8 ± 0[2]	5	95.1 ± 0.2[2]	3	nd	nd	nd	nd
	6	nd	5	97.7 ± 0.6[3]	3 - 4	nd	nd	nd	nd
1.2 g cm^{-3} NaCl	24	nd	nd	nd	nd	nd	nd	99.6 ± 0.3[1]	5
1.7 g cm^{-3} KI	24	nd	nd	nd	nd	nd	nd	99.9 ± 0[1]	5

Digestion with HNO_3 is often replaced by less harsh alkaline chemicals such as KOH (Hermabessiere et al., 2019; Karami et al., 2017a; Phuong et al., 2018) to reduce potential impacts on microplastics. However, mean clarification rate of alkaline digestions, using 1 M and 10% KOH for 24 and 48 hr at room temperature, was < 25% for coral and sponge tissues and sea cucumber GIT contents (Table 2.1). In addition, visual assessment of all retentates confirmed samples were 'partially intact' (score 2 for all three taxa). In addition, visual assessment of all KOH digestions of sea squirt pharynges revealed they were only 'partially digested' (score 3), despite of the mean clarification rates being high for sea squirt pharynges (> 70%), with 1 M KOH for 24 hr resulting in almost complete clarification (98.8%). Thus, digestion with KOH, regardless of concentration and exposure time tested, did not meet both sub-criteria, nor achieve efficient clarification for any of the four taxa, and was not considered any further. The underperformance of the KOH treatments might suggest that it is ineffective in dissolving the calcium carbonate in coral skeleton, as well as sediment in sea cucumber GIT contents, spongin and silica spicules in sponge skeleton, and the muscular pharynx of ascidians. However, recent studies suggest the use of 20% KOH instead of 10% to increase the clarification efficiency of this alkaline reagent (Jones et al., 2021, Kashiwabara et al, 2021). That being so, 20% KOH should be explored for the tested matrices in future studies applying this workflow.

2.3.1.2. Efficiency of density (NaCl, KI) flotations

Clarification of sea cucumber GIT content with both 1.2 g cm^{-3} NaCl and 1.7 g cm^{-3} KI was efficient with mean clarification rates >99% and mean visual ranking scores of 'digested' (score 5) (Table 2.1). Other studies on sea cucumber GITs have used chemical digestion methods, such as HNO_3, in preference to density flotation without clear justification (Mohsen et al., 2019; Sayogo et al., 2020). Because the GIT content, having minimal organic matter, is compositionally analogous to marine sediment, effective clarification can be expected with density floatation methods that are commonly applied to separate microplastics from sediment matrices (Graham and Thompson, 2009; Quinn et al., 2017). Here, while also effective in clarifying sea cucumber GIT content, 70% HNO_3 was not further considered due to its hazardous nature; sound chemical risk management requires 'replacing dangerous by non-

dangerous or less dangerous' chemicals where practicable (89/391/EEC, 1989). While brine solutions of NaCl have been used previously to separate microplastics from sea cucumber GIT content (Graham and Thompson, 2009; Wicaksono et al., 2021), KI has only been used for sediments and soils (Aslam et al., 2020; Mu et al., 2019). Prior to this study, neither density flotation method has been thoroughly validated based on clarification efficiency of this type of sample while also assessing impacts on microplastics, or microplastic recovery rates (Aslam et al., 2020; Graham and Thompson, 2009; Wicaksono et al., 2021). This possibly generated unrealistic microplastic contamination estimates inadvertently, so future studies need to address this. Based on their clarification efficiencies of sea cucumber GIT content, both density flotation methods progressed to the next stage of the workflow.

2.3.2. Criterion 2: Impacts on microplastic physical and chemical characteristics

Based on clarification efficiencies achieved for the four tissue matrices, the impacts of the three reagents HNO_3, NaCl and KI on the physical and chemical characteristics of microplastics were examined.

2.3.2.1.Impacts of Milli-Q water exposure

Exposure to Milli-Q water (used as a positive control) did not significantly impact PE, PET, PS or PVC size ($p > 0.05$, Appendix A – Figure S4, Table S4) or shape. Changes in colour were observed for 42% of PET fragments (Figure 2.2a), transitioning from transparent and clear to transparent and yellow/orange (change in colour value from 6.6. to 6.2; Appendix A – Figure S2). Similar yellowing was subsequently observed in PET fragments across all separation methods tested (see below), possibly as a result of UV degradation (Pastorelli et al., 2014; Sang et al., 2020). In contrast to the microplastic fragments, size and shape of rayon threads changed dramatically, with threads unravelling almost immediately into multiple (n~60) monofilament fibres upon exposure to Milli-Q water (Appendix A – Figure S5), as well as following exposure to any of the other chemical reagents (see below). The unravelling of rayon threads complicated pre- and post-treatment comparisons and demonstrated that the impact of any separation method on rayon size (SC-3) and shape (SC-4) is considerable. These

results, under control conditions, further highlight the importance of examining the potential impacts of separation methods for specific microplastics, including thread fibres. It also suggests that such unravelling may contribute, at least in part, to the prevalence of microfibres in the marine environment (Hernandez et al., 2017; Özkan and Gündoğdu, 2020). Rayon colour, on the other hand, was unaffected by control conditions. (Fig 2b).

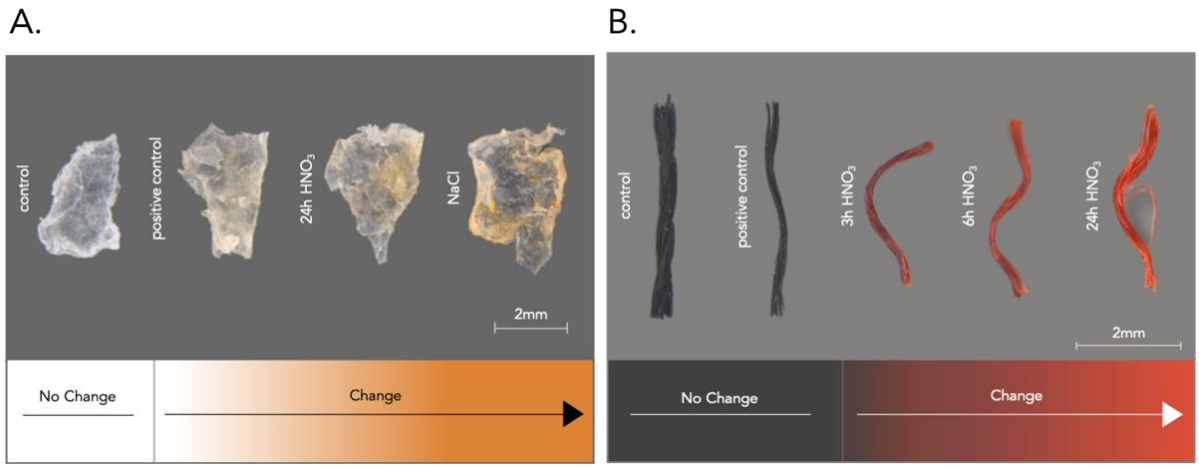

Figure 2.2: Colour changes in microplastic fragments and fibres following exposure to various chemical reagents. (a) Increased yellowing of polyester fragments following exposure to Milli-Q water (positive control), 70% HNO_3 and 1.2 g cm^{-3} NaCl for 24 h. (b) Discolouration of rayon fibres following exposure to Milli-Q water (positive control) for 24 h, and 70% HNO_3 for 3, 6 and 24 h.

The spectral similarity between untreated control and positive control microplastics was high for PE, PS, PET and PVC fragments (≥ 0.98), but somewhat lower for rayon fibres (0.88 ± 0.01 SE) (Table 2.2). The IR spectral profile of rayon changed in the O-H region of the spectrum, which became more prominent than in control. However, no changes were observed for the characteristic IR absorption bands (Comnea-Stancu et al., 2017) (Appendix A – Table S5). Similar changes in IR profiles have been reported for cellulose-based fibres in the presence of humidity and are associated with the inherently hygroscopic nature of cellulose-based materials (Celino et al., 2018). The rayon CI ratio also differed significantly before and after treatment, indicating oxidation ($p < 0.05$, Appendix A – Table S6), but did not impede polymer identification. All polymer types returned ≥ 0.70 spectral match to reference spectra (Table 2.2), including rayon, lending confidence to their chemical assignment.

Table 2.2: Average spectral similarities of treated microplastics to untreated controls ('SS'), and spectral match of treated microplastics to polymers in the NICDOCOM IR spectral library ('SM') (criterion 2). The five microplastics polymer types were treated with either Milli-Q water (positive control), 70% nitric acid (HNO_3), 1.2 g cm^{-3} sodium chloride (NaCl), or 1.7 g cm^{-3} potassium iodide (KI) for 24 h. Spectra were determined using infrared spectroscopy. PE = polyethylene, PS = polystyrene, PET = polyester and PVC = polyvinylchloride. nd = not done.

Polymer type	Treatment											
	Milli-Q water		70% HNO_3						1.2 g cm^{-3} NaCl		1.7 g cm^{-3} KI	
	24 h		3 h		6 h		24 h		24 h		24 h	
	SS	SM	SS	SM	SS	SM	SS	SM	SS	SM	SS	SM
PE	0.99 ± 0.00	0.98 ± 0.01	nd	nd	nd	nd	0.97 ± 0.00	0.96 ± 0.00	0.97 ± 0.00	0.96 ± 0.01	0.98 ± 0.00	0.96 ± 0.04
PS	0.99 ± 0.00	0.99 ± 0.00	nd	nd	nd	nd	0.96 ± 0.00	0.97 ± 0.03	0.95 ± 0.00	0.98 ± 0.01	0.97 ± 0.00	0.98 ± 0.02
PET	0.98 ± 0.00	0.99 ± 0.00	nd	nd	nd	nd	0.98 ± 0.00	0.99 ± 0.00	0.95 ± 0.01	0.98 ± 0.01	0.95 ± 0.00	0.98 ± 0.01
PVC	0.99 ± 0.00	0.86 ± 0.03	nd	nd	nd	nd	0.95 ± 0.00	0.86 ± 0.02	0.92 ± 0.01	0.85 ± 0.04	0.98 ± 0.00	0.84 ± 0.04
Rayon	0.88 ± 0.01	0.96 ± 0.01	0.74 ± 0.01	0.87 ± 0.02	0.74 ± 0.01	0.87 ± 0.01	0.69 ± 0.01	0.83 ± 0.09	0.88 ± 0.01	0.95 ± 0.01	0.89 ± 0.00	0.96 ± 0.01

2.3.2.2.Impacts of acid (HNO3) digestion

Exposure to 70% HNO_3 did not significantly impact PE, PET, PS or PVC size ($p > 0.05$, Appendix a – Figure S4, Table S4) or shape. As for Milli-Q water, colour change was observed for 38% of PET fragments (Figure 2.2a). While these results are consistent with some studies (Miller et al., 2021; Pfeiffer and Fischer, 2020; Yu et al., 2019), it also contradicts others reporting on the effects of HNO_3 on size, shape and/or colour of irregular microplastics –

especially for PS, PET and PVC (Prata et al., 2019; Roch and Brinker, 2017). This contradiction may be due, in part, to different protocols or experimental designs across studies, particularly reaction temperature and microplastic size. Heating potentially promotes the reaction between HNO_3 and microplastics (Pfeiffer and Fischer, 2020), with several studies reporting changes in microplastic size, shape and/or colour after exposure to hot acid (Claessens et al., 2013; De Witte et al., 2014; Roch and Brinker, 2017; Zhang et al., 2020b). Exposures conducted at room temperature, including this study, circumvents such impacts of heating (Miller et al., 2021; Yu et al., 2019). Size is also known to alter the potential reactivity of microplastics, with smaller, irregular fragments having higher reactivity (Lubken et al., 2021) and sensitivity to reagents (Guilizia et al, submitted). While changes in rayon size and shape were not further assessed for reasons outlined previously (section 6.1), its colour changed from black to red (i.e., from -5.6 to -5.2; Figure 2.2b, Appendix A – Figure S2), even after shorter exposure times (6 and 3 hr) to 70% HNO_3. Such discoloration could be due to chemical modification (e.g., oxidation) of the black pigment/dye.

The spectral similarity between treated microplastics to untreated controls was high for PE, PS, PET and PVC fragments (≥ 0.95), but lower for rayon fibres (0.69 ± 0.01 SE) (Table 2.2, Appendix A – Table S5). The CI ratio of treated rayon IR profiles was significantly different to control rayon IR profiles ($p < 0.05$, Appendix A – Table S6). These impacts on rayon were evident even after reducing the HNO_3 digestion time to 3 hr. Such spectral changes have been reported previously for rayon specifically, and for cellulose-based materials in general, and are associated with water absorption (Comnea-Stancu et al., 2017; Huntley et al., 2015), oxidation (da Silva Souza et al., 2018) and nitration (Gismatulina et al., 2017; Heredia-Guerrero et al., 2014; Jamal et al., 2020). These changes, however, did not affect the accuracy of polymer assignment, with PE, PS, PET, PVC, and rayon all having spectral matches ≥ 0.73 to reference spectra (Table 2.2).

Overall, not all sub-criteria were met for all microplastics after exposure to the 70% HNO_3 digestion methods. PE, PS and PVC fragments were unaltered by 70% HNO_3, whilst PET fragments were discoloured (SC-5). For rayon fibres shape (SC-3), size (SC-4), colour (SC-5), and spectral similarity (SC-6) were all impacted. Regardless, all five polymers were still accurately assigned (SC-7) following exposure. Given rayon shape and size is impacted by positive control conditions (i.e., Milli-Q water), and the high clarification efficiency afforded

by 70% HNO_3 for the biological matrices examined, this digestion method was progressed to the next stage in the workflow, with the caveat that physical and/or chemical characteristics of spiked PET and rayon could be impacted and affect recovery rates.

2.3.2.3.Impacts of density (NaCl, KI) flotation

Exposure to brine solutions did not significantly impact PE, PET, PS or PVC size ($p > 0.05$, Appendix A – Figure S4, Table S3) or shape. Similar to the other treatments, yellowing of PET was observed (Figure 2.2a). Changes in size and shape of rayon were not further assessed for reasons outlined previously (section 6.1), while rayon colour was unaffected. It should be noted that KI brine solutions were observed to yellow over time (i.e., up to one week) as a result of oxidation but did not impact the microplastic's colour when exposed up to 24 hr. Microplastic discoloration should be investigated for prolonged exposure times.

The spectral similarity to control microplastics was high for PE, PS, PET and PVC fragments (≥ 0.92), but was just below the 0.9 threshold for rayon fibres (0.88 ± 0.01 SE for NaCl; 0.89 ± 0.00 SE for KI) (Table 2.2). IR absorption bands associated with water absorption (Comnea-Stancu et al., 2017) and degradation were observed in the treated rayon spectrum (Appendix A – Table S5). Oxidation of rayon polymer was evident from the change in CI ratio following NaCl ($p < 0.05$), but not KI ($p > 0.05$) exposures (Appendix – Table S6). Regardless, all five microplastics showed strong similarity to reference spectra (≥ 0.84) (Table 2.2), providing confidence in these polymer assignments.

Again, not all sub-criteria were met. Both NaCl and KI density flotation methods were deemed suitable for PE, PS and PVC fragments, but less so for PET fragments - due to impacts on colour (SC-5) and rayon fibres - due to impacts on shape (SC-3), size (SC-4), and spectral similarity (SC-6). Given all five polymers were still accurately assigned (SC-7) following exposure to NaCl and to KI, both separation methods progressed to the next stage in the workflow, with the understanding that recovery rates could be somewhat affected by the impacts observed.

2.3.3. Criterion 3: Microplastic recovery rates from biological material

Based on the minimal impacts on the physical and chemical characteristics of the microplastics tested, recovery rates of spiked microplastics from coral, sponge and sea squirts were determined for 70% HNO_3. For sea cucumber GIT contents, recovery rates of spiked microplastics were determined for NaCl and KI.

2.3.3.1. Microplastic recovery rates from coral, sponge and ascidian tissues using 70% HNO3

Mean recovery rates of PE, PS, PET and PVC from spiked biological tissues were high, ranging from 80% ± 11.6 SE (PE from sponge) to 100% ± 0.00 (PE, PS, PET and PVC from coral; PE and PS from sea squirt) (Table 2.3). In contrast, mean recovery rates of rayon fibres were low and variable, ranging from 50% ± 10 SE for sea squirts, to 70% ± 10 SE for sponge.

The spectral similarity to control microplastics was high for PE, PS and PET fragments (≥ 0.94), but below the 0.9 threshold for PVC fragments and rayon fibres (Table 2.3, Appendix A – Table S7-S9). IR spectra of PVC recovered from digested coral, sponge and sea squirt tissues contained additional peaks not observed after treatment with 70% HNO_3 only (Appendix A – Table S10). Some of these peaks are potentially associated with oxidation, formation of carbonyl groups (Hutabarat et al., 2016; Ternero-Hidalgo et al., 2016) and/or nitration (Hadjiivanov et al., 2002). Other peaks are characteristic of lipids (Liang et al., 2010), and could be a result of residual biological matter after digestion (Miller et al., 2021; Scheurer and Bigalke, 2018). The impact of the biological matrix on recovered rayon was similar to treatment with 70% HNO_3 only at various exposure times, with evidence of oxidation (new peak at 1730 cm-1 (Moosavinejad et al., 2019; Ramírez-Flores et al., 2009)) (Appendix A – Table S10). Spectral similarity of all recovered microplastics to reference spectra was above the 0.7 threshold value (Table 2.3, Appendix A – Table S7-S9), again providing confidence in the chemical assignment.

Table 2.3: Microplastics recovery rates (criterion 3) from coral, sponge, sea squirt and sea cucumber matrices. For each of the matrices and five microplastics examined, the mean (± standard error) microplastic recovery rate ('RR'), spectral similarities of recovered microplastics to untreated control ('SS'), and spectral match of recovered spiked microplastics to polymers in the NICDOCOM IR spectral library ('SM') were determined following exposure to four separation methods. Digestion of coral, sponge and sea squirt tissues with 70% HNO_3, and density flotation of sea cucumber gastro-intestinal tract (GIT) contents with 1.2 g cm^{-3} NaCl and 1.7 g cm^{-3} KI. PE = polyethylene, PS = polystyrene, PET = polyester and PVC = polyvinylchloride. Rayon monofilaments were tested here (see methods for details). nd = not done.

Plastic	Coral (70% HNO_3)			Sponge (70% HNO_3)			Sea squirt (70% HNO_3)			Sea cucumber					
										1.2 g cm^{-3} NaCl			1.7 g cm^{-3} KI		
	RR	SS	SM	RR	SS	SM	RR	SS	SM	RR	SS	SM	RR	SS	SM
PE	100 ± 0.0	0.99 ± 0.0	94 ± 1.0	100.0 ± 0.0	0.96 ± 0.0	97 ± 1.0	80.0 ± 11.6	0.99 ± 0.0	96 ± 1.0	100 ± 0.0	0.99 ± 0.0	98 ± 0.0	100 ± 0.0	0.99 ± 0.0	99 ± 1.0
PS	100 ± 0.0	0.98 ± 0.01	95 ± 3.0	100 ± 0.0	0.96 ± 0.01	94 ± 1.0	86.7 ± 6.7	0.99 ± 0.0	98 ± 0.0	93.3 ± 6.7	0.99 ± 0.0	97 ± 1.0	80 ± 11.6	0.99 ± 0.0	99 ± 0.0
PET	100 ± 0.0	0.94 ± 0.01	99 ± 0.0	93.3 ± 6.7	0.98 ± 0.0	99 ± 0.0	86.7 ± 6.7	0.98 ± 0.0	99 ± 0.0	53.3 ± 6.7	0.97 ± 0.01	98 ± 0.0	86.7 ± 6.7	0.99 ± 0.0	99 ± 0.0
PVC	100 ± 0.0	0.79 ± 0.02	86 ± 2.0	93.3 ± 6.7	0.71 ± 0.09	86 ± 5.0	93.3 ± 6.7	0.84 ± 0.0	94 ± 0.0	46.7 ± 6.7	0.95 ± 0.01	90 ± 2.0	93.3 ± 6.7	0.98 ± 0.0	87 ± 1.0
Rayon (24 h)	60 ± 0.0	0.80 ± 0.05	82 ± 5.0	50 ± 10.0	0.71 ± 0.04	86 ± 4.0	70 ± 10.0	0.85 ± 0.05	78 ± 2.0	50 ± 10.0	0.97 ± 0.0	97 ± 0.0	100 ± 0.0	0.90 ± 0.02	96 ± 0.0
Rayon (3 h)	70 ±10.0	0.83 ± 0.0	90 ± 1.0	nd	nd	nd	nd	nd	nd	nd	nd	nd	nd	nd	nd
Rayon (6 h)	nd	nd	nd	nd	nd	nd	70 ± 10.0	0.66 ± 0.0	86 ± 1.0	nd	nd	nd	nd	nd	nd

Given the overall high recovery rates achieved for PE, PET and PS, 70% HNO_3 was deemed the preferred method for microplastic separation from coral, sponge and sea squirt tissues. PVC recovery from the biological matrices was also generally high, but the spectral similarity to reference spectra was lower across the board (SC-9), and such interactive effects must be considered when validating separation methods. While recovered rayon monofilament were still correctly assigned, physical recovery rates following HNO_3 digestions were low and resulted in underestimates of rayon contamination, similar to that reported for polyamides (PA or nylon) (Claessens et al., 2013; Pfeiffer and Fischer, 2020; Roch and Brinker, 2017).

2.3.3.2. Microplastic recovery rates from sea cucumber GIT contents using NaCl and KI

Mean recovery rates of PE and PS from spiked sea cucumber GIT contents were high using both brine solutions (≥ 80%). For PET, PVC and rayon, rates of ≥ 70% could only be achieved with the denser KI solution, Table 2.3), approximately double that using NaCl. High recovery rates of dense polymers are particularly important when assessing contamination of benthic detritus-feeding organisms, including sea cucumbers, as such polymers are abundant on the ocean floor (Cheang et al., 2018; Uddin et al., 2021; Woodall et al., 2014). The high density of KI (1.7 g cm^{-3}) increases recovery rates of denser microplastics (e.g., rayon, PET and PVC) from environmental samples, although it is still not suited to more dense polymer types such as Teflon (2.1–2.3 g cm^{-3}) (Lusher et al., 2020). Other salts such as zinc bromide (ZBr2), sodium iodide (NaI), sodium polytungstate, calcium chloride, zinc chloride (ZnCl2), and potassium formate have also been used to separate microplastics from environmental matrices (Lusher et al., 2020; Mai et al., 2018), with only ZBr2 and NaI achieving similar densities as KI. All three salt solutions can be prepared at room temperature (Kedzierski et al., 2017) (Rodrigues et al., 2020) without supersaturating the solution and precipitating salts, facilitating sample washing and reuse of solutions after appropriate filtration to remove potential contamination (e.g., at 0.45 μm). However, unlike KI, both ZBr2 and NaI are highly toxic to aquatic life (Quinn et al., 2017; Zhang et al., 2020c), undermining their safe handling and disposal after use. The spectral similarity of recovered spiked microplastics to untreated

controls and reference spectra was high for all five polymers (≥ 0.90 and ≥ 87%, respectively, Table 2.3, Appendix A – Tables S11 and S12).

Given the higher recovery rates of spiked microplastics using KI compared to NaCl, in particular, for denser polymers, KI was deemed the preferred method for microplastic separation from sea cucumber GIT content. The non-hazardous nature of KI, and the potential for KI solutions to be reused, further informed this decision.

2.4. Conclusion

A variety of separation methods, specifically designed to liberate microplastics from environmental samples, have been published (Lusher et al., 2020). These can be used to guide new studies on microplastic contamination of underreported taxa, including taxa that are critical in marine ecological processes and uniquely susceptible to microplastic uptake. However, in many instances one 'generic' separation method is chosen to process different matrices without prior validation of its use for the target taxa. Based on the presented results, it is recommended that microplastic separation methods are validated for new taxa, and their potential limitations reported to ensure reliable use of published contamination data. Here, the application of the criteria-guided workflow facilitated a systematic assessment of microplastic separation methods for coral, sponge and sea squirt tissues and sea cucumber GIT contents. Importantly, it provided accurate information on i) clarification efficiency of biological matrices, ii) physical and chemical impacts of treatments on target polymers, and iii) microplastic recovery rates from diverse tissues, thereby enabling sound and robust decision-making for microplastic processing pipelines that will provide reliable estimates of microplastic contamination in marine organisms. Following this workflow, 3, 6, and 24-hour 70% HNO_3 digestion was the preferred separation method for coral, sponge and sea squirt tissues respectively, while 24-hour KI density flotation was better suited to processing sea cucumber GIT contents. Limitations of each separation method were established for each of four taxa and five polymers examined. In particular, while rayon was chemically identifiable against reference spectra across all separation methods, accurate estimates of rayon contamination in environmental samples will be complicated by disintegration of rayon threads into multiple monofilament fibres, which have low recovery rates inherently. Other studies

have reported physical and chemical deterioration of rayon due to microplastic sample processing (Dawson et al., 2020), further highlighting the need to develop efficient and reliable methods to effectively separate and quantify these and other modified cellulose-based polymer fibres from environmental samples.

Chapter 3: Distribution and compartmentalisation of microplastic contamination in abiotic and biotic matrices of Lizard Island coral reef, Australia

Abstract

Microplastic contamination in abiotic and biotic compartments of the remote Lizard Island coral reefs was determined to (i) generate baseline information for underexplored coral reef ecosystems, and (ii) explore interactions between available microplastics in abiotic compartments and their inhabitant organisms. Microplastic abundance and characteristics (shape, size, colour, and polymer type) were analysed and compared amongst samples of seawater (surface and mid-column), seafloor sediment, and five marine organisms (planktivorous fish, ascidian, sponge, coral, and sea cucumber) feeding in these compartments, respectively. Lizard Island abiotic and biotic compartments were all contaminated with microplastics. Microplastic concentrations increased with depth, while microplastics contamination levels amongst organisms did not significantly vary. Positive relationships between environmental exposure concentration and uptake by resident organisms was observed for all tested representative species, except coral. Yet, physical and chemical characteristics of microplastics recovered from organisms did not always reflect what was present in the environment. In fish specifically, fibres were more abundant than fragments. Across the five taxa assessed, microplastics < 500 μm were most prevalent. Differences in microplastic colour and polymer type were also observed in some taxa, and the potential reasons for such results are deserving of further investigation. This study suggests microplastic contamination in marine organisms may increase with predicted marine microplastics increases, and the biological risks of microplastic uptake may be greater for some microplastics than for others, particularly in relation to a subset of shapes, sizes, colour and polymers of encountered microplastics.

Key words: marine debris, Great Barrier Reef, marine organisms, baseline, uptake, risk

3.1. Introduction

Plastics are considered one of the main marine environmental issues of global priority (UN, 2019), and microplastics (plastics 1µm to 5mm long) are of greatest concern. This suite of contaminants encompasses a complex variety of plastic particulates that are either manufactured in this size range for commercial use (i.e., primary microplastics) or result from the fragmentation of larger plastic products (i.e., secondary microplastics). Consequently, microplastics occur in various sizes, shapes, colours and chemical compositions (Rochman et al., 2019), which in the marine environment, along with environmental forces and conditions, can influence microplastic distribution (GESAMP, 2015) and bioavailability (Ajith et al., 2020; Kaiser et al., 2017).

To date, microplastics have been detected in every marine ecosystem and organism investigated, including abiotic and biotic compartments of remote locations such as the Antarctic (Cincinelli et al., 2017; Reed et al., 2018; Sfriso et al., 2020), ocean gyres (Brach et al., 2018; Goldstein and Goodwin, 2013), and the deep sea (Courtene-Jones et al., 2017; Zhang et al., 2020a). Dense plastics such as polyvinyl chloride (PVC) and polyester (PET), for example, sink and are deposited on the sea floor (Corcoran et al., 2015), potentially becoming more bioavailable to organisms that inhabit this compartment. Pelagic organisms, on the other hand, are likely exposed to less dense plastics dispersed in the water column. In addition to their presence in the environment, microplastic bioavailability depends on the susceptibility of organisms to take up these plastics, which can occur through passive (unintentional) or active ingestion – the latter in organisms reliant on visual or chemical cues that may actively choose to ingest microplastics of similar size, shape colour, or smell and taste to their natural food (Roch et al., 2020). As such, the now known ubiquitous nature of microplastics raises additional questions regarding contamination patterns across environmental compartments and their respective biotic interactions, in order to better assess microplastic ecological risks.

Relationships between microplastics in abiotic and biotic compartments are often suggested by field studies (Jensen et al., 2019) (Zhang et al., 2020a). However, validating the existence of such relationships relies on relating spatial and temporal field data to determine microplastics presence in a given compartmentalised place at a given time. Field experimental designs that accommodate concurrent abiotic and biotic sampling, therefore offer a reliable

approach by enabling direct comparisons of microplastic contamination and inference of transfer of microplastics between abiotic and biotic compartments. Although controlled laboratory experiments can assess patterns of microplastic distribution and relationships between abiotic and biotic compartments (Setala et al., 2014), these are inherently restricted by their inability to simulate *in situ* spatio-temporal environmental conditions or the highly variable fluctuations in microplastic contamination distributions and composition in these compartments.

Coral reefs are directly associated with many ecosystem services beneficial to humans including fisheries, recreation, and coastal protection (Woodhead et al., 2019), and are suitable environments for field experiments that sample both abiotic and biotic microplastics for assessment. Coral reefs are highly biodiverse ecosystems (Fisher et al., 2015) wherein many different species can co-occur within a small area, making them spatially and temporally ideal for undertaking microplastics research *in situ*. Furthermore, as coral reefs are suffering significant anthropogenic pressures (e.g., climate change and land runoff containing urban and/or agricultural contaminants) that disrupt their natural functionality (Woodhead et al., 2019), it is important to understand whether environmentally pervasive microplastic contamination constitutes another threat to coral reef biota. Although limited information is available on contamination levels and potential impacts of microplastics on reef ecosystems (Huang et al., 2021), recent studies have reported microplastics of various sizes, shapes, colours and polymers contaminating coral reef waters (Jensen et al., 2019) (Nie et al., 2019; Tan et al., 2020), sediments (Patti et al., 2020; Portz et al., 2020; Zhang et al., 2019) and biota (Kroon et al., 2018b) (La Beur et al., 2019; Rotjan et al., 2019).

In this study, the relationship between microplastic contamination in abiotic and biotic compartments was assessed at Lizard Island, a group of remote islands located within the mid-shelf of the Great Barrier Reef, where land based (industrial, urban, agricultural) runoff is not expected to be a major source of these contaminants. Currently no baseline microplastic information exists for Lizard Island, therefore, microplastic abundance and characteristics were analysed in both abiotic and biotic compartments across an environmental gradient. Specifically, samples of surface and mid-column seawater as well as seafloor sediment were collected as representatives of the abiotic compartment, and organisms inhabiting these strata at the time (pelagic: planktivorous fish; sedentary benthic: filter feeders - ascidian and sponge,

and suspension feeder - coral; and mobile benthic: deposit feeder - sea cucumber) were collected as representatives of the inhabitant biotic compartments. The studied taxa are ecologically relevant, supporting both habitat-formation and nutrient cycling on coral reefs (Knowlton, 2001; Mohsen et al., 2019). In addition, the taxa examined are vulnerable to microplastic uptake and deleterious effects thereof (Critchell and Hoogenboom, 2018; Kroon et al., 2018b; Messinetti et al., 2018; Mohsen et al., 2021; Reichert et al., 2018). Whilst previous studies have assessed field microplastic contamination of the studied taxa (Ding et al., 2019; Girard et al., 2021; Jensen et al., 2019; Mohsen et al., 2019; Vered et al., 2019) (Chapter 4), this is the first to directly relate microplastics contamination in these species with abiotic contamination within a coral reef ecosystem. Comparisons between each abiotic and respective biotic compartment was made taking into account the most likely mode of microplastics uptake by the studied organisms (e.g., selective active or non-selective passive uptake).

3.2. Methods

3.2.1. Lizard Island and sampling sites

Lizard Island (14°40′08″S 145°27′34″E) is located approximately 30 km northeast of the Australian continent, in the Northern Great Barrier Reef (Figure 3.1). This coral reef system is 250 km north of the largest city in the region (Cairns; population ~151,000) and 200 km from the nearest agricultural industry (Douglas Shire) (https://qldglobe.information.qld.gov.au/). Because of its ecological and economical importance, it is protected within a Marine National Park and Conservation Park zone, which regulates and restricts extractive and recreational uses. In recent years, microplastic contamination has been reported for coral reef fish collected from Lizard Island reefs (Kroon et al., 2018b) (Chapter 4), and beach clean-up surveys have identified substantial marine debris contaminating the island's coastline (http://amdi.tangaroablue.org/), a high proportion (> 70 %) of which is plastic remnants.

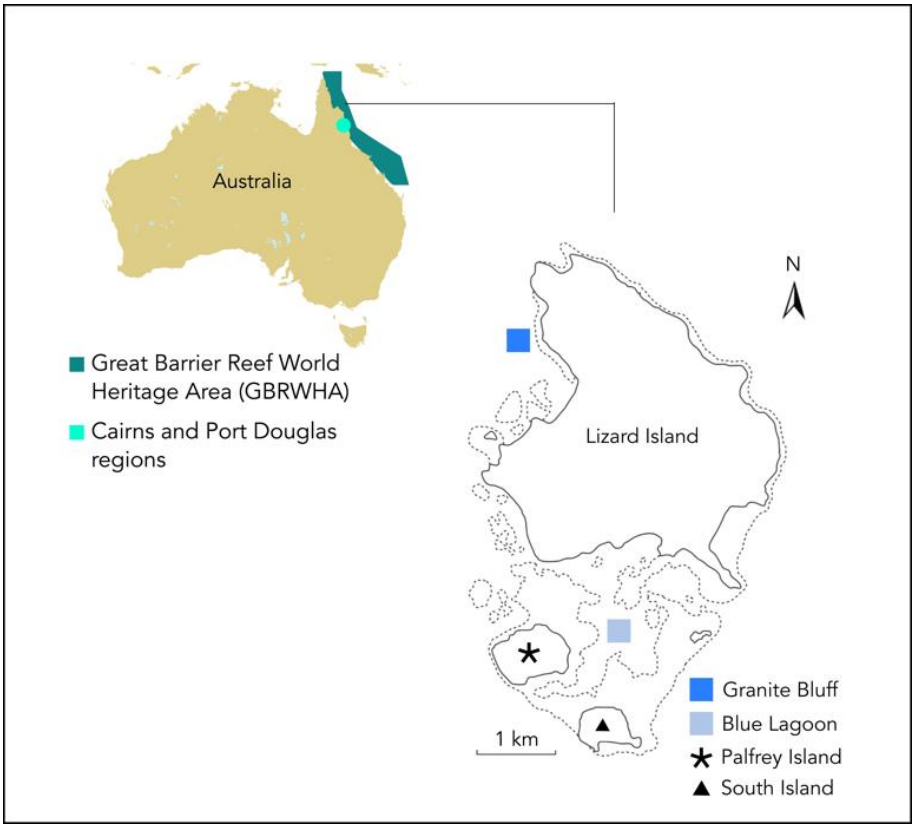

Figure 3.1: Location of Lizard Island, in the Northern Great Barrier Reef (Australia); closest urban centre and agricultural industry; and sampling sites (Granite Bluff and Blue Lagoon).

The Lizard Island group consists of three islands: Lizard, Palfrey and South Islands. Narrow fringing reefs surround most of the main island, while between Palfrey and South Islands the reef forms an enclosed lagoon (~90 m wide and ~10 m deep, with a 3 m tidal range and fast flowing currents (Hamylton et al., 2014)). The hydrodynamics around the Lizard Island group are strongly influenced by wind (Frith et al., 1986), which occurs predominantly from the southeast (referred to as the Southeast Trade wind) during March to September. This trade wind reaches speeds of up to 30 $m.s^{-1}$ (Hamylton et al., 2014) and circulates to the northwest (Frith et al., 1986). From October to February the wind direction is unpredictable, as are circulation patterns, which present more frequent current reversals and cross-shelf motion (Frith et al., 1986). Northwest winds are the second most common Lizard Island wind feature, with maximum speeds of 20 $m.s^{-1}$ (Hamylton et al., 2014). Lizard Island is also susceptible to cyclones during summer months, which increases wind speed and may disrupt shallow coral reefs (Lassig, 1983).

3.2.2. Sample collection

Sample collection was conducted at Lizard Island from 1st to 12th October 2018, including abiotic (surface seawater, mid-column seawater, and seafloor sediment) and biotic (planktivorous fish, hard coral, sponge, sea squirt and sea cucumber) samples. All collections were conducted in accordance with ethics permit A2506 (James Cook University) and national regulation (Great Barrier Reef Marine Park Authority permit G12/35236.1). Samples were obtained from two different coral reefs: Granite Bluff and Blue Lagoon (Figure 3.1). Five replicates of each abiotic sample were collected per site (total N = 30). For each biotic sample, ten individuals were collected per taxon per site (total N = 100) to enable method validation for these taxa which are not well represented in the microplastic literature. Collections were conducted using neuston tows (surface seawater), a submersed pump sampler (mid-column seawater) and SCUBA (seafloor sediment and organisms). Species sampled were *Pomacentrus amboinensis* (fish – pelagic planktivore), *Holothuria edulis* (sea cucumber – mobile benthic deposit feeder), *Polycarpa pigmentata* (sedentary benthic sea squirt – filter feeder), *Dipsastraea lizardensis* (sedentary benthic hard coral – suspension feeder) and *Neopetrosia chaliniformis* (sedentary benthic sponge – filter feeder). Relevant Lizard Island environmental information (e.g., weather and sea conditions) at the time of field sampling was obtained from the Australian Bureau of Meteorology (BOM; http://www.bom.gov.au/) and the Australian Institute of Marine Science (AIMS; https://www.aims.gov.au/docs/research/monitoring/weather/weather.html) weather stations. Observations of wind (speed and direction), swell and depth were also documented for each site during seawater sampling.

3.2.2.1.Seawater

Surface tows (10 min) and mid-column pumping (20 min) were conducted at both sites in waters immediately adjacent to the coral reefs to avoid reef disturbance. Following Kroon et al. (2018a), surface tows were conducted at boat speeds < 4 knots, with a 355 µm plankton net (254 cm length) attached to a neuston frame (74.5 diameter x 30.0 cm height) positioned on the port side of the boat such that the net was half immersed in the water. GPS coordinates

(Garmin GPS76) were recorded to establish the tow distance from which the volume of seawater filtered was calculated. After each tow, captured material was rinsed into a 750 mL cod end which was sealed with a lid and stored in a nally bin for transport to Lizard Island Research Station (LIRS).

Mid-column seawater sampling was conducted using a custom-built submersible pump sampler. The pump sampling protocol was adapted from previous environmental studies (Lusher et al., 2014, Setäla et al, 2016, Bannick et al, 2019) for application at various depths. Briefly, the pumping device consisted of a battery driven impeller pump (MEI standard 2.2 kW motor, 3phase @ 400 V) connected to a hose (PVC, 18 mm internal diameter x 7 m length), through which seawater was pumped at a flowrate of 45 L min^{-1}. Diving weights (4 kg total) were attached to ensure the pump and hose remained vertical at each sampling depth. Prior to each sampling event, the pump was operated *in situ* for 2 min to flush the device and avoid cross contamination between samples (i.e., seawater was not sampled at this time). Mid-column sampling was conducted at five different depths per sampling site, with seawater pumped into stacked 263 and 37 µm mesh sieves. After each sampling event, the pair of stacked mesh sieves was fully covered with aluminium foil and stored upright in nally bins for transport to LIRS. As mesh sieves on the deck are exposed to potential airborne contamination while conducting the mid-column seawater sampling, Milli-Q blanks were placed adjacent to sampling sieves and covered contemporaneously with sampling sieves (see item 2.5 for more information).

3.2.2.2.Sediment

Sediment samples were collected on SCUBA, using 0.5 m^2 PVC quadrats from five different locations on both Granite Bluff and Blue Lagoon reefs, respectively. Quadrats were placed on relatively flat areas of the seafloor (i.e., absence of sand banks or ripples) in the vicinity of sea cucumber sightings. The top 3 cm of sediment was carefully scraped, using a stainless-steel trowel and placed into a 15 L polyethylene (PE) plastic bag laid flat against the quadrat edge, with the bag opening folded shut. With each trowel load of sediment collected the bag was lifted upright and sediment was allowed to settle for ~1 min. The bag was gently squeezed to push out excess water and the opening sealed with a knot and rubber band. Once

sediment had been collected for any given quadrat, samples were transferred to nally bins on the boat for transport to LIRS.

3.2.2.3.Organisms

All sampled organisms were collected from different locations along the Granite Bluff and Blue Lagoon reefs using SCUBA. Fish were exposed to diluted natural clove oil (1:3:3 parts clove oil:ethanol:seawater), corralled into a fencing net then captured by hand net (Kroon, 2015). Individual fish were subsequently placed into PE ziplock bags, whereafter they were immediately and humanely euthanized by adding a lethal overdose of clove oil (100% clove oil and > 80% ethanol (EtOH) in a final ratio of 1:3.5) to the bag. Fragments of coral and sponge colonies, and whole sea squirt individuals were collected using hammer and chisel. Sea cucumbers were collected by hand. Each invertebrate sample was immediately placed in its own PE ziplock bag, sealed and transferred to the boat for euthanasia on ice. Storage in individual bags prevented microplastic cross-contamination between samples and preserved any faeces or regurgitated material for subsequent microplastic analysis if and when these events occurred. All sampled organisms were stored on ice in a cool box and transported to LIRS where they were immediately pre-processed and preserved.

3.2.3. Sample processing

At LIRS, surface tow samples were filtered into stacked 263 and 37 µm mesh sieves, the retained items transferred to 50 mL jars (polypropylene (PP) cup, high density polyethylene (HDPE) screw cap; Sarstedt) and preserved in 70% EtOH (to a final volume of 50 mL) for processing and analysis at the Australian Institute of Marine Science (AIMS) in Townsville (Kroon et al., 2018a). Similarly, contents of mid-column samples retained on stacked 263 and 37 µm mesh sieves (i.e., already concentrated during field collection) were also transferred into 50 mL jars. Sediment samples were frozen at -20˚C for transportation and processing at AIMS. Organisms were measured (standard and fork length, 0.1 cm, Kincrome, 1/1000 in), weighed (0.01 g, AND EK-410i) and the gastrointestinal tracts (GIT) of fish and sea cucumbers and the tunic and pharynx of sea squirts were respectively removed by dissection. GIT contents and

sea squirt innards were transferred to 50 mL PP jars sealed with HDPE lids. Whole coral and sponge samples were transferred into 600 mL PP jars. All biological material was preserved in 70% EtOH for transport and storage prior to processing and analysis at AIMS laboratories.

3.2.3.1.Seawater

Surface seawater samples were processed using a density separation method adapted from (Kroon et al., 2018a). Briefly, samples were transferred to 400 mL glass beakers and topped up with 300 mL of 1.2 g cm^{-3} sodium chloride (NaCl; AR, Fisher Chemical, CAS No. 7647-14-5) brine solution, manually stirred for 3 min using a glass stirring rod and subsequently left overnight (~18 hr) to settle. Approximately 100 mL of the surface supernatant was then decanted into a second glass beaker and an additional 100 mL NaCl brine solution added to the remaining 200 mL of sample. The sample was again stirred for 3 min, left to settle for 1 hr, and a second 100 mL of surface supernatant syphoned into the aforementioned 2nd glass beaker. This process was repeated once more. The combined decanted supernatant (total ~ 3 x 100 mL) was filtered through a customized filtration apparatus consisting of tiered 263 and 26 µm stainless steel filters (Schlawinsky, 2020). A similar protocol was used to process mid-column seawater samples, but instead using 1.7 g cm^{-3} potassium iodide (KI; AR, Univar, CAS No. 7681-11-0), based on the assumption that denser microplastics would likely be present in this abiotic compartment (Cheang et al., 2018; Uddin et al., 2021; Woodall et al., 2014)). In addition, supernatant of mid-column seawater samples was syphoned into the second beaker using a silicone tube rather than decanted to avoid disturbing settled material.

3.2.3.2.Sediment

Frozen sediment samples were freeze-dried (~2 days) and processed using 1.7 g cm^{-3} KI density separation as per mid-column seawater samples. An additional 547 µm stainless-steel filter was added to the top of the z-stacked filtration apparatus to capture larger items, e.g. shell fragments, fine sand particles and organic matter.

3.2.3.3.Organisms

Each fish GIT was cut open using dissecting scissors and gut content scraped into a Bogorov counting chamber for exhaustive visual inspection under stereomicroscope (Leica M165C, 0.73x - 12.0x magnification) (Kroon et al., 2018b). Putative microplastics identified in each fish GIT were picked from the chamber using a glass pipette and transferred to 26 µm stainless steel filters for further physical and chemical characterization. Each fish GIT wall was inspected in a petri dish containing Milli-Q water. All invertebrates were processed following Chapter 2 with some slight modification. Briefly, corals were digested using 70% nitric acid (HNO_3; AR, Univar, CAS No. 7697-37-2) for 6 hours. Sponges were digested using a step-wise protocol, in which samples were first digested using 70% HNO_3 for 6 hours and residual material density separated using an overnight 1.7 g cm^{-3} KI procedure. Sea squirt innards were digested using 70% HNO_3 for 24 hours. Lastly, each dissected sea cucumber GIT was excised and gut content removed and processed using 1.7g cm^{-3} KI. All clarified invertebrate samples were subsequently filtered through the filtration apparatus onto stainless steel filters, as described above (2.3.1 Seawater).

3.2.4. Microplastic identification and characterization

Microplastic identification, based on physical and chemical characterization, was done following Kroon et al. (2018a) with some modifications. First, all putative microplastics were visually identified using stereomicroscopy (Leica MZ16A) and microphotographed (Leica DFC 500, Leica Application Suite LAS 4.4.0). All putative microplastics were then characterized based on size, shape, and colour (Hidalgo-Ruz et al., 2012; Norén, 2007, Chapter 2). Size (maximum length) was acquired using Fiji (Image J software), and items were grouped into one of five size classes (class 1: < 500 µm, class 2: ≥ 500 µm and < 1mm, class 3: ≥ 1 and < 2.5 mm, class 4: ≥ 2.5 and < 5 mm, class 5: ≥ 5 mm). Class 5 was included to capture plastics larger than the micro scale). Shape and colour of all examined items were categorized based on Chapter 2. Polymer composition of every putative microplastic was chemically confirmed by Fourier-transform infrared spectroscopy (FTIR). Only putative microplastics not found in the filter after microscopy analysis were not chemically analysed (refer to results for

information on total number of putative microplastics, as well as number of items analysed and not analysed by FTIR). FTIR spectra were obtained using either PerkinElmer Spectrum 100 FTIR [1 mm ATR window, pressure gauge = 150, 16 scans at 4 cm^{-1} resolution, wavenumber range 4000 - 600 cm^{-1}, atmospheric (CO_2/H_2O) suppression, atmospheric vapor compensation, and background scans acquired every 10 acquired spectra] or PerkinElmer Spotlight 200i FTIR microscope [100 µm ATR aperture, pressure gauge = 5%, 32 scans at 4 cm^{-1} resolution, wavenumber range 4000 - 600 cm^{-1}, atmospheric (CO_2/H_2O) suppression, atmospheric vapor compensation, and background scans acquired for every spectrum], affording 10 µm size limit of detection. Spectra were processed using PerkinElmer Data Tune-up and searched against NICDOCOM IR spectral libraries (Polymers and Additives, Coatings, Fibers, Dyes and Pigments, Petrochemicals; NICODOM Ltd., Czechia, excluding CO_2 and H_2O ranges) for final chemical assignment, as per Kroon et al. (2018a). All items were categorized as either (i) synthetic or semi-synthetic items (i.e., items manufactured by chemical synthesis, e.g., plastics, or synthetically modified from natural materials, e.g., rayon, cellophane), (ii) naturally derived (i.e., items manufactured from natural materials, e.g., cotton), and (iii) natural (i.e., not manufactured). Items categorized as synthetic and semi-synthetic were deemed microplastics and grouped based on their primary assignment obtained by FTIR and following Kroon et al. (2018a). Semi-synthetic items comprising natural fibres and plastic polymers were grouped based on their synthetic composition (e.g., mixture of rayon and polyester was assigned into the polyester group). Synthetic items made of more than one synthetic polymer were grouped based on their main synthetic compound when possible (e.g., mixture of 30% polypropylene and 70% polyester was assigned into the polyester group; and polyvinylchloride, polyvinyl alcohol and polyvinyl benzyl chloride were assigned into the polyvinyl-based polymer group).

3.2.5. Quality assurance and quality control (QA/QC)

3.2.5.1. Recovery Rates

All separation methods described above were validated using spike-recovery tests prior to final use in the study. Spike-recovery tests consisted of three replicates of each seawater, sediment (~ 3 g, d.w.) and organism (~ 3 g of tissue, d.w.) samples that were spiked by adding 15 microplastic particles, including irregular particles (< 1.0 mm) of yellow PE (N = 5);

transparent polystyrene (PS, N = 5), and monofilament fibres (approx. 2 mm) of black rayon (N = 5). Spiked samples were then processed as described for field samples and recovered spiked microplastics were visually identified and counted using a stereomicroscope (Leica MZ16A).

3.2.5.2. Microplastic contamination control

Prevention and monitoring of extraneous microplastic contamination followed protocols described in Kroon et al. (2018a) and Chapter 4. The unavoidable use of plastic-based utensils during sample collection and processing was recognised, and a representative sample of each was collected and added into a project-specific plastic contaminant library (Appendix B – Table S1) (Kroon et al., 2018a). Airborne contamination was monitored and also added in the contaminant library. Airborne contamination was monitored using Milli-Q blanks for those collection and processing steps where samples were exposed to air. Thus, during field collection, Milli-Q blanks were collected concurrently with mid-column seawater sampling only as this was the only sampling technique during which midwater samples were exposed to air. Laboratory procedures from all sample types included Milli-Q blanks, i.e., sample pre-processing at LIRS, and sample processing (including during dissections, Bogorov sorting, sample clarification and filtration) at AIMS. Milli-Q blanks were treated as samples were and exposed to air whenever samples were also exposed to air. These blanks were then filtered onto 26 µm stainless steel filters for verification under microscopy and FTIR. To establish and correct for unintentional contamination, all microplastics found in samples were compared with those in the contaminant library (Kroon et al., 2018a). Specifically, if the spectral match to an item in the spectral library was ≥ 90%, and both shape and colour also matched, the microplastic in the sample was considered to be a result of extraneous contamination and was excluded from further analysis. Measures to reduce the likelihood of extraneous microplastic contamination were applied during all lab-based processing conducted, including wearing cotton clothes and delinting lab coats prior to sample handling. Furthermore, equipment, tools and working area were cleaned prior to use as per Chapter 4. For sample processing, both NaCl and KI brine solutions were filtered to 0.45 µm (Millipore® HA filters); 70% HNO_3 was not filtered for safety reasons. Instead, to assess HNO_3 as a potential source of extraneous

microplastic contamination, 15 mL of the acid was neutralized using 0.45 µm pre-filtered 10% potassium hydroxide (KOH) solution and filtered onto 26 µm stainless steel filters for verification under microscopy and, if necessary, FTIR. No microplastics were found in HNO_3 samples neutralized in this manner. Density separations and acid digestions were conducted in a fume hood.

3.2.6. Data analysis of field collected samples

All statistical data analysis was conducted using RStudio, version 1.2.5042. Best fitted models were chosen using an Akaike Information Criterion (AIC) test and DHARMa residual diagnostics. Differences in microplastic concentration within abiotic (microplastics m^{-3}) or biotic (microplastics g^{-1} of tissue processed) (equation 1) compartments and the influence of sampling site were investigated by general linear models (GLM, $p < 0.05$). To account for skew and overdispersion of data, models were fitted using Poisson distribution for the logarithmic transformation of the abiotic compartment, while a negative binomial distribution was used for the biotic compartment.

$$\text{concentration of microplastics} = \text{matrix} + \text{sampling site} + \text{constant} \quad \text{(Eq. 1)}$$

where,

matrix = surface seawater, mid-column seawater and sediment (i.e., abiotic compartment); or fish, sea squirt, sponge, coral and sea cucumber (i.e., biotic compartment) analyses, sampling site = Granite Bluff or Blue Lagoon.

To compare the level of microplastic contamination between abiotic and biotic compartments based on shape (fragments vs fibres), size (size-class 1 to 5), colour and polymer, Chi-squared ($p < 0.05$) and Fisher's Exact tests ($p < 0.05$) were performed. Microplastic contamination in fish, corals, sea squirts and sponges were compared to levels found in the mid-column seawater, while that in sea cucumbers was compared to contamination found in the sediment.

3.3. Results

3.3.1. General environmental conditions during field sampling

Maximum temperatures throughout the field collection varied from 29.2 to 31.1˚C. No rain events occurred during this sampling period. Wind speed at the Granite Bluff and Blue Lagoon sampling sites varied from 0 to 20 knots and 0 to 5 knots, respectively. Wind direction was predominantly south-easterly and swell at both sites varied little, from 0 to 0.5 m. Detailed environmental conditions corresponding to specific sample collection times are reported in Table S2 (Appendix B). GPS coordinates for surface and mid-column seawater sampling sites are reported in Table S3 (Appendix B).

3.3.2. QA/QC

3.3.2.1.Spiked microplastic recovery rates

Overall, recovery rates of > 70% were achieved for spiked microplastics across all matrices and sample processing activities with the exception of rayon fibres recovered from sponges, which was slightly lower at 66.67 ± 9.43 % (mean ± standard deviation [SE]). Complete recovery was achieved for spiked PE recovered from all matrices except sponges, and for rayon monofilament fibres recovered from sea cucumber GIT contents treated with 1.7 g cm^{-3} KI. Recovery rates of spiked PS varied between 80.00 ± 16.33 % (sea cucumber GIT contents) and 93.33 ± 9.43% (for surface seawater, mid-column seawater and sponge samples). Recovery rates of spiked microplastics from each sample matrix and respective separation method are reported in Table S4 (Appendix B).

3.3.2.2.Microplastic presence and abundance in abiotic and biotic samples

This study isolated a total of 2,137 putative microplastics from samples. Of these, 318 were excluded from final analysis, either because the chemical composition could not be confirmed (i.e., poor quality of acquired FTIR spectra, N = 100), or because an item matched physically and chemically with an item from the contaminant library (N = 221). Another 1,115 items were

further excluded based on being assigned to either a natural item or a naturally-derived polymer (e.g., cotton). The remaining 701 (32.8%) putative microplastics were confirmed to be synthetic (N = 535) and semi-synthetic (N = 169) polymers. Total numbers of putative microplastics, excluded items, and final plastic counts per matrix are reported in Table S5 (Appendix B). Items categorized as synthetic and semi-synthetic were deemed microplastics and grouped as per Table S6 (Appendix B).

3.3.3. Microplastic contamination of coral reefs

3.3.3.1. Presence and abundance in abiotic and biotic compartments

Microplastics were found in all abiotic compartments sampled from Granite Bluff and Blue Lagoon. Combining results from both sampling sites, mean concentration (± SD) of microplastics (expressed as microplastics m^{-3} $matrix^{-1}$) varied one thousand-fold, with 0.15 ± 0.12 microplastics m^{-3} in surface seawater, 39.78 ± 12.85 microplastics m^{-3} in mid-column seawater, and 909.91 ± 463.67 microplastics m^{-3} in seafloor sediment. Microplastic concentrations differed significantly amongst abiotic compartments ($p < 0.05$, Figure 3.2a, Appendix B –Table S7a). Per sampling site, microplastic concentrations were significantly greater in the Granite Bluff water and sediment than these same matrices in the Blue Lagoon ($p < 0.05$, Appendix B –Table S7b), with the exception of the coral community, where this was apparently inverted. Mean microplastic concentration per sampling site and matrix is detailed in Table 3.1.

Microplastic concentrations did not differ significantly amongst the four taxa ($p > 0.05$, Figure 3.2b, Appendix B – Table S7b). Considering both sampling sites together, mean concentration of microplastics per taxon was 1.49 ± 1.70 microplastics g^{-1} fish GIT, 1.04 ± 1.37 microplastics g^{-1} sea squirt, 0.18 ± 0.15 microplastics g^{-1} sponge, 0.09 ± 0.08 microplastics g^{-1} coral, and 0.02 ± 0.01 microplastics g^{-1} sea cucumber GIT. However, microplastic contamination was not present in every biotic replicate, except for fish where the number of items found per fish GIT ranged from 1 to 14. In contrast, for all taxa, microplastic concentrations were significantly greater in specimens collected from Granite Bluff compared to those from Blue Lagoon ($p < 0.05$, Appendix B – Table S7b), trend that seems to be driven

by fish and sea quirt, although not indicated by the statistical analysis. Mean microplastic concentration per sampling site and taxon is detailed in Table 3.1.

Table 3.1: Mean concentration (± standard deviation; SD) of microplastics per abiotic (microplastic m^{-3}) and biotic compartment (microplastic g^{-1}) from Granite Bluff and Blue Lagoon sampling sites (n = 5 replicates per sampling site). Concentration reported as number of microplastics m^{-3} (surface seawater, mid-column seawater, sediment) and number of microplastics g^{-1} of animal tissue processed (fish GIT, sea squirt innards, whole sponge, whole coral, and sea cucumber GIT).

	Abiotic			Biotic				
Sampling site	Surface seawater	Mid-column seawater	Sediment	Fish	Sea squirt	Sponge	Coral	Sea cucumber GIT contents
Granite Bluff	0.23 ± 0.12	43.56 ± 15.06	1127.77 ± 439.48	2.31 ± 2	1.68 ± 0.40	0.26 ± 0.10	0.04 ± 0.04	0.02 ± 0.02
Blue Lagoon	0.06 ± 0.01	36 ± 8.65	692.04 ± 376.70	0.67 ± 0.63	0.01 ± 0.01	0.14 ± 0.08	1.55 ± 0.73	0.01 ± 0.01

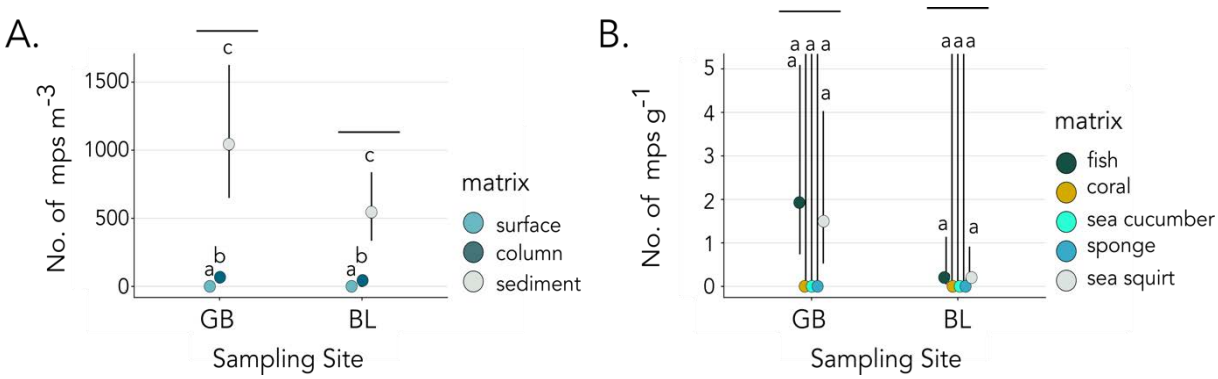

Figure 3.2: Microplastic counts m^{-3} (A) of abiotic surface, mid-column and sediment compartments; and microplastic counts g^{-1} (B) in fish, sea squirt, coral, sponge, and sea cucumber. Colour key insets for panel A compartmental sample representation and for panel B organismal sample representation. Horizontal axis represents the two sampling sites: Granite Bluff and Blue Lagoon. Symbols and vertical lines represent estimated marginal means and 95% confidence intervals. Letters (a, b, c) represent significant differences ($p < 0.05$) within the abiotic (A) and biotic (B) compartments for each sampling site. Horizontal bars represent differences ($p < 0.05$) between the two Lizard Island sampling sites examined for each compartment analysed.

3.3.3.2.Physical and chemical characteristics in the abiotic compartment

The abiotic compartments of Lizard Island presented a similar ratio of microplastic fibres to fragments (N = 270 and 298, respectively). Most microplastics were < 500 µm in maximum length (size class 1, N = 205), followed by those between 1.0 and 2.5 mm (size class 3, N = 141). The other sizes classes, including those considered to be macroplastics (> 5 mm), were present in similar but lesser numbers (size class 2, N = 74; size class 4, N = 72; size class 5, N = 73). Blue (n = 202) and transparent (n = 104) microplastics were the most common colours found, followed by white (N = 50), pink (N = 45) and red (N = 41), with other colours (e.g., brown, green and orange) being less common. PP (N = 154) and PET (N = 113) were the most common polymers detected, followed by rayon (N = 83), polyacrylate (N = 48) and PE (N = 46). Other polymers such as polyvinyl, polysiloxane, nylon and PS were observed, but in much lesser numbers. Total number of microplastics sampled per compartment (surface seawater, mid-column seawater and sediment) and shape, size, colour and polymer characteristics is presented in Table S8 (Appendix B).

3.3.3.2.1. Surface seawater compartment

Surface seawater samples contained more fragments (79%) than fibres (21%) (Appendix B – Table S8, Figure S1). Microplastic size varied from 72.3 µm to 11.2 mm, with size classes 1 (40%) and 3 (32%) most abundant, followed by size classes 2 (14%), 4 (11%), and 5 (3%). The most abundant microplastic colours were blue (27%) and pink (25%), followed by white (19%), transparent (12%), black (8%). Other microplastics colours such as green, grey and yellow collectively represented less than 10%. The most abundant microplastics polymer types were PP (40%) and PE (25%), followed by polyacrylate (14%), PET (9%), and rayon (6%). Other microplastics polymer types, such as polyvinyl and nylon were rare and made up a combined 6 % of the total.

3.3.3.2.2. Mid-column seawater compartment

Mid-column seawater samples contained similar numbers of microplastic fragments and fibres (47 and 53%, respectively) (Appendix B – Table S8, Figure S1). Microplastic size varied

from 10.5 µm to 13.3mm, with the majority in the smallest size class 1 (56%), followed by those in classes 2 (22%), 3 (17%), 4 (3%), and 5 (< 1%). 1.4% of microplastics (5 fibres) could not be measured for being tangled. Blue (39%) and transparent (20%) microplastics were the most abundant colours, followed by black (10%), red (8%) and white (6%), with other colours combined representing less than 20%. PP (26%), PET (22%), and rayon (17%) polymers were the most abundant polymer types, followed by polyacrylate (7%) and polyvinyl (6%), with others such as nylon, PE and PS making up a combined 22%.

3.3.3.2.3. Sediment compartment

Sediment samples contained more fibres (72%) than fragments (28%) (Appendix B – Table S8, Figure S1). Microplastic size varied from 33.0 µm to 2.9 mm and, as for the other two abiotic compartments, the smallest microplastic size class 1 was most abundant (47%), with microplastic numbers decreasing as item size increased, i.e., 2 (30%), 3 (20%) and 4 (3%), respectively. Size class 5 microplastics were not present in sediments. Blue (35%) and transparent (23%) microplastics were the most abundant colour, followed by red (13%) and green (9%), with other colours making up only 20%. PET (32%) and rayon (18%) polymers were the most abundant polymer types, followed by nylon (9%), acrylonitrile (7%), acrylate (6%) and PP (6%), with others such as polyvinyl, epoxy and PE making up a combined 22%.

3.3.3.3. Physical and chemical characteristics in the biotic compartment and comparison of microplastic distribution with the abiotic compartment

In the Lizard Island biotic compartment microplastics fibres (n=77) were moderately higher in number than fragments (n=59). An inverse relationship between microplastic size and number was observed. The majority of microplastics measured < 500 µm in maximum length (size class 1, N = 71), followed by microplastics between 500 µm and 1.0 mm (size class 2, N = 19), and between 1.0 and 2.5 mm (size class 3, N = 30). Plastic items >2.5 mm, including those in the macroplastic category, were still present but in much lower numbers (size class 4, N = 2, and size class 5, N = 4). Transparent (N = 55), blue (N = 23) and white (N = 23) microplastics were the most common colours found, followed by black (N = 16) and red (N = 8). The most common microplastic types were PP (N = 154) and PET polymers (N = 46),

followed by rayon (N = 24), PP (N = 15), polyacrylate (N = 11), and polyglycol (N = 10). Other polymers such as polyvinyl, polysiloxane, nylon and PS were also observed but in lesser numbers. Total number of microplastics sampled per compartment (surface seawater, mid-column seawater and sediment) and shape, size, colour and polymer characteristics is presented in Table S8 (Appendix B). Detailed characterization of microplastic contamination per taxon, including influence of the abiotic compartment (sampling site) is provided below.

3.3.3.3.1. Fish

Fish GITs contained more fibres (72%) than fragments (28%) (Appendix B – Table S8, Figure S2). Only microplastics in the smaller size classes 1 (42%), 2 (26%) and 3 (32%) were present. Minimum and maximum microplastic sizes were 33.6 µm and 1.7 mm, respectively. Transparent (44%) and blue (28%) microplastics were the most abundant colour, followed by black (7%), red (7%), orange (5%), yellow (5%), pink (2%) and white (2%). PET polymer (63%) was the most abundant polymer type, followed by rayon (14%) and PP (7%), with others such as PS and polysiloxane making up a combined 12%. Microplastics recovered from fish GITs differed from those found in the seawater column according to shape (X-squared = 5.614, $p < 0.05$) and polymer type (Fisher's $p < 0.001$) distribution, while microplastic sizes and colours were similarly distributed between these two compartments (Fisher's $p > 0.05$) (Figure 3.3a).

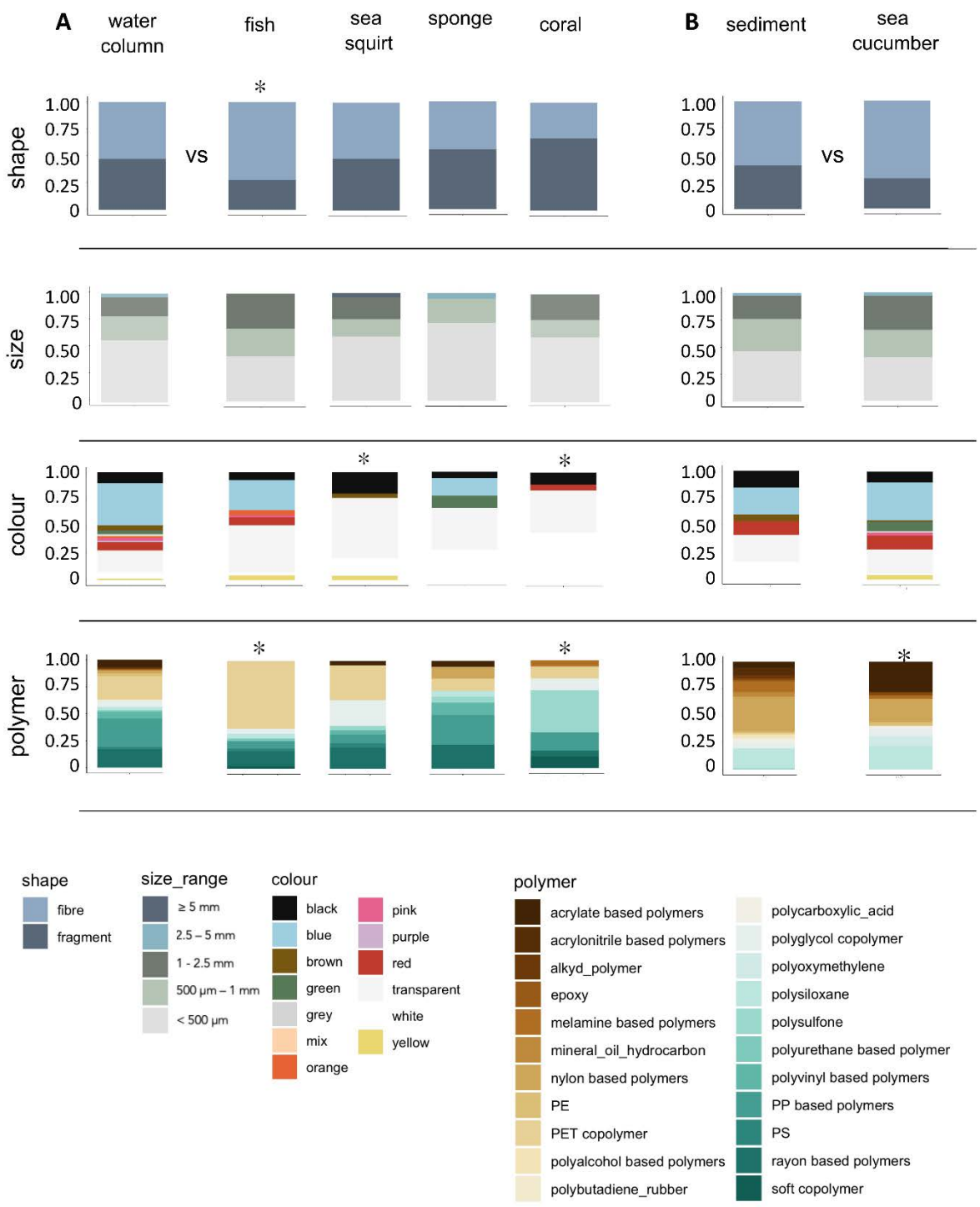

Figure 3.3: Relative number of microplastics found in abiotic (seawater column (A) and sediment (B)) and biotic (fish gastrointestinal tract (GIT), sea squirt, sponge, coral and sea cucumber GIT) compartments from Lizard Island coral reefs. Each row represents the distribution of a microplastic characteristic (shape, size, colour and polymer) within each abiotic compartment and associated taxa. *

Represents significant differences in microplastic physical and/or chemical characteristic between abiotic and biotic compartments ($p < 0.05$, Chi-square or Fisher test).

3.3.3.3.2. Sea squirt

Sea squirt GIT samples contained similar numbers of microplastic fragments and fibres (48 and 52%, respectively) (Appendix B – Table S8, Figure S2). Microplastic size varied from 73.6 µm to 1.5 mm, with most from size class 1 (60%), followed by size classes 2 and 3 with similar numbers (16% and 24%, respectively). Microplastics in size classes 4 and 5 were absent. Transparent (56%) microplastics were the most abundant colour, followed by black (20%) and white (16%), brown and yellow (4% each), while only one blue item was found. PET polymer (32%) was the most abundant polymer type, followed by polyglycol (24%), rayon (20%) and PP (8%), with others such as PS and polyvinyl contributing a combined 16%. Microplastics recovered from sea squirt GITs differed from those obtained from the seawater column in relation to microplastic colour (Fisher's $p < 0.001$), unlike microplastic shape (X-squared = 0.010793, $p > 0.05$), size (Fisher's $p > 0.05$) and polymer type (Fisher's $p > 0.05$) which were comparable between their GITs and the seawater column (Figure 3.3a).

3.3.3.3.3. Sponge

Sponge samples contained similar numbers of microplastic fragments and fibres (56 and 44%, respectively) (Appendix B – Table S8, Figure S2). Microplastics in size class 1 (72%) were highly abundant. Size classes 2 (22%) and 4 (6%) comprised the remaining microplastics, with none found in size classes 3 and 5. Minimum and maximum microplastic sizes were 20.0 µm and 3.7 mm, respectively. Transparent microplastics (39%) were the most abundant colour, followed by white (28%), blue (17%), green (11%) and black (6%). PP (28%), rayon (22%), PET (11%), polyvinyl (11%), and nylon (11%) polymers were the most abundant polymer types, with others such as acrylate and polysiloxane contributing a combined 17%. Microplastics recovered from sponges were similar to that of the seawater column in relation to all characteristics, including shape (X-squared = 0.5118, $p > 0.05$), size (Fisher's $p > 0.05$), colour (Fisher's $p > 0.05$) and polymer (Fisher's $p > 0.05$) (Figure 3.3a).

3.3.3.3.4. Coral

Coral samples contained more microplastic fragments (67%) than fibres (33%) (Appendix B – Table S8, Figure S2). Microplastic size varied from 139.5 µm to 2.7 mm and, as for the other sessile benthic taxa, microplastics in size class 1 (< 500 µm, 72%) were most abundant, with size classes 2 (11%), 3 (11%) and 4 (6%) representing the remaining items. Microplastics in size class 5 were absent. White (44%) and transparent (39%) microplastics were the most abundant colours, followed by black (11%), and red (6%). Polysulfone polymers (39%) were the most abundant polymer type, followed by PP (17%), PET (11%), rayon (11%), and polyglycol (11%) polymers, with polytetrafluoroethylene (PTFE) and melamine contributing a combined 11%. Microplastics recovered from corals differed from those recovered from the seawater column in relation to colour (Fisher's $p < 0.001$) and polymer type (Fisher's $p < 0.001$), but not shape (X-squared = 2.6759, $p > 0.05$) or size (Fisher's $p > 0.05$) (Figure 3.3a).

3.3.3.3.5. Sea cucumber

Sea cucumber GIT contents contained more microplastic fibres (60%) than fragments (40%) (Appendix B – Table S8, Figure S2). As for the other taxa microplastics in size class 1 (41%) were most abundant. Those in size classes 2 and 3 were present in similar numbers (25% and 31%, respectively), with 3% belonging to size class 4. Microplastics in size class 5 were absent. Minimum and maximum microplastic sizes were 149.2 µm and 4.9 mm, respectively. Transparent (25%) and blue (25%) microplastics were the most abundant colours, followed by white (16%), black (16%), red (12%) and brown (6%). Polyacrylate (28%), PET (22%) and rayon (22%) polymers were the most abundant polymer types recovered, followed by PS (9%) and PP (6%), with others such as nylon and polyvinyl contributing a combined 13%. Microplastics recovered from sea cucumber GIT contents differed from those recovered from the sediment with respect to polymer type (Fisher's $p < 0.05$), but not polymer shape (X-squared = 1.5718, $p > 0.05$), size (Fisher's $p > 0.05$) or colour (Fisher's $p > 0.05$) (Figure 3.3b).

3.4. Discussion

3.4.1. Presence and abundance of marine microplastics in abiotic and biotic compartments

Microplastic contamination was prevalent at Lizard Island, with 88% of all compartments (abiotic and biotic) containing microplastics despite the remote location of this coral reef. Sea surface, mid-column and sediment samples collected from both Granite Bluff and Blue Lagoon reefs all contained microplastics. Similarly, microplastics contamination was revealed in at least 70% of individuals of each species examined, except for fishes, which exhibited microplastics contamination in every individual sampled. These findings in a remote and relatively pristine environment not only highlight the ubiquitous nature of microplastics contamination but also the current lack of robust and broad scale baseline data for such environments (Tan et al., 2020). Similar observations have been reported in other studies conducted in remote areas, including coral reef ecosystems (Huang et al., 2021). For mid-shelf reefs in the central GBR, a recent biophysical modelling study reported that most of the microplastic contamination found was unlikely to have originated from continental sources (Jensen et al., 2019). Whether this holds true for Lizard Island remains to be determined. The highly dynamic oceanographic features associated with GBR coral reef ecosystems (Monismith, 2007; Taebi et al., 2011), including Lizard Island, likely contribute to microplastic dispersion and highlights the need for further investigation.

At Lizard Island, microplastic contamination in surface seawater was within the range reported for other coral reefs (Huang et al., 2021), but lower than concentrations reported for the central GBR (Jensen et al., 2019) and higher than for the remote Nansha Islands atoll reefs (Tan et al., 2020). To date, only one other study has assessed microplastic contamination in the mid-column waters of coral reefs (Xisha Islands coral reefs) (Ding et al., 2019) and reported concentrations lower than those found at Lizard Island. This difference could be due to a multitude of local environmental factors including microplastic sources, hydrodynamics, and weather conditions during sampling (Kane et al., 2020; van Sebille et al., 2015), extent of biological interactions such as biofouling (Kooi et al., 2017; Liu et al., 2020a), and methodological differences in sample collection, processing and analysis (e.g., this study sampled 900 L of water per replicate while Ding et al. (2019) sampled only 5 L). Microplastic

concentrations in Lizard Island sediment samples were similar to or lower than those recently reported in the sediment beds of other coral reefs (Huang et al., 2021). In sampled species, microplastics contamination was also lower (Fallon and Freeman, 2021; Wicaksono et al., 2021) or similar (Ding et al., 2019; Vered et al., 2019) to those found in other reef systems.

Microplastic contamination at Lizard Island increased with increasing water depth, and sediment samples were the most contaminated. Similar vertical distributions have been described for other shallow coastal marine environments (Liu et al., 2020a; Song et al., 2018) and are influenced by physical oceanographic parameters (e.g., wind, currents and tides), microplastic features (e.g., shape and polymer) (Liu et al., 2020a), and/or biological activities (e.g., biofouling) (Liu et al., 2020a; Song et al., 2018). However, the positive correlation between microplastic concentration and depth does not hold true for every marine environment. For example, deep ocean studies have reported non-linear vertical distribution patterns for microplastics relative to the vertical thermohaline (Zobkov et al., 2019). These differences in distribution highlight the complexity surrounding vertical transport of microplastics from surface seawater to sediment beds and the need for compartmentalised sampling across a depth gradient to permit robust data comparisons and inferences on patterns of distribution.

Sediment samples were collected within a 0.5 m wide x 0.5 m long x 0.03 m deep transect, with microplastic concentrations reported m^{-3}. Thus, this sampling design represents a broad spatial coverage of the sediment surface layer, and while a high microplastic loading was estimated from replicate samples, this does not necessarily indicate higher bioavailability for organisms that live in or feed on the sediment bed. Accordingly, sea cucumbers, which are benthic deposit feeders, did not exhibit higher microplastics contamination than the other species sampled, all of which feed from the water column. In fact, no significant difference in microplastic contamination was observed amongst the different biota examined, which is possibly promoted by variable microplastics contamination within the same species suggesting biotic contamination is not homogeneous. Such variability also highlights the complexity inherent in identifying species that are vulnerable to microplastic contamination and supports arguments for long-term spatial and temporal biological microplastic monitoring.

Granite Bluff was found to be more contaminated than Blue Lagoon, irrespective of sample type (both abiotic and biotic) apart from corals. This was somewhat surprising, considering the low number of plastic debris, including microplastics, found on the beaches surrounding

Granite Bluff compared to beaches surrounding Blue Lagoon (http://amdi.tangaroablue.org/). Blue Lagoon is, however, less protected from the south-easterly winds than Granite Bluff and these predominant winds (from March to September) drive stronger water currents which may have assisted in dispersal (and therefore dilution) of any microplastic debris present at the time of sampling. Microplastic input from local land and sea-based activities could have also played an important role in the observed differences in microplastic contamination levels; Lizard Island Resort and a public mooring are both located in the vicinity of Granite Bluff, while Blue Lagoon is largely sanctioned for research with minimal tourism. A positive relationship between environmental exposure concentration and uptake by resident organisms (i.e., levels of biotic microplastic contamination reflect levels of abiotic microplastic contamination) was observed, with species from Blue Lagoon having lower microplastic loadings than their counterparts from Granite Bluff. This relationship between abiotic and biotic contamination is commonly reported in aquarium-based studies, including of *P. amboinensis* collected from Lizard Island and exposed to environmentally relevant microplastics and concentration (Chapter 4). Together, these studies support the hypothesis that an increase in marine abiotic microplastic concentrations can cause concomitant increases in marine biotic microplastic contamination; hence increasing the risks of ecological effects. If proven, this hypothesis is of clear concern given that marine microplastic concentrations are predicted to increase up to 10-fold by 2100 if no major changes are enacted to reduce plastic use and disposal practices (Everaert et al., 2020).

3.4.2. Physical and chemical microplastic characteristics across abiotic and biotic compartments

Microplastic contamination in all tiers of the seawater column and in sediments provided a baseline against which microplastics contamination in the inhabiting species could be assessed. Significantly different distributions of microplastic shapes, sizes, colour, and polymers were found between environmental exposure and uptake by resident organisms (i.e., types of biotic microplastic contamination do not reflect types of abiotic microplastic contamination). These differences appear to result from various and potentially synergistic environmental and/or biological factors.

Microplastics found in fish differed from those found in the mid-column seawater samples in shape and polymer type. Fish had ingested more fibres than fragments, which corroborates with other field studies (Filgueiras et al., 2020; Jensen et al., 2019; Kroon et al., 2018b; Xu et al., 2020a). This suggests active (i.e., selective) uptake of microplastic fibres, possibly due to their similar appearance to natural food sources (e.g., filamentous algae) (Peters et al., 2017; Roch et al., 2020). Alternatively, this finding may result from the longer depuration rates of microplastic fibres compared to fragments (Xiong et al., 2019) (Chapter 4). Only microplastics < 2.5 mm were present in fish samples, with the majority being < 500 µm. High presence of small microplastics (generally < 1 mm) versus larger ones is commonly reported in field (Avio et al., 2015b; Ding et al., 2019; Garnier et al., 2019; Su et al., 2019) and laboratory (Critchell and Hoogenboom, 2018; Xiong et al., 2019) fish studies, with this size being more readily swallowed (Xiong et al., 2019), or having slower depuration rates (Liu et al., 2021), or both. Here, microplastic sizes in fish were not statistically different from those found in the water column, fish displayed high susceptibility to take up the most abundant microplastic sizes present in the water column of Lizard Island. While colour has been suggested to influence microplastic uptake by fish (Ory et al., 2017; Sa et al., 2015; Santos et al., 2016), this is not evident here suggesting that for *P. amboinensis* microplastic uptake might be better correlated with other microplastic characteristics, such as shape. Lastly, differences in polymer types present in fish compared to the mid-water column are likely to be intrinsically related to the prevalence of microplastic fibres over fragments observed in fish samples. PET and rayon, the main polymer types found in fish GIT contents, were also predominantly found as fibres in mid-column seawater samples. However, the direct influence of polymer type on uptake by fish cannot be excluded, especially because of associated biofouling (Savoca et al., 2017), which can vary based on polymer type (Agostini et al., 2021; Feng et al., 2020; Kirstein et al., 2019) and produce chemical cues that mimic natural food, making them more bioavailable to a range of marine organisms (Corona et al., 2020; Procter et al., 2019; Savoca et al., 2017). Regardless of the mechanism of uptake, findings here suggest that microplastic fibres made of PET or rayon, and of < 2.5 mm (especially < 500µm) in size may pose greater risks to fish than other microplastics (primarily fragments and/or larger microplastics) present in the abiotic compartment.

Microplastics found in sea squirts, sponges, and corals were similar in shape and size to those found in the mid-column. As discussed for fish, these either suggest lack of influence of microplastic characteristic on uptake, or high susceptibility to take up the most abundant microplastics present at the water column of Lizard Island. The feeding strategy and mechanisms of these organisms suggest that shape should not influence microplastic uptake. For size, however, sea squirts are filter feeders that trap filtered food and other particulate matter in a mucus net within the pharynx which is subsequently transported into the esophagus. Undesirable items are selectively expelled from the pharynx with the filtered water. Through this feeding process sea squirts have been observed to take up ≤ 1.3 mm long particles (Tatianan et al., 2004), as well as abundant amounts of microplastics < 400 µm (Vered et al., 2019), aligning with the microplastic sizes observed in this study. Sponges also filter the water column for food via ostia, mainly drawing in items smaller than 100 µm, i.e., within the morphological size range of their pore structure (Reiswig, 1971; Simpson, 2012). However, larger microplastics may have been endocytosed by the sampled sponges, a mechanism suggested to explain microplastic uptake by various sponge species at Bocas del Toro, Panamá (Fallon and Freeman, 2021). In corals, the majority of microplastics resembled the size of their prey items such as zooplankton (Fabricius et al., 1995; Ferrier-Pagès et al., 2010), although, plastic fibres > 2 mm were also present. As coral samples were digested whole, it is not known whether larger fibres were actively ingested or representative of passive contamination through tissue overgrowth (Ferrier-Pagès et al., 2010; Martin et al., 2019; Reichert et al., 2018). Thus, as for fish, is likely that the invertebrates tested in this study are highly susceptible to take up the most abundant microplastic sizes present at the water column of Lizard Island. Microplastics found in sea squirts and corals differed in colour from those found in the mid-column. Considering that these taxa are only capable of light sensing (Picciani et al., 2021; Rivera et al., 2012) and not colour detection, it is likely that these organisms were selectively ingesting microplastics with other specific characteristics, i.e. shape, size and polymer, that so happen to be mainly transparent or white. However, for sea squirts, the variety in shape and polymer type of recovered microplastics suggest uptake is driven by size. For corals, 40% of the white items were also polysulfone fragments potentially indicating uptake of white microplastics driven by polymer type. Similarly, sea cucumbers seemingly selectively ingested specific polymer types from the sediment. In fact, polymer type was the only microplastic characteristic with different

distributions between sea cucumber and the sediment. It is possible that polymer chemistry is driving this process in corals and sea cucumbers given these two taxa rely on chemosensation for feeding. Furthermore, microplastic biofouling can result in increased uptake by corals (Corona et al., 2020), although this has not been confirmed for sea cucumbers. Overall, findings suggest that sea squirts, sponges, and corals take up microplastics of similar size of what was found in the water column of Lizard Island, and specially microplastics < 500µm in size, regardless of other physical and chemical characteristics. This microplastic size range may pose a higher risk to a multitude of invertebrate taxa than microplastics of other sizes, a trend that corroborates laboratory studies on other invertebrate taxa (Lehtiniemi et al., 2018; Wang et al., 2021b). The impacts of colour and polymer type deserve further assessment.

3.5. Conclusion

With growing concerns around environmental microplastic contamination, extensive baseline information on both abiotic and biotic compartments is paramount. Similarly, it is also important to understand microplastic bioavailability, and decouple interactions between available microplastics in abiotic compartments and exposed organisms that encounter and feed on these, to elucidate risks of microplastic bioavailability and effects to reef ecosystems. The abiotic and biotic compartments of Lizard Island coral reefs analysed in this study were all found to be contaminated with microplastics. As in other shallow water systems, microplastic concentrations increased with depth, while the levels of microplastics contamination in the study species were consistent regardless of their position in the habitat or feeding regime. Levels of microplastic contamination between marine abiotic and biotic compartments were shown to be mostly positively correlated, indicating that microplastic contamination in marine organisms is likely to increase with the predicted increase in marine microplastic concentrations. Yet, physical and chemical characteristics of microplastics found in organisms did not always reflect what was present in the abiotic compartment in which they live and/or feed on. In fish GITs specifically, fibres were more abundant than fragments. Across the five taxa assessed, microplastics < 500 µm were consistently most prevalent. Together with the high abundance of these items in the water column and sediment, these results suggest more attention should be given to the abundance, distribution, and effects of

microplastics < 500 μm at Lizard Island. Overall, these findings suggest greater biological risks of some microplastics in relation to others, based primarily on shape and most likely size.

Chapter 4: Ingestion and depuration of microplastics by a planktivorous coral reef fish, *Pomacentrus amboinensis*

Abstract

Microplastics are ubiquitous contaminants in marine environments and organisms. Concerns about potential impacts on marine organisms are usually associated with uptake of microplastics, especially via ingestion. This study used environmentally relevant exposure conditions to investigate microplastic ingestion and depuration kinetics of the planktivorous damselfish, *Pomacentrus amboinensis*. Irregular shaped blue polypropylene (PP) particles (longest length 125 to 250 µm), and regular shaped blue polyester (PET) fibers (length 600 to 700 µm) were selected based on physical and chemical characteristics of microplastics commonly reported in the marine environment, including in coral reef ecosystems. Individual adult damselfish were exposed to a single dose of PP particles and PET fibers at concentrations reported for waters of the Great Barrier Reef (i.e., environmentally relevant concentrations, ERC), or future projected higher concentrations (10x ERC, 100x ERC). Measured microplastic concentrations were similar to their nominal values, confirming that PP particles and PET fibers were present at the desired concentrations and available for ingestion by individual damselfish. Throughout the 128-h depuration period, the 88 experimental fish were sampled 2, 4, 8, 16, 32, 64 and 128-h post microplastic exposure and their gastrointestinal tracts (GIT) analyzed for ingested microplastics. While damselfish ingested both experimental microplastics at all concentrations, body burden and depuration rates of PET fibres were significantly larger and longer, respectively, compared to PP particles. For both microplastic types, exposure to higher concentrations led to an increase in body burden and lower depuration rates. These findings confirm ingestion of PP particles and PET fibers by *P. amboinensis* and demonstrate for the first time the influence of microplastic characteristics and concentrations on body burden and depuration rates. Finally, despite measures put in place to prevent contamination, extraneous microplastics were recovered from experimental fish, highlighting the challenge to completely eliminate contamination in microplastic exposure studies. These results are critical to inform and continuously improve protocols for future microplastics

research, and to elucidate patterns of microplastic contamination and associated risks in marine organisms.

Key words: polypropylene, polyester, particle, fiber, marine environment, uptake, impacts, damselfish.

4.1. Introduction

Contamination of the marine environment with microplastics (plastic items 1 μm - 5 mm in length) is prevalent, with up to 51 trillion floating microplastics estimated to occur in this environment globally (van Sebille et al., 2015). This staggering amount is also predicted to significantly increase if the global community does not address plastic production, use, reuse and disposal management (Everaert et al., 2020; Jambeck et al., 2015b). Under a "business as usual scenario", concentrations of marine microplastic contamination are estimated to increase up to 10 times by 2100 (Everaert et al., 2020).

Microplastics are frequently found contaminating marine organisms (Halstead et al., 2018; Kroon et al., 2018b; Qu et al., 2018), and may disrupt physiological processes resulting in, for example, cellular stress (Espinosa et al., 2017; Jeong et al., 2016), and energy (Lo and Chan, 2018; Welden and Cowie, 2016) and hormonal (Zhao et al., 2020) imbalances. As a consequence, microplastics and their associated impacts could ultimately affect marine organisms by changing growth, reproduction and/or mortality of individuals (Liu et al., 2020c). Reports of microplastic-related risks for marine organisms have, for the most part, been associated with their uptake, and specifically direct ingestion of microplastic items (GESAMP, 2019). Other pathways, however, such as passive uptake through the gills (Bour et al., 2020a) or via trophic transfer from prey items (Miller et al., 2020; Santana et al., 2017) have been demonstrated in controlled laboratory experiments. Thus, similar to other contaminants (Amoroso et al., 2020; Blanco et al., 2018; Hassell et al., 2020), depuration is a major factor influencing the potential effects of microplastics following ingestion. Microplastic depuration alters the amount of contamination present within the gastrointestinal tract (GIT) of organisms over time, thereby influencing toxicity, vectorization of additives and sorbed chemicals, and the likelihood of trophic transfer (Bour et al., 2020b; Dawson et al., 2018). Hence, a better understanding of microplastic ingestion and depuration kinetics of marine organisms may help elucidate risks posed by this contaminant.

Microplastic ingestion and depuration kinetics have not been rigorously evaluated in marine organisms under controlled exposures, and rarely reflect environmentally relevant exposure characteristics, such as microplastic polymer composition, shape, size, color, and concentration (Cong et al., 2019; Lu et al., 2016) (Table 4.1). For example, polystyrene (PS) beads represent

the most common microplastic evaluated in controlled ingestion and depuration studies, yet microfibers and irregular microparticles comprising of other polymers, such as polyester (PET), polyethylene (PE), and polypropylene (PP) are more abundant in marine environments (Coyle et al., 2020). Furthermore, experimental microplastic concentrations are generally much higher than reported environmental concentrations (Xu et al., 2020a). In terms of suitable species, controlled exposure studies specifically examining ingestion and depuration kinetics rarely consider organisms likely exposed to and contaminated with microplastics in the marine environment. For example, ingestion and depuration studies have mainly focused on aquatic invertebrates (Chae and An, 2020; Ehlers et al., 2020; Wang et al., 2019a), and freshwater fish (Grigorakis et al., 2017; Hoang and Felix-Kim, 2020; Xiong et al., 2019). In contrast, only four ingestion and depuration studies have been conducted on brackish/marine fish (Bour et al., 2020b; Cong et al., 2019; Manabe et al., 2011) despite these being some of the most frequently reported organisms contaminated with microplastics (Jensen et al., 2019; Kroon et al., 2018b; Lusher, 2015). Hence, there is a major shortcoming in the current literature limiting the understanding of microplastic ingestion and depuration kinetics in marine organisms. A more comprehensive exploration of environmentally relevant exposure conditions on a broader range of organisms in the marine environment is warranted (Bour et al., 2020b).

Table 4.1: Summary of microplastic ingestion and depuration studies conducted on aquatic species. PE = polyethylene, PS = polystyrene, PET = polyethylene terephthalate (also polyester), PP = polypropylene, HDPE = high density polyethylene. S = sphere, Fg = fragment, Fb = fiber, Fl = film. Sizes reported as one unique size, and as a size range (either min. and max., or average ± standard deviation). Only laboratory studies reporting on microplastic ingestion and depuration kinetics were considered. Note that the number of rows in this table does not correspond to the total number of studies published on the topic because studies reporting on more than one species are included multiple times.

Taxa	Species	Life stage	Environment	Polymer	Shape	Size	Color	Concentration	Reference
Fish	*Pimephales promelas*	larval	freshwater	PE	S	63-75 µm and 125-150 µm	green	25 mg L^{-1} and 50 mg mps L^{-1} (145,343 mps L^{-1} and 290,686 mps L^{-1} for 63-75 mm mps or 18,367 mps L^{-1} and 36,734 mps L^{-1} for 125-150 mm mps)	Hoang and Felix-Kim (2020)
	Carassius auratus	n/a		PE	Fg, Fb, Fl	3-5 mm, 2-3 mm, and 0. 5-2 mm	white, transparent, and cyan	100 mps L^{-1}	Xiong et al. (2019)
		adult		PE, PET	S, Fb	50-500 µm and ≥ 63 µm	n/a	50 mps food $pellet^{-1}$	Grigorakis et al. (2017)
	Oryzias melastigma	larval and adults	brackish	PS	S	10 µm	green	$1x10^5$ mps L^{-1} (each 30 larvae)	Cong et al. (2019)
	Oryzias latipes	embryos and larvae		latex	S	50 and 500 nm	n/a	10 mg L^{-1} in embryo culture medium	Manabe et al. (2011)
	Gasterosteus aculeatus	n/a	freshwater and marine	PE, PET	S, Fb	27-32 and 500 µm	blue and black	100,000 mps L^{-1} (1:1 per plastic type)	Bour et al. (2020b)

	Seriolella violacea	juvenile	marine	nylon	tubular	1.2 ± 0.2 mm (length), 1.0 ± 0.1 mm (width)	black, blue, translucent, and yellow	10 food pellets and 2 microplastics	Ory et al. (2018)
	Pomacentrus amboinensis	larval		PS	S	200-300 µm	transparent	167 mps L^{-1} (each 10 larvae)	McCormick et al. (2020)
Snail	*Achatina fulica*	"growing period"	terrestrial	PET	Fb	1257.8 µm (length) and 76.3 µm (width)	n/a	0.01-0.71 g kg^{-1} (dry soil) (6.4% of fodder/lettuce mass rate)	Song et al. (2019)
	Radix balthica	adult	freshwater	PS, polyacrylic wool	Fg, Fb	up to 200 µm; 30 and 2,000 µm	blue and green	15% (fragment or fiber) of available biofilm (4.24g mps/biofilm)	Ehlers et al. (2020)
Frog	*Xenopus tropicalis*	tadpole	freshwater	PS	S	1 and 10 µm	green	10^3 mps mL^{-1}	Hu et al. (2016)
Zooplankton	*Hyalella azteca*	adult	freshwater	PE, PP	Fg, Fb	10-27 µm and 20-75 µm	blue	0-10^4 mps mL^{-1} (acute) and 0-20x10^3 mps mL^{-1} (chronic); 0-90 mps mL^{-1}	Au et al. (2015)

	Daphnia magna	adult	freshwater	PE	S, Fg	10-106 µm and 10-75 µm	white and black	10^{-4}-10 g L^{-1}	Frydkjaer et al. (2017)
		juvenile	freshwater	PS	S	2 µm and 100 nm	n/a	1 mg L^{-1}	Rist et al. (2017)
	Artemia sp.	larval	marine	PS	S	10 µm		10^3 mps mL^{-1}	Wang et al. (2019b)
	various	various		PS	S, Fg	15 and 30 µm	green	50-200 microplastics mL^{-1}	Elizalde-Velazquez et al. (2020)
Crab	*Carcinus maenas*	n/a	marine	PS	S	8-10 µm	n/a	n/a (gives nominal concentration of mussel exposure but not concentration in contaminated mussels)	Watts et al. (2014)
Bivalve	*Mytilus galloprovincialis*	adult	marine	PE	S	180-212 µm (203.84 ± 13.76 µm)	n/a	10 mg L^{-1} ($2x10^3$ particles L^{-1})	Chae and An (2020)
		adult	marine	PS	S	2, 6 and 10 µm	yellow-green, red	10 and 1000 mps mL^{-1}	Goncalves et al. (2019)
		adult	marine	HDPE	Fg	up to 22 µm, mean of 4-6 µm	n/a	3 mg L^{-1}	Fernandez and Albentosa (2019a)

	Mytilus edulis	adult	marine	HDPE	Fg	up to 22 µm, mean of 4-6 µm	n/a	3 mg L^{-1}	Fernandez and Albentosa (2019b)
		adult	marine	PET	Fb	459 ± 2.25 µm	pink	up to 30 mps mL^{-1} (0.374% of available seston)	Woods et al. (2018)
		adult	marine	PS	S	49.1 ± 1.3 µm	black	5 mps L^{-1} and 100 mps L^{-1}	Rist et al. (2019)
	Magallana gigas	adult	marine	PS	Fg	100, 250 and 500 µm	orange	60 mps L^{-1} (30 mps per size)	Graham et al. (2019)
Sea urchin	*Tripneustes gratilla*	larval	marine	PE	S	10-45 µm, majority 25-32 µm	green	aprox. 500 spheres mL^{-1} (for retention study)	Kaposi et al. (2014)

In this controlled exposure study, microplastic ingestion, body burden and depuration kinetics of the planktivorous damselfish *Pomacentrus amboinensis* were investigated. Adults of this species, common to shallow Indo-Pacific coral reefs, actively feed on food particles carried on water currents (McCormick and Weaver, 2012), playing a key role in transferring energy from plankton up the food web (Emslie et al., 2019). Microplastic contamination in adult *P. amboinensis* was common among individuals collected on reefs in the central Great Barrier Reef, Australia (Jensen et al., 2019), making this a relevant species for studies on microplastic impacts resulting from ingestion. Here, adult ambon damselfish were exposed once to environmentally relevant types (irregular shaped blue PP particles and regular shaped blue PET fibers) and concentrations (ERC) of microplastics, based on characteristics or estimations of microplastics found in sea surface waters (Abayomi et al., 2017; Cole et al., 2014; Cozar et al., 2014; Kanhai et al., 2017; Syakti et al., 2017), including at the Great Barrier Reef (Everaert et al., 2020; Jensen et al., 2019) and Lizard Island (Chapter 3). Dose response was also assessed by exposing the damselfish to a range of microplastic concentrations (Critchell and Hoogenboom, 2018), including future scenarios of marine microplastic contamination, i.e., 10X ERC and 100X ERC – extending concentrations beyond 2100 predictions (Everaert et al., 2020). To elucidate ingestion and depuration kinetics, ambon damselfish were sampled incrementally at 2, 4, 8, 16, 32, 64 and 128-h post microplastic exposure and GITs analyzed for ingested microplastic body burden. Finally, unintended sample contamination with extraneous microplastics, generally not monitored or reported in the current literature, was determined during the controlled exposure and/or sample processing. The presented findings on the residence time of these items within a marine fish and under different exposure scenarios of exposure contribute to improved understanding of the potential ecological risks posed by microplastic contamination in marine environments.

4.2. Material and methods

4.2.1. Study Area

Fish collection and the controlled exposure experiment were conducted at the Australian Museum's Lizard Island Research Station (LIRS). Lizard Island (14˚40'08''S 145˚27'34''E)

is a mid-shelf reef located in the northern area of the Great Barrier Reef World Heritage Area (GBR WHA). The reef system is situated approximately 30 km northeast from the Australian continent and 250 km north from the largest city in the region (Cairns; population ~151,000). Despite its relatively remote location, there is potential for microplastic contamination coral reefs and in reef fish of Lizard Island based on recent studies reporting microplastic contamination from surface waters nearby (Hall et al., 2015; Jensen et al., 2019; Reisser et al., 2013b) and from reef fish collected at Lizard Island(Jensen et al., 2019; Kroon et al., 2018b).

4.2.2. Fish Collection and Husbandry

The fish collection and experiment were performed in accordance with relevant institutional and national guidelines and regulations (Great Barrier Reef Marine Park Authority permit G12/35236.1 and James Cook University Animal Ethics Committee Approval Number A2635). In total, 92 adult *P. amboinensis* were captured on SCUBA using fence and dip nets, and temporarily immobilized using a diluted solution containing clove oil (Kroon, 2015). Immediately following collection, four of the 92 fish were individually placed in resealable zip lock plastic bags and euthanized with an overdose of clove oil to establish the background level of microplastics in the study species. These four fish were processed as per laboratory fish (refer to 'Quantification of Ingested Microplastics') and GITs analyzed for putative microplastics (refer to 'Preventing and Monitoring Contamination'). A sample of these plastic bags was included in the customized contaminant library to monitor unintended sample contamination with extraneous microplastics (refer to 'Preventing and Monitoring Contamination'). The remaining 88 fish were transported to LIRS, placed in individual 12 L transparent polystyrene (PS) tanks (34 cm x 20 cm x 21 cm) with PP lids, and given 3 to 6 days to recover and acclimate prior to microplastic exposure. The use of plastic tanks and lids was due to logistical, financial and safety risks of shipping glass aquaria via road and sea for experimental use.

The 88 experimental tanks were located in two enclosed and inter-connected laboratory rooms at LIRS, with restricted access throughout the duration of the study. Both rooms and all tanks were thoroughly cleaned with fresh bore water prior the experiment. After cleaning, tanks were air dried overnight, subsequently filled with filtered (50 µm; Puretec®, PP Series Pleated

Sediment Cartridge) natural seawater from the Lizard Island lagoon and left in flow-through mode for 48 h prior to introducing the fish. Once individual fish were introduced, tanks were operated in flow-through mode with a complete tank turnover of 1.5 L h^{-1} to ensure good water quality and adequate aeration. The room temperature was maintained at 24˚C and fish were subjected to a 12:12 h artificial light:dark cycle. Basic seawater physical (temperature, T; pH, dissolved oxygen, DO) and chemical (ammonia, NH_3; nitrate, NO_3) parameters were monitored with a HACH 40 portable multi-parameter meter (T, 0.1˚C; DO, 0.01 mg L^{-1}), Fisherbrand™ strips (pH, 0.1) and Aquasonic test kits (NH_3, 0.1 ppm; NO_3, 5 ppm), respectively. Measurements were taken either directly from the tank (T and DO) or from a subsample taken with a syringe (pH and chemical parameters) every second day during the acclimation, exposure and depuration periods in at least 30% of tanks using a random number generator each time. During the 128 h depuration period, the random number generator was only applied to those tanks that still contained fish.

Throughout the study, fish were fed with an equivalent of 1.25% of the average adult *P. amboinensis* biomass, adapted from Critchell and Hoogenboom (2018). Food comprised of 125 to 250 µm irregular shaped commercial food pellets (INVE Aquaculture; proteins min. 55%, lipids min. 9% and natural fibrous materials max. 1.9%), and post-hatched artemia (500-800 µm) reared from a frozen artemia culture at LIRS. Food items were of similar size dimensions to experimental microplastics (Figure 4.1). Individual fish were considered acclimated when observed consuming the food pellets and artemia.

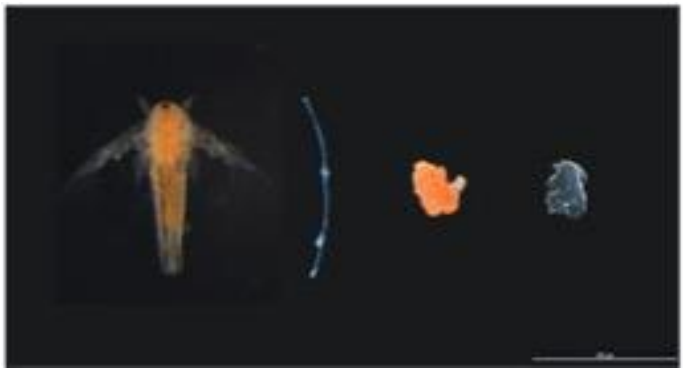

Figure 4.1: Comparable shapes and sizes of food and experimental microplastics given to adult damselfish *Pomacentrus amboinensis* in a controlled laboratory experiment. Food included orange post-hatched artemia (far left) and orange food pellet (second right). Experimental microplastics included blue polyester fiber (2nd left) and blue polypropylene particle (far right), with photo taken before biofouling of microplastics.

4.2.3. Experimental Microplastics

The following two experimental microplastics were used: irregular shaped blue secondary PP particles (longest length 125 to 250 µm), and regular shaped blue secondary PET fibers (length 600 to 700 µm) (Figure 4.1). Both microplastics were artificially produced at the Australian Institute of Marine Science (AIMS) laboratories in Townsville, Australia. The PP particles were sourced from 15 mL falcon tube lids (Greiner), milled with a commercial blender (up to 10 000 RPM), and dry sieved through two stainless steel laboratory test sieves (Endecotts) of 125 and 250 µm aperture sizes. The PET fibers were sourced from sewing thread (Gütermann, CA 02776), cut with sterile surgical blades (Paramount, BS EN 27740), and sized using calipers (Kincrome, 1/1000 in). The chemical composition of both PP particles and PET fibers were confirmed by Fourier transform infrared spectroscopy (FTIR) (Appendix C – Figure S1).

To simulate microplastics found in the marine environment, PP particles and PET fibers were biofouled at AIMS using a method modified from Kulcsár (2019). Briefly, both experimental microplastics were loosely packed into 85 mL opaque cartridges (Telos-Kinesis) (one polymer type per cartridge) each capped with a 263 µm stainless steel mesh on the outflow. Both cartridges were then connected to an overflow from a 2500 L flow-through seawater system inhabited by coral reef organisms including invertebrates (e.g. corals, sea

urchins and sea stars) and fish. To facilitate biofouling of experimental microplastics, cartridges were exposed to natural day:night conditions and ambient temperature for seven days. Ambient seawater temperature in the cartridges was maintained by immersing both cartridges in a 13 L seawater tank connected to the same flow-through seawater system used to supply seawater for the cartridges. After seven days, biofouled PP particles and PET fibers were hand picked and individually transferred into 20 mL scintillation vials containing 15 mL filtered (0.45µm) natural seawater and individual doses of the three concentrations (i.e., ERC, 10x ERC and 100x ERC) were prepared. ERC was based on monitored (0.04 to 0.48 m^{-3}) (Jensen et al., 2019) and modeled (0.01 – 0.02 microplastic/m^2) (Everaert et al., 2020) microplastic concentrations in sea surface of the Great Barrier Reef Region. Nominal microplastic concentrations were manually prepared at 1 PP particle and 1 PET fiber per 12 L (37 (h) x 22 (d) cm) tank (ERC), 10xERCs at 10 PP particles and 10 PET fibers per 12 L tank, and 100xERCs at 100 PP particles and 100 PET fibers per 12 L tank (Table 4.2). Prepared microplastic doses were kept at room temperature and exposed to an artificial 12:12 light:dark cycle for a maximum of 15 days prior to use. On the day of the exposure, standard concentrations of food pellets and cultured artemia (see "Fish Collection and Husbandry") were added to each vial, and to four control vials containing 15 mL filtered (0.45µm) natural seawater. Each vial was shaken and their entire contents transferred to the designated tank. The vials were rinsed liberally with filtered natural seawater to ensure all contents were transferred.

Table 4.2: Nominal (1, 10 or 100 particles or fibers 12 L^{-1}) and measured (mean ± standard deviation) concentrations of microplastics in three treatment groups during single exposure of adult damselfish *Pomacentrus amboinensis* to blue polypropylene (PP) particles and polyester (PET) fibers in this controlled laboratory experiment. ERC = environmentally relevant concentration. Control treatment was not included as no microplastics were added. Microplastic concentrations were measured in nine 12 L control tanks (n = 3 tanks per ERC treatment; seawater without damselfish).

Treatment	PP (particle 12 L^{-1})		PET (fiber 12 L^{-1})	
	Nominal concentration	Measured concentration	Nominal concentration	Measured concentration
ERC	1.0	1.0 ± 0.0	1.0	0.7 ± 0.5
10x ERC	10.0	9.3 ± 0.5	10.0	9.0 ± 0.8
100x ERC	100.0	95.0 ± 2.5	100.0	94.3 ± 1.3

4.2.4. Experimental Design and Conduct

Individual fish were acclimated for 3 to 6 days and fed twice daily as described above. Following acclimation, each of the 88 tanks were assigned randomly to one of four treatment groups and seven sampling periods (customized random generator script, RStudio version 1.1.463). Pre-prepared microplastic doses were added to the three exposure treatments: ERC (n = 28 tanks), 10x ERC (n = 28) and 100x ERC (n = 28) (Table 4.2). No experimental microplastics were added to the control group (n = 4). Space restrictions within the laboratory influenced the design of the experiment and the number of controls, precluding an equivalent number of fish for the control replicates, and the use of tanks without fish to monitor for airborne and seawater contaminants.

Prior to exposure with the experimental microplastics, all fish were starved for 24 h. Starvation was imposed to 1) ensure clear GITs prior to experimental procedure, thereby reducing any uncontrolled variability within and between treatments, and 2) increase the likelihood of microplastic ingestion by increasing the desire/need to feed (Grigorakis et al., 2017; Song et al., 2019). On the day of exposure, individual fish received their normal food as well as their randomly assigned and pre-prepared doses of PP particles and PET fibers simultaneously, as described above. During the first 30 seconds of microplastic exposure, tanks continued to operate in flow-through mode to abet microplastic and food dispersion in the water column. After 30 seconds, all tanks were switched from flow-through to circulation mode to increase the likelihood of the fish encountering the microplastics. After 2 h exposure, flow-through mode was resumed, and fish were left to depurate for up to a total of 128 h. During depuration, fish were fed as usual - without additional microplastics - twice daily. Excess food and excretions were removed by siphon daily to avoid reingestion of depurated microplastics. Filters were applied to the seawater outflow to prevent the discharge of microplastics (experimental and extraneous) into the Lizard Island coral reef environment.

4.2.5. Quantification of Ingested Microplastics

At 2, 4, 8, 16, 32, 64 and 128-h post exposure, four individual fish randomly chosen from each treatment were removed from their tanks and humanely euthanized using ice slurry. Fish

were measured (standard and fork length, 0.1 cm, Kincrome, 1/1000 in), weighed (0.01 g, AND EK-410i), and preserved in 70% ethanol (EtOH) for transport and storage. All control fish (n = 4) were sampled at the first sampling time (2 h) to accurately demonstrate if, during the exposure period, fish were exposed to microplastics other than those intentionally offered (i.e. other than the experimental microplastics).

Individual fish were dissected to remove the entire GIT from the top of the esophagus to the rectum. Individual GITs were weighed (wet weight, w.w., Sartorius TE31025, max 3100g, d 0.01 g) and subjected to alkaline digestion using a method adapted from Karami et al. (2017b) to recover PP particles and PET fibers. Briefly, GIT digestion was conducted with 10% potassium hydroxide (KOH; AR, Fisher, CAS No. 1310-58) at 40˚C for 48 h in a ratio of 1:20 of GIT wet weight (g) to volume of KOH (mL). Digested GIT solutions were filtered through 77 and 26 µm stainless steel mesh filters (19 mm diameter) (Schlawinsky, 2020), and rinsed with 70% EtOH to remove fat vestiges (Dawson et al., 2020). Microplastics retained on mesh filters were visually identified, counted and photographed using stereomicroscopy (Leica MZ16A, Leica DFC 500, Leica Application Suite LAS 4.4.0). PP particles and PET fibers were readily distinguishable from other particulates based on the combinations of shape, size and color.

4.2.6. Microplastic Exposure Validation and Spike-Recovery Tests

To validate the nominal concentrations of experimental microplastics, nine individual 12 L tanks without fish were dosed with biofouled and pre-prepared experimental PP and PET doses (ERC n=3, 10x ERC n=3 and 100x ERC n=3) and left for 30 seconds in flow-through mode. Each tank was then emptied via a drain over a 40 µm nylon mesh to capture microplastics. Experimental microplastics (PP and PET) retained on mesh filters were visually identified and counted using stereomicroscopy (Zeiss SteREO Discovery.V8).

A spike-recovery test was conducted, to (1) account for impacts of the adapted KOH method on the experimental microplastics, and (2) establish recovery rates for spiked PP particles and PET fibers after the KOH digestion. Specifically, biofouled PP particles and PET fibers at the three concentrations of exposure (ERC, 10x ERC and 100x ERC) were exposed to 1.5 mL of 10% KOH and processed as above. Three replicates were spiked for each treatment

(ERC n=3, 10X ERC n=3, 100X ERC n=3). Following digestion at 40˚C for 48 h, samples were filtered, rinsed and the 77 and 26 µm stainless steel mesh filters visually assessed using stereomicroscopy. Recovered spiked microplastics were counted to estimate recovery rates for experimental PP particles and PET fibres after the KOH digestion.

4.2.7. Preventing and Monitoring Contamination

A range of measures were implemented to minimize potential microplastic contamination during room preparation, experimental procedure, and sample processing including fish dissection, and GIT digestion and filtration. As previously stated, all experimental tanks were placed in a closed room and isolated from potential air and waterborne microplastic contaminants (as much as possible) using lids and filters. Throughout the study, and whenever used, equipment and tools were sequentially cleaned with reverse osmosis H_2O, Milli-Q H_2O, 70% EtOH, or a combination of these. Cellulose-based cloths were used to wipe surfaces with 70% EtOH. Prior to use, 10% KOH and 70% EtOH solutions were filtered to 0.45 µm (Millipore® HA filters). Clothing and lab coats worn during microplastic preparation, dosing and sample processing were made from naturally-derived materials (e.g. cotton) to eliminate introducing synthetic fibers and specifically non-experimental PETs. All clothing was also delinted using a lint roller (Scotch-Brite®, 3M) prior to sample handling. Nevertheless, the use of plastic material was unavoidable as described above, including consumables such as zip lock bags for fish collection, and plastic gloves and parafilm during sample processing. To control for these sources of plastic items that could be unintentionally introduced into the experiment, a customized contaminant library was developed following Kroon et al. (2018a) to enable detection of such extraneous microplastic contamination from either the environment, the experimental procedure, or during sample processing. Briefly, samples of plastic gear used during fish collection (e.g. fish net and zip lock bag), experimental procedures (e.g. exposure tanks and lids, seawater pipeline) and sample processing (e.g. spray bottle and gloves) were included in a customized contaminant library (Appendix C –Table S1), along with any airborne putative microplastic identified from filtered blank processing controls (i.e. Petri dishes with 20 mL of Milli-Q H2O). Materials from other equipment, such as probes from the HACH 40 portable multi-parameter meter and the cartridge from the Puretec® filter, were not included

to avoid damage to expensive and delicate instruments. All items in the contaminant library were photographed for shape and color characterization and analyzed by FTIR for chemical composition.

To determine the occurrence and potential sources of microplastic contamination throughout the study, all putative microplastics (i.e. non-test PP and PET microplastics) identified in fish GITs (including field, control and exposed fish) and blank processing controls were physically and chemically characterized following Kroon et al. (2018a); Kroon et al. (2018b). Items were tentatively identified as microplastics based on key physical parameters (i.e. size, shape, color) commonly used in the literature (Hidalgo-Ruz et al., 2012; Norén, 2007). All putative microplastics were then analyzed by FTIR to confirm polymer composition using either PerkinElmer Spectrum 100 FTIR (1 mm ATR window, pressure gauge = 150, 8 scans at 4 cm^{-1} resolution, wavenumber range between 4000 and 600 cm^{-1}, atmospheric (CO_2/H_2O) suppression, atmospheric vapor compensation, and background scans acquired every 10 acquired spectra) or PerkinElmer Spotlight 200i FT-IR microscope (100µm ATR aperture, pressure gauge = 5%, 32 scans at 4 cm^{-1} resolution, wavenumber range between 4000 and 600 cm^{-1}, atmospheric (CO_2/H_2O) suppression, atmospheric vapor compensation, and background scans acquired for every acquired spectrum). FTIR spectra were searched against the NICDOCOM IR spectral libraries (Polymers and Additives, Coatings, Fibers, Dyes and Pigments, Petrochemicals; NICODOM Ltd., Czech Republic) and the matching polymer type assigned. FTIR spectra of microplastics retrieved from fish GITs were then compared with those in the custom-built contaminant library to identify potential microplastic contamination throughout the study, and infer possible sources of contamination (i.e. due to being inadvertently introduced from the environment, the experimental procedure, or during sample processing.

4.2.8. Data Analyses

Based on the size range of the two experimental microplastics and the limited evidence of microplastic translocation into fish tissue after uptake (Cong et al., 2019; Lu et al., 2016), microplastic body burden was defined as the amount of microplastics present in the fish GIT.

Microplastics body burden was quantified for PP particles and PET fibers separately and per individual fish GIT analyzed.

To determine whether microplastic body burden over time was affected by microplastic type or concentration, a general linear model (GLM, $p < 0.05$) was used following the equation:

$$\text{body burden} = \text{type} + \text{concentration} + \text{time} + \text{weight} + \text{constant} \quad \text{(Eq. 1)}$$

where,

type = PP particles or PET fibers

concentration = ERC, 10x ERC, or 100x ERC

time = time of collection (or depuration time)

weight = fish weight (in g)

Fish weight was included as a covariant in the GLM because body weight is a common variable to be considered in toxicokinetic studies (Hendriks and Heikens, 2001; Lebrun et al., 2014; Miller et al., 2016). Based on the GLM model, effects of microplastic type, concentration of exposure and depuration period were calculated as:

Plastic type:

$$e^{\text{intercept estimate}} / e^{(\text{intercept estimate} - \text{PETvsPP intercept})} \quad \text{(Eq. 2)}$$

Concentration of exposure:

$$e^{(\text{intercept estimate} + \text{ERCvs10xERC intercept})} / e^{(\text{intercept estimate})} \quad \text{(Eq. 3)}$$

$$e^{(\text{intercept estimate} + \text{ERCvs100xERC intercept})} / e^{(\text{intercept estimate})} \quad \text{(Eq. 4)}$$

Depuration period:

$$\left(1 - \left(\log_t{}^{\log(\text{depuration}) \text{ intercept})} / \log_2{}^{\log(\text{depuration}) \text{ intercept})}\right)\right) \quad \text{(Eq. 5)}$$

where t = depuration period, ranging from 4 to 128-h).

Although fish had been randomly assigned to the four different treatments and seven sampling periods, fish weight was included in the model to account for potential variation in the amount of microplastics ingested and depurated due to fish size. To accommodate overdispersion resulting from high numbers of zero's in the data set, the model followed a negative binomial distribution linked with log function. This data analysis was conducted with RStudio, version 1.1.463. The four control fish were not included in the GLM as these fish were never exposed to the experimental microplastics (see "Results").

The microplastics body burden as a function of time was used to estimate the depuration rates and elimination half-life of PP particles and PET fibers at the different exposure concentrations. Depuration rate constants were calculated based on the following first-order kinetics model, assuming that the ratio of microplastic elimination is directly proportional to microplastics concentration in the fish (Newman, 2012):

$$C_t = C_0 e^{-k_e t} \quad \text{(Eq. 6)}$$

where,

C_t = amount of microplastics in the fish GIT at a particular time

C_0 = initial amount of microplastics in the fish GIT

k_e = elimination rate constant as number of microplastics per h

t = time of measured concentration (C_t)

From this model, microplastic elimination half-life was calculated following:

$$t_{1/2} = \ln(2)\, k_e \quad \text{(Eq. 7)}$$

where,

$t_{1/2}$ = microplastic elimination half-life

k_e = elimination rate constant as number of microplastics per h

Microplastic depuration rates and elimination half-life were calculated using GraphPad, version 8.4.1. Significant differences among depuration rates were compared using one-way ANOVA and Tukey's multiple comparisons tests. Interaction between experimental microplastics and concentration was considered a factor (with 6 levels; $p < 0.05$).

4.3. Results

4.3.1. Basic Water Quality and Fish Condition

Water quality was measured on acclimation days 1, 2, 3, 4 and 5; on the day prior microplastic exposure (starvation day) and on two depuration days (2 and 4), totaling 132 times in randomly assigned tanks. Variability in seawater T (24.6˚C ± 0.7), pH (8.0), and DO (8.19 mg L^{-1} ± 0.1) was negligible. Further, concentrations of NH_3 (0 ppm) and NO_3 (≤ 5 ppm) were consistently below limits considered harmful to marine fish.

Throughout the study, none of the fish presented any signs of stress and no mortality was recorded. Following establishment in their individual tanks, all 88 fish commenced feeding on the first day of the acclimation period and continued to do so throughout the experiment. Following microplastic exposure, no changes in fish behavior were observed across any of the four treatments.

4.3.2. Microplastic Exposure Validation and Spike-Recovery Tests

Measured concentrations of experimental microplastics in seawater across the three experimental treatments were similar to their nominal values (Table 4.2). This confirmed that irregular shaped blue PP particles and regular shaped blue PET fibers were present in the water at the desired concentrations and available for ingestion by individual damselfish.

No discernible changes in the blue color of spiked particles and fibres were observed by stereomicroscopy. Results from the spike-recovery test showed high efficiency for recovering both experimental microplastics after exposure to 10% KOH at 40˚C for 48 h (Table 4.3). Specifically, the mean recovery rates for both PP particles and PET fibers were > 85% (SD < 10) in all treatments, except for PP particles in the ERC treatment (67% ± 47).

Table 4.3: Percentage (mean ± standard deviation) of microplastic recovery rates of from spike-recovery test in three treatment groups during single exposure of adult damselfish *Pomacentrus amboinensis* to blue polypropylene (PP) particles and polyethylene (PET) fibers in this controlled laboratory experiment. Control treatment was not included as no microplastics were added. Spike-recovery test was done in triplicate per treatment group. ERC = environmentally relevant concentration. Spike-recovery test was conducted with experimental microplastics and KOH only but following the protocol used for sample processing.

Treatment	PP (% of particle 12 L^{-1})	PET (% of fiber 12 L^{-1})
ERC (n = 3)	66.7 ± 47.1	100.0 ± 0.0
10x ERC (n = 3)	93.3 ± 9.3	96.7 ± 4.7
100x ERC (n = 3)	88.7 ± 4.9	88.7 ± 5.4

4.3.3. Microplastic Body Burden

Both PP particles and PET fibers were observed in the GITs of exposed fish, confirming ingestion of experimental microplastics by *P. amboinensis* (Table 4.4**,** Appendix C – Table S2). PET fibers from the 100x ERC treatment were occasionally found entangled, sometimes with other organic materials (Figure 4.2).

Table 4.4: Mean microplastic body burden fish^{-1} (absolute number ± standard deviation; n = 4 fish per treatment and depuration time) in three treatment groups (n = 84 tanks) during a single exposure of adult damselfish *Pomacentrus amboinensis* to blue polypropylene (PP) particles and polyester (PET) fibers in a controlled laboratory experiment. Proportional decline in microplastic body burden over the 128 h-depuration period, relative to body burden at 2 h depuration. Proportional decline was estimated across the three treatment groups and two experimental microplastic (n = 84 tanks) following the same microplastic exposure as described above. ERC = environmentally relevant concentrations. Control fish treatment was not included as no microplastics were added. Refer to Appendix C – Table S2 for raw data.

Depuration times (h)			2	4	8	16	32	64	128
microplastic body burden fish^{-1} (mean ± standard deviation)	Treatment	Microplastic type							
	ERC	PP particle	0.8 ± 0.5	0.8 ± 0.5	0.0 ± 0.0	0.0 ± 0.0	0.0 ± 0.0	0.0 ± 0.0	0.0 ± 0.0
		PET fiber	0.5 ± 06	0.8 ± 0.5	0.0 ± 0.0	0.0 ± 0.0	0.0 ± 0.0	0.0 ± 0.0	0.0 ± 0.0
	10 x ERC	PP particle	6.8 ± 1.3	3.5 ± 1.3	0.0 ± 0.0	0.0 ± 0.0	0.0 ± 0.0	0.0 ± 0.0	0.0 ± 0.0
		PET fiber	7.5 ± 2.4	6.8 ± 1.0	0.0 ± 0.0	0.3 ± 0.5	0.0 ± 0.0	0.0 ± 0.0	0.0 ± 0.0
	100x ERC	PP particle	55.8 ± 15.0	39.5 ± 10.8	1.3 ± 2.5	0.0 ± 0.0	0.0 ± 0.0	0.0 ± 0.0	0.0 ± 0.0
		PET fiber	58.5 ± 38.5	65.5 ± 18.8	10.5 ± 7.1	3.3 ± 2.1	1.0 ± 2.0	2.5 ± 4.4	0.8 ± 1.0
Microplastic depuration in relation to first sampling time (2 h) (%)			n/a	67.0	83.0	89.0	92.0	94.0	96.0

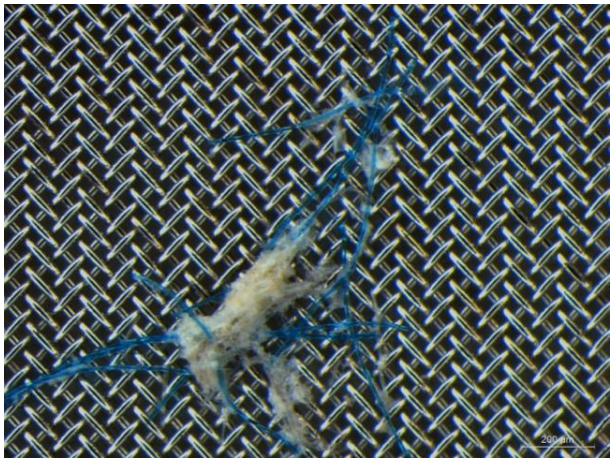

Figure 4.2: Polyester (PET) fibers, entangled with other ingested materials, recovered from an adult damselfish *Pomacentrus amboinensis*. Gut contents presented were recovered after 2 h of depuration following a single exposure to polypropylene particles and PET fibers at 100x environmentally relevant concentration.

At the 2-h depuration period, all fish exposed to the future projected concentrations of 10x ERC and 100x ERC contained both experimental microplastic types in their GIT (Figure 4.3). The microplastic body burden for these fish represented 25 - 98% of the total microplastics offered in these treatments. Of fish exposed to the ERC treatment, two contained both microplastic types, one contained a single microplastic type, and one did not contain either of the microplastics offered. Similar trends were observed at the 4-h depuration time point. Both microplastic types offered were present in all fish exposed to the 10x ERC and 100x ERC concentrations, while fish from the ERC treatment contained only one microplastic type each (one a PET fiber; the other a PP particle). While microplastic body burden was similar at the 2 and 4 h depuration periods, it decreased dramatically following 8 h of depuration. At this time, the experimental microplastics were only observed in individuals exposed to the 100x ERC treatment, at a maximum of 5% of the PP particle dose and 20% of the PET fiber dose. In addition, PP were only isolated from one fish, while PET fibers were still present in all four fish sampled at 8 h depuration. After 16 h, PP particles were completely depurated from all fish across all treatments. In contrast, PET fibers were still detected in two individual fish from the 100x ERC treatment up to and including 128 h, albeit at low abundances (< 2% of the body burden at 2 h depuration). Based on the fitted GLM ($R^2 = 0.86$), mean microplastic body burden was influenced by the type of microplastic offered, the exposure concentration and the depuration period ($p < 0.001$), but not by fish weight ($p = 0.49$) (Table 4.5). Overall, mean body burden for PET fibers was 2.2 times higher than for PP particles (Figure 4.3). Within individual treatments, body burden increased as concentration of exposure increased. Fish exposed to the 10x and 100x ERC treatments contained 8.5 and 91.8 times more experimental microplastics than ERC, respectively. Finally, the most significant change in body burden over time occurred within 8 h, when, considering all concentrations of exposure, the number of experimental microplastics in the GIT dropped 83% from the first sampling time (2 h) (Table 4.4).

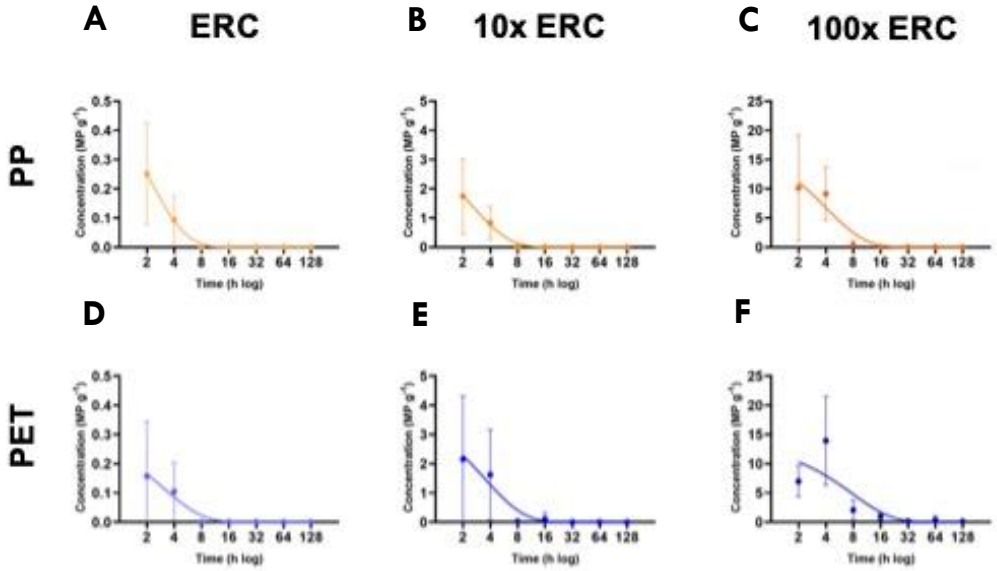

Figure 4.3: Mean microplastic body burden fish-1 (± standard deviation) in three treatment groups (n = 84 tanks) during a single exposure of adult damselfish *Pomacentrus amboinensis* to polypropylene (PP) particles and polyethylene (PET) fibers in a controlled laboratory experiment. Mean body burden is presented for four damselfish collected at each of the seven depuration times (2, 4, 8, 16, 32, 64 and 128 h). ERC = environmentally relevant concentrations. Each graph corresponds to a combination of experimental microplastic and concentration of exposure. (A) PP-ERC (B) PP-10x ERC (C) PP-100x ERC (D) PET-ERC (E) PET- 10x ERC (F) PET- 100x ERC.

Table 4.5: Differences in body burden over time due to microplastic type, microplastic concentration or fish weight, following a single exposure of adult damselfish *Pomacentrus amboinensis* to blue polypropylene (PP) particles and polyester (PET) fibers in a controlled laboratory experiment. Estimated regression parameters, standard errors (Std. error), z-values and p-values for the general linear model presented in Eq 1.

	Estimate	Std. error	z-value	p-value
Intercept	1.32094	0.42367	3.11800	0.00182
PP	-0.78655	0.22393	-3.51200	0.00044
10x ERC	2.14352	0.40928	5.23700	1.63e-07
100x ERC	4.51990	0.39654	11.39800	< 2e-16
Log(depuration)	-1.59942	0.11341	-14.10300	< 2e-16
Weight	0.02199	0.03213	0.68400	0.49371

4.3.4. Microplastic Depuration Rates and Elimination Half-life

Depuration rates varied from 0.13 microplastics h^{-1} (PET 100x ERC) to 0.52 microplastics h^{-1} (PP ERC) (Table 4.6), and were significantly influenced by microplastic type and

concentration offered (Welch's ANOVA W (5, 72.49) = 41.48 , $p < 0.0001$) (Figure 4.3). PP depuration rates were significantly faster than those of PET at all concentrations tested ($p < 0.05$) (Appendix C –Table S3). However, regardless of microplastic type encountered, depuration rates decreased with increasing concentration. Fish from the 100x ERC treatment had significantly slower depuration rates than fish from the two lower ERC treatments ($p < 0.0001$). The shortest elimination half-life was observed for PP particles at the lowest ERC (1.34 h); the longest was for PET fibers at 100x ERC (5.41 h) (Table 4.6).

Table 4.6: Microplastics depuration rate (in items h^{-1}) with 95% confidence interval (CI), and elimination half-life (h) of polypropylene (PP) particles and polyester (PET) fibers in three treatment groups (n = 84 tanks) following a single exposure of adult damselfish *Pomacentrus amboinensis* in a controlled laboratory experiment. ERC = environmentally relevant concentrations.

	PP particles			PET fibers		
	ERC	10x ERC	100x ERC	ERC	10x ERC	100x ERC
Depuration rate (item h^{-1})	0.52	0.42	0.25	0.33	0.29	0.13
95% CI	0.26 to 1.14	0.21 to 0.87	0.12 to 0.49	0.10 to 0.96	0.10 to 0.72	0.05 to 0.26
Elimination Half-life (h)	1.34	1.64	2.77	2.12	2.4	5.41

4.3.5. Monitoring Contamination

No experimental microplastics (PP particles and PET fibers) were found in the GITs of the four control fish, nor in blank processing controls collected during fish dissection, GIT digestion and filtration, confirming that (cross-)contamination over the course of the study was not evident. On the other hand, extraneous putative microplastics were visually identified in the GITs of all field control, experimental control and experimental fish (n = 92) and likewise in all blank processing controls (n = 7, one per sampling time) despite best efforts to minimize such contamination. In total, 374 putative microplastics were visually identified across all 92 fish. Forty-four putative microplastics were excluded from further analysis as polymer composition could not be determined due to the poor quality of acquired FTIR spectra. Of the remaining 330 extraneous putative microplastics, 67 matched physical and chemical characteristics of items from the contaminant library (i.e. same shape, color and $\geq$ 90% spectral match) and were deemed to have originated from sample processing activities (Figure 4.4a).

From these items, the majority was airborne contamination (n= 56), the rest originated from clothing, including the lab coat, and was comprised of cellulose-based items (n = 11). No microplastic contamination from the experimental set up was observed (e.g. tanks, pipelines and filtration system). The other 263 items did not match physical and chemical characteristics of items from the contaminant library, including equipment such as fish tanks and tank lids, and were deemed to come from experimental procedures (i.e. experimental air, water or fish food). While it is possible that some of these items came with the fish from the environment, the pre-depuration time of 3-6 days should preclude this.

Physical and chemical characterization of these 263 extraneous putative microplastics revealed that 57 were synthetic plastics, 26 were semi-synthetic plastics (Figure 4.4b) and 100 were naturally derived anthropogenic polymers. For example, many fibers were identified as being cellulose-based but were highly colored with uniform shape and/or were intertwined (i.e. anthropogenic but naturally derived). The remaining 80 items were determined to be naturally-derived and a natural origin could not be discounted. Three of the four field control fish contained microplastics in their GITs including both synthetic (e.g. 2 PP, 1 PE, and 1 with both PE and PP) and semi-synthetic (e.g. 2 rayon:PET) items. In contrast, none of the four laboratory acclimated control fish contained any synthetic items and only one contained a semi-synthetic item (cotton:rayon fiber). Similarly, the majority of laboratory exposed fish were not contaminated with microplastics (n = 56 of 84; 67%). Most of those that were contaminated with extraneous microplastics contained either one (n = 14 fish) or two (n = 9 fish) items, which were predominantly polyacrylate, polyester and nylon-based synthetic fibers (e.g. cotton:PET, rayon:PET, and rayon:nylon) (Figure 4.4c). Nine synthetic items were isolated from a single treated fish, and semi-synthetic items were found in 16 treated fish. Overall, contamination of field, control and treated fish with synthetic and semi-synthetic extraneous items comprised predominantly of fibers (n = 64) rather than particles (n = 19).

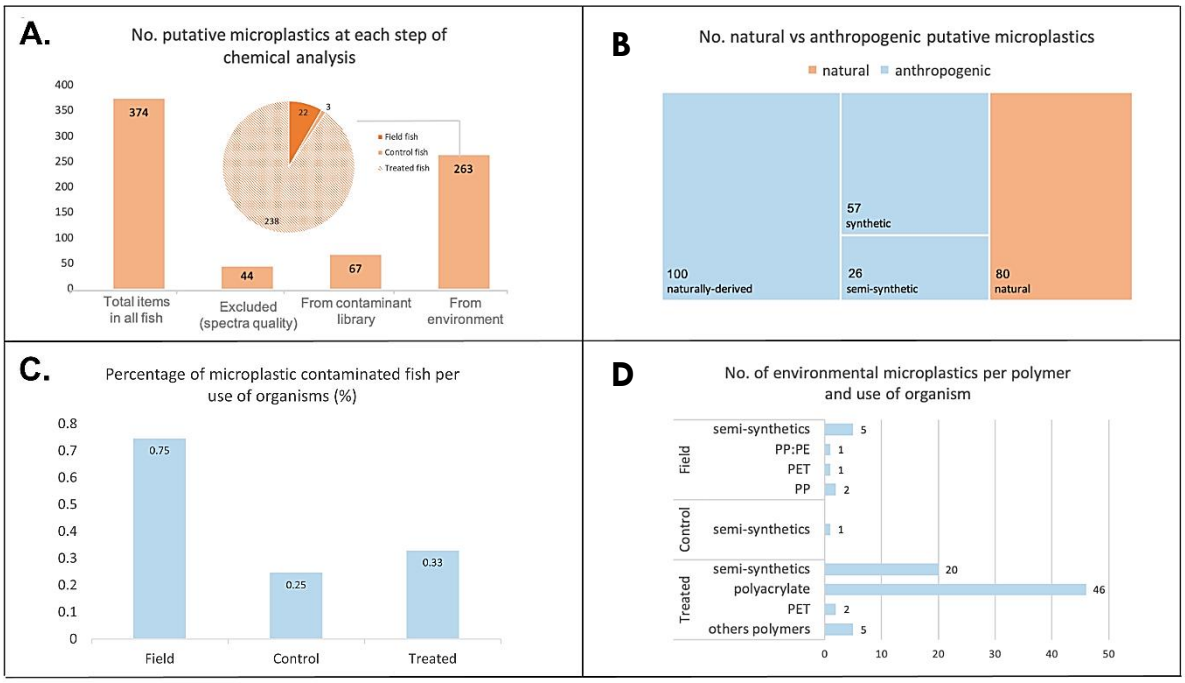

Figure 4.4: Quantification and potential sources of extraneous microplastic contamination throughout a single exposure study of adult damselfish *Pomacentrus amboinensis* to polypropylene (PP) particles and polyethylene (PET) fibers in a controlled laboratory experiment. (A) Total number of putative microplastics visually identified in the fishes' gastrointestinal tracts (GIT), with 67 items likely originating from sample processing procedures, and 263 items deemed to come from experimental system and procedures. (B) Assignment of 263 putative microplastics to natural, and anthropogenic – naturally-derived, semi-synthetic, or synthetic items. (C) Percentage of field control, experimental control and experimental treated fish contaminated with extraneous microplastics. (D) Polymer type and number of extraneous microplastics found in field control, experimental control and experimental treated fish.

4.4. Discussion

Ours is one of the first studies to investigate and confirm microplastic ingestion using environmentally relevant exposure conditions in a controlled laboratory experiment (Rochman et al., 2019), and provide strong support for microplastic contamination trends observed in marine organisms collected in the field. Specifically, microplastic ingestion by adult *P. amboinensis,* a planktivorous coral reef fish, occurred regardless of the microplastic polymer type (PP, PET), shape (irregular fragments, regular fibers), size (125 to 250 µm, 600 to 700 µm) or exposure concentration (ERC, 10x ERC, 100x ERC). Importantly, the measured microplastic concentrations in this experiment were similar to their nominal values, confirming

that PP particles and PET fibers were present at the desired concentrations and available for ingestion by individual damselfish. Both body burdens and depuration rates differed between the two experimental microplastics, with body burden of PET fibers being 2.2 times greater, and depuration rates of PET fibers being significantly lower than that for PP particles. For both microplastic types, exposure to higher concentrations led to an increase in microplastic body burden and lower depuration rates. These findings confirm ingestion of environmentally relevant PP particles and PET fibers by *P. amboinensis* and demonstrate for the first time the influence of microplastic characteristics and concentration on depuration rates of coral reef fish.

Ingestion of microplastic fragments and fibers has been reported for a variety of marine planktivorous fish species, both in the field (Compa et al., 2018; Jensen et al., 2019; Tanaka and Takada, 2016) and in the laboratory (Cong et al., 2019; Critchell and Hoogenboom, 2018; Xiong et al., 2019). Based on the literature, two mechanisms could explain the pattern of microplastic ingestion observed in this study: 1) fish selectively or non-randomly ingesting microplastics (Bour et al., 2020b; Jensen et al., 2019; Mizraji et al., 2017; Ory et al., 2018), or 2) fish passively or inadvertently ingesting microplastics while feeding (Roch et al., 2020). In this study, selective feeding cannot be ruled out as the experimental fish were pre-starved and the biofouled experimental microplastics, likely emitting dimethyl sulfide, may have acted as an attractant as has been reported for seabirds (Savoca et al., 2016), fish (Savoca et al., 2017) and copepods (Procter et al., 2019). Conversely, passive or inadvertent ingestion may have occurred given that exposures were conducted concurrently with normal feeding, and microplastic body burden appeared proportional to the exposure concentration. Passive or inadvertent microplastic ingestion could also explain the observed variabilities in body burden within the same exposure treatments, such as those ranging from 0 to 100% in the ERC treatment. Highly variable microdebris ingestion, including microplastic ingestion, is commonly reported for fish, both in field (Compa et al., 2018; Garnier et al., 2019; Jensen et al., 2019; Kroon et al., 2018b) and in experimental (Hoang and Felix-Kim, 2020; Lu et al., 2016; Xiong et al., 2019) studies. For example, adult *P. amboinensis* collected in the central GBR WHA contained an average of four microdebris items per individual fish, with a range from zero to 131 items (Jensen et al., 2019). In the laboratory, larvae of the same species also showed high variability in microplastic intake (McCormick et al., 2020). Together, these results

and those of previous studies indicate likely but inconsistent ingestion of microplastics by fish, particularly at environmentally relevant levels of exposure. With increasing exposure concentrations, however, variability in microplastic ingestion decreased suggesting that it may become more difficult for fish like *P. amboinensis* to avoid ingesting microplastics inadvertently while feeding.

The depuration rate of experimental microplastics ingested by *P. amboinensis* was relatively short, with most being eliminated within 8 h. At this timepoint, PP particles and PET fibers were only observed in the GITs of fish exposed to the 100x ERC treatment. After 16 h, PP particles were no longer observed in any of the fish, and after 128 h only two fish contained a small number of PET fibers. The observed residence time of microplastics in fish GITs suggests temporary microplastic contamination and a low likelihood of accumulation after ingestion. Although microplastics are commonly reported in coastal and marine fish collected in the field, when these studies are more closely evaluated, as in Kroon et al. (2018b), the majority of individual fish examined (i.e. >80%) do not appear to be contaminated. This may indicate that microplastics are transitory in wild fish and may not accumulate at current or future ERCs (Santana et al., 2017). Nonetheless, compared with natural food, which is depurated by *P. amboinensis* typically within 3-5 h and at the most <10 h after ingestion (Marnane and Bellwood, 1997), PP and PET microplastics were substantially slower to traverse the GIT. Whether these differences in depuration rates between natural food and microplastics affect energy acquisition for this species is unknown, but possible in theory. For example, the longer residency time of microplastics compared to natural food items could support the hypothesis that microplastic ingestion can impact organism fitness (Besseling et al., 2013; Cole et al., 2015; Lo and Chan, 2018).

Similar or even shorter microplastic depuration periods have been reported for various aquatic organisms, including fish (Dawson et al., 2018; Mazurais et al., 2015; Xiong et al., 2019). The subtle differences in depuration periods among studies could be related to variations in experimental design, including characteristics of microplastics used, such as polymer type, shape, size, color, and concentration (Xiong et al., 2019). Furthermore, characteristics of the species being investigated (such as feeding habits, trophic levels, morphology, and life stage) may also influence ingestion and depuration rates (Bour et al., 2018a; Xu et al., 2020b). For example, *P. amboinensis* larvae were reported to take up to 14 hours to depurate transparent

PS microspheres (200-300µm, 167 microsphere L^{-1}) ingested during a one hour exposure experiment (McCormick et al., 2020). In turn, microplastic exposure (i.e. 50 PET fibers of 50 to 500 µm in length, and 50 PE irregular fragments > 63µm per food pellet, with no color specification) of planktivorous adult goldfish *Carassius auratus* resulted in similar microplastic retention as the fish used in the present study (up to 3 of 50 beads and fibers ingested after six days), but in slower depuration rate (Grigorakis et al., 2017). To better elucidate patterns of microplastic contamination and associated risks in marine organisms, future depuration studies should compare and investigate the role of physical and chemical properties of different microplastics, as well as biological and ecological characteristics of the species under investigation.

This study showes that fish body burden and depuration rates were significantly affected by the experimental microplastic they were exposed to. At all doses, body burdens were lower and depuration rates faster for PP particles compared to PET fibers. Considering that the tested microplastics differed in (i) polymer composition, (ii) size, and (ii) shape, any or all of these factors could potentially influence the observed results. To be best of my knowledge, studies comparing microplastic uptake and depuration rates across different polymer compositions are still missing (Grigorakis et al., 2017). In contrast, larger microplastics have been observed to be depurated more quickly (Xiong et al., 2019), suggesting that the shape and size of the experimental microplastics used here may be likely explanations for the observed patterns. The slower depuration of PET fibers observed here corroborates studies that report the prevalence of fibers in wild organisms, including fish, from coastal and marine environments (Filgueiras et al., 2020; Jensen et al., 2019; Kroon et al., 2018b; Xu et al., 2020a). Moreover, it supports the hypothesis that microplastic fibers may pose a greater risk to marine organisms than microplastic particles (Au et al., 2015; Song et al., 2019), although few studies to date have examined potential biological effects of microplastic fibers. Accumulation and entanglement of fibers in the GIT has been observed in fish (Jensen et al., 2019) and may impact the gut passage time of microplastics in fish and other marine organisms (Welden and Cowie, 2016; Xiong et al., 2019). Xiong et al. (2019) also suggested that the presence of food along with microplastics in the GIT can increase microplastic retention. In the present study, clumps of PET fibers entangled with gut contents were occasionally found in the GIT of exposed fish (Figure 4.2), however, they were not observed consistently enough to confidently state that

they contributed to the differences in depuration rates. Another hypothesis is that the GIT morphology may contribute to retention of fibers, potentially influencing fiber gut passage time (Welden and Cowie, 2016); whether this is true for *P. amboinensis* remains to be determined.

For both experimental microplastics, body burdens and depuration rates increased with increasing exposure concentrations. This is opposite to patterns for natural food which moves faster through fish GITs with increasing concentration (German, 2011). This suggests that microplastic ingestion, and potential effects on planktivorous fish like *P. amboinensis*, are strongly influenced by the amount of microplastics present in their environment (Ding et al., 2018; Roch et al., 2020). Thus, higher risk of biological contamination and subsequent effects are likely associated with environments that are more contaminated (Everaert et al., 2020), such as accumulation zones (e.g. gyres (Eriksen et al., 2013) and benthic habitats (Barrett et al., 2020; Ogata et al., 2009), as well as areas adjacent to highly populated regions or areas of industrial (Li et al., 2020a) and commercial fishery (Xue et al., 2020) interest. Similarly, the presented findings are consistent with predictions that microplastic body burdens will increase in marine fish along with projected increases in marine microplastic contamination (Everaert et al., 2020; Geyer et al., 2017; Jambeck et al., 2015b), driven by the estimated 400% rise in annual plastic production by 2100 (Everaert et al., 2020).

Complete elimination of contamination with extraneous microplastics is challenging (Prata et al., 2021) and efforts to do so are rarely quantified and reported on in microplastic exposure studies (e.g. Nanninga et al., 2020; Zhao et al., 2020). Ours is the first to quantify extraneous microplastics in the GITs of individual fish and link them to potential sources (i.e. field, experimental system or sample processing procedures) to discuss potential elimination strategies. Control fish collected and euthanized in the field contained both synthetic and semi-synthetic extraneous items different to those found in experimental control and exposed fish. This corroborates that experimental fish had depurated any microplastics brought in from the field during acclimation. Despite measures put in place to prevent contamination, 67 extraneous putative microplastics were retrieved from experimental control and exposed fish, with 20% of these putative microplastics linked with items used and recovered during sample processing procedures, specifically airborne items and clothing. All clothing, including lab coats, worn during this study were cellulose-based, thus were not considered further. Nevertheless, monitoring it highlighted how important is to avoid synthetic and semi-synthetic

clothing while conducting microplastic studies, including experimental procedures. The remaining 80%, primarily polyacrylate and semi-synthetics fibers, could not be linked to specific items and is assumed to have originated from the experimental air, water or fish food. Whether these extraneous microplastics influenced the ingestion and depuration rates of experimental microplastics remains unknown. This exposure study was conducted in a general use laboratory at a remote field research station, and access to sophisticated filtration systems to clarify incoming air and seawater, was not available. Similar limitations could be faced by many experimental researchers, however, these are not frequently considered or discussed in the microplastic literature (Prata et al., 2021). Results from this study highlight the need for elimination of contamination sources where possible, and importantly for enhanced data quality control through robust study design with relevant experimental controls and stringent monitoring of background contamination. This is particularly important for microplastic studies using exposure conditions that reflect ERCs.

4.5. Conclusion

In summary, this study confirmed that the planktivorous damselfish *P. amboinensis* ingests environmentally relevant types (specifically irregular shaped blue PP particles and PET fibers) and concentrations of microplastics. After a single exposure to experimental microplastics, the majority of PP particles and PET fibers were eliminated from the GIT within 8 h, with most items completely purged by 128 h. Damselfish ingested both experimental microplastics at all concentrations, with body burden of PET fibers being 2.2 times greater, and depuration rates of PET fibers significantly lower than that for PP particles. For both microplastic types, exposure to higher concentrations led to an increase in body burden and lower depuration rates. These results corroborate the higher abundance of microplastic fibers versus particles reported in many wild-caught marine organisms, and highlight the need for more research on the impacts of microplastic fibers on marine organisms. The presented findings also support the hypothesis that environments with higher levels of microplastic contamination (e.g. current “hotspots”) pose a greater risk to marine organisms due to increased microplastic ingestion and prolonged depuration rates, and that sporadic exposure to microplastics might have lower microplastic-associated risks. Finally, despite measures put in place to prevent contamination, extraneous

microplastics were recovered from experimental fish, highlighting the challenge to completely eliminate contamination in microplastic exposure studies. This is of particular concern for experiments examining the impacts of environmentally relevant microplastic exposure. Thus, it is strongly recommended that controlled exposure studies quantify and report on contamination with extraneous microplastics to inform and continuously improve protocols for future microplastics research.

Chapter 5: Elevated seasonal temperatures increase the risk profile of microplastic fibres for juvenile *Acanthochromis polyacanthus*

Abstract

Effect studies using environmentally relevant microplastic exposure levels, under various warming scenarios, are relevant to ecological risk assessments and environmental management. Yet scenario of exposure in laboratory studies are often not aligned with field conditions. To assess the concurrent effects that microplastics and temperature exposure have on the health and fitness of juvenile *Acanthochromis polyacanthus*, this study, conducted during the austral winter, used environmentally relevant predicted concentrations of polyester (PET) fibres (0, 1.1 and 11 PET L^{-1}) and predicted elevated winter seawater temperatures experienced on the central Great Barrier Reef (GBR) (2020 23.7, 2050 25.2 and 2100 26.7˚C). An 8-week chronic microplastic exposure was simulated using a custom-built automated dosing system, developed specifically for this experiment. During this period, the system was maintained at seawater temperatures representing a 5-year averaged July daily temperature based on observations from Davis Reef, central GBR (ambient), or predicted future temperatures. Multiple physiological endpoints were examined to comprehensively assess effects of concurrently increasing microplastics and temperature on key molecular and phenotypic health and fitness parameters such as cortisol, total lipids, growth and condition factor were measured under the conditions evaluated. Microplastic uptake by *A. polyacanthus* only occurred via ingestion and was influenced solely by microplastic concentration. Increased daily winter temperature correlated to elevated levels of cortisol, but this was significantly decreased by concomitant exposure to the highest tested PET concentration. However, no measurable effects on growth, body condition and total lipid content were observed, suggesting that the impact of continued unabated microplastic contamination whilst mean GBR winter seawater temperatures increase, will be subtle.

Key words: effects, damselfish, microplastic fibre, PET, climate change

5.1. Introduction

Marine ecosystems are increasingly affected by anthropogenic factors, such as climate change and pollution. Microplastics (1 µm to 5mm in length) are ubiquitous and, based on their various shapes, sizes, colours and chemical composition (Rochman et al., 2019), are considered a complex pollutant (Everaert et al., 2020; Huang et al., 2021) (Horton and Barnes, 2020). Under laboratory conditions, microplastic exposure and uptake (via either passive or selective ingestion) has been shown to cause adverse health effects in organisms at molecular and individual levels of organization (Tort, 2011). For marine fishes, such effects include DNA damage and other oxidative stress (Avio et al., 2015b; Espinosa et al., 2017; Pannetier et al., 2020), disruption in feeding, body weight and reproduction (Naidoo and Glassom, 2019; Yin et al., 2018), along with behavioural disturbances that alter predator-prey dynamics including shoaling, boldness and distance from shelter (Barboza et al., 2018; McCormick et al., 2020; Yin et al., 2018). Consequently, there is widespread concern that such effects on organisms may lead to broader ecological changes and a decline in overall ecosystem health (DAWE, 2021; Karasaki et al., 2020; SAM, 2019).

To elucidate the nature and extent of microplastic effects in the marine environment, and the immediate and long-term impacts of microplastic presence on the overall health of ecosystems, experimental studies should apply environmentally relevant parameters and exposure concentrations (Horton, 2021) (GESAMP, 2016; Rochman et al., 2019). Environmentally relevant parameters can include the physical and chemical characteristics resembling those found in the environment, as well as realistic concentration (Horton, 2021; Rochman et al., 2019) and exposure regimes (Horton, 2021). Thus far, in studies of microplastic impacts on fish, only polymer type has been extensively explored in terms of environmental relevance (Besseling et al., 2013; Jeong et al., 2016; Santana et al., 2018). In contrast, the size of microplastics generally used in experiments is often much smaller than that reported in the field (McCormick et al., 2020) (Fonte et al., 2016; Jensen et al., 2019; Yin et al., 2018) (Chapter 3), although some argue that this may be due to logistical constraints of field studies resulting in under sampling of smaller items. Similarly, spheres (i.e., perfectly round manufactured microplastics) are the most frequently used microplastic shape (Cole and Galloway, 2015; Guven et al., 2018), whereas irregular or fibrous microplastics are far more

commonly reported in the marine environment and within organisms (Horton, 2021) (Chapter 3, Chapter 4). Frequently, microplastic colours are either not reported (Guven et al., 2018; Jeong et al., 2016; Naidoo and Glassom, 2019) or not justified based on field observations (Brun et al., 2019; Fonte et al., 2016), although colour can play an important role in microplastic uptake for fish that rely on visual cues when foraging (Ory et al., 2017; Sa et al., 2015; Xiong et al., 2019). Unrealistic nominal concentrations are also often used and can represent many orders of magnitude or more than what is found in the field (Santana and Turra, 2020; Yin et al., 2018). Lastly, constant exposures throughout time are not well explored, largely due to logistical constraints. Such studies are usually conducted with one or two intermittent exposure events per day in parallel with a feeding regime (Critchell and Hoogenboom, 2018; Rochman et al., 2014). However chronic exposures to microplastics might better represent what is occurring in the field (Horton, 2021).

As marine microplastics do not occur in isolation from other anthropogenic pressures, the inclusion of multiple stressors should also be explored to reveal environmentally relevant outcomes (Horton and Barnes, 2020). In coral reef ecosystems, for example, climate change and associated warming seawater temperatures represent imminent threats to organisms due to their naturally low tolerance to temperature fluctuations (Johansen and Jones, 2011; Stuart-Smith et al., 2017). When reef fishes are exposed to predicted increased summer seawater temperatures, changes in physiological traits are observed, for example reduced growth rates and lower reproductive success (Donelson et al., 2010; Munday et al., 2008). Similarly, fish behaviour has been reported to be affected by extreme seawater temperatures (Hoegh-Guldberg and Bruno, 2010), with potential adverse impacts on population structure (Johansen and Jones, 2011). Although underexplored for reef fishes, thresholds of stress and effects might change seasonally for other coral reef organisms, such as corals (Berkelmans and Willis, 1999), highlighting the importance of undertaking seasonal investigations to understand the full extent of climate change effects due to deviations from mean temperatures throughout the year. Regarding tropical coral reef fishes, only one study has investigated the effects of increasing winter seawater temperatures on health (Donelson et al., 2011) and observed an elevation in resting metabolism rates, which could potentially lead to changes in energy allocation and altered ecologically relevant traits, such as growth, reproduction, and behaviour. In other environments, such as temperate waters, warmer winter temperatures lead to smaller egg sizes

of Arctic char fish, as well as decreased hatching success and smaller larvae (Farmer et al., 2015). Hence, microplastic exposure and increased seasonal seawater temperatures are likely to occur simultaneously and potentially act synergistically. Despite this threat, only two studies have assessed cumulative effects of these two stressors on marine fishes within a multifactorial experiment. Synergistic influences of microplastics and temperature on temperate estuarine gobies have been demonstrated through changes in metabolic activity (i.e., ethoxyresorufin O-deethylase and glutathione S-transferase) (Ferreira et al., 2016; Fonte et al., 2016), changes in behaviour (Fonte et al., 2016), and increased mortality rate (Ferreira et al., 2016). Together, these studies also highlight the need to further explore synergistic effects of microplastics and changes in seawater temperature due to climate change. Furthermore, these studies also stress the importance to measure multiple endpoints from different levels of biological organization to establish comprehensive and relevant impacts on organisms (Ankley et al., 2010; USEPA, 1998).

This study assessed the combined effects of predicted (i.e. elevated) microplastic concentrations and austral winter temperatures on important health and fitness parameters in a coral reef fish at ecologically relevant levels. Spiny chromis (*Acanthochromis polyacanthus*) is a model species (Fakan and McCormick, 2019; Hannan et al., 2020; Hilder and Pankhurst, 2003; Laubenstein et al., 2019) which experiences both microplastic and seawater warming pressures throughout the Great Barrier Reef (Hall et al., 2015; Jensen et al., 2019; Kroon et al., 2018b) (Chapter 4). Juveniles represent an important developmental life stage, which includes post-brooding dispersal, establishment of new territory (Kavanagh, 1996) and have been used in microplastic ingestion laboratory experiments (Critchell and Hoogenboom, 2018). Here, juvenile *A. polyacanthus* were exposed to both microplastic contamination and elevated winter seawater temperatures, to test the hypothesis that combined increase in stressors would increase chronic fish stress (bound cortisol in tissues) and decrease energy reserves (total lipids), causing detrimental effects in fish growth and condition factor (Tort, 2011).

5.2. Materials and Methods

5.2.1. Experimental animals and husbandry

Animal collection and experimentation were conducted in accordance with ethics permit A2678 (James Cook University). Juvenile fish were sourced from the Northern regions of the Great Barrier Reef (Upolu Reef and Vlasoff Cay) by Cairns Marine, a commercial supplier of wild caught fishes (n = 240), and from reared stock held at James Cook University's Marine and Aquaculture Research Facilities Unit (MARFU, n = 84). Wild caught fish were kept in holding tanks (24˚C) at Cairns Marine facility for 4 days between collection and transportation to the experimental facility. Fish from MARFU were kept in outdoor holding tanks (ambient temperature) from hatching (summer) to the time of transportation to the experimental facility (late autumn). All fish were transported to the Australian Institute of Marine Science (AIMS, Townsville, Australia) National Sea Simulator. Upon arrival at AIMS, fish were homogenously distributed with 12 individuals per a tank (110 L; acrylic) based on fork length and weight. After four days of the acclimation period, fish were weighed (AND EK-410i, d=0.01g), sized (fork length) (SPI 2000, 1/1000 in) and tagged with elastomer (VIE, 20g x 1.5'' TERUMO needle).

Experimental tanks were supplied with temperature controlled filtered seawater (FSW; 0.5 µm) and operated in flow-through mode with a complete water exchange of 0.8 L h^{-1} to maintain water quality and provide adequate aeration. The room temperature was maintained at 23.0°C and seawater temperature was monitored in each tank (probe RTD-Pt100) to maintain treatment conditions (Section 2.3). Fish were subjected to a 10:14 h artificial light:dark cycle, using panel lights (300W LED full spectrum lights) controlled by a PAR sensor (Kye, SKL 26250). The light profile started at 7:00 (i.e., dawn) emitting 50 PAR and was slowly increased to 130 PAR at 12:30 (i.e., midday), then gradually returned to 50 PAR by 18:30 (i.e., dusk) after which fish were maintained in darkness. Dissolved oxygen (DO), ammonia (NH_3) and nitrate (NO_3) concentrations were monitored twice weekly in three randomly chosen tanks per treatment. DO was measured with a HQ40d portable multi-parameter meter (DO, 0.01 mg L^{-1}) and maintained at an average DO of 8.44 mg/L ± 0.19 (± 0.19). NH_3 and NO_3 were measured using Aquasonic test kits (NH_3, 0.1 ppm; NO_3, 5 ppm) and maintained at concentrations of 0

ppm and <5ppm, respectively. Tanks were cleaned twice weekly on non-sampling days to limit algae growth (e.g., crustose coralline algae).

Throughout the 21-day acclimation and the experimental period, fish were fed twice daily at an equivalent of 1.25% of their average initial weight following Critchell and Hoogenboom (2018). After four weeks, the food provided was doubled to account for fish growth. The first daily feeding comprised of post-hatched enriched artemia (500–800 μm) reared from a live artemia culture. The second feed comprised of ~ 800 μm irregularly shaped commercial food pellets (THERA +A; proteins min. 39%, fat min. 9%, and fibre max. 8%). Both food items were chosen based on having similar dimensions to experimental microplastics.

5.2.2. Experimental microplastics

Secondary (i.e., fragmented from primary plastics) blue polyester (polyethylene terephthalate; PET) textile fibres were chosen as experimental microplastics due to their ubiquitous presence in marine environments (Rebelein et al., 2021), including in coral reef ecosystems of the Great Barrier Reef and in resident fish (Jensen et al., 2019; Kroon et al., 2018b) (Chapter 3 and 4). PET fibres (500 to 750 μm in length) were artificially produced at AIMS from sewing thread (Gütermann, CA 02776) cut using sterile surgical blades (Paramount, BS EN 27740) and callipers (Kincrome, 1/1000 in). The chemical composition of PET fibres was confirmed by Fourier transform infrared spectroscopy (FTIR) (Appendix D). Stock solutions of virgin PET (58500 [MP_{low}] and 1350000 [MP_{high}] fibres in 20 ml of FSW [0.45 μm, Millipore® PTFE filters]) were prepared every 2 days. FSW was used as control ($MP_{control}$).

5.2.3. Experimental design

Fish were continuously exposed to the microplastics, via a custom-built automated dosing system that periodically released known concentrations of PET fibres from a header tank into experimental tanks. The use of the automated dosing system compensated for the loss of PET fibres due to the flowthrough experimental set-up and kept the concentration of exposure consistent over time. The system was designed, constructed, and validated to facilitate studying

the impacts of chronic exposure of juvenile *A. polyacanthus* to environmentally relevant concentrations of textile PET fibres on the Grreat Barrier Reef. Details of the design and validation of the automated dosing system are provided in the Appendix D. PET concentrations in tanks prior to exposing fish, and after the experiment, were measured and reported as the expected concentration in experimental tanks throughout the 8 weeks of exposure.

Fish (n = 12 fish per tank, and three tanks per treatment) were exposed to nine treatments over eight weeks, representing a factorial combination of three nominal microplastic concentrations ($MP_{control}$ – 0 PET L^{-1}; MP_{low} – approx. 1.1 PET L^{-1}; and MP_{high} – approx. 11 PET L^{-1}) and three different seawater temperatures: $T_{23.7}$ – ambient (at 23.7˚C); $T_{25.2}$ – ambient + 1.5°C (at 25.2˚C); and $T_{26.7}$ – ambient + 3.0°C (at 26.7˚C). Environmentally relevant concentrations of microplastic were extrapolated from monitored (Jensen et al., 2019, Chapter 3) and modelled (Everaert et al., 2020) microplastic concentrations in surface seawaters of the Great Barrier Reef. Future scenarios used here goes beyond concentrations predicted to 2100 (Everaert et al., 2020).

Ambient temperature was based on a 5-year averaged July daily temperature at Davis Reef, central GBR (Appendix D – Table S1). The elevated temperatures reflect future predicted values (IPCC, 2018). Three microplastic controls were used, one for each temperature treatment: $MP_{control}$: $T_{23.7}$, $MP_{control}$: $T_{25.2}$ and $MP_{control}$: $T_{26.7}$. During the acclimation period, tank temperatures were slowly increased by 0.5˚C per day (0.25˚C twice daily, over 3 days for $T_{25.2}$ and over 5 days for $T_{26.7}$). All fish were acclimated at the designated treatment temperature for another four days prior to commencing MP exposure treatments, including fish exposed to ambient temperature to ensure same start of the experimental exposure for all treatments.

To validate microplastic uptake, two fish per tank were randomly sacrificed using ice slurry after 1 week of exposure. Fish were then rinsed using Milli-Q water to remove any PET fibres that may have adhered to their skin. Fish were dissected to assess presence and quantity of PET in their gills and gastrointestinal tracts (GIT). This data was excluded from the final statistical analysis. The remaining fish (n=10 fish per tank) were exposed for a further seven weeks, after which they were euthanised using ice slurry, rinsed, weighed, sized and dissected to quantify microplastic uptake and evaluate health and fitness parameters (described in section 2.5, below).

5.2.4. Microplastics isolation from fish

Dissected fish gills and GIT were air dried, weighed (wet weight, w.w., Sartorius TE31025, max 3100 g, d 0.01 g) and subjected to alkaline digestion as per Chapter 4 to recover PET fibres. Briefly, fish tissues were treated with 10% potassium hydroxide (KOH, AR, Fisher, CAS No. 1310-58) at 40°C for 48 h using a ratio of 1:20 of GIT wet weight (g) to volume of KOH (mL). Digested samples were filtered through tiered 77 and 26 µm stainless-steel filters (19 mm diameter)(Schlawinsky, 2020), and rinsed with 70% EtOH to remove fat vestiges (Dawson et al., 2020). Retained experimental PET and other potential extraneous microplastic contamination were visually identified, counted and photographed using stereomicroscopy (Leica MZ16A, Leica DFC 500, Leica Application Suite LAS 4.4.0). PET fibres were readily distinguishable from other particulates based on the combination of shape, size and colour.

5.2.5. Health and fitness parameters

5.2.5.1. Cortisol and total lipids

Fish tissues (muscle, skin, scale and bones) (Sadoul and Geffroy, 2019) were lyophilized (LabConco, Free Zone 1) for 24 hours and weighed (Sartorius TE31025, max 3100 g, d 0.01 g). Dried tissue was ground using pestle and mortar, to which 10 mL of cold (4˚C) 1x PBS solution (Phosphate buffered saline, Sigma-Aldrich) was added and homogenized for 3 min using a bead beater (Biospec Products, Mini Beadbeater TM; 4 and 8 mm stainless-steel beads).

To estimate the bound cortisol and total lipids per gram of dry sample (i.e., dry weight or d.w.) an aliquot of fish homogenate (4 ml) was transferred to a borosilicate glass vial (40 ml) and extracted with ethyl acetate (35 ml, approx. 1:9 ratio). The homogenate was vortexed (Lab-Line Instruments, Super-Mixer 1291, 3x speed, 1 min), centrifuged (Beckman Coutler, Allegra X-15R, 1000 rpm, 2 min, 4 °C) and the ethyl acetate phase transferred to a pre-weighed glass vial for total lipid analysis. This was repeated once more and the combined ethyl acetate extract evaporated to dryness under a constant stream of N_2 (Techne Dri-Block DB.3D Sample Concentrator, 40˚C) and weighed for total lipids.

For cortisol analysis, a second aliquot (1 mL) of the homogenate was reconstituted by shaking (BioSan, PSU-20i shaker| 250 rpm, 90min) in 1 mL of ELISA buffer and analysed by Enzyme-linked Immunoassay (ELISA, Cayman Chemical Kit, Kit N° 500360). The cortisol analysis was validated using steps suggested in Metcalfe et al. (2018), including tests for parallelism (optimum dilution), extraction efficiency, and accuracy (spiking test). The results of the protocol validation are detailed in the Appendix D.

5.2.5.2. Growth and condition factor

Growth was calculated based on the initial and final wet weight (w.w.) of fish after eight weeks exposure, following the Specific Growth Rate equation (SGR, eq. 1) (Houde and Schekter, 1981; Lugert et al., 2016).

$$SGR = \{[\log(size_f) - \log(size_i)]/t\} * 100 \quad \text{(Eq. 1)}$$

where $size_i$ and $size_f$ are the initial and final w.w., respectively, and t is the time of the experiment in days. Condition factor was calculated based on Fulton's somatic condition factor equation (S_{CF}, eq. 2) adapted from Illing et al. (2018):

$$S_{CF} = 10^4(w.w./L^b) \quad \text{(Eq. 2)}$$

where w.w. is the fish wet weight (g), *L* the fish fork length (mm), and *b* is the slope of the linear regression of *log(w.w.)*.

5.2.6. Extraneous microplastic contamination control

Prior to the experiment, tanks were thoroughly washed using fresh water, soaked with 0.1% H_2O_2 solution for 4 h and again thoroughly washed using fresh water. Cleaned tanks were filled with FSW (1 µm; Waterco polyester thread bags, and 0.5 µm; HPF Water quality polypropylene sediment cartridge GT2-0K) in flow-through configuration (complete water exchange of 0.8 L h^{-1}). Seawater supplying the automated dosing system was similarly filtered (1 µm; Davey polyspun microlene filter). To prevent extraneous airborne microplastics

contaminating the system during the experiment, all experimental procedures were conducted in an enclosed room with restricted access. Prior to entering the room, clothes were delinted using a lint roller (Scotch-Brite®, 3M). The header tank and experimental tanks were covered with lids, except when stock solutions were replenished (header tank) or during cleaning (experimental tanks). Experimental tanks were cleaned using cellulose-based cloths and abrasive synthetic (mixture of polyester and viscose, transparent colour) sponges. Clothes and cotton laboratory coats were also delinted prior to sample collection, dissection and microplastic separation and characterisation. All equipment and tools used in these procedures were sequentially cleaned with reverse osmosis H_2O water, Milli-Q H_2O, 70% EtOH, or a combination of these. Cellulose-based cloths were used to wipe surfaces with filtered 70% EtOH. For sample processing, 10% KOH and 70% EtOH solutions were filtered to 0.45 µm (Millipore® PTFE filters).

5.2.7. Data analysis

Statistical data analysis was conducted using RStudio, version 1.3.1093. Best fitted models were chosen using an Akaike Information Criterion (AIC) test and DHARMa residual diagnostics. Differences in PET uptake within treatments were investigated by general linear models (GLM) with random effects (glmmTMB, $p < 0.05$). The model followed equation 3:

$$\text{Number of PET} = \text{mp} * \text{temperature} + \text{size} + (1 \mid \text{tank}) + \text{constant} \quad \text{(Eq. 3)}$$

Where "mp" corresponds to the microplastic treatments excluding control (MP_{low} and MP_{high}), and "temperature" corresponds to all seawater temperature treatments ($T_{23.7}$, $T_{25.2}$ and $T_{26.7}$). Fish size (fork length, mm) was included as a covariate in the GLM to account for its potential influence on microplastics uptake. Experimental tank was included in the model as a random factor since the experimental design included multiple fish per tank and three tanks per treatment. The model was fitted using a negative binomial distribution. Post-hoc comparisons were conducted using the package 'emmeans' (version 1.6.0), based on marginal means and predictive test distributions.

Similarly, differences in cortisol, total lipids, growth and condition factor between treatments were assessed following either equations 4, 5 or 6, respectively:

$$\text{cortisol} = \text{mp} * \text{temperature} + \text{size} + (1\,|\text{tank}) + \text{constant} \quad \text{(Eq. 4)}$$

$$\text{total lipis} = \text{mp} + \text{temperature} + \text{size} + (1\,|\text{tank}) + \text{constant} \quad \text{(Eq. 5)}$$

$$\text{growth or condition factor} = \text{mp} + \text{temperature} + (1\,|\text{tank}) + \text{constant} \quad \text{(Eq. 6)}$$

In these models, the factor "mp" included the microplastic control as well as exposed treatments ($MP_{control}$, MP_{low}, and MP_{high}) while "temperature" was considered as above. Factors "size" and "tank" were included in the model as per PET uptake analysis. Growth and condition factor models were fitted using gaussian distributions. Total lipids used beta distribution. For the analysis of cortisol, data were log transformed and models fitted using gaussian distributions. Post-hoc comparisons were conducted as described above.

5.3. Results

5.3.1. Validation and estimation of microplastic uptake

No PET fibres were found in $MP_{control}$ *A. polyacanthus* throughout the experiment. PET fibres were recovered from the GIT after both one and eight weeks of exposure confirming ingestion by *A. polyacanthus*; gills were clear of microplastics at both timepoints. However, microplastics were not isolated from every individual in the low exposure treatment at both timepoints. Despite the low replication, overall PET uptake after one week of exposure increased with increasing microplastic concentration, especially at the highest temperature (Appendix E – Table S1). The fitted glmmTBM confirmed microplastic uptake after 8-weeks exposure was only influenced by the exposure concentration ($p < 0.01$, Appendix E –Table S2, Figure 5.1). Overall, fish exposed to the highest concentration had 9.6 times more PET in their GIT than fish exposed to the lower concentration (Table 5.1). Temperature and fish size did not influence mean PET uptake ($p > 0.05$).

Table 5.1: Impacts of increasing microplastic (MP) exposure and elevated sea water temperature (T) on fish cortisol levels, total lipids, growth and condition factor. Control = $MP_{control}$, low PET exposure at

1.1 fibres L^{-1} = MP_{low} and high PET exposure at 11 fibres L^{-1} of filtered seawater = MPhigh. Values reported as mean ± SE. Polyethylene terephthalate = PET, dry weight = d.w., wet weight = w.w.

Treatment		Stress and fitness parameters				
MP	T ($T_{°C}$)	PET uptake (PET $fish^{-1}$)	Cortisol levels (pg g^{-1} d.w.)	Total lipids (g d.w.)	Growth (mm % day^{-1})	Condition Factor (g w.w. mm^{-3})
$MP_{control}$	$T_{23.7}$	0 ± 0	555.59 ± 76.10	0.048 ± 0.006	1.79 ± 0.08	0.91 ± 0.03
MP_{low}	$T_{23.7}$	6.97 ± 1.05	559.69 ± 170.92	0.038 ± 0.005	1.98 ± 0.09	0.88 ± 0.02
MP_{high}	$T_{23.7}$	70.07 ± 33.94	622.52 ± 81.90	0.048 ± 0.004	1.66 ± 0.10	0.92 ± 0.02
$MP_{control}$	$T_{25.2}$	0 ± 0	564.29 ± 78.05	0.035 ± 0.004	1.75 ± 0.08	0.85 ± 0.01
MP_{low}	$T_{25.2}$	9.20 ± 3.07	468.47 ± 89.14	0.038 ± 0.003	1.65 ± 0.10	0.90 ± 0.01
MP_{high}	$T_{25.2}$	239.20 ± 44.49	603.67 ± 69.39	0.039 ± 0.005	1.96 ± 0.09	0.92 ± 0.02
$MP_{control}$	$T_{26.7}$	0 ± 0	1017.74 ± 237.67	0.043 ± 0.005	1.97 ± 0.07	0.92 ± 0.02
MP_{low}	$T_{26.7}$	13.23 ± 3.37	649.20 ± 66.90	0.035 ± 0.005	1.83 ± 0.07	0.90 ± 0.02
MP_{high}	$T_{26.7}$	88.60 ± 34.19	434.81 ± 68.37	0.044 ± 0.005	1.98 ± 0.09	0.91 ± 0.01

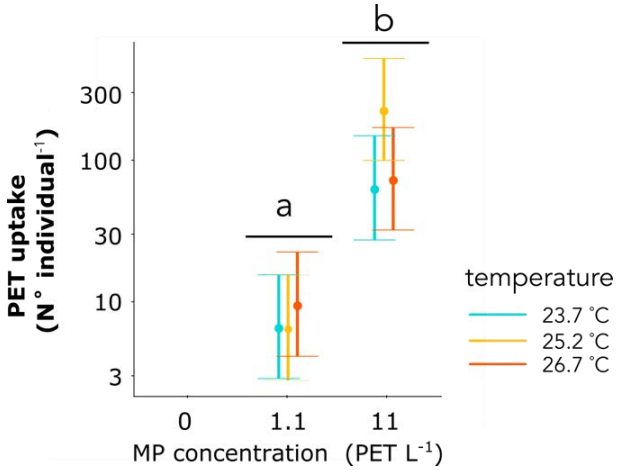

Figure 5.1: Number of ingested microplastic fibres in Spiny chromis (*Acanthochromis polyacanthus*) juveniles after an 8-week exposure to combined treatments of three microplastic concentrations (0, 1.1 and 11 PET L^{-1}) and three winter seawater temperatures (23.7, 25.2, and 26.7˚C). Symbols and error bars represent estimated marginal means and 95% confidence intervals. Letters indicate significant differences across the treatments with elevated microplastic concentrations (glmmTMB, Tukey post-hoc tests, $p<0.05$). Polyethylene terephthalate = PET.

5.3.2. Cortisol and total lipids

Visual observations of fish indicated no signs of stress, and feeding behaviour was normal throughout the experiment. Bound cortisol in the control group ($MP_{control}$:$T_{23.7}$) averaged 555.59 ± 76.10 pg g^{-1} (mean ± SE) (Table 5.1) and increased to 1017.74 ± 237.67 pg g^{-1} ($MP_{control}$:$T_{26.7}$) when exposed to the highest temperature. The introduction of low levels of microplastics (1.1 PET L^{-1}) followed the same trend (559.69 ± 170.92 to 649.20 ± 66.90 PET fibres per fish), but not significantly, whereas this trend was significantly reversed in fish exposed to the highest microplastics level (11 PET L^{-1}). Fitted glmmTBM and post hoc tests revealed significant interactions between microplastic concentration and seawater temperature resulting in a large reduction of cortisol at the highest temperature ($T_{26.7}$) as microplastic levels increased (622.52 ± 89.14 pg g^{-1} at $T_{23.7}$ to 434.81 ± 68.37 pg g^{-1} at $T_{26.7}$) ($p < 0.05$, Appendix E – Table S3, Figure 5.2a). At ambient and intermediate temperatures there was a negligible increase in cortisol as microplastic concentrations increased. Fish size, even in the control group, influenced cortisol ($p > 0.05$), which decreased with increasing weight.

Total lipid content in the control group ($MP_{control}$:$T_{23.7}$) averaged 0.048 ± 0.006 g d.w.$^{-1}$ (mean ± SE) (Table 5.1). Regardless of microplastic concentration (0, 1.1 or 11 PET L^{-1}), lipid content showed a non-significant inverse relationship with increasing temperature. The fitted glmmTBM revealed that microplastic concentration and seawater temperature did not influence mean total lipid content ($p > 0.05$, Appendix E – Table S4, Figure 5.2b). Fish size also inversely influenced total lipid content ($p < 0.05$), with decreasing total lipids at increasing wet weights.

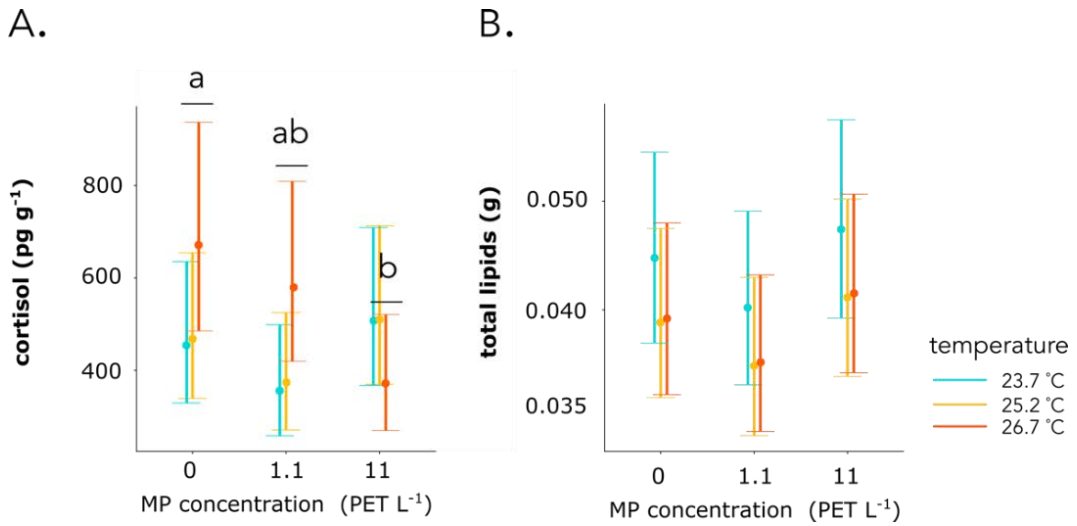

Figure 5.2: (A) Bound cortisol and (B) total lipids in whole body tissues of Spiny chromis (*Acanthochromis polyacanthus*) after an 8-week exposure to combined treatments of three microplastic concentrations (0, 1.1. and 11 PET L^{-1}) and three winter seawater temperatures (23.7, 25.2, and 26.7˚C). Symbols and error bars represent estimated marginal means and 95% confidence intervals. Letters indicate significant differences across the treatments with elevated microplastic concentrations (glmmTMB, Tukey post-hoc tests, $p<0.05$). Polyethylene terephthalate = PET.

5.3.3. Growth and Condition factor

Fish growth in the control group ($MP_{control}$:$T_{23.7}$) averaged 1.79 ± 0.08% day^{-1} (mean ± SE) (Table 5.1). Growth rates increased slightly with increasing temperature from 1.79 ± 0.08% day^{-1} ($MP_{control}$: $T_{23.7}$) to 1.97 ± 0.07% day^{-1} ($MP_{control}$:$T_{26.7}$). Fish exposed to the low microplastic concentrations and increased temperatures showed no change in growth rate, while fish exposed to the high microplastic treatment were marginally larger (1.66 ± 0.10 % day^{-1} at MP_{high}:$T_{23.7}$). However, the fitted glmmTBM indicates that microplastic exposure and seawater temperature did not significantly affect fish growth ($p > 0.05$, Appendix E – Table S5) (Figure 5.3a).

Fish condition factor in the control group ($MP_{control}$:$T_{23.7}$) averaged 0.91 ± 0.03 (mean ± SE) (Table 5.1), and did not significantly vary (glmmTMB, $p > 0.05$) across treatments ($p > 0.05$, Appendix E – Table S6, Figure 5.3b).

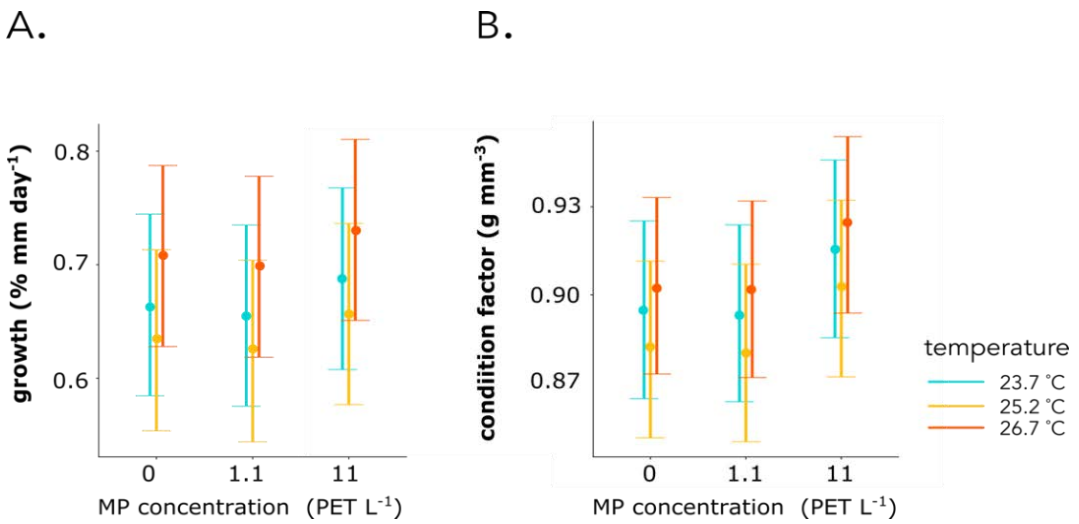

Figure 5.3: (A) Growth and (B) condition factor of Spiny chromis (*Acanthrochromis polyacanthus*) after an 8-week exposure to combined treatments of three microplastic concentrations (0, 1.1. and 11 PET L^{-1}) and three winter seawater temperatures (23.7, 25.2, and 26.7˚C). Symbols and error bars represent estimated marginal means and 95% confidence intervals. Polyethylene terephthalate = PET.

5.4. Discussion

Concerns about the effects of microplastics on marine organisms have resulted in numerous studies examining biological exposure and effects. However, exposure effect studies often employ unrealistic (or environmentally irrelevant) microplastic concentrations and physical characteristics (GESAMP, 2016; Horton, 2021; Rochman et al., 2019), and do not consider the impacts of other co-occurring environmental stressors, such as climate change associated warming (Horton and Barnes, 2020). As a result, findings do not readily translate to the environment and are therefore not suited to informing ecological risk assessments. To address this, the present study simulated environmentally relevant conditions of microplastic exposure in combination with elevated winter seawater temperatures and assessed key phenotypic and molecular health and fitness parameters of exposed fish to identify any associated ecological risks. By developing and using a "fit for purpose" microplastic automated dosing system, this study was able to gain novel insights into what effects future predicted microplastic contamination alone and in combination with seasonal temperature stress due to climate change have on the model coral reef fish, *A. polyacanthus.*

In fishes, uptake of microplastics can occur through ingestion and/or retention by gill rakers (Bour et al., 2020a; Yin et al., 2018; Zitouni et al., 2021). Here, PET fibres were solely ingested, with no microplastics found in gills of *A. polyacanthus* after one or eight weeks of exposure. Considering the highly elevated exposure concentrations employed in previous studies (e.g., 100,000 microplastics L^{-1}, Yin et al. (2018) and Bour et al. (2020a)), compared to the maximum 11 microplastics L^{-1} in this study), the findings presented suggest the route of microplastic uptake by fish is dose dependant, with predominantly passive uptake through the gills occurring with unrealistically high microplastic concentrations. This should, however, be validated by further studies, including with fish of different feeding strategies (e.g., carnivorous). Ingestion, on the other hand, occurred throughout the chronic exposure (8 weeks) to 1.1 and 11 PET fibres L^{-1}, irrespective of the seawater temperature, supporting ingestion as a major pathway of microplastic uptake (GESAMP, 2019; Roch et al., 2020). Irrespective of fish size, increased PET exposure resulted in increased ingestion, a relationship supported by previous studies reporting uptake of PET fragments by juvenile *A. polyacanthus* (Critchell and Hoogenboom, 2018) and of PET fibres and polypropylene (PP) fragments by adult *Pomacentrus amboinensis*, another planktivorous coral reef damselfish (Chapter 4). Together, these findings support the hypothesis that there is an increased risk to fish health resulting from ingestion of ever increasing microplastic contamination in marine environments (Everaert et al., 2020). Nonetheless, influences of seawater temperature, and in particular winter temperatures, on microplastics ingestion is poorly explored in the scientific literature, with no definitive relationship between temperature and microplastic uptake reported (Ferreira et al., 2016; Fonte et al., 2016). In this study, increased winter seawater temperature had no effect on microplastic uptake. This suggests that higher mean winter seawater temperatures, predicted to occur in the RCP 8.5 climate change scenarios (IPCC, 2018), are unlikely to increase juvenile *A. polyachantus* susceptibility to microplastic ingestion. The observed results could be related to the optimal thermal conditions of this fish species (Zarco-Perelló et al., 2012), which are close to the exposed increased seawater temperatures, and could be maintaining similar fish activity across temperature treatments, including feeding and susceptibility of microplastic uptake through ingestion. Further studies, however, should assess whether this holds true for fish using other feeding strategies (e.g., carnivorous) or for predicted higher summer seawater

temperatures, when fish are more likely to exceed their thermal tolerance and have altered feeding habits (Scott et al., 2017).

The four phenotypic health and fitness parameters measured revealed that microplastic uptake significantly inhibits or downregulates tissue bound cortisol at the highest seawater temperature examined. This confirms that microplastic contamination is a significant environmental stressor acting in combination with forecasted warming temperatures. Cortisol was affected by both microplastic exposure and elevated winter seawater temperature, and was also influenced by fish size. Cortisol is important in the vertebrate response to acute and chronic stress and acts by mediating the immune response - including immunosuppression - depending on the stressor (Rohonczy et al., 2021). Fish cortisol is known to increase when seawater temperature increases (Goikoetxea et al., 2021; Planas et al., 1990). This relationship was exhibited by control fish exposed to the highest tested temperatures, albeit non-significant. However, fish exposed to increased microplastic at the highest temperature tested displayed an antagonistic effect, with significant reduction in bound cortisol levels, which dropped below basal (i.e. $MP_{control}$) levels. Such downregulation (i.e., depletion) of cortisol may result from either dose-dependent PET toxicity, or associated PET additives (Gayathri et al., 2004; Singh and Bhalla, 2017), or due to a chronic stress response mechanism whereby cortisol is downregulated in fish tissues (Barton, 2002; Pickering and Pottinger, 1987; Pottinger, 1990; Shrimpton and Randall, 1994) or, a combination of the abovementioned scenarios.

Little information is available regarding specific toxicity pathways of PET and PET-associated chemical additives on cortisol in coral reef fishes. However, related literature reports toxicity of PET and PET-associated chemical additives to other aquatic and non-aquatic life, including humans (Mathieu-Denoncourt et al., 2015; Rodrigues et al., 2019). Toxic monomers such as phytoestrogens can leach from PET and act as endocrine disrupters (Singh and Bhalla, 2017). Similarly, low doses of di (2-ethyl hexyl) phthalate (DEHP), a plastic additive commonly used as a carrier in the textile dying process (Schönberger and Graf, 2018), was shown to decrease levels of cortisol in rats after 14 days of exposure. This was attributed to the toxic effect DEHP has on the adrenal gland (Gayathri et al., 2004). Generally, plastic monomers and additives are known to leach from plastic polymers under temperatures well in excess of the highest winter temperature treatment used here (26.7°C) (Saido and Taguichi, 2004). Yet, for some polymers, such as polystyrene (PS), monomer leachate into the

environment was reported at 30˚C, and is prevalent in various marine ecosystems, potentially at higher concentrations than the polymers themselves (Saido et al., 2020). Here, fish were chronically exposed to virgin PET textile fibres, thus leachates (monomers and chemical additives) may have supressed the high cortisol levels induced by the highest temperature tested, considering the temperature dependence of the leaching process. Nevertheless, further investigation of leachates associated with PET fibres used here, and the leaching rate as a function of moderate increase in temperature, is warranted to establish whether this process underlies the observations reported here.

Cortisol has been reported to be downregulated due to negative feedback. Cortisol in fish tissues, such as gills and liver, is mediated by corticoid-associated receptors (Barton, 2002; Pickering and Pottinger, 1987; Pottinger, 1990; Shrimpton and Randall, 1994), and the more receptors that are available in the target organ, the more cortisol it may contain (Danielsen and Stallcup, 1985). However, under conditions of chronic, repeated or multiple stressors, elevated levels of free or plasma-bound cortisol in fish downregulate corticoid-associated receptors in tissues and reduce cortisol responsiveness (Barton, 2002; Pickering and Pottinger, 1987; Pottinger, 1990; Shrimpton and Randall, 1994). In this study, the stress induced by increased microplastic exposure could be acting to suppress the bound cortisol in the thermally stressed fish, attenuating the effects of increased temperature. To verify this hypothesis, potential biomarkers including cortisol pathway metabolites, free and bound cortisol, and corticoid receptors in target tissues should be investigated.

Regardless of the mechanisms driving the cortisol downregulation, findings reported here suggest juvenile *A. polyacanthus* can cope with chronic exposure to realistic increases in marine microplastic contamination and winter seawater temperatures, likely because the combination of both stressors resulted in an antagonistic response in the fish. However, additional studies using other biomarkers responsive to heat stress in coral reef fishes (Madeira et al, 2017, Johansen et al, 2021) and/or exposures under predicted future summer temperatures are needed to determine whether microplastic uptake by this coral reef fish further exacerbates any stress associated with extreme future ocean temperatures forecasted for the Great Barrier Reef throughout the year. Likewise, it has been shown that predicted future temperatures affect many metabolic pathways in transgenerational juvenile *A. polyacanthus* raised at predicted future summer seawater temperatures (Veilleux et al., 2015), the altered metabolic pathways

thought to be associated with observed shifts in energy production in support of the maintenance of fish performance (Veilleux et al., 2015). It remains to be seen whether increased microplastic exposure alters this response in thermally adapted transgenerational fish.

In the present study, a correlation between levels of bound cortisol and fish size was observed, with smaller fish having significantly more cortisol than larger ones. Basal levels of cortisol underpin regular metabolic and behavioural functions (Mommsen et al., 1999), with natural changes in cortisol expected with growth (Barcellos et al., 2012). The relationship observed here has been reported previously and it was theorised that smaller sized fish have a stronger response to stressors (Kortet et al., 2019). Here, fish size was evenly distributed across treatment tanks thus smaller fish may have also been distressed by the presence of larger dominant individuals (Barlow et al., 1986), resulting in increased cortisol levels due to hierarchy/social interaction (Fox et al., 1997; Zhang et al., 2021). Regardless, effects of fish size on cortisol were overshadowed by both increasing microplastic concentration and elevated winter seawater temperature, highlighting the synergistic impact of both pervasive stressors on juveniles.

Fish exposed to chronic stress may regulate their energetic metabolism to cope with the new demands, a process often involving energy allocation to stress-related functions at the expense of primary functions, such as growth (Tort, 2011). However, total lipid content, growth and condition factor were not affected by the experimental treatments, suggesting the observed changes in cortisol did not require a significant energy allocation. These results contrast with a previous study where ingestion of PET fragments in the absence of food resulted in decreased growth in juvenile *A. polyacanthus* (Critchell and Hoogenboom, 2018), and differs from other studies reporting changes in total fish lipid content, growth or condition factor. However, in the aforementioned studies elevated microplastic concentrations were used, which were substantially higher (Lu et al., 2016; Naidoo and Glassom, 2019; Yin et al., 2018) than in this present study. *A. polyacanthus* fed *ad libitum* and exposed to environmentally relevant microplastic concentrations represents a more realistic microplastic exposure scenario. Findings also indicate that even with chronic microplastic exposure, the predicted elevated winter seawater temperatures for the central GBR are not detrimental to the fitness of juvenile *A. polyacanthus*, likely because these future seawater temperatures still fall close to the

optimum thermal range of this species (Zarco-Perelló et al., 2012). Cortisol, however, is also known to affect other fish traits, such as behaviour (Brun et al., 2019; Tang et al., 2021), and changes in behaviour have been shown to be directly influenced by microplastics (Critchell and Hoogenboom, 2018) (Ferreira et al., 2016) and by increased seawater temperature (Kua et al., 2020; Warren et al., 2016; Wen et al., 2018). Thus, assessing additional ecologically-related endpoints may provide further insights into the ecological risks associated with these two pervasive stressors when applied independently or concurrently.

5.5. Conclusion

Establishing fish response to cumulative stress exposure is of high relevance to ecological risk assessments. This study suggests that during the austral winter, juveniles of the planktivorous *A. polyacanthus* from the Great Barrier Reef will increasingly ingest PET fibres in a dose-dependent manner, irrespective of seawater temperature. Furthermore, concurrent exposure to environmentally relevant estimates of future microplastic contamination and winter seawater temperatures induced stress but did not detrimentally affect energy reserves or overall fitness of juvenile *A. polyacanthus.* This suggests that predicted increases in microplastic contamination levels on the GBR and warmer upper seawater mean temperatures during winter will have minimal impacts on energy metabolism in juvenile *A. polyacanthus*. However, given cortisol levels were altered, further investigation into the underlying metabolic processes, including the identification of additional biomarkers to assess toxicity of microplastic polymers, such as PET, are required. In addition, the effects of cortisol level changes along with the cumulative impacts of these pervasive stressors on fish behaviour and on other individual ecologically relevant traits, should be assessed. Similarly, further research should investigate the effects of chronic microplastic exposure at average summer conditions, predicted for 2050 and 2100, that could exceed optimal thermal conditions for coral reef fishes.

Chapter 6: General Discussion

Microplastics are of immediate concern due to their increasing abundance, bioavailability, and potential biological effects (Santana and Turra, 2020), and given their persistence in the environment, they are predicted to have long-lasting dire consequences on the health of marine ecosystems (Adam et al., 2021; Everaert et al., 2020; Jung et al., 2021), including the Great Barrier Reef (GBR) off the tropical east coast of Australia (GBRMPA, 2019). Risk and uncertainty regarding microplastic presence, abundance and impacts in marine ecosystems has motivated the need for ecological risk assessments (ERAs), but implementation has suffered from a lack of consistent and comprehensive scientific information. Research over the past two decades has focussed on addressing these knowledge gaps and led to a better understanding of the potential impacts of microplastic contamination. However, the lack of realistic environmental data on the biological effects resulting from microplastic contamination means it is still not possible to accurately evaluate the likelihood of adverse effects on ecological entities. Similarly, not enough information is available to determine how these effects may change with varying microplastic exposure levels or whether they compound the impacts of other stressors, such as elevated future temperature due to climate change (USEPA, 1998).

This PhD thesis examined the extent and effects of microplastic contamination on a GBR coral reef ecosystem (Lizard Island) following ERA principles for the formulation of hypotheses and experimental designs to better inform effective and realistic policies that address growing concerns of microplastic impacts on marine ecosystems. Specifically, validated field and laboratory-based methodologies were either tailored or developed to accurately assess: (i) microplastic contamination levels in - and relationships between - coral reef abiotic and biotic compartments (Chapters 2 and 3) and (ii) the effects of environmentally relevant conditions of present and predicted future microplastic exposure on microplastic uptake, depuration kinetics, and fish health and fitness (Chapters 4 and 5). Lizard Island was chosen as the study site given its remote location, ecological relevance (GBRMPA, 2019) and existing evidence of microplastics contamination (Kroon et al., 2018b). Following ERA principles, the microplastic concentrations recorded at Lizard Island (Chapter 3) were used as the baseline for subsequent laboratory microplastic exposure experiments that assessed dose responsiveness in two damselfish species (*Pomacentrus amboinensis* and *Acanthochromis*

polyacanthus) (Chapters 4 and 5). Furthermore, as microplastics represent but one environmental stressor, potential health effects of such contamination in fish were investigated under environmentally relevant present and predicted future climate change scenarios (winter temperatures ranging from ambient 23.7 ˚C to moderate 25.2 ˚C and extreme 26.7˚C; Chapter 5) (IPCC, 2018).

The outcomes of these interdependent studies address three topics critical to microplastic ERAs: (1) data quality assurance and quality control (QA/QC), (2) microplastic exposure thresholds, and (3) effect on coral reef fish health resulting from microplastic exposure. Findings and their implications are discussed here and the potential ecological risks identified to better inform effective environmental management.

6.1. Quality assurance and quality control (QA/QC): a microplastics perspective

ERAs require reliable data to inform subsequent environmental management decisions (SAM, 2019) and as such rely on stringent QA/QC measures (USEPA, 1998). Unfortunately, unrealistic estimates of microplastic concentrations reported in marine ecosystems remains a concern (Kroon et al., 2018a) and limits the suitability of much of the data in the microplastic literature for inclusion in an ERA (USEPA, 1998). As such, validation of methods used to estimate environmental microplastic concentrations is crucial to ensure data accuracy and robustness. Hence, improving the efficiency and reducing the limitations of microplastic methods (i.e., field collection, separation from a multitude of sample matrices, identification, quantification, and characterization) have recently become important research topics (Lusher et al., 2020; Miller et al., 2017; Rochman et al., 2019). Efforts to establish a single universal microplastic separation method have fallen short when applied to vastly different sample matrices, i.e., abiotic (surface water vs sediment) vs biotic (whole organism vs dissected organs) (Lusher et al., 2020), primarily due to a focus on methods that work with 'model' sample types, i.e., seawater, sediment, fish, and bivalves (Avio et al., 2015b; Bellasi et al., 2021; Jaafar et al., 2020; Karlsson et al., 2017). Findings reported here (Chapter 2) corroborate this and confirm that methods need to be tailored to the specific sample matrix, especially for those that are understudied (i.e., sea squirt, sponge, coral and sea cucumber). Here, taxon-

specific microplastic separation methods were determined using a criteria-guided workflow that assessed three main factors: (i) efficiency of matrix clarification, (ii) physical and chemical impacts of the method on target polymers, and (iii) microplastic recovery rates from the sample matrix. Although these factors are important for efficient and accurate estimations of environmental microplastic contamination (Lusher et al., 2020) (Lusher et al., 2020; Miller et al., 2017; Rochman et al., 2019) they are not always considered prior to or reported in microplastic field studies (Alfaro-Nunez et al., 2021; Fathoniah and Patria, 2021; Wang et al., 2021a).

Using the criteria-guided workflow developed here, the limitations of each separation method with respect to each of the targeted organisms (sea squirt, sponge, coral and sea cucumber) and polymer types examined (polyethylene, polystyrene, polyethylene terephthalate, polyvinyl chloride, and rayon) were exposed. For example, digestion with potassium hydroxide (KOH) proved totally ineffectual for all taxa. Testing of the separation methods found coral, sponge and sea squirt tissues required 70% nitric acid (HNO_3) digestion (3, 6, and 24 h), while potassium iodide (KI) density flotation (24 h) performed best for sea cucumber gastrointestinal tract (GIT) contents. Accurate estimates of nearly all polymer types were achieved using these two methods, however, rayon fibres proved the exception. Although rayon was chemically identifiable, its recovery was complicated by its tendency to discolour and disintegrate into multiple monofilament fibres. Other studies have reported similar physical and chemical deterioration of rayon due to processing reagents (Dawson et al., 2020; Thiele et al., 2019), and combined with results from this thesis, further highlight the need to develop tailored methods to ensure effective separation and quantification of microplastic fibres, especially as interest is now focussing on their impacts, including of semi-synthetic ones such as rayon (Rebelein et al., 2021).

The application of the tailored methods to closely related, field-caught taxa (only certain species could be collected from Lizard Island) resulted in unexpectedly low clarification rates, with each method having to be modified accordingly (Chapter 3). This finding highlights the diversity in anatomy and body composition even within genera which precludes the use of a universal microplastic separation technique. To ensure accurate reporting of microplastic contamination it is imperative to validate separation methods prior to conducting ERAs on each new species and to not rely on methods tailored to the higher taxa level (e.g., genus and family).

Prevention and monitoring of contamination from extraneous sources is also paramount to achieving accurate microplastic estimations. As such, field studies usually include procedural blanks (i.e., controls) in their sample processing protocols (e.g., airborne contamination) (Prata et al., 2020); and account for the unavoidable use of plastic instruments and gear by building contaminant libraries against which samples are compared (Kroon et al., 2018a). However, often overlooked, is the need to control and monitor for extraneous microplastic contamination in laboratory-based studies which aim to determine the biological effects of deliberately introduced (i.e., spiked) microplastics. Experimental microplastic exposures often rely on experimental systems that, to some extent, are constructed with plastic materials or which may introduce plastics. Furthermore, the use of raw seawater, which can potentially be contaminated with microplastics, is often described, but many studies do not explicitly report whether or not the seawater was filtered and verified as contamination-free for experimental use (Brun et al., 2019; Naidoo and Glassom, 2019; Zitouni et al., 2021), which is a required standard procedure for testing uptake and effects of chemicals in fish (OECD, 2012). Similarly, the food provided to test organisms (Thiele et al., 2021) and the air in the experimental environment (Prata et al., 2020) represent potential sources of extraneous microplastic contamination and should also be accounted for. For data accuracy and use in ERAs, reducing extraneous microplastic contamination from experimental sources is as important as monitoring and reporting its occurrence. This is especially relevant for future research investigating environmentally relevant microplastic exposure concentrations (usually less than 1 microplastic L^{-1} of surface seawater) (Everaert et al., 2020, Chapter 3) as improper accounting of extraneous microplastics contamination could generate false estimates of effects and dose-responses.

Chapter 4 represents the first microplastic exposure study to also assess spiked experimental organisms for extraneous microplastic contamination and link the observations to potential sources (e.g., field, experimental system, or sample processing procedures). Despite the implementation of preventative measures, putative extraneous microplastics were still retrieved from experimental control and exposed fish. Twenty percent were from cellulose-based clothing worn throughout the experiment and sample processing with the remaining 80% most likely originating from the air, filtered seawater, or fish food as they differed from microplastics found in field samples and from plastic instruments and gear. This finding reveals the challenges associated with the complete elimination of all potential contamination sources in

microplastic exposure studies. As such, future studies should quantify and report background contamination in all experiments, strive to eliminate the use of plastics were possible, develop plastic-free sampling and processing methods, and implement stringent use of controls. Implementing these QA/QC measures during the design phase and throughout the study will generate data that is reliable and accurate, and therefore more informative for ERAs.

6.2. Microplastic exposure thresholds: a survey of Lizard Island coral reefs

While microplastic contamination is considered prevalent and ubiquitous in marine environments, not every marine ecosystem type has been comprehensively assessed. Coral reef ecosystems, for example, are estimated to cover 249,713 km^2 of the global oceans and are recognized by their ecological and social importance, yet remain understudied for microplastic contamination (Huang et al., 2021); only 21 microplastic field studies have been conducted in coral reefs globally. Of these, most focussed on surface seawater, while less than ten analysed sediment and organisms. These studies revealed coral reef ecosystems in Southeast Asia and India have the potential to be microplastic contamination hotspots given the high microplastic concentrations reported, such as 45,200 items m^{-3} in reef lagoons of the Xisha Islands (South China Sea) (Ding et al., 2019) and 126,000 items m^{-3} on reefs of Tuticorin and Vembar Islands (India) (Patterson et al., 2020). Conversely, surface seawater samples from the Central GBR were estimated to be between 0.04 and 0.48 items m^{-3} (Jensen et al., 2019), and the pristine waters on atoll reefs surrounding the Nansha Islands had 0.01 - 0.15 items m^{-3} (Tan et al., 2020). The low microplastic concentrations in the sea surface waters of Lizard Island (0.15 ± 0.12 microplastics m^{-3}, Chapter 3) corroborates the findings of Jensen et al.(2019) and indicates microplastics do not pose a significant risk to the GBR in comparison to other coral reefs.

Nevertheless, microplastic concentration was observed to increase with depth at Lizard Island, as previously observed in other shallow environments (Liu et al., 2020b; Song et al., 2018), and suggests that coral reef organisms living and feeding in the water column (e.g., fish) and on the sea floor (e.g., sea squirts, sponges, corals, and sea cucumbers) might be exposed to higher microplastic concentrations than are currently postulated in the literature. In Chapter 3, the concentration of microplastics isolated from the target species was consistent amongst taxa regardless of their feeding regime or vertical distribution throughout the habitat. Yet, fish were

the only organism found to be 100% contaminated with microplastics, suggesting they are at higher risk than invertebrate species inhabiting the same environment. Reasons for that could include fish taking up and/or retaining microplastics more frequently than invertebrates, and should be investigated. Overall, polymer composition and concentration of microplastics isolated from within each organism reflected those found in the immediate surrounding environment, and suggests that environments with higher microplastic loads (e.g., "hotspots") pose a greater risk than less contaminated environments. As such, future predicted increases in microplastic concentrations (Everaert et al., 2020; Jambeck et al., 2015b) could potentially lead to an overall increase in organismal contamination and, thus, an increase in the potential for adverse health effects associated with microplastic contamination.

Microplastic concentrations in biotic compartments of Lizard Island coral reefs positively correlated to those in the abiotic compartments; however, sampled compartments did not exhibit similar distributions of microplastic shapes, sizes, colours, or polymer types. These results support the hypothesis that microplastic bioavailability, and thus ecological risk, not only depends on presence in the environment but also on the susceptibility of organisms to take up these microplastics. Uptake can occur through passive (unintentional) or active (intentional) ingestion (Roch et al., 2020) as well as be influenced by various biological factors such as species-specific morphology (Kumkar et al., 2021; Welden and Cowie, 2016) and feeding mechanism (Li et al., 2021; Scherer et al., 2017). For example, it was observed that there were more fibres than fragments in the GIT of damselfish, which agrees with the findings reported for the same damselfish species previously collected from other reefs on the GBR (Jensen et al., 2019), and for many non-coral reef fish species (Rebelein et al., 2021). Furthermore, across the five taxa assessed, small microplastics (< 500 μm) were consistently observed to be the most abundant, which agrees well with previous field studies that also surveyed a variety of marine organisms (Lehtiniemi et al., 2018; Wang et al., 2021b). The relatively high abundance of specific microplastic shapes and size classes found in the organisms may be attributed to their (visual/chemical/shape/colour) similarity to natural food/prey items, or to variation in depuration rates as a function of these same two features (Xiong et al., 2019). For some organisms there were marked differences in colour and polymer type as compared to their immediate abiotic environment suggesting selective uptake. Future studies should explore this observation and aim to elucidate the influence of visual and chemical cues, including the role

of biofouling, on the uptake of specific microplastics across a range of marine organisms. Overall, findings indicate there is greater risk of uptake of microplastic fibres - for fish specifically - and < 500 μm in length - for all target species.

6.3. Effects of microplastic exposure: a case study of the coral reef damselfish

Laboratory experiments based on environmentally relevant exposures highlight the real and present risks facing natural ecosystems. Microplastic features that are associated with higher risk need to be incorporated into laboratory experiments (Katsnelson, 2015; Rochman et al., 2019), including those investigating future predicted exposure scenarios. Features to consider include: (i) ubiquitous presence of microplastic fibres and irregular fragments, (ii) varying microplastic sizes, colours, and polymer types, (iii) realistic concentrations representing present and future estimates, (iv) persistence in the environment leading to chronic exposure, and (v) potential to compound the impacts caused by other anthropogenic stressors such as thermal stress due to climate change (Horton, 2021; Rochman et al., 2019).

Water column samples from Lizard Island were found to be commonly contaminated with 600 - 700 μm blue polyester (PET) fibres and 125 - 250 μm blue polypropylene (PP) irregular fragments (Chapter 3). To investigate the ingestion and depuration kinetics of these two microplastics, adult damselfish were exposed to simulated environmentally relevant concentrations (ERC; Chapter 4) using baseline contamination estimates from Lizard Island (Chapter 2; one fragment or fibre per fish per 12 L tank). Fish were also exposed to 10x and 100x ERC to establish a dose-response relationship. Exposed fish ingested both PP fragments and PET fibres at all three concentrations, with most ingested microplastics depurated within 8 hours. Microplastic presence in organisms increased for both polymers with increasing concentration, while depuration rates slowed. PET fibres were found in higher numbers in organisms and had a slower depuration rate than PP fragments at all exposure concentrations, including ERC, which possibly explains the higher abundance of microplastic fibres found in this, and other, fish species collected from various marine environments (Jensen et al., 2019; Rebelein et al., 2021) (Chapter 3). Overall, this supports the hypothesis that intermittent exposure to microplastics may have lower associated risks as compared to chronic exposure (Horton, 2021), as most ingested microplastics will be depurated within 8 hours. In addition,

this supports the idea that current microplastic "hotspots" and predicted increases in microplastic loads pose greater risks to marine organisms (Everaert et al., 2020) due to increased ingestion and slower depuration rates. Lastly, the higher quantities of PET fibres in the GIT of fish highlights the need to understand the health impacts such exposure may have on marine organisms.

Chronic exposure to microplastic PET fibres over 8 weeks (Chapter 5) revealed juvenile damselfish ingested fibres in an exclusively dose-dependent manner, as observed in adults in Chapter 4, independent of seawater temperature. However, at elevated temperatures, representing their upper winter thermal tolerance limit, the bound cortisol levels decreased significantly as microplastic concentration (and thus uptake) increased. Meanwhile, no effects were observed at the phenotypic levels on fish health and fitness. This suggests an underlying relationship between microplastic ingestion and heat stress manifesting itself at the molecular level. At molecular and phenotypic levels, synergistic effects between microplastic ingestion and thermal stress have been reported in a temperate estuarine fish species (Ferreira et al., 2016; Fonte et al., 2016). Given many tropical species are already experiencing temperatures nearing their upper thermal tolerance limit, with elevated temperatures known to affect the health and performance of damselfish (Munday et al., 2008; Nilsson et al., 2009), this relationship between microplastic ingestion and temperature warrants further investigation at elevated summer temperatures. In addition, as cortisol response has been linked with changes in behaviour, this endpoint should also be investigated under summer scenarios (Brun et al., 2019) (Tang et al., 2021).

6.4. Ecological risks posed by microplastics

Criteria-guided workflows to assess microplastic separation methods are critical to ensure data accuracy and reliability suited to an ERA. This is evident for microplastics research based on the findings presented in this thesis. Validation of species-specific microplastic separation methods using the workflow developed here (Chapter 2) proved critical during the field survey of previously underexplored species (Chapter 3) and its adoption in future field studies is recommended to continuously improve the quality of microplastics data for ERAs. Establishing the baseline information on microplastic contamination in both abiotic and biotic matrices at

Lizard Island revealed the prevalence of microplastics in the water, sediment and organisms of this coral reef system and the risks the inhabiting organism face from specific microplastics in the environment. It also highlighted the need for more research into the mechanisms that influence active microplastic uptake, including the physical and chemical characteristics of microplastics and biofouling, and why microplastic uptake varies amongst even closely related species, to more accurately determine ecological risk.

Adoption of the baseline level of microplastic contamination at Lizard Island as the ambient experimental exposure concentration, and the use of PET fibres, ensured experiments conducted here were relevant to an ERA and addressed the demand for research on the biological effects of microplastic fibres. An increase in microplastic concentration correlated to an increase in microplastic quantities and lower depuration rates, while fibres were also found to cause higher loads in the fish and be retained for longer than fragments (Chapter 4). In addition, high concentrations of microplastic fibres in combination with increased winter seawater temperatures induced a stress response in fish, indicating these two stressors act synergistically and may be exacerbated under future summer conditions (Chapter 5). These findings should be considered in any future microplastics exposure study to ensure environmental relevance.

6.5. Concluding remarks

By advancing the technical approaches used to conduct accurate microplastics research, their application in the four independent studies that comprise this thesis has contributed to the understanding of the key environmental and ecological factors that influences the risk microplastics pose in the marine environment (Figure 6.1). These include microplastic contamination in abiotic and biotic compartments of coral reefs, microplastic ingestion and depuration kinetics by coral reef fish, and synergistic effects of microplastics and future predicted climate change temperatures. This thesis has delivered best practices for revealing the risks associated with microplastic exposure in the marine environment and contributes to sound microplastic ERAs (Adam et al., 2021; Everaert et al., 2020; Li et al., 2020b) through provision of the most current and relevant QA/QC data, ultimately providing certainty to reef managers and improving environmental decision making.

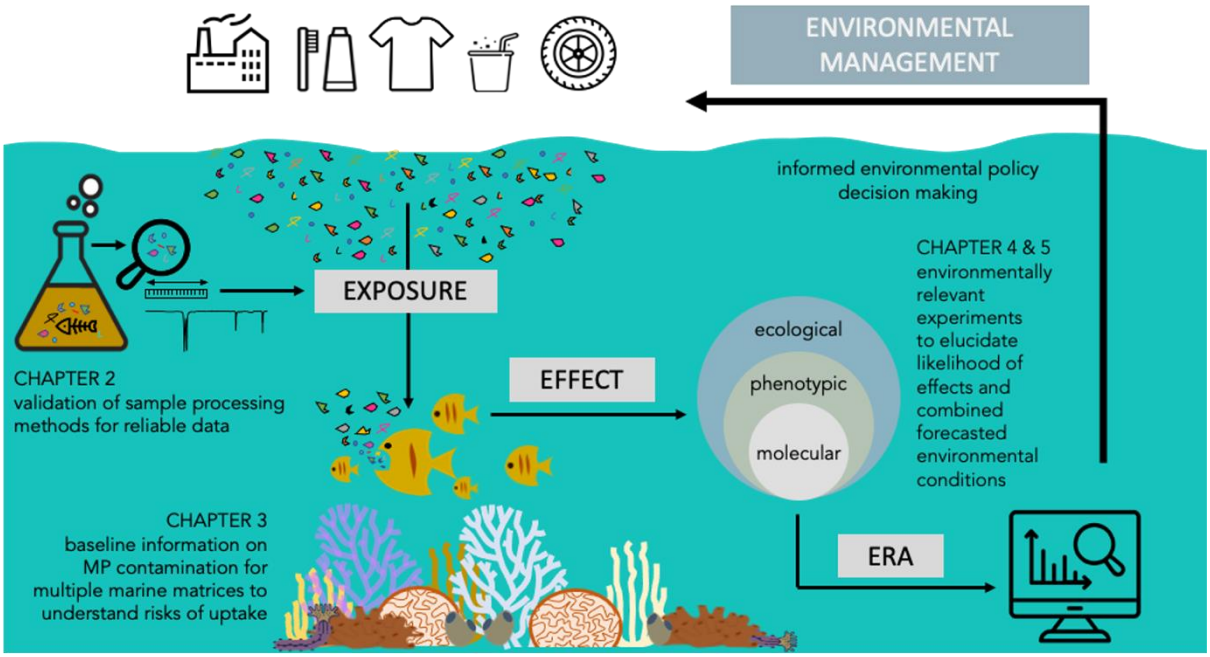

Figure 6.1: Goals of each data chapter in the context of Ecological Risk Assessment (ERA). Chapter 2 validated methods of sample processing for microplastic (MP) separation, further providing data accuracy to Chapter 3, in which baseline information on MP contamination was generated for abiotic and biotic compartments of Lizard Island to understand risks of biological uptake. Based on data generated in Chapter 3, Chapters 4 and 5 analysed MP effects of environmental and ecological relevance. The four studies are expected to contribute to sound ERAs on marine MP contamination and to informed environmental policy and decision making encompassing this issue. Icons sourced from: ProSymbols, Iconsdb, and Flaticon.

References

89/391/EEC, C.D., 1989. Council Directive 89/391/EEC of 12 June 1989 on the introduction of measures to encourage improvements in the safety and health of workers at work, , Official Journal of the European Communities

Abayomi, O.A., Range, P., Al-Ghouti, M.A., Obbard, J.P., Almeer, S.H., Ben-Hamadou, R., 2017. Microplastics in coastal environments of the Arabian Gulf. Mar Pollut Bull 124, 181-188.

Adam, V., von Wyl, A., Nowack, B., 2021. Probabilistic environmental risk assessment of microplastics in marine habitats. Aquat Toxicol 230, 105689.

Agostini, L., Moreira, J.C.F., Bendia, A.G., Kmit, M.C.P., Waters, L.G., Santana, M.F.M., Sumida, P.Y.G., Turra, A., Pellizari, V.H., 2021. Deep-sea plastisphere: Long-term colonization by plastic-associated bacterial and archaeal communities in the Southwest Atlantic Ocean. Sci Total Environ 793, 148335.

Ajith, N., Arumugam, S., Parthasarathy, S., Manupoori, S., Janakiraman, S., 2020. Global distribution of microplastics and its impact on marine environment-a review. Environ Sci Pollut Res Int 27, 25970-25986.

Alfaro-Nunez, A., Astorga, D., Caceres-Farias, L., Bastidas, L., Soto Villegas, C., Macay, K., Christensen, J.H., 2021. Microplastic pollution in seawater and marine organisms across the Tropical Eastern Pacific and Galapagos. Sci Rep 11, 6424.

Amoroso, M.G., Langellotti, A.L., Russo, V., Martello, A., Monini, M., Di Bartolo, I., Ianiro, G., Di Concilio, D., Galiero, G., Fusco, G., 2020. Accumulation and Depuration Kinetics of Rotavirus in Mussels Experimentally Contaminated. Food Environ Virol 12, 48-57.

Andrady, A.L., 2011. Microplastics in the marine environment. Mar Pollut Bull 62, 1596-1605.

Ankley, G.T., Bennett, R.S., Erickson, R.J., Hoff, D.J., Hornung, M.W., Johnson, R.D., Mount, D.R., Nichols, J.W., Russom, C.L., Schmieder, P.K., Serrrano, J.A., Tietge, J.E., Villeneuve, D.L., 2010. Adverse outcome pathways: a conceptual framework to support ecotoxicology research and risk assessment. Environ Toxicol Chem 29, 730-741.

Aragaw, T.A., Mekonnen, B.A., 2021. Distribution and Impact of Microplastics in the Aquatic Systems: A Review of Ecotoxicological Effects on Biota, Microplastic Pollution, pp. 65-104.

Arthur, C., Baker, J., Bamford, H., 2009. Proceedings of the International Research Workshop on the Occurrence, Effects, and Fate of Microplastic Marine Debris, in: Arthur, C., Baker, J., Bamford, H. (Eds.), Workshop on the Occurrence, Effects and Fate of Microplastic Marine Debris. National Oceanic and Atmospheric Administration, Tacpma, WA, USA.

Aslam, H., Ali, T., Mortula, M.M., Attaelmanan, A.G., 2020. Evaluation of microplastics in beach sediments along the coast of Dubai, UAE. Mar Pollut Bull 150, 110739.

Astudillo-Garcia, C., Bell, J.J., Montoya, J.M., Moitinho-Silva, L., Thomas, T., Webster, N.S., Taylor, M.W., 2020. Assessing the strength and sensitivity of the core microbiota approach on a highly diverse sponge reef. Environ Microbiol 22, 3985-3999.

Au, S.Y., Bruce, T.F., Bridges, W.C., Klaine, S.J., 2015. Responses of *Hyalella azteca* to acute and chronic microplastic exposures. Environ Toxicol Chem 34, 2564-2572.

Avio, C.G., Gorbi, S., Milan, M., Benedetti, M., Fattorini, D., d'Errico, G., Pauletto, M., Bargelloni, L., Regoli, F., 2015a. Pollutants bioavailability and toxicological risk from microplastics to marine mussels. Environ Pollut 198, 211-222.

Avio, C.G., Gorbi, S., Regoli, F., 2015b. Experimental development of a new protocol for extraction and characterization of microplastics in fish tissues: First observations in commercial species from Adriatic Sea. Mar Environ Res 111, 18-26.

Balthazar-Silva, D., Turra, A., Moreira, F.T., Camargo, R.M., Oliveira, A.L., Barbosa, L., Gorman, D., 2020. Rainfall and tidal cycle regulate seasonal inputs of microplastic pellets to sandy beaches. Frontiers in Environmental Science 8.

Barboza, L.G.A., Vieira, L.R., Guilhermino, L., 2018. Single and combined effects of microplastics and mercury on juveniles of the European seabass (Dicentrarchus labrax): Changes in behavioural responses and reduction of swimming velocity and resistance time. Environ Pollut 236, 1014-1019.

Barcellos, L.J., Kreutz, L.C., Koakoski, G., Oliveira, T.A., da Rosa, J.G., Fagundes, M., 2012. Fish age, instead of weight and size, as a determining factor for time course differences in cortisol response to stress. Physiol Behav 107, 397-400.

Barlow, G.W., Rogers, W., Fraley, N., 1986. Do Midas cichlids win through prowess or daring? It depends. Behaviour Ecology and Sociology 19, 1 - 8.

Barrett, J., Chase, Z., Zhang, J., Holl, M.M.B., Willis, K., Williams, A., Hardesty, B.D., Wilcox, C., 2020. Microplastic pollution in deep-sea sediments from the Great Australian Bight. Frontiers in Marine Science 7.

Barton, B.A., 2002. Stress in fishes: A diversity of responses with particular reference to changes in circulating corticosteroids. Integ. and comp. biol. 45, 517 - 525.

Bellasi, A., Binda, G., Pozzi, A., Boldrocchi, G., Bettinetti, R., 2021. The extraction of microplastics from sediments: An overview of existing methods and the proposal of a new and green alternative. Chemosphere 278, 130357.

Berkelmans, R., Willis, B.L., 1999. Seasonal and local spatial patterns in the upper thermal limits of corals on the inshore Central Great Barrier Reef. Coral Reefs 18, 219-228.

Berry, K.L.E., Epstein, H.E., Lewis, P.J., Hall, N.M., Negri, A.P., 2019. Microplastic contamination has limited effects on coral fertilisation and larvae. Diversity 11.

Besseling, E., Wegner, A., Foekema, E.M., van den Heuvel-Greve, M.J., Koelmans, A.A., 2013. Effects of microplastic on fitness and PCB bioaccumulation by the lugworm *Arenicola marina* (L.). Environ Sci Technol 47, 593-600.

Blanco, J., Alvarez, G., Rengel, J., Diaz, R., Marino, C., Martin, H., Uribe, E., 2018. Accumulation and biotransformation of dinophysis toxins by the surf clam *Mesodesma donacium*. Toxins (Basel) 10.

Bour, A., Avio, C.G., Gorbi, S., Regoli, F., Hylland, K., 2018a. Presence of microplastics in benthic and epibenthic organisms: Influence of habitat, feeding mode and trophic level. Environ Pollut 243, 1217-1225.

Bour, A., Haarr, A., Keiter, S., Hylland, K., 2018b. Environmentally relevant microplastic exposure affects sediment-dwelling bivalves. Environ Pollut 236, 652-660.

Bour, A., Hossain, S., Taylor, M., Sumner, M., Almroth, B.C., 2020a. Synthetic microfiber and microbead exposure and retention time in model aquatic species under different exposure scenarios. Fronteirs in Environmental Science 8, 1-10.

Bour, A., Sturve, J., Höjesjö, J., Carney Almroth, B., 2020b. Microplastic vector effects: Are fish at risk when exposed via the trophic chain? Frontiers in Environmental Science 8.

Brach, L., Deixonne, P., Bernard, M.F., Durand, E., Desjean, M.C., Perez, E., van Sebille, E., Ter Halle, A., 2018. Anticyclonic eddies increase accumulation of microplastic in the North Atlantic subtropical gyre. Mar Pollut Bull 126, 191-196.

Browne, M.A., Niven, S.J., Galloway, T.S., Rowland, S.J., Thompson, R.C., 2013. Microplastic moves pollutants and additives to worms, reducing functions linked to health and biodiversity. Curr Biol 23, 2388-2392.

Brun, N.R., van Hage, P., Hunting, E.R., Haramis, A.G., Vink, S.C., Vijver, M.G., Schaaf, M.J.M., Tudorache, C., 2019. Polystyrene nanoplastics disrupt glucose metabolism and cortisol levels with a possible link to behavioural changes in larval zebrafish. Commun Biol 2, 382.

Caron, A.G.M., Thomas, C.R., Berry, K.L.E., Motti, C.A., Ariel, E., Brodie, J.E., 2018. Ingestion of microplastic debris by green sea turtles (Chelonia mydas) in the Great Barrier Reef: Validation of a sequential extraction protocol. Mar Pollut Bull 127, 743-751.

Carpenter, E.J., Anderson, S.J., Harvey, G.R., Miklas, H.P., Peck, B.B., 1972. Polystyrene spherules in coastal waters. Science 178, 749-750.

Carpenter, E.J., Smith, K.L., Jr., 1972. Plastics on the Sargasso sea surface. Science 175, 1240-1241.

Cashman, M.A., Ho, K.T., Boving, T.B., Russo, S., Robinson, S., Burgess, R.M., 2020. Comparison of microplastic isolation and extraction procedures from marine sediments. Mar Pollut Bull 159, 111507.

Celino, A., Goncalves, O., Jacquemin, F., Freour, S., 2018. Qualitative and quantitative assessment of water sorption in natural fibres using ATR-FTIR spectroscopy. Carbohydr Polym 101, 163-170.

Chae, Y., An, Y.J., 2020. Effects of food presence on microplastic ingestion and egestion in *Mytilus galloprovincialis*. Chemosphere 240, 124855.

Cheang, C.C., Ma, Y., Fok, L., 2018. Occurrence and composition of microplastics in the seabed sediments of the coral communities in proximity of a metropolitan area. Int J Environ Res Public Health 15.

Cincinelli, A., Scopetani, C., Chelazzi, D., Lombardini, E., Martellini, T., Katsoyiannis, A., Fossi, M.C., Corsolini, S., 2017. Microplastic in the surface waters of the Ross Sea (Antarctica): Occurrence, distribution and characterization by FTIR. Chemosphere 175, 391-400.

Claessens, M., Van Cauwenberghe, L., Vandegehuchte, M.B., Janssen, C.R., 2013. New techniques for the detection of microplastics in sediments and field collected organisms. Mar Pollut Bull 70, 227-233.

Cole, M., Lindeque, P., Halsband, C., Galloway, T.S. 2011. Microplastics as contaminants in the marine environment: A review. Mar Pollut Bull 26, 2588 – 2597.

Cole, M., Webb, H., Lindeque, P.K., Fileman, E.S., Halsband, C., Galloway, T.S., 2014. Isolation of microplastics in biota-rich seawater samples and marine organisms. Sci Rep 4, 4528.

Cole, M., Galloway, T.S., 2015. Ingestion of nanoplastics and microplastics by pacific oyster larvae. Environ Sci Technol 49, 14625-14632.

Cole, M., Lindeque, P., Fileman, E., Halsband, C., Galloway, T.S., 2015. The impact of polystyrene microplastics on feeding, function and fecundity in the marine copepod *Calanus helgolandicus*. Environ Sci Technol 49, 1130-1137.

Colton, J.B., Knapp, D.F., Burns, B.R., 1974. Plastic particles in surface waters of the Northwestern Atlantic. Science 185, 491-497.

Comnea-Stancu, I.R., Wieland, K., Ramer, G., Schwaighofer, A., Lendl, B., 2017. On the Identification of rayon/viscose as a major fraction of microplastics in the marine environment: Discrimination between natural and manmade cellulosic fibers using Fourier Transform Infrared Spectroscopy. Appl Spectrosc 71, 939-950.

Compa, M., Ventero, A., Iglesias, M., Deudero, S., 2018. Ingestion of microplastics and natural fibres in *Sardina pilchardus* (Walbaum, 1792) and *Engraulis encrasicolus* (Linnaeus, 1758) along the Spanish Mediterranean coast. Mar Pollut Bull 128, 89-96.

Cong, Y., Jin, F., Tian, M., Wang, J., Shi, H., Wang, Y., Mu, J., 2019. Ingestion, egestion and post-exposure effects of polystyrene microspheres on marine medaka (*Oryzias melastigma*). Chemosphere 228, 93-100.

Corcoran, P.L., Norris, T., Ceccanese, T., Walzak, M.J., Helm, P.A., Marvin, C.H., 2015. Hidden plastics of Lake Ontario, Canada and their potential preservation in the sediment record. Environ Pollut 204, 17-25.

Corona, E., Martin, C., Marasco, R., Duarte, C.M., 2020. Passive and active removal of marine microplastics by a mushroom coral (*Danafungia scruposa*). Frontiers in Marine Science 7.

Courtene-Jones, W., Quinn, B., Gary, S.F., Mogg, A.O.M., Narayanaswamy, B.E., 2017. Microplastic pollution identified in deep-sea water and ingested by benthic invertebrates in the Rockall Trough, North Atlantic Ocean. Environ Pollut 231, 271-280.

Coyle, R., Hardiman, G., Driscoll, K.O., 2020. Microplastics in the marine environment: A review of their sources, distribution processes and uptake into ecosystems. Case Studies in Chemical and Environmental Engineering.

Cozar, A., Echevarria, F., Gonzalez-Gordillo, J.I., Irigoien, X., Ubeda, B., Hernandez-Leon, S., Palma, A.T., Navarro, S., Garcia-de-Lomas, J., Ruiz, A., Fernandez-de-Puelles, M.L., Duarte, C.M., 2014. Plastic debris in the open ocean. Proc Natl Acad Sci U S A 111, 10239-10244.

Critchell, K., Hoogenboom, M.O., 2018. Effects of microplastic exposure on the body condition and behaviour of planktivorous reef fish (*Acanthochromis polyacanthus*). PloS one 13, e0193308.

da Silva Souza, D.R., Caminhas, L.D., de Mesquita, J.P., Pereira, F.V., 2018. Luminescent carbon dots obtained from cellulose. Materials Chemistry and Physics 203, 148-155.

Danielsen, M., Stallcup, M.R., 1985. Down-regulation of glucocorticoid receptors in mouse lymphoma cell variants. Mollecular and Cellular Biology 4, 449 - 453.

DAWE, 2021. National Plastics Plan 2021, in: Department of Agriculture, W.a.t.E. (Ed.). Commonwealth of Australia, Camberra, p. 12.

Dawson, A., Huston, W., Kawaguchi, S., King, C., Cropp, R., Wild, S., Eisenmann, P., Townsend, K., Bengtson Nash, S., 2018. Uptake and depuration kinetics influence microplastic bioaccumulation and toxicity in antarctic krill (*Euphausia superba*). Environ Sci Technol 52, 3195-3201.

Dawson, A.L., Motti, C.A., Kroon, F.J., 2020. Solving a sticky situation: Microplastic analysis of lipid-rich tissue. Frontiers in Environmental Science 8.

Dawson, A.L., Santana, M.F.M., Miller, M.E., Kroon, F.J., 2021. Relevance and reliability of evidence for microplastic contamination in seafood: A critical review using Australian consumption patterns as a case study. Environ Pollut 276, 116684.

De Witte, B., Devriese, L., Bekaert, K., Hoffman, S., Vandermeersch, G., Cooreman, K., Robbens, J., 2014. Quality assessment of the blue mussel (*Mytilus edulis*): comparison between commercial and wild types. Mar Pollut Bull 85, 146-155.

Devriese, L.I., van der Meulen, M.D., Maes, T., Bekaert, K., Paul-Pont, I., Frere, L., Robbens, J., Vethaak, A.D., 2015. Microplastic contamination in brown shrimp (*Crangon crangon*, Linnaeus 1758) from coastal waters of the Southern North Sea and Channel area. Mar Pollut Bull 98, 179-187.

Ding, J., Jiang, F., Li, J., Wang, Z., Sun, C., Wang, Z., Fu, L., Ding, N.X., He, C., 2019. Microplastics in the coral reef systems from Xisha Islands of South China Sea. Environ Sci Technol 53, 8036-8046.

Ding, J., Zhang, S., Razanajatovo, R.M., Zou, H., Zhu, W., 2018. Accumulation, tissue distribution, and biochemical effects of polystyrene microplastics in the freshwater fish red tilapia (*Oreochromis niloticus*). Environ Pollut 238, 1-9.

Donelson, J.M., Munday, P.L., McCormick, M.I., Nilsson, G.E., 2011. Acclimation to predicted ocean warming through developmental plasticity in a tropical reef fish. Global Change Biology 17, 1712-1719.

Donelson, J.M., Munday, P.L., McCormick, M.I., Pankhurst, N.W., Pankhurst, P.M., 2010. Effects of elevated water temperature and food availability on the reproductive performance of a coral reef fish. Marine Ecology Progress Series 401, 233-243.

Donohue, M.J., Masura, J., Gelatt, T., Ream, R., Baker, J.D., Faulhaber, K., Lerner, D.T., 2019. Evaluating exposure of northern fur seals, *Callorhinus ursinus*, to microplastic pollution through fecal analysis. Mar Pollut Bull 138, 213-221.

Ehlers, S.M., Maxein, J., Koop, J.H.E., 2020. Low-cost microplastic visualization in feeding experiments using an ultraviolet light-emitting flashlight. Ecological Research 35, 265-273.

Elizalde-Velazquez, A., Carcano, A.M., Crago, J., Green, M.J., Shah, S.A., Canas-Carrell, J.E., 2020. Translocation, trophic transfer, accumulation and depuration of polystyrene microplastics in *Daphnia magna* and *Pimephales promelas*. Environ Pollut 259, 113937.

Emslie, M.J., Logan, M., Cheal, A.J., 2019. The distribution of planktivorous damselfishes (Pomacentridae) on the Great Barrier Reef and the relative influences of habitat and predation. Diversity 11.

Enders, K., Lenz, R., Beer, S., Stedmon, C.A., Browman, H., 2017. Extraction of microplastic from biota: recommended acidic digestion destroys common plastic polymers. ICES Journal of Marine Science 74, 326-331.

EPA, U.S., 1992. Framework for Ecological Risk Assessment. U. S. EPA, p. 41.

Eriksen, M., Maximenko, N., Thiel, M., Cummins, A., Lattin, G., Wilson, S., Hafner, J., Zellers, A., Rifman, S., 2013. Plastic pollution in the South Pacific subtropical gyre. Mar Pollut Bull 68, 71-76.

Espinosa, C., Cuesta, A., Esteban, M.A., 2017. Effects of dietary polyvinylchloride microparticles on general health, immune status and expression of several genes related to stress in gilthead seabream (*Sparus aurata* L.). Fish Shellfish Immunol 68, 251-259.

Europe, P., 2020. Plastics - the Facts: An analysis of European plastics production, demand and waste data, in: Europe, P. (Ed.). Plastics Europe, Belgium, p. 62.

Everaert, G., De Rijcke, M., Lonneville, B., Janssen, C.R., Backhaus, T., Mees, J., van Sebille, E., Koelmans, A.A., Catarino, A.I., Vandegehuchte, M.B., 2020. Risks of floating microplastic in the global ocean. Environ Pollut 267, 115499.

Fabricius, K.E., Genin, A., Benayahu, Y., 1995. Flow-dependent herbivory and growth in zooxanthellae-free soft corals. Limnology and Oceanography 40, 1290-1301.

Fakan, E.P., McCormick, M.I., 2019. Boat noise affects the early life history of two damselfishes. Mar Pollut Bull 141, 493-500.

Fallon, B.R., Freeman, C.J., 2021. Plastics in Porifera: The occurrence of potential microplastics in marine sponges and seawater from Bocas del Toro, Panama. PeerJ 9, e11638.

Farmer, T.M., Marschall, E.A., Dabrowski, K., Ludsin, S.A., 2015. Short winters threaten temperate fish populations. Nat Commun 6, 7724.

Fathoniah, I., Patria, M.P., 2021. Abundance of microplastic in green mussel Perna viridis, water, and sediment in Kamal Muara, Jakarta Bay. Journal of Physics: Conference Series 1725.

Feng, L., He, L., Jiang, S., Chen, J., Zhou, C., Qian, Z.J., Hong, P., Sun, S., Li, C., 2020. Investigating the composition and distribution of microplastics surface biofilms in coral areas. Chemosphere 252, 126565.

Fernandez, B., Albentosa, M., 2019a. Dynamic of small polyethylene microplastics (< 10µm) in mussel's tissues. Mar Pollut Bull 146, 493-501.

Fernandez, B., Albentosa, M., 2019b. Insights into the uptake, elimination and accumulation of microplastics in mussel. Environ Pollut 249, 321-329.

Ferreira, P., Fonte, E., Soares, M.E., Carvalho, F., Guilhermino, L., 2016. Effects of multi-stressors on juveniles of the marine fish *Pomatoschistus microps*: Gold nanoparticles, microplastics and temperature. Aquat Toxicol 170, 89-103.

Ferrier-Pagès, C., Hoogenboom, M., Houlbrèque, F., 2010. The role of plankton in coral trophodynamics, in: Dubinsky, Z., Stambler, N. (Eds.), Coral Reefs: An Ecosystem in Transition. Springer, Dordrecht, pp. 215 - 229.

Filgueiras, A.V., Preciado, I., Carton, A., Gago, J., 2020. Microplastic ingestion by pelagic and benthic fish and diet composition: A case study in the NW Iberian shelf. Mar Pollut Bull 160, 111623.

Fisher, R., O'Leary, R.A., Low-Choy, S., Mengersen, K., Knowlton, N., Brainard, R.E., Caley, M.J., 2015. Species richness on coral reefs and the pursuit of convergent global estimates. Curr Biol 25, 500-505.

Fonte, E., Ferreira, P., Guilhermino, L., 2016. Temperature rise and microplastics interact with the toxicity of the antibiotic cefalexin to juveniles of the common goby (*Pomatoschistus microps*): Post-exposure predatory behaviour, acetylcholinesterase activity and lipid peroxidation. Aquat Toxicol 180, 173-185.

Fox, H.E., White, S.A., Kao, M.H.F., Fernald, R.D., 1997. Stress and dominance in a social Fish. The Journal of Neuroscience 17, 6463 - 6469.

Frere, L., Paul-Pont, I., Rinnert, E., Petton, S., Jaffre, J., Bihannic, I., Soudant, P., Lambert, C., Huvet, A., 2017. Influence of environmental and anthropogenic factors on the composition, concentration and spatial distribution of microplastics: A case study of the Bay of Brest (Brittany, France). Environ Pollut 225, 211-222.

Frith, C.A., Leis, J.M., Goldman, B., 1986. Currents in the Lizard Island region of the Great Barrier Reef Lagoon and their relavance to potential movements of larvae. Coral Reefs 5, 81 - 92.

Frydkjaer, C.K., Iversen, N., Roslev, P., 2017. Ingestion and egestion of microplastics by the cladoceran *Daphnia magna*: Effects of regular and irregular shaped plastic and sorbed phenanthrene. Bull Environ Contam Toxicol 99, 655-661.

Fu, Z., Chen, G., Wang, W., Wang, J., 2020. Microplastic pollution research methodologies, abundance, characteristics and risk assessments for aquatic biota in China. Environ Pollut 266, 115098.

Galgani, F.F., D.; Van Franeker, J.; Katsanevakis, S.; Maes, T.; Mouat, J.; Oosterbaan, L.; Poitou, I.; Hanke, G.; Thompson, R.; Amato,E.; Birkun, A.; Janssen, C., 2010. Task Group 10 Report Marine litter, in: Zampoukas, N. (Ed.), p. 57.

Galloway, T.S., Cole, M., Lewis, C., 2017. Interactions of microplastic debris throughout the marine ecosystem. Nat Ecol Evol 1, 116.

Gambardella, C., Morgana, S., Ferrando, S., Bramini, M., Piazza, V., Costa, E., Garaventa, F., Faimali, M., 2017. Effects of polystyrene microbeads in marine planktonic crustaceans. Ecotoxicol Environ Saf 145, 250-257.

Garnier, Y., Jacob, H., Guerra, A.S., Bertucci, F., Lecchini, D., 2019. Evaluation of microplastic ingestion by tropical fish from Moorea Island, French Polynesia. Mar Pollut Bull 140, 165-170.

Gayathri, C.R., Dhanya, A.R., Indu, A.R., Kurup, P.A., 2004. Changes in some hormones by low doses of di(2-ethyl. hexyl) phtalate (DEHP), a commonly used plasticizer in PVC blood storage bags & medical tubing. Indian Journal of Medical Research 119, 139 - 144.

GBRMPA, 2014. Great Barrier Reef Marine Park Authority Science Strategy and Information Needs 2014-2019. GBRMPA, Townsville, p. 32.

GBRMPA, G.B.R.M.P.A., 2019. Great Barrier Reef Outlook Report. Great Barrier Reef Marine Park Authority, Townsville, p. 354.

German, D.P., 2011. Digestive ffficiency, encyclopedia of fish physiology: From genome to environment. Elsevier, Amsterda, pp. 1596-1607.

Germanov, E.S., Marshall, A.D., Bejder, L., Fossi, M.C., Loneragan, N.R., 2018. Microplastics: No small problem for filter-feeding megafauna. Trends in Ecology and Evolution 33, 1-6.

GESAMP, 2015. Sources, fate and effects of microplastics in the marine environment: a global assessment. International Maritime Organization.

GESAMP, 2016. Sources, fate and effects of microplastics in the marine environment: part two of a global assessmen. International Maritime Organization, London.

GESAMP, 2019. Guidelines for the monitoring and assessment of plastic litter in the ocean, in: Kershaw, P., Turra, A., Galgani, F. (Eds.). United Nations Environmental Program (UNEP), p. 130.

Geyer, R., Jambeck, J.R., Law, K.L., 2017. Production, use, and fate of all plastics ever made. Science Advances 3, e1700782.

Girard, E.B., Fuchs, A., Kaliwoda, M., Lasut, M., Ploetz, E., Schmahl, W.W., Worheide, G., 2021. Sponges as bioindicators for microparticulate pollutants? Environ Pollut 268, 115851.

Gismatulina, Y.A., Budaeva, V.V., Sakovich, G.V., 2017. Nitrocellulose synthesis from miscanthus cellulose. Propellants, Explosives, Pyrotechnics 43, 96-100.

Goikoetxea, A., Sadoul, B., Blondeau-Bidet, E., Aerts, J., Blanc, M.-O., Parrinello, H., Barrachina, C., Pratlong, M., Geffroy, B., 2021. Genetic pathways underpinning hormonal stress responses in fish exposed to short- and long-term warm ocean temperatures. Ecological Indicators 120.

Goldstein, M.C., Goodwin, D.S., 2013. Gooseneck barnacles (Lepas spp.) ingest microplastic debris in the North Pacific Subtropical Gyre. PeerJ 1, e184.

Goncalves, C., Martins, M., Sobral, P., Costa, P.M., Costa, M.H., 2019. An assessment of the ability to ingest and excrete microplastics by filter-feeders: A case study with the Mediterranean mussel. Environ Pollut 245, 600-606.

Graham, E.R., Thompson, J.T., 2009. Deposit- and suspension-feeding sea cucumbers (Echinodermata) ingest plastic fragments. Journal of Experimental Marine Biology and Ecology 368, 22-29.

Graham, P., Palazzo, L., Andrea de Lucia, G., Telfer, T.C., Baroli, M., Carboni, S., 2019. Microplastics uptake and egestion dynamics in Pacific oysters, *Magallana gigas* (Thunberg, 1793), under controlled conditions. Environ Pollut 252, 742-748.

Grigorakis, S., Mason, S.A., Drouillard, K.G., 2017. Determination of the gut retention of plastic microbeads and microfibers in goldfish (*Carassius auratus*). Chemosphere 169, 233-238.

Guven, O., Bach, L., Munk, P., Dinh, K.V., Mariani, P., Nielsen, T.G., 2018. Microplastic does not magnify the acute effect of PAH pyrene on predatory performance of a tropical fish (*Lates calcarifer*). Aquat Toxicol 198, 287-293.

Hadjiivanov, K., Avreyska, V., Klissurski, D., Marinova, T., 2002. Surface Species Formed after NO Adsorption and NO + O2 Coadsorption on ZrO2 and Sulfated ZrO2: An FTIR Spectroscopic Study. Langmuir 18, 1619-1625.

Hall, N.M., Berry, K.L.E., Rintoul, L., Hoogenboom, M.O., 2015. Microplastic ingestion by scleractinian corals. Marine Biology 162, 725-732.

Halstead, J.E., Smith, J.A., Carter, E.A., Lay, P.A., Johnston, E.L., 2018. Assessment tools for microplastics and natural fibres ingested by fish in an urbanised estuary. Environ Pollut 234, 552-561.

Hamylton, S.M., Leon, J.X., Saunders, M.I., Woodroffe, C.D., 2014. Simulating reef response to sea-level rise at Lizard Island: A geospatial approach. Geomorphology 222, 151-161.

Hannan, K.D., Munday, P.L., Rummer, J.L., 2020. The effects of constant and fluctuating elevated pCO2 levels on oxygen uptake rates of coral reef fishes. Sci Total Environ 741, 140334.

Hartmann, N.B., Huffer, T., Thompson, R.C., Hassellov, M., Verschoor, A., Daugaard, A.E., Rist, S., Karlsson, T., Brennholt, N., Cole, M., Herrling, M.P., Hess, M.C., Ivleva, N.P., Lusher, A.L., Wagner, M., 2019. Are we speaking the same language? Recommendations for a definition and categorization framework for plastic debris. Environ Sci Technol 53, 1039-1047.

Hassell, K.L., Coggan, T.L., Cresswell, T., Kolobaric, A., Berry, K., Crosbie, N.D., Blackbeard, J., Pettigrove, V.J., Clarke, B.O., 2020. Dietary uptake and depuration kinetics of perfluorooctane sulfonate, perfluorooctanoic scid, and hexafluoropropylene oxide dimer acid (GenX) in a Benthic Fish. Environ Toxicol Chem 39, 595-603.

Hendriks, A.J., Heikens, A., 2001. The power of size. 2. Rate constants and equilibrium ratios for accumulation of inorganic substances related to species weight. Environmental Toxicology and Chemistry 20, 1421-1437.

Heredia-Guerrero, J.A., Benitez, J.J., Dominguez, E., Bayer, I.S., Cingolani, R., Athanassiou, A., Heredia, A., 2014. Infrared and Raman spectroscopic features of plant cuticles: A review. Front Plant Sci 5, 305.

Hermabessiere, L., Paul-Pont, I., Cassone, A.L., Himber, C., Receveur, J., Jezequel, R., El Rakwe, M., Rinnert, E., Riviere, G., Lambert, C., Huvet, A., Dehaut, A., Duflos, G., Soudant, P., 2019. Microplastic contamination and pollutant levels in mussels and cockles collected along the channel coasts. Environ Pollut 250, 807-819.

Hernandez, E., Nowack, B., Mitrano, D.M., 2017. Polyester textiles as a source of microplastics from households: A mechanistic study to understand microfiber release during washing. Environ Sci Technol 51, 7036-7046.

Hidalgo-Ruz, V., Gutow, L., Thompson, R.C., Thiel, M., 2012. Microplastics in the marine environment: a review of the methods used for identification and quantification. Environ Sci Technol 46, 3060-3075.

Hilder, M.L., Pankhurst, N.W., 2003. Evidence that temperature change cues reproductive development in spiny damselfish, *Acanthochromis polyacanthus*. Environmental Biolofy of Fishes 66, 187-196.

Hoang, T.C., Felix-Kim, M., 2020. Microplastic consumption and excretion by fathead minnows (*Pimephales promelas*): Influence of particles size and body shape of fish. Sci Total Environ 704, 135433.

Hoegh-Guldberg, O., Bruno, J.F., 2010. The impact of climate change on the world's marine ecosystems. Science 328, 1523-1528.

Horton, A.A., 2021. Plastic pollution: When do we know enough? J Hazard Mater 422, 126885.

Horton, A.A., Barnes, D.K.A., 2020. Microplastic pollution in a rapidly changing world: Implications for remote and vulnerable marine ecosystems. Sci Total Environ 738, 140349.

Houde, E.D., Schekter, R.C., 1981. Growth rates, rations and cohort consuption of marine fish larvae in relation to prey concentrations. Rapports et proces-verbaux des reunions//Conseil permanent international pour l'exploration de la mer 178, 441–453.

Hu, L., Su, L., Xue, Y., Mu, J., Zhu, J., Xu, J., Shi, H., 2016. Uptake, accumulation and elimination of polystyrene microspheres in tadpoles of *Xenopus tropicalis*. Chemosphere 164, 611-617.

Huang, W., Chen, M., Song, B., Deng, J., Shen, M., Chen, Q., Zeng, G., Liang, J., 2021. Microplastics in the coral reefs and their potential impacts on corals: A mini-review. Sci Total Environ 762, 143112.

Huntley, C.J., Crews, K.D., Curry, M.L., 2015. Chemical functionalization and characterization of cellulose extracted from wheat straw using acid hydrolysis methodologies. International Journal of Polymer Science 2015, 1-9.

Hurley, R.R., Lusher, A.L., Olsen, M., Nizzetto, L., 2018. Validation of a method for extracting microplastics from complex, organic-rich, environmental matrices. Environ Sci Technol 52, 7409-7417.

Hutabarat, J.T.P., Wirjosentono, B., Marpaung, H., Agusnar, H., 2016. The study of degdradation cable isolation of PVC (Polyvinil Chloride) : A comparison of isolation cable between short circut and open flame. Chemistry and Materials Research, 8-22.

Illing, B., Moyano, M., Berg, J., Hufnagl, M., Peck, M.A., 2018. Behavioral and physiological responses to prey match-mismatch in larval herring. Estuarine, Coastal and Shelf Science 201, 82-94.

IPCC, 2018. Global Warming of 1.5°C. An IPCC Special Report on the impacts of global warming of 1.5°C above pre-industrial levels and related global greenhouse gas emission pathways, in the context of strengthening the global response to the threat of climate change, sustainable development, and efforts to eradicate poverty.

Ivar do Sul, J.A., Costa, M.F., 2014. The present and future of microplastic pollution in the marine environment. Environ Pollut 185, 352-364.

Iwalaye, O.A., Moodley, G.K., Robertson-Andersson, D.V., 2021. Water temperature and microplastic concentration influenced microplastic ingestion and retention rates in sea cucumber (*Holothuria cinerascens* Brandt, 1835). Ocean Science Journal 56, 141-155.

Jaafar, N., Musa, S.M., Azfaralariff, A., Mohamed, M., Yusoff, A.H., Lazim, A.M., 2020. Improving the efficiency of post-digestion method in extracting microplastics from gastrointestinal tract and gills of fish. Chemosphere 260, 127649.

Jamal, S.H., Roslan, N.J., Shah, N.A.A., Noor, S.A.M., Ong, K.K., Yunus, W.M.Z.W., 2020. Preparation and characterization of nitrocellulose from bacterial cellulose for propellant uses. Materials Today: Proceedings 29, 185-189.

Jambeck, J.R., Geyer, R., Wilcox, C., Siegler, T.R., Perryman, M., Andrady, A., Narayan, R., Law, K.L., 2015. Plastic waste inputs from land into the ocean. Science 347.

Jensen, L.H., Motti, C.A., Garm, A.L., Tonin, H., Kroon, F.J., 2019. Sources, distribution and fate of microfibres on the Great Barrier Reef, Australia. Sci Rep 9, 9021.

Jeong, C.B., Won, E.J., Kang, H.M., Lee, M.C., Hwang, D.S., Hwang, U.K., Zhou, B., Souissi, S., Lee, S.J., Lee, J.S., 2016. Microplastic size-dependent toxicity, oxidative stress induction, and p-JNK and p-p38 activation in the monogonont rotifer (*Brachionus koreanus*). Environ Sci Technol 50, 8849-8857.

Johansen, J.L., Nadler, L.E., Habary, A., Bowden, A.J., Rummer, J. 2021. Thermal acclimation of tropical reef fishes to global heat waves, eLife 10e59162.

Johansen, J.L., Jones, G.P., 2011. Increasing ocean temperature reduces the metabolic performance and swimming ability of coral reef damselfishes. Global Change Biology 17, 2971-2979.

Jones, J.S., Porter, A., Munoz-Perez, J.P., Alarcon-Ruales, D., Galloway, T.S., Godley, B.J., Santillo, D., Vagg, J., Lewis, C. 2021. Plastic contamination of a Galapagos Island (Ecuador) and the relative risks to native marine species. Sci. Total Environ 789, 147704.

Jung, J.W., Park, J.W., Eo, S., Choi, J., Song, Y.K., Cho, Y., Hong, S.H., Shim, W.J., 2021. Ecological risk assessment of microplastics in coastal, shelf, and deep sea waters with a consideration of environmentally relevant size and shape. Environ Pollut 270, 116217.

Kaiser, D., Kowalski, N., Waniek, J.J., 2017. Effects of biofouling on the sinking behavior of microplastics. Environmental Research Letters 12.

Kane, I.A., Clare, M.A., Miramontes, E., Wogelius, R., Rothwell, J.J., Garreau, P., Pohl, F., 2020. Seafloor microplastic hotspots controlled by deep-sea circulation. Science 368, 1140-1145.

Kanhai, D.K., Officer, R., Lyashevska, O., Thompson, R.C., O'Connor, I., 2017. Microplastic abundance, distribution and composition along a latitudinal gradient in the Atlantic Ocean. Mar Pollut Bull 115, 307-314.

Kaposi, K.L., Mos, B., Kelaher, B.P., Dworjanyn, S.A., 2014. Ingestion of microplastic has limited impact on a marine larva. Environ Sci Technol 48, 1638-1645.

Karami, A., Golieskardi, A., Choo, C.K., Romano, N., Ho, Y.B., Salamatinia, B., 2017a. A high-performance protocol for extraction of microplastics in fish. Sci Total Environ 578, 485-494.

Karami, A., Golieskardi, A., Ho, Y.B., Larat, V., Salamatinia, B., 2017b. Microplastics in eviscerated flesh and excised organs of dried fish. Sci Rep 7, 5473.

Karami, A., Romano, N., Galloway, T., Hamzah, H., 2016. Virgin microplastics cause toxicity and modulate the impacts of phenanthrene on biomarker responses in African catfish (*Clarias gariepinus*). Environ Res 151, 58-70.

Karasaki, R., BVegh, T., Diana, Z., Bering, J., Caldas, J., Pickle, A., Rittschof, D., Virdin, J., 2020. 20 years of government responses to the global plastic pollution problem. Duke University, Durham, NC, p. 308.

Karbalaei, S., Golieskardi, A., Watt, D.U., Boiret, M., Hanachi, P., Walker, T.R., Karami, A., 2020. Analysis and inorganic composition of microplastics in commercial Malaysian fish meals. Mar Pollut Bull 150, 110687.

Karlsson, T.M., Vethaaka, A.D., Almrothd, B.C., Ariesee, F., van Velzena, M., Hassellövb, M., Lesliea, H.A., 2017. Screening for microplastics in sediment, water, marine invertebrates and fish: Method development and microplastic accumulation. Marine Pollution Bulletin 122, 403-408.

Kashiwabara, L.M., Kahane-Rapport, S.R., King, C., DeVogelaere, M., Goldbogen, J.A., Savoca, M.S. 2021. Microplastics and microfibres in surface waters of Monterey Bay National Marine Sancturary, California. Mar Pollut Bull 165, 112148.

Katsnelson, A., 2015. News Feature: Microplastics present pollution puzzle. PNAS 112, 5547-5549.

Kavanagh, K.D., 1996. The early life history of the brooding damselfish *Acanthochromis polycanthus*: effects of environment and ancestry. PhD thesis. James Cook University, p. 150.

Kedzierski, M., Le Tilly, V., Cesar, G., Sire, O., Bruzaud, S., 2017. Efficient microplastics extraction from sand. A cost effective methodology based on sodium iodide recycling. Mar Pollut Bull 115, 120-129.

Kirstein, I.V., Wichels, A., Gullans, E., Krohne, G., Gerdts, G., 2019. The Plastisphere - Uncovering tightly attached plastic "specific" microorganisms. PloS one 14, e0215859.

Knowlton, N., 2001. The future of coral reefs. Proc Natl Acad Sci U S A 98, 5419-5425.

Kooi, M., Nes, E.H.V., Scheffer, M., Koelmans, A.A., 2017. Ups and downs in the ocean: Effects of biofouling on vertical transport of microplastics. Environ Sci Technol 51, 7963-7971.

Kortet, R., Laakkonen, M.V.M., Tikkanen, J., Vainikka, A., Hirvonen, H., 2019. Size-dependent stress response in juvenile Arctic charr (*Salvelinus alpinus*) under prolonged predator conditioning. Aquaculture Research 50, 1482-1490.

Kroon, F., Motti, C., Talbot, S., Sobral, P., Puotinen, M., 2018a. A workflow for improving estimates of microplastic contamination in marine waters: A case study from North-Western Australia. Environ Pollut 238, 26-38.

Kroon, F.J., 2015. The efficacy of clove oil for anaesthesia of eight species of Australian tropical freshwater teleosts. Limnology and Oceanography: Methods 13, 463-475.

Kroon, F.J., Motti, C.E., Jensen, L.H., Berry, K.L.E., 2018b. Classification of marine microdebris: A review and case study on fish from the Great Barrier Reef, Australia. Sci Rep 8, 16422.

Kua, Z.X., Hamilton, I.M., McLaughlin, A.L., Brodnik, R.M., Keitzer, S.C., Gilliland, J., Hoskins, E.A., Ludsin, S.A., 2020. Water warming increases aggression in a tropical fish. Sci Rep 10, 20107.

Kuhn, S., van Werven, B., van Oyen, A., Meijboom, A., Bravo Rebolledo, E.L., van Franeker, J.A., 2017. The use of potassium hydroxide (KOH) solution as a suitable approach to isolate plastics ingested by marine organisms. Mar Pollut Bull 115, 86-90.

Kulcsár, D., 2019. Microplastic ingestion and selectivity in anemonefish (*Amphiprion melanopus*) from field observations (Great Barrier Reef) and controlled laboratory exposures. MSc. thesis. Faculty of Science. University of Copenhagen, p. 71.

Kumar, A.S., Varghese, G.K., 2021. Source apportionment of marine microplastics: First step towards Managing microplastic pollution. Chemical Engineering & Technology 44, 906-912.

Kumkar, P., Gosavi, S.M., Verma, C.R., Pise, M., Kalous, L., 2021. Big eyes can't see microplastics: Feeding selectivity and eco-morphological adaptations in oral cavity affect microplastic uptake in mud-dwelling amphibious mudskipper fish. Sci Total Environ 786, 147445.

Kurniawan, S.B., Said, N.S.M., Imron, M.F., Abdullah, S.R.S., 2021. Microplastic pollution in the environment: Insights into emerging sources and potential threats. Environmental Technology & Innovation 23.

La Beur, L., Henry, L.-A., Kazanidis, G., Hennige, S., McDonald, A., Shaver, M.P., Roberts, J.M., 2019. Baseline assessment of marine litter and microplastic ingestion by cold-water coral reef benthos at the East Mingulay Marine Protected Area (Sea of the Hebrides, Western Scotland). Frontiers in Marine Science 6.

Landis, W.G., Yu, M.-H., 2004. Introduction to environmental toxicology: impacts of chemicals upon ecological systems. CRC Press LLC, Florida.

Lassig, B.R., 1983. The effects of a cyclonic storm on coral reef assemblages. Environmntal Biology of Fishes 9, 55 - 63.

Laubenstein, T.D., Rummer, J.L., McCormick, M.I., Munday, P.L., 2019. A negative correlation between behavioural and physiological performance under ocean acidification and warming. Sci Rep 9, 4265.

Lebrun, J.D., Leroy, D., Giusti, A., Gourlay-France, C., Thome, J.P., 2014. Bioaccumulation of polybrominated diphenyl ethers (PBDEs) in *Gammarus pulex*: relative importance of different exposure routes and multipathway modeling. Aquat Toxicol 154, 107-113.

Lehtiniemi, M., Hartikainen, S., Näkki, P., Engström-Öst, J., Koistinen, A., Setälä, O., 2018. Size matters more than shape: Ingestion of primary and secondary microplastics by small predators. Food Webs 17.

Li, B., Liang, W., Liu, Q.X., Fu, S., Ma, C., Chen, Q., Su, L., Craig, N.J., Shi, H., 2021. Fish ingest microplastics unintentionally. Environ Sci Technol 55, 10471-10479.

Li, B., Su, L., Zhang, H., Deng, H., Chen, Q., Shi, H., 2020a. Microplastics in fishes and their living environments surrounding a plastic production area. Sci Total Environ 727, 138662.

Li, J., Qu, X., Su, L., Zhang, W., Yang, D., Kolandhasamy, P., Li, D., Shi, H., 2016. Microplastics in mussels along the coastal waters of China. Environ Pollut 214, 177-184.

Li, J., Yang, D., Li, L., Jabeen, K., Shi, H., 2015. Microplastics in commercial bivalves from China. Environ Pollut 207, 190-195.

Li, R., Yu, L., Chai, M., Wu, H., Zhu, X., 2020b. The distribution, characteristics and ecological risks of microplastics in the mangroves of Southern China. Sci Total Environ 708, 135025.

Liang, Z., Li, W., Yang, S., Du, P., 2010. Extraction and structural characteristics of extracellular polymeric substances (EPS), pellets in autotrophic nitrifying biofilm and activated sludge. Chemosphere 81, 626-632.

Liu, K., Courtene-Jones, W., Wang, X., Song, Z., Wei, N., Li, D., 2020a. Elucidating the vertical transport of microplastics in the water column: A review of sampling methodologies and distributions. Water Res 186, 116403.

Liu, W., Zhao, Y., Shi, Z., Li, Z., Liang, X., 2020c. Ecotoxicoproteomic assessment of microplastics and plastic additives in aquatic organisms: A review. Comp Biochem Physiol Part D Genomics Proteomics 36, 100713.

Liu, Y., Qiu, X., Xu, X., Takai, Y., Ogawa, H., Shimasaki, Y., Oshima, Y., 2021. Uptake and depuration kinetics of microplastics with different polymer types and particle sizes in Japanese medaka (*Oryzias latipes*). Ecotoxicol Environ Saf 212, 112007.

Lo, H.K.A., Chan, K.Y.K., 2018. Negative effects of microplastic exposure on growth and development of Crepidula onyx. Environ Pollut 233, 588-595.

Lu, Y., Zhang, Y., Deng, Y., Jiang, W., Zhao, Y., Geng, J., Ding, L., Ren, H., 2016. Uptake and accumulation of polystyrene microplastics in zebrafish (*Danio rerio*) and toxic effects in liver. Environ Sci Technol 50, 4054-4060.

Lubken, R.M., de Jong, A.M., Prins, M.W.J., 2021. How reactivity variability of biofunctionalized particles is determined by superpositional heterogeneities. ACS Nano 15, 1331-1341.

Lugert, V., Thaller, G., Tetens, J., Schulz, C., Krieter, J., 2016. A review on fish growth calculation: multiple functions in fish production and their specific application. Reviews in Aquaculture 8, 30-42.

Lusher, A., 2015. Microplastics in the marine environment: Distribution, interactions and effects, in: al, B.e. (Ed.), Marine Anthropogenic Litter, pp. 245-307.

Lusher, A., Brate, I.L.N., Hurkey, R., Iversen, K., Oslen, M., 2017a. Testing of methodology for measuring microplastics in blue mussels (*Mytilus spp*) and sediments, and recommendations for future monitoring of microplastics (R & D-project). Norwegian Institute for Water Research, Norway.

Lusher, A.L., McHugh, M., Thompson, R.C., 2013. Occurrence of microplastics in the gastrointestinal tract of pelagic and demersal fish from the English Channel. Mar Pollut Bull 67, 94-99.

Lusher, A.L., Munno, K., Hermabessiere, L., Carr, S., 2020. Isolation and extraction of microplastics from environmental samples: An evaluation of practical approaches and recommendations for further harmonization. Appl Spectrosc 74, 1049-1065.

Lusher, A.L., Welden, N.A., Sobral, P., Cole, M., 2017b. Sampling, isolating and identifying microplastics ingested by fish and invertebrates. Analytical Methods 9, 1346-1360.

Madeira, C., Mendonca, V., Leal, M.C., Flores, A.A.V., Cabral, H.N., Diniz, M.S., Vinagre, C. 2017. Thermal stress, thermal safety margins and acclimation capacity in tropical shallow waters – an experimental approach testing multiple end-points in two common fish. Ecol. Indic. 81, 146-158.

Mai, L., Bao, L.J., Shi, L., Wong, C.S., Zeng, E.Y., 2018. A review of methods for measuring microplastics in aquatic environments. Environ Sci Pollut Res Int 25, 11319-11332.

Manabe, M., Tatarazako, N., Kinoshita, M., 2011. Uptake, excretion and toxicity of nano-sized latex particles on medaka (*Oryzias latipes*) embryos and larvae. Aquat Toxicol 105, 576-581.

Markic, A., Gaertner, J.-C., Gaertner-Mazouni, N., Koelmans, A.A., 2019. Plastic ingestion by marine fish in the wild. Critical Reviews in Environmental Science and Technology 50, 657-697.

Marnane, M.J., Bellwood, D.R., 1997. Marker technique for investigating gut throughput rates in coral reef fishes. Marine Biology 129, 15-22.

Martin, C., Corona, E., Mahadik, G.A., Duarte, C.M., 2019. Adhesion to coral surface as a potential sink for marine microplastics. Environ Pollut 255, 113281.

Martin, J., Lusher, A., Thompson, R.C., Morley, A., 2017. The Deposition and accumulation of microplastics in marine sediments and bottom water from the Irish Continental Shelf. Sci Rep 7, 10772.

Mathieu-Denoncourt, J., Wallace, S.J., de Solla, S.R., Langlois, V.S., 2015. Plasticizer endocrine disruption: Highlighting developmental and reproductive effects in mammals and non-mammalian aquatic species. Gen Comp Endocrinol 219, 74-88.

Mazurais, D., Ernande, B., Quazuguel, P., Severe, A., Huelvan, C., Madec, L., Mouchel, O., Soudant, P., Robbens, J., Huvet, A., Zambonino-Infante, J., 2015. Evaluation of the impact of polyethylene microbeads ingestion in European sea bass (*Dicentrarchus labrax*) larvae. Mar Environ Res 112, 78-85.

McCormick, M.I., Chivers, D.P., Ferrari, M.C.O., Blandford, M.I., Nanninga, G.B., Richardson, C., Fakan, E.P., Vamvounis, G., Gulizia, A.M., Allan, B.J.M., 2020. Microplastic exposure interacts with habitat degradation to affect behaviour and survival of juvenile fish in the field. Proc Biol Sci 287, 20201947.

McCormick, M.I., Weaver, C.J., 2012. It pays to be pushy: intracohort interference competition between two reef fishes. PloS one 7, e42590.

Mendrik, F.M., Henry, T.B., Burdett, H., Hackney, C.R., Waller, C., Parsons, D.R., Hennige, S.J., 2021. Species-specific impact of microplastics on coral physiology. Environ Pollut 269, 116238.

Messinetti, S., Mercurio, S., Parolini, M., Sugni, M., Pennati, R., 2018. Effects of polystyrene microplastics on early stages of two marine invertebrates with different feeding strategies. Environ Pollut 237, 1080-1087.

Metcalfe, S.S., Kroon, F.J., Beale, D.J., Miller, G., 2018. Development of a validation protocol of enzyme immunoassay kits used for the analysis of steroid hormones in fish plasma. Journal of Experimental Marine Biology and Ecology 499, 26-34.

Miller, M.E., Hamann, M., Kroon, F.J., 2020. Bioaccumulation and biomagnification of microplastics in marine organisms: A review and meta-analysis of current data. PLoS ONE 15, e0240792.

Miller, M.E., Kroon, F.J., Motti, C.A., 2017. Recovering microplastics from marine samples: A review of current practices. Mar Pollut Bull 123, 6-18.

Miller, M.E., Motti, C.A., Menendez, P., Kroon, F.J., 2021. Efficacy of microplastic separation techniques on seawater samples: Testing accuracy using high-density polyethylene. Biol Bull 240, 52-66.

Miller, T.H., McEneff, G.L., Stott, L.C., Owen, S.F., Bury, N.R., Barron, L.P., 2016. Assessing the reliability of uptake and elimination kinetics modelling approaches for estimating bioconcentration factors in the freshwater invertebrate, Gammarus pulex. Sci Total Environ 547, 396-404.

Mizraji, R., Ahrendt, C., Perez-Venegas, D., Vargas, J., Pulgar, J., Aldana, M., Patricio Ojeda, F., Duarte, C., Galban-Malagon, C., 2017. Is the feeding type related with the content of microplastics in intertidal fish gut? Mar Pollut Bull 116, 498-500.

Mohsen, M., Wang, Q., Zhang, L., Sun, L., Lin, C., Yang, H., 2019. Microplastic ingestion by the farmed sea cucumber *Apostichopus japonicus* in China. Environ Pollut 245, 1071-1078.

Mohsen, M., Zhang, L., Sun, L., Lin, C., Wang, Q., Liu, S., Sun, J., Yang, H., 2021. Effect of chronic exposure to microplastic fibre ingestion in the sea cucumber *Apostichopus japonicus*. Ecotoxicol Environ Saf 209, 111794.

Mommsen, T.P., Vijayan, M.M., Moon, T.W., 1999. Cortisol in teleosts: dynamics, mechanisms of action, and metabolic regulation. Reviews in Fish Biology and Fisheries 9, 211 - 268.

Monismith, S.G., 2007. Hydrodynamics of coral reefs. Annual review of fluid mechanics 39, 37-55.

Moosavinejad, S.M., Madhoushi, M., Vakili, M., Rasouli, D., 2019. Evaluation of degradation in chemical compounds of wood in historical buildings using FT-IR and FT-Raman vibrational spectroscopy. Maderas. Ciencia y tecnología, 0-0.

Mu, J., Qu, L., Jin, F., Zhang, S., Fang, C., Ma, X., Zhang, W., Huo, C., Cong, Y., Wang, J., 2019. Abundance and distribution of microplastics in the surface sediments from the northern Bering and Chukchi Seas. Environ Pollut 245, 122-130.

Munday, P.L., Kingsford, M.J., O'Callaghan, M., Donelson, J.M., 2008. Elevated temperature restricts growth potential of the coral reef fish *Acanthochromis polyacanthus*. Coral Reefs 27, 927-931.

Munno, K., Helm, P.A., Jackson, D.A., Rochman, C., Sims, A., 2018. Impacts of temperature and selected chemical digestion methods on microplastic particles. Environ Toxicol Chem 37, 91-98.

Naidoo, T., Glassom, D., 2019. Decreased growth and survival in small juvenile fish, after chronic exposure to environmentally relevant concentrations of microplastic. Mar Pollut Bull 145, 254-259.

Naidoo, T., Goordiyal, K., Glassom, D., 2017. Are nitric acid (HNO_3) digestions efficient in isolating microplastics from juvenile fish? Water, Air, & Soil Pollution 228.

Nanninga, G.B., Scott, A., Manica, A., 2020. Microplastic ingestion rates are phenotype-dependent in juvenile anemonefish. Environ Pollut 259, 113855.

Newman, M.C., 2012. Bioaccumulation, in: press., C. (Ed.), Quantitative ecotoxicology pp. 77-138.

Nie, H., Wang, J., Xu, K., Huang, Y., Yan, M., 2019. Microplastic pollution in water and fish samples around Nanxun Reef in Nansha Islands, South China Sea. Sci Total Environ 696, 134022.

Nilsson, G.E., Crawley, N., Lunde, I.G., Munday, P.L., 2009. Elevated temperature reduces the respiratory scope of coral reef fishes. Global Change Biology 15, 1405-1412.

Norén, F., 2007. Small plastic particles in Coastal Swedish waters. KIMO Sweden, p. 11.

Obbard, R.W., Sadri, S., Wong, Y.Q., Khitun, A.A., Baker, I., Thompson, R.C., 2014. Global warming releases microplastic legacy frozen in Arctic Sea ice. Earth's Future 2, 315-320.

OECD, 2012. 305 - Guidelines for testing of chemicals - Bioaccumulation in fish: aqueous and dietary. exposure, p. 72.

Ogata, Y., Takada, H., Mizukawa, K., Hirai, H., Iwasa, S., Endo, S., Mato, Y., Saha, M., Okuda, K., Nakashima, A., Murakami, M., Zurcher, N., Booyatumanondo, R., Zakaria, M.P., Dung le, Q., Gordon, M., Miguez, C., Suzuki, S., Moore, C., Karapanagioti, H.K., Weerts, S., McClurg, T., Burres, E., Smith, W., Van Velkenburg, M., Lang, J.S., Lang, R.C., Laursen, D., Danner, B., Stewardson, N., Thompson, R.C., 2009. International Pellet Watch: global monitoring of persistent organic pollutants (POPs) in coastal waters. 1. Initial phase data on PCBs, DDTs, and HCHs. Mar Pollut Bull 58, 1437-1446.

Ory, N., Chagnon, C., Felix, F., Fernandez, C., Ferreira, J.L., Gallardo, C., Garces Ordonez, O., Henostroza, A., Laaz, E., Mizraji, R., Mojica, H., Murillo Haro, V., Ossa Medina, L., Preciado, M., Sobral, P., Urbina, M.A., Thiel, M., 2018. Low prevalence of microplastic contamination in planktivorous fish species from the southeast Pacific Ocean. Mar Pollut Bull 127, 211-216.

Ory, N.C., Sobral, P., Ferreira, J.L., Thiel, M., 2017. Amberstripe scad *Decapterus muroadsi* (Carangidae) fish ingest blue microplastics resembling their copepod prey along the coast of Rapa Nui (Easter Island) in the South Pacific subtropical gyre. Sci Total Environ 586, 430-437.

Özkan, İ., Gündoğdu, S., 2020. Investigation on the microfiber release under controlled washings from the knitted fabrics produced by recycled and virgin polyester yarns. The Journal of The Textile Institute 112, 264-272.

Pan, Z., Liu, Q., Jiang, R., Li, W., Sun, X., Lin, H., Jiang, S., Huang, H., 2021. Microplastic pollution and ecological risk assessment in an estuarine environment: The Dongshan Bay of China. Chemosphere 262, 127876.

Pannetier, P., Morin, B., Le Bihanic, F., Dubreil, L., Clerandeau, C., Chouvellon, F., Van Arkel, K., Danion, M., Cachot, J., 2020. Environmental samples of microplastics induce significant toxic effects in fish larvae. Environ Int 134, 105047.

Pastorelli, G., Cucci, C., Garcia, O., Piantanida, G., Elnaggar, A., Cassar, M., Strlič, M., 2014. Environmentally induced colour change during natural degradation of selected polymers. Polymer Degradation and Stability 107, 198-209.

Patterson, J., Jeyasanta, K.I., Sathish, N., Edward, J.K.P., Booth, A.M., 2020. Microplastic and heavy metal distributions in an Indian coral reef ecosystem. Sci Total Environ 744, 140706.

Patti, T.B., Fobert, E.K., Reeves, S.E., Burke da Silva, K., 2020. Spatial distribution of microplastics around an inhabited coral island in the Maldives, Indian Ocean. Sci Total Environ 748, 141263.

Peters, C.A., Thomas, P.A., Rieper, K.B., Bratton, S.P., 2017. Foraging preferences influence microplastic ingestion by six marine fish species from the Texas Gulf Coast. Mar Pollut Bull 124, 82-88.

Pfeiffer, F., Fischer, E.K., 2020. Various digestion protocols within microplastic sample processing — evaluating the resistance of different synthetic polymers and the efficiency of biogenic organic matter destruction. Frontiers in Environmental Science 8.

Phuong, N.N., Zalouk-Vergnoux, A., Kamari, A., Mouneyrac, C., Amiard, F., Poirier, L., Lagarde, F., 2018. Quantification and characterization of microplastics in blue mussels (*Mytilus edulis*): protocol setup and preliminary data on the contamination of the French Atlantic coast. Environ Sci Pollut Res Int 25, 6135-6144.

Phuong, N.N., Zalouk-Vergnoux, A., Poirier, L., Kamari, A., Chatel, A., Mouneyrac, C., Lagarde, F., 2016. Is there any consistency between the microplastics found in the field and those used in laboratory experiments? Environ Pollut 211, 111-123.

Picciani, N., Kerlin, J.R., Jindrich, K., Hensley, N.M., Gold, D.A., Oakley, T.H., 2021. Light modulated cnidocyte discharge predates the origins of eyes in Cnidaria. Ecol Evol 11, 3933-3940.

Pickering, A.D., Pottinger, T.G., 1987. Poor water quality suppresses the cortisol response of salmonid fish to handling and confinement. Journal of Fish Biology 30, 363-374.

Planas, J., Gutierrez, J., Fernandez, J., Carrilho, M., Canals, P., 1990. Annual and daily variations of plasma cortisol in sea bass, *Dicentrarchus labrax* L. Aquaculture 91, 171 -178.

Portz, L., Manzolli, R.P., Herrera, G.V., Garcia, L.L., Villate, D.A., Ivar do Sul, J.A., 2020. Marine litter arrived: Distribution and potential sources on an unpopulated atoll in the Seaflower Biosphere Reserve, Caribbean Sea. Mar Pollut Bull 157, 111323.

Pottinger, T.G., 1990. The effct of stress and exogenous cortisol on receptor-like binding of cortisol in the liver of rainbow trout, *Oncorhynchus mykiss*. General and Comparative Endocrinology 78, 194 - 203.

Prata, J.C., Castro, J.L., da Costa, J.P., Duarte, A.C., Rocha-Santos, T., Cerqueira, M., 2020. The importance of contamination control in airborne fibers and microplastic sampling: Experiences from indoor and outdoor air sampling in Aveiro, Portugal. Mar Pollut Bull 159, 111522.

Prata, J.C., da Costa, J.P., Duarte, A.C., Rocha-Santos, T., 2019. Methods for sampling and detection of microplastics in water and sediment: A critical review. TrAC Trends in Analytical Chemistry 110, 150-159.

Prata, J.C., Reis, V., da Costa, J.P., Mouneyrac, C., Duarte, A.C., Rocha-Santos, T., 2021. Contamination issues as a challenge in quality control and quality assurance in microplastics analytics. J Hazard Mater 403, 123660.

Procter, J., Hopkins, F.E., Fileman, E.S., Lindeque, P.K., 2019. Smells good enough to eat: Dimethyl sulfide (DMS) enhances copepod ingestion of microplastics. Mar Pollut Bull 138, 1-6.

Prokić, M.D., Radovanović, T.B., Gavrić, J.P., Faggio, C., 2019. Ecotoxicological effects of microplastics: Examination of biomarkers, current state and future perspectives. TrAC Trends in Analytical Chemistry 111, 37-46.

Provencher, J.F., Covernton, G.A., Moore, R.C., Horn, D.A., Conkle, J.L., Lusher, A.L., 2020. Proceed with caution: The need to raise the publication bar for microplastics research. Sci Total Environ 748, 141426.

Qu, X., Su, L., Li, H., Liang, M., Shi, H., 2018. Assessing the relationship between the abundance and properties of microplastics in water and in mussels. Sci Total Environ 621, 679-686.

Quinn, B., Murphy, F., Ewins, C., 2017. Validation of density separation for the rapid recovery of microplastics from sediment. Analytical Methods 9, 1491-1498.

Ragoobur, D., Huerta-Lwanga, E., Somaroo, G.D., 2021. Microplastics in agricultural soils, wastewater effluents and sewage sludge in Mauritius. Sci Total Environ 798, 149326.

Ramírez-Flores, J., Rubio, E., Rodríguez-Lugo, V., Castaño, V.M., 2009. Purification of polluted waters by functionalized membranes Rev. Adv. Mater. Sci. 21, 211-216.

Rebelein, A., Int-Veen, I., Kammann, U., Scharsack, J.P., 2021. Microplastic fibers - Underestimated threat to aquatic organisms? Sci Total Environ 777, 146045.

Reed, S., Clark, M., Thompson, R., Hughes, K.A., 2018. Microplastics in marine sediments near Rothera Research Station, Antarctica. Mar Pollut Bull 133, 460-463.

Rehm, R., Zeyer, T., Schmidt, A., Fiener, P., 2021. Soil erosion as transport pathway of microplastic from agriculture soils to aquatic ecosystems. Sci Total Environ 795, 148774.

Reichert, J., Schellenberg, J., Schubert, P., Wilke, T., 2018. Responses of reef building corals to microplastic exposure. Environ Pollut 237, 955-960.

Reisser, J., Shaw, J., Wilcox, C., Hardesty, B.D., Proietti, M., Thums, M., Pattiaratchi, C., 2013a. Marine Plastic Pollution in Waters around Australia: Characteristics, Concentrations, and Pathways. PLoS One 8, e80466.

Reisser, J., Shaw, J., Wilcox, C., Hardesty, B.D., Proietti, M., Thums, M., Pattiaratchi, C., 2013b. Marine plastic pollution in waters around Australia: characteristics, concentrations, and pathways. PloS one 8, e80466.

Reiswig, H.M., 1971. In situ pumping activities of tropical Demospongiae. Marine Biology 9, 38 - 50.

Ripken, C., Kotsifaki, D.G., Nic Chormaic, S., 2021. Analysis of small microplastics in coastal surface water samples of the subtropical island of Okinawa, Japan. Sci Total Environ 760, 143927.

Rist, S., Baun, A., Hartmann, N.B., 2017. Ingestion of micro- and nanoplastics in *Daphnia magna* - Quantification of body burdens and assessment of feeding rates and reproduction. Environ Pollut 228, 398-407.

Rist, S., Steensgaard, I.M., Guven, O., Nielsen, T.G., Jensen, L.H., Moller, L.F., Hartmann, N.B., 2019. The fate of microplastics during uptake and depuration phases in a blue mussel exposure system. Environ Toxicol Chem 38, 99-105.

Rivera, A.S., Ozturk, N., Fahey, B., Plachetzki, D.C., Degnan, B.M., Sancar, A., Oakley, T.H., 2012. Blue-light-receptive cryptochrome is expressed in a sponge eye lacking neurons and opsin. J Exp Biol 215, 1278-1286.

Roch, S., Brinker, A., 2017. Rapid and efficient method for the detection of microplastic in the gastrointestinal tract of fishes. Environ Sci Technol 51, 4522-4530.

Roch, S., Friedrich, C., Brinker, A., 2020. Uptake routes of microplastics in fishes: practical and theoretical approaches to test existing theories. Sci Rep 10, 3896.

Rochman, C.M., Brookson, C., Bikker, J., Djuric, N., Earn, A., Bucci, K., Athey, S., Huntington, A., McIlwraith, H., Munno, K., Frond, H.D., Kolomijeca, A., Erdle, L., Grbic, J., Bayoumi, M., Borrelle, S.B., Wu, T., Santoro, S., Werbowski, L.M., Zhu, X., Giles, R.K., Hamilton, B.M., Thaysen, C., Kaura, A., Klasios, N., Ead, L., Kim, J., Sherlock, C., Ho, A., Hunga, C., 2019. Rethinking microplastics as a diverse contaminant suite. Environmental Toxicology and Chemistry 38, 703-711.

Rochman, C.M., Kurobe, T., Flores, I., Teh, S.J., 2014. Early warning signs of endocrine disruption in adult fish from the ingestion of polyethylene with and without sorbed chemical pollutants from the marine environment. Sci Total Environ 493, 656-661.

Rodrigues, M.O., Abrantes, N., Goncalves, F.J.M., Nogueira, H., Marques, J.C., Goncalves, A.M.M., 2019. Impacts of plastic products used in daily life on the environment and human health: What is known? Environ Toxicol Pharmacol 72, 103239.

Rodrigues, M.O., Goncalves, A.M.M., Goncalves, F.J.M., Abrantes, N., 2020. Improving cost-efficiency for MPs density separation by zinc chloride reuse. MethodsX 7, 100785.

Rohonczy, J., O'Dwyer, K., Rochette, A., Robinson, S.A., Forbes, M.R., 2021. Meta-analysis shows environmental contaminants elevate cortisol levels in teleost fish - Effect sizes depend on contaminant class and duration of experimental exposure. Sci Total Environ 800, 149402.

Rotjan, R.D., Sharp, K.H., Gauthier, A.E., Yelton, R., Lopez, E.M.B., Carilli, J., Kagan, J.C., Urban-Rich, J., 2019. Patterns, dynamics and consequences of microplastic ingestion by the temperate coral, *Astrangia poculata*. Proc Biol Sci 286, 20190726.

Sa, L.C., Luis, L.G., Guilhermino, L., 2015. Effects of microplastics on juveniles of the common goby (*Pomatoschistus microps*): confusion with prey, reduction of the predatory performance and efficiency, and possible influence of developmental conditions. Environ Pollut 196, 359-362.

Sadoul, B., Geffroy, B., 2019. Measuring cortisol, the major stress hormone in fishes. J Fish Biol 94, 540-555.

Saido, K., Kodera, Y., Kimukai, H., Sato, H., Okabe, A., Koizumi, K., Takatama, K., Kwon, B.G., Chung, S.-Y., Nishimura, M., Mentese, S., 2020. Waste polystyrene degradation in the world cceans: Newly identi. Research Square, 1 - 7.

Saido, K., Taguichi, H., 2004. Low-temperature decomposition of epoxy resin. Macromolecular Research 12, 490 - 492.

SAM, S.A.M., 2019. Environmental and health risks of microplastic pollution, Brussels, p. 60.

Sang, T., Wallis, C.J., Hill, G., Britovsek, G.J.P., 2020. Polyethylene terephthalate degradation under natural and accelerated weathering conditions. European Polymer Journal 136.

Santana, M.F.M., Dawson, A.L., Motti, C.A., van Herwerden, L., Lefevre, C., Kroon, F.J., 2021. Ingestion and depuration of microplastics by a planktivorous coral reef fish, *Pomacentrus amboinensis*. Frontiers in Environmental Science 9.

Santana, M.F.M., Moreira, F.T., Pereira, C.D.S., Abessa, D.M.S., Turra, A., 2018. Continuous exposure to microplastics does not cause physiological effects in the cultivated mussel *Perna perna*. Arch Environ Contam Toxicol 74, 594-604.

Santana, M.F.M., Moreira, F.T., Turra, A., 2017. Trophic transference of microplastics under a low exposure scenario: Insights on the likelihood of particle cascading along marine food-webs. Mar Pollut Bull 121, 154-159.

Santana, M.F.M., Turra, A., 2020. Toxicity of microplastics in the marine environment, in: D'Mello, J.P.F. (Ed.), A handbook of environmental toxicology, 1 ed. CAB International, Edinburgh, UK, pp. 436-454.

Santillo, D., Miller, K., Johnston, P., 2017. Microplastics as contaminants in commercially important seafood species. Integr Environ Assess Manag 13, 516-521.

Santos, I.R., Neto, J.A.B., Wallner-Kersanach, M., 2008. Resíduos Sólidos. , in: Neto, J.A.B., Wallner-Kersanach, M., Patchineelam, S.M. (Eds.), Poluição Marinha. Interciência, Rio de Janeiro, pp. 309–334.

Santos, R.G., Andrades, R., Fardim, L.M., Martins, A.S., 2016. Marine debris ingestion and Thayer's law - The importance of plastic color. Environ Pollut 214, 585-588.

Savoca, M.S., Tyson, C.W., McGill, M., Slager, C.J., 2017. Odours from marine plastic debris induce food search behaviours in a forage fish. Proc Biol Sci 284.

Savoca, M.S., Wohlfeil, M.E., Ebeler, S.E., Nevitt, G.A., 2016. Marine plastic debris emits a keystone infochemical for olfactory foraging seabirds. Sci Adv 2, e1600395.

Sayogo, B.H., Patria, M.P., Takarina, N.D., 2020. The density of microplastic in sea cucumber (*Holothuria sp.)* and sediment at Tidung Besar and Bira Besar island, Jakarta. Journal of Physics: Conference Series 1524.

Scherer, C., Brennholt, N., Reifferscheid, G., Wagner, M., 2017. Feeding type and development drive the ingestion of microplastics by freshwater invertebrates. Sci Rep 7, 17006.

Scheurer, M., Bigalke, M., 2018. Microplastics in Swiss floodplain soils. Environ Sci Technol 52, 3591-3598.

Schlawinsky, M., 2020. The intake of microplastic debris by marine organisms on the Great Barrier Reef. Msc Thesis. Oldenburg University, p. 87.

Schoⷈnberger, H., Graf, K., 2018. Di(ethylhexyl)phthalate (DEHP). Partnership for sustainable textiles.

Scott, M., Heupel, M., Tobin, A., Pratchett, M., 2017. A large predatory reef fish species moderates feeding and activity patterns in response to seasonal and latitudinal temperature variation. Sci Rep 7, 12966.

Setala, O., Fleming-Lehtinen, V., Lehtiniemi, M., 2014. Ingestion and transfer of microplastics in the planktonic food web. Environ Pollut 185, 77-83.

Sfriso, A.A., Tomio, Y., Rosso, B., Gambaro, A., Sfriso, A., Corami, F., Rastelli, E., Corinaldesi, C., Mistri, M., Munari, C., 2020. Microplastic accumulation in benthic invertebrates in Terra Nova Bay (Ross Sea, Antarctica). Environ Int 137, 105587.

Shrimpton, J.M., Randall, D.J., 1994. Downsregulation of corticosteroid receptors in gills of coho salmon due to stress and cortisol treatment. American Physiology Socioety, R432 - R438.

Simpson, T.L., 2012. Functional morphology and morphological variation, in: Simpson, T.L. (Ed.), The cell biology of sponges. Springer, New York, pp. 1 - 41.

Singh, Z., Bhalla, S., 2017. Toxicity of synthetic fibres and health. Advance Research in Textile Engineering 2, 1 - 4.

Song, Y., Cao, C., Qiu, R., Hu, J., Liu, M., Lu, S., Shi, H., Raley-Susman, K.M., He, D., 2019. Uptake and adverse effects of polyethylene terephthalate microplastics fibers on terrestrial snails (*Achatina fulica*) after soil exposure. Environ Pollut 250, 447-455.

Song, Y.K., Hong, S.H., Eo, S., Jang, M., Han, G.M., Isobe, A., Shim, W.J., 2018. Horizontal and vertical distribution of microplastics in Korean coastal waters. Environ Sci Technol 52, 12188-12197.

Stuart-Smith, R.D., Edgar, G.J., Bates, A.E., 2017. Thermal limits to the geographic distributions of shallow-water marine species. Nat Ecol Evol 1, 1846-1852.

Su, L., Nan, B., Hassell, K.L., Craig, N.J., Pettigrove, V., 2019. Microplastics biomonitoring in Australian urban wetlands using a common noxious fish (Gambusia holbrooki). Chemosphere 228, 65-74.

Su, L., Sharp, S.M., Pettigrove, V.J., Craig, N.J., Nan, B., Du, F., Shi, H., 2020. Superimposed microplastic pollution in a coastal metropolis. Water Res 168, 115140.

Sussarellu, R., Suquet, M., Thomas, Y., Lambert, C., Fabioux, C., Pernet, M.E., Le Goic, N., Quillien, V., Mingant, C., Epelboin, Y., Corporeau, C., Guyomarch, J., Robbens, J., Paul-Pont, I., Soudant, P., Huvet, A., 2016. Oyster reproduction is affected by exposure to polystyrene microplastics. Proc Natl Acad Sci U S A 113, 2430-2435.

Syakti, A.D., Bouhroum, R., Hidayati, N.V., Koenawan, C.J., Boulkamh, A., Sulistyo, I., Lebarillier, S., Akhlus, S., Doumenq, P., Wong-Wah-Chung, P., 2017. Beach macro-litter monitoring and floating microplastic in a coastal area of Indonesia. Mar Pollut Bull 122, 217-225.

Syakti, A.D., Jaya, J.V., Rahman, A., Hidayati, N.V., Raza'i, T.S., Idris, F., Trenggono, M., Doumenq, P., Chou, L.M., 2019. Bleaching and necrosis of staghorn coral (*Acropora formosa*) in laboratory assays: Immediate impact of LDPE microplastics. Chemosphere 228, 528-535.

Syberg, K., Khan, F.R., Selck, H., Palmqvist, A., Banta, G.T., Daley, J., Sano, L., Duhaime, M.B., 2015. Microplastics: addressing ecological risk through lessons learned. Environ Toxicol Chem 34, 945-953.

Taebi, S., Lowe, R.J., Pattiaratchi, C.B., Ivey, G.N., Symonds, G., Brinkman, R., 2011. Nearshore circulation in a tropical fringing reef system. Journal of Geophysical Research 116.

Tan, F., Yang, H., Xu, X., Fang, Z., Xu, H., Shi, Q., Zhang, X., Wang, G., Lin, L., Zhou, S., Huang, L., Li, H., 2020. Microplastic pollution around remote uninhabited coral reefs of Nansha Islands, South China Sea. Sci Total Environ 725, 138383.

Tanaka, K., Takada, H., 2016. Microplastic fragments and microbeads in digestive tracts of planktivorous fish from urban coastal waters. Sci Rep 6, 34351.

Tang, Y., Mi, P., Li, M., Zhang, S., Li, J., Feng, X., 2021. Environmental level of the antidepressant venlafaxine induces behavioral disorders through cortisol in zebrafish larvae (*Danio rerio*). Neurotoxicol Teratol 83, 106942.

TatianN, M., Sahade, R., Esnal, G.B., 2004. Diet components in the food of Antarctic ascidians living at low levels of primary production. Antarctic Science 16, 123-128.

Ternero-Hidalgo, J.J., Rosas, J.M., Palomo, J., Valero-Romero, M.J., Rodríguez-Mirasol, J., Cordero, T., 2016. Functionalization of activated carbons by HNO_3 treatment: Influence of phosphorus surface groups. Carbon 101, 409-419.

Thiele, C.J., Hudson, M.D., Russell, A.E., 2019. Evaluation of existing methods to extract microplastics from bivalve tissue: Adapted KOH digestion protocol improves filtration at single-digit pore size. Mar Pollut Bull 142, 384-393.

Thiele, C.J., Hudson, M.D., Russell, A.E., Saluveer, M., Sidaoui-Haddad, G., 2021. Microplastics in fish and fishmeal: an emerging environmental challenge? Sci Rep 11, 2045.

Thomas, M.E., 1997. Potassium Iodide (KI), in: Palik, E.D., Ghosh, G. (Eds.), Handbook of Optical Constants of Solids. Elsevier Inc, pp. 807-820.

Thompson, R.C., Olsen, Y., Mitchell, R.P., Davis, A., Rowland, S.J., John, A.W.G., McGonigle, D., Russell, A.E., 2004. Lost at sea: where is all the plastic? Science 304, 1.

Tort, L., 2011. Stress and immune modulation in fish. Dev Comp Immunol 35, 1366-1375.

Turra, A., Manzano, A.B., Dias, R.J., Mahiques, M.M., Barbosa, L., Balthazar-Silva, D., Moreira, F.T., 2014. Three-dimensional distribution of plastic pellets in sandy beaches: shifting paradigms. Sci Rep 4, 4435.

Uddin, S., Fowler, S.W., Uddin, M.F., Behbehani, M., Naji, A., 2021. A review of microplastic distribution in sediment profiles. Mar Pollut Bull 163, 111973.

UN, U.N.E.P., 2019. Plastics and shallow water coral reefs. Synthesis of the science for policy-makers. UN, p. 50.

USEPA, 1992. Framework for Ecological Risk Assessment. U.S. Environmental Protection Agency, Washington, DC, p. 41.

USEPA, 1998. Guidelines for Ecological Risk Assessment. U.S. Environmental Protection Agency, Washington, DC, p. 171.

Van Cauwenberghe, L., Janssen, C.R., 2014. Microplastics in bivalves cultured for human consumption. Environ Pollut 193, 65-70.

Van Cauwenberghe, L., Vanreusel, A., Mees, J., Janssen, C.R., 2013. Microplastic pollution in deep-sea sediments. Environ Pollut 182, 495-499.

van Sebille, E., Wilcox, C., Lebreton, L., Maximenko, N., Hardesty, B.D., van Franeker, J.A., Eriksen, M., Siegel, D., Galgani, F., Law, K.L., 2015. A global inventory of small floating plastic debris. Environmental Research Letters 10.

Vandermeersch, G., Van Cauwenberghe, L., Janssen, C.R., Marques, A., Granby, K., Fait, G., Kotterman, M.J., Diogene, J., Bekaert, K., Robbens, J., Devriese, L., 2015. A critical view on microplastic quantification in aquatic organisms. Environ Res 143, 46-55.

Veilleux, H.D., Ryu, T., Donelson, J.M., van Herwerden, L., Seridi, L., Ghosheh, Y., Berumen, M.L., Leggat, W., Ravasi, T., Munday, P.L., 2015. Molecular processes of transgenerational acclimation to a warming ocean. Nature Climate Change 5, 1074-1078.

Vered, G., Kaplan, A., Avisar, D., Shenkar, N., 2019. Using solitary ascidians to assess microplastic and phthalate plasticizers pollution among marine biota: A case study of the Eastern Mediterranean and Red Sea. Mar Pollut Bull 138, 618-625.

von Moos, N., Burkhardt-Holm, P., Kohler, A., 2012. Uptake and effects of microplastics on cells and tissue of the blue mussel *Mytilus edulis* L. after an experimental exposure. Environ Sci Technol 46, 11327-11335.

Wang, Q., Zhu, X., Hou, C., Wu, Y., Teng, J., Zhang, C., Tan, H., Shan, E., Zhang, W., Zhao, J., 2021a. Microplastic uptake in commercial fishes from the Bohai Sea, China. Chemosphere 263, 127962.

Wang, S., Hu, M., Zheng, J., Huang, W., Shang, Y., Kar-Hei Fang, J., Shi, H., Wang, Y., 2021b. Ingestion of nano/micro plastic particles by the mussel *Mytilus coruscus* is size dependent. Chemosphere 263, 127957.

Wang, X., Huang, W., Wei, S., Shang, Y., Gu, H., Wu, F., Lan, Z., Hu, M., Shi, H., Wang, Y., 2019a. Microplastics impair digestive performance but show little effects on antioxidant activity in mussels under low pH conditions. Environ Pollut, 113691.

Wang, Y., Mao, Z., Zhang, M., Ding, G., Sun, J., Du, M., Liu, Q., Cong, Y., Jin, F., Zhang, W., Wang, J., 2019b. The uptake and elimination of polystyrene microplastics by the brine shrimp, *Artemia parthenogenetica*, and its impact on its feeding behavior and intestinal histology. Chemosphere 234, 123-131.

Warren, D.T., Donelson, J.M., McCormick, M.I., Ferrari, M.C., Munday, P.L., 2016. Duration of exposure to elevated temperature affects competitive interactions in juvenile reef fishes. PloS one 11, e0164505.

Watts, A.J., Lewis, C., Goodhead, R.M., Beckett, S.J., Moger, J., Tyler, C.R., Galloway, T.S., 2014. Uptake and retention of microplastics by the shore crab *Carcinus maenas*. Environ Sci Technol 48, 8823-8830.

Welden, N.A.C., Cowie, P.R., 2016. Environment and gut morphology influence microplastic retention in langoustine, *Nephrops norvegicus*. Environ Pollut 214, 859-865.

Wen, B., Zhang, N., Jin, S.R., Chen, Z.Z., Gao, J.Z., Liu, Y., Liu, H.P., Xu, Z., 2018. Microplastics have a more profound impact than elevated temperatures on the predatory performance, digestion and energy metabolism of an Amazonian cichlid. Aquat Toxicol 195, 67-76.

Wicaksono, K.B., Patria, M.P., Suryanda, A., 2021. Microplastic ingestion in the black sea cucumber *Holothuria leucospilota* (Brandt, 1835) collected from Rambut Island, Seribu Islands, Jakarta, Indonesia. IOP Conference Series: Materials Science and Engineering 1098.

Woodall, L.C., Sanchez-Vidal, A., Canals, M., Paterson, G.L., Coppock, R., Sleight, V., Calafat, A., Rogers, A.D., Narayanaswamy, B.E., Thompson, R.C., 2014. The deep sea is a major sink for microplastic debris. R Soc Open Sci 1, 140317.

Woodhead, A.J., Hicks, C.C., Norström, A.V., Williams, G.J., Graham, N.A.J., Fox, C., 2019. Coral reef ecosystem services in the Anthropocene. Functional Ecology.

Woods, M.N., Stack, M.E., Fields, D.M., Shaw, S.D., Matrai, P.A., 2018. Microplastic fiber uptake, ingestion, and egestion rates in the blue mussel (*Mytilus edulis*). Mar Pollut Bull 137, 638-645.

Wootton, N., Ferreira, M., Reis-Santos, P., Gillanders, B.M., 2021. A comparison of microplastic in fish from Australia and Fiji. Frontiers in Marine Science 8.

Wright, S.L., Rowe, D., Thompson, R.C., Galloway, T.S., 2013. Microplastic ingestion decreases energy reserves in marine worms. Curr Biol 23, R1031-1033.

Wu, X., Zhong, C., Wang, T., Zou, X., Zang, Z., Li, Q., Chen, H., 2021. Occurrence and distribution of microplastics on recreational beaches of Haichow Bay, China. Environ Sci Pollut Res Int 28, 6132-6145.

Xiong, X., Tu, Y., Chen, X., Jiang, X., Shi, H., Wu, C., Elser, J.J., 2019. Ingestion and egestion of polyethylene microplastics by goldfish (*Carassius auratus*): influence of color and morphological features. Heliyon 5, e03063.

Xu, S., Ma, J., Ji, R., Pan, K., Miao, A.J., 2020a. Microplastics in aquatic environments: Occurrence, accumulation, and biological effects. Sci Total Environ 703, 134699.

Xu, X., Wong, C.Y., Tam, N.F.Y., Lo, H.S., Cheung, S.G., 2020b. Microplastics in invertebrates on soft shores in Hong Kong: Influence of habitat, taxa and feeding mode. Sci Total Environ 715, 136999.

Xue, B., Zhang, L., Li, R., Wang, Y., Guo, J., Yu, K., Wang, S., 2020. Underestimated microplastic pollution derived from fishery activities and "hidden" in deep sediment. Environ Sci Technol 54, 2210-2217.

Yan, Z., Zhao, H., Zhao, Y., Zhu, Q., Qiao, R., Ren, H., Zhang, Y., 2020. An efficient method for extracting microplastics from feces of different species. J Hazard Mater 384, 121489.

Yang, D., Shi, H., Li, L., Li, J., Jabeen, K., Kolandhasamy, P., 2015. Microplastic pollution in table salts from China. Environ Sci Technol 49, 13622-13627.

Yin, L., Chen, B., Xia, B., Shi, X., Qu, K., 2018. Polystyrene microplastics alter the behavior, energy reserve and nutritional composition of marine jacopever (*Sebastes schlegelii*). J Hazard Mater 360, 97-105.

Yu, X., Peng, J., Wang, J., Wang, K., Bao, S., 2016. Occurrence of microplastics in the beach sand of the Chinese inner sea: the Bohai Sea. Environ Pollut 214, 722-730.

Yu, Z., Peng, B., Liu, L.Y., Wong, C.S., Zeng, E.Y., 2019. Development and validation of an efficient method for processing microplastics in biota samples. Environ Toxicol Chem 38, 1400-1408.

Zarco-Perelló, S., Pratchett, M., Liao, V., 2012. Temperature-growth performance curves for a coral reef fish, *Acanthochromis polyacanthus*. Galaxea, Journal of Coral Reef Studies 14, 97-103.

Zhang, D., Liu, X., Huang, W., Li, J., Wang, C., Zhang, D., Zhang, C., 2020a. Microplastic pollution in deep-sea sediments and organisms of the Western Pacific Ocean. Environ Pollut 259, 113948.

Zhang, L., Zhang, S., Wang, Y., Yu, K., Li, R., 2019. The spatial distribution of microplastic in the sands of a coral reef island in the South China Sea: Comparisons of the fringing reef and atoll. Sci Total Environ 688, 780-786.

Zhang, X., Yan, B., Wang, X., 2020b. Selection and optimization of a protocol for extraction of microplastics from Mactra veneriformis. Sci Total Environ 746, 141250.

Zhang, X., Yu, K., Zhang, H., Liu, Y., He, J., Liu, X., Jiang, J., 2020c. A novel heating-assisted density separation method for extracting microplastics from sediments. Chemosphere 256, 1-6.

Zhang, Z., Bai, Q., Xu, X., Zhang, X., 2021. Effects of the dominance hierarchy on social interactions, cortisol level, HPG-axis activities and reproductive success in the golden cuttlefish *Sepia esculenta*. Aquaculture 533.

Zhao, H.J., Xu, J.K., Yan, Z.H., Ren, H.Q., Zhang, Y., 2020. Microplastics enhance the developmental toxicity of synthetic phenolic antioxidants by disturbing the thyroid function and metabolism in developing zebrafish. Environ Int 140, 105750.

Zitouni, N., Bousserrhine, N., Missawi, O., Boughattas, I., Chevre, N., Santos, R., Belbekhouche, S., Alphonse, V., Tisserand, F., Balmassiere, L., Dos Santos, S.P., Mokni, M., Guerbej, H., Banni, M., 2021. Uptake, tissue distribution and toxicological effects of environmental microplastics in early juvenile fish *Dicentrarchus labrax*. J Hazard Mater 403, 124055.

Zobkov, M.B., Esiukova, E.E., Zyubin, A.Y., Samusev, I.G., 2019. Microplastic content variation in water column: The observations employing a novel sampling tool in stratified Baltic Sea. Mar Pollut Bull 138, 193-205.

Appendix A

Supplementary Information for Chapter 2 An assessment workflow to recover microplastics from complex biological matrices

1. Supplementary Methods

Table S1: Chemical and physical characteristics of laboratory prepared microplastics. Polymer type was confirmed using infrared spectroscopy. PE = polyethylene, PS = polystyrene, PET = polyester, PVC = polyvinylchloride. SD = standard deviation.

Experiment	Polymer	Size range (mm)	Average size (± SD, mm)	Shape	Colour
Effects of reagents and separation methods on polymer physical and chemical characteristics	PE	1.6 – 4.3	2.7 ± 0.6	Irregular fragment, non-film, rough	yellow, opaque, vivid
	PS	1.4 – 3.5			clear, transparent
	PET	2.3 – 4.5			clear, transparent
	PVC	2.2 – 3.6			grey, opaque, vivid
	Rayon thread	Approx. 4	Approx. 4	Regular fibre, non-film, rough	black, opaque, vivid
Microplastic recovery rates	PE	≤ 0.5	≤ 0.5	Irregular fragment, non-film, rough	yellow, opaque, vivid
	PS	≤ 0.5			clear, transparent
	PET	≤ 0.5			clear, transparent
	PVC	≤ 0.5			grey, opaque, vivid
	Rayon monofilament*	Approx. 2	Approx. 2	Regular fibre, non-film, rough	black, opaque, vivid

Table S2: Spectral match (percentage) of control microplastics to reference spectra in the NICDOCOM IR spectral libraries. Control microplastics include polyethylene (PE), polystyrene (PS), polyester (PET), polyvinylchloride (PVC), and rayon (n = 5 replicates per microplastic; #).

Plastic	Spectrum search	
PE # 1	98.68	PAD0151.SPC POLYETHYLENE, HOSTALEN GM 7040;9002-88-4;(C2H4)N, NICODOM;
PE # 2	97.68	PAD0153.SPC POLYETHYLENE, LUPOLEN 6021 D;9002-88-4;(C2H4)N, NICODOM; LY
PE # 3	97.67	PAD3075.SPC LUWAX AF 32, NICODOM, MICRONIZED POLYETHYLENE WAXES; BASF
PE # 4	97.57	PAD2543.SPC DIOCTADECYL SULFIDE;1844-09-3;C36H74S, COPYRIGHT NICODOM; H
PE # 5	97.50	CO1121.SP POLYETHYLENE;9002-88-4;(C)NICODOM 2009 IR-SPECTRA.COM
PS # 1	98.71	PAD0207.SPC POLYSTYRENE, MONOCARBOXY TERMINATED;9003-70-7,9003-53-6;(C8
PS # 2	98.16	PAD0208.SPC POLYSTYRENE, NOPE PS-NETSARK 336M;9003-70-7,9003-53-6;(C8H8
PS # 3	97.74	PEC0349.SPC POLYSTYRENE, 9003-70-7, COPYRIGHT NICODOM 2012
PS # 4	97.74	PAD0004.SPC POLYSTYRENE;9003-70-7;(C8H8)N,WWW.IR-SPECTRA.COM, COPYRIGHT
PS # 5	97.71	CO1126.SP POLYSTYRENE;9003-70-7;(C)NICODOM 2009 IR-SPECTRA.COM
PET # 1	99.20	FB001.SP FB001, COMFORTREL, POLYESTER, WELLMAN, COPYRIGHT NICODOM 2007
PET # 2	99.14	FB450.SP FB450, DACRON, POLYESTER, DUPONT, COPYRIGHT NICODOM 2007 IR-SP
PET # 3	99.13	FB443.SP FB443, AVLIN, POLYESTER, AVTEX, COPYRIGHT NICODOM 2007 IR-SPEC
PET # 4	99.13	FB451.SP FB451, DIOLEN, POLYESTER, DIOLEN INDUSTRIAL FIBERS, COP. NICOD
PET # 5	98.99	FB440.SP FB440, MICRODENIER SENSURA, POLYESTER, WELLMAN, COPYRIGHT NICO
PVC # 1	87.06	PAD3433.SPC POLYVINYLCHLORIDE - HARD, NICODOM
PVC # 2	87.03	CO1129.SP POLYVINYLCHLORIDE - HARD;(C)NICODOM 2009 IR-SPECTRA.COM
PVC # 3	75.75	FB317.SP FB317, RHOVYL, PVC, RHONE-POULENC, COPYRIGHT NICODOM 2007 IR-S
PVC # 4	75.60	PAD0412.SPC POLYVINYLCHLORIDE #2;9002-86-2;(C2H3CL)N,WWW.IR-SPECTRA.COM
PVC # 5	74.61	PAD3886.SPC VINYL CHLORIDE/VINYL ACETATE/VINYL TERPOLYMER, NICODOM
Rayon # 1	92.58	FB286.SP FB286, FIBRO, RAYON, COURTAULDS, COPYRIGHT NICODOM 2007 IR-SPE
Rayon # 2	92.36	FB349.SP FB349, CREPE WELNETTE, MIXED YARN, WONOCO, COPYRIGHT NICODOM 2

Rayon # 3	91.80	FB374.SP FB374, BERMUDA TWEED, MIXED YARN, WONOCO, COPYRIGHT NICODOM 20
Rayon # 4	91.30	FB267.SP FB267, COTTON 33%, RAYON 49%, NYLON 16%, ELASTAN 2%, COTTON NY
Rayon # 5	91.30	FB252.SP FB252, BAMBOO FIBER, NATURAL, BAMBUS ELEGANG, COPYRIGHT NICODO

Table S3: Initial experimental parameters (technical information and step-by-step procedural description) of each of the four microplastic separation methods tested, namely alkaline (potassium hydroxide; KOH) and acid (nitric acid; HNO3) digestions, and sodium chloride (NaCl) and potassium iodide (KI) density flotations, to determine suitability for microplastic recovery from coral, sponge and sea squirt tissues and sea cucumber GIT content.

(a) Experimental parameters

Separation method	Chemical digestion		Density separation	
Reagent	HNO_3 *	KOH *	NaCl *	KI *
Concentration	70% (15.9 M)	5.6% (1 M) and 10% (1.8 M)	1.2 $g.cm^{-3}$	1.7 $g.cm^{-3}$
Ratio of reagent:biological matrix (v:d.w in ml:g)	4:1	4:1	4:1	4:1
Processing time (hr)	24, 6 and 3	24 and 48	24	24
Temperature	22 ± 1˚C	22 ± 1˚C	22 ± 1˚C	22 ± 1˚C

(b) Step-by-step procedural description

Separation method	Chemical digestion		Density separation	
Reagent	HNO_3 *	KOH *	NaCl *	KI *
step 1	dry, dissect ** and weigh			
step 2	transfer into 150 ml beaker			
step 3	add reagent			
step 4	n/a		manually stir 5 min	
step 5	digest 24, 3, or 6 h	digest 24 or 48 h	settle for 24 h	
step 6	filter processed sample[1]			
step 7	dry in fume hood for minimum of 2 days			

* Reagent details: NaCl (AR, Fisher Chemical, CAS No. 7647-14-5); KI (AR, Univar, CAS No. 7681-11-0); HNO_3 (70% AR, Univar, CAS No. 7697-37-2); KOH (AR, Fisher, CAS No. 1310-58). All reagent solutions were prepared with Milli-Q water except HNO_3, which was used neat.

** Only sea cucumber and sea squirt specimens were dissected. Coral and sponge specimens were digested entirely as detailed in section 2.1.

1.1. Shape chart

The shape descriptors proposed here systematically organize microplastic shapes reported in the scientific literature to improve consistency in microplastic characterization across studies. The descriptors consider shape categories already used in the microplastic literature [2, 3] grouped according to shape definitions commonly applied in other fields of research, such as geology and polymer production. Microplastic shapes are organized in three defining attributes: (i) surface shape, (ii) thickness, and (iii) texture. Surface shape (SFigure 2) relates to the two-dimensional outline of microplastics and includes regular and irregular items. Regular microplastics are symmetric in shape, with fibers, threads and lines being longer than it is wide, and round items having the same radius from any perimeter point. Irregular microplastics embraces all asymmetric items, regardless of roundness and sphericity (see Vepraskas and Cassel [4] for concepts of sphericity and roundness for sediment grains). Thickness divides microplastics between film (< 254 µm height when measured perpendicular to the horizontal plane of the item) (modified from Headley Pratt [5]) and non-film which are any microplastic that is thicker than film (Supplementary Figure 1). Texture indicates if the microplastic is rough or smooth. The proposed descriptors are suggestions of how standardizing terminology can assist the scientific community for more accurate microplastic characterization.

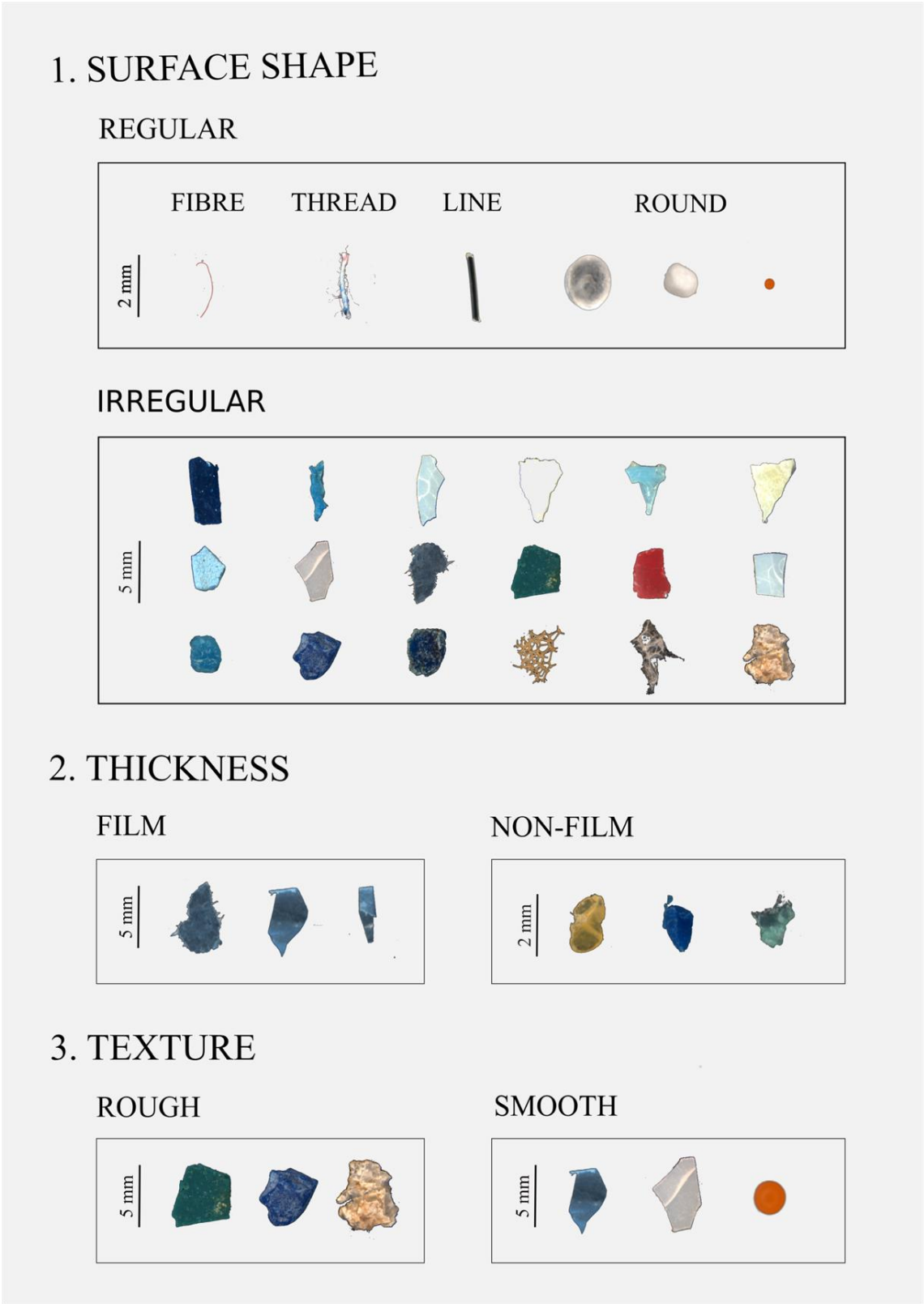

Figure S1: Microplastic shape descriptors based on (1) surface shape (regular and irregular), (2) thickness (film or non-film) and (3) texture (rough or smooth). Image created by the first author with microplastics recovered from beach sediment samples and prepared from larger plastic items sourced in the laboratory.

1.2. Colour chart

This colour chart systematically organizes microplastic colour descriptions reported in the scientific literature to improve consistency in microplastic characterization across studies. In this colour chart, microplastic colours are described by three different and complementary elements: (i) colour value, (ii) clarity, and (iii) chroma. Colour value is the combination between hue (i.e., colour) and lightness/darkness (i.e., value). Hue (x axis, Supplementary Figure 2) is the main colour descriptor that corresponds to what is considered basic colours: primary (red, yellow, blue), secondary (orange, green, purple), tertiary (brown) and shades (black, white and gray). Value (y axis, Supplementary Figure 2) is the descriptor of hue lightness/darkness. Value changes the hue scale in a vertical axis, with pure white being 6 and pure black the opposite extreme (-6). Colour and value were divided into 11 and 12 increments, respectively, although they could in theory be divided into infinite steps within. Every colour and value step has a number that together corresponds to a colour value and ultimately represents different shades of a hue. Clarity is an additional category for colour description that concerns transparency of microplastic particles, being either clear or opaque (Supplementary Figure 2). Of note is that clear white items can be considered transparent. Chroma indicates how faded the colour appears. In the proposed chart, chroma is considered either faded or vivid. The use of hue, value and chroma to systematize the proposed characterization is based on Munsell's colour scale (https://munsell.com/). The proposed colour chart is an illustration of how subjective descriptions as "light yellow" and "beige" can be replaced for more accurate and reproducible methods of characterization.

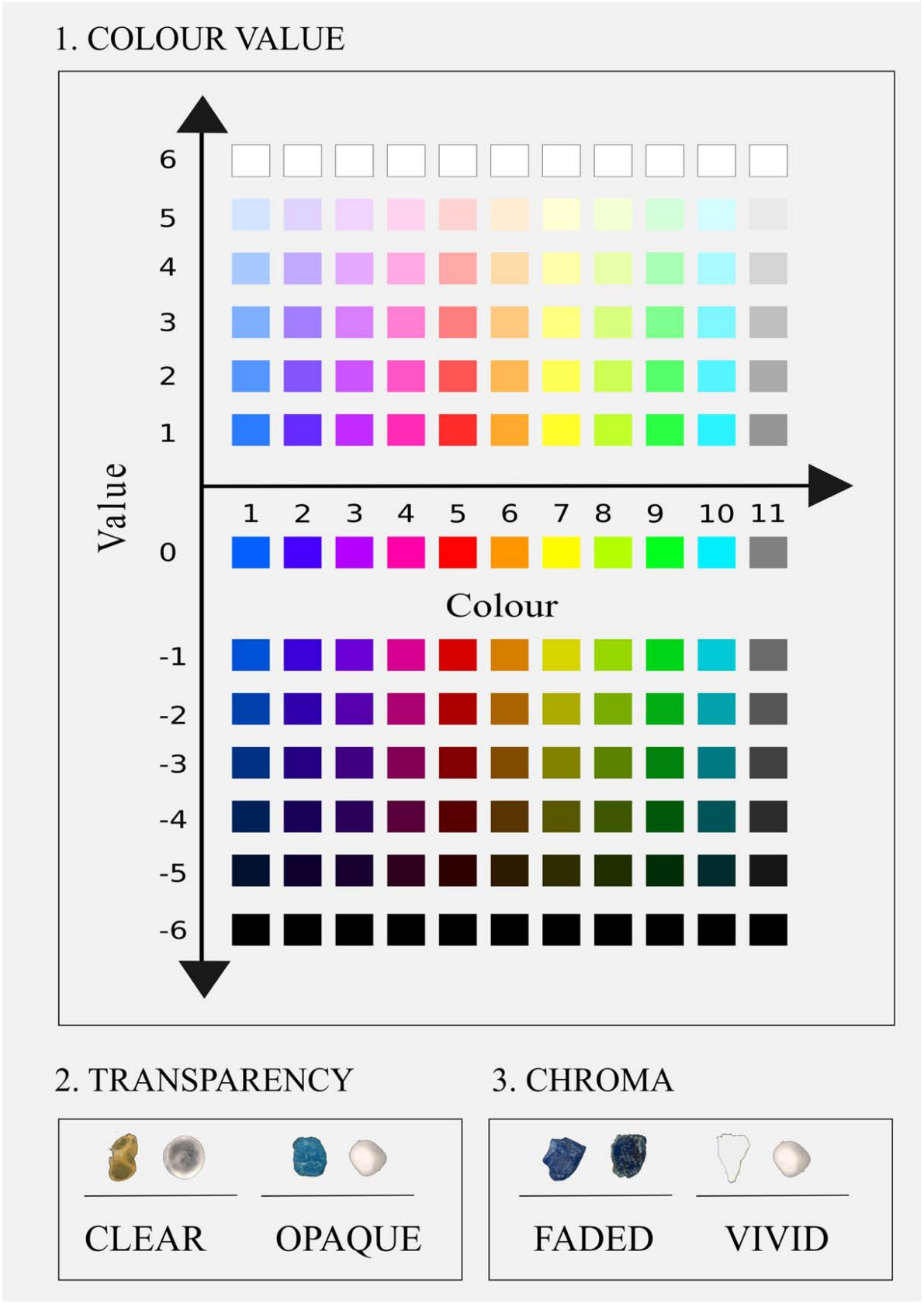

Figure S2: Microplastics colour description and colour chart based on (1) colour value defined by the combination of hue (x axis of graph; 1: blue, 2: blue-purple, 3: purple, 4: purple-red or pink, 5: red, 6: red-yellow or orange, 7: yellow, 8: yellow-green, 9: green, 10: green-blue, 11: grey), (2) transparency (clear or opaque) and (3) chroma (faded or vivid).

1.3. Matrix clarification efficiency

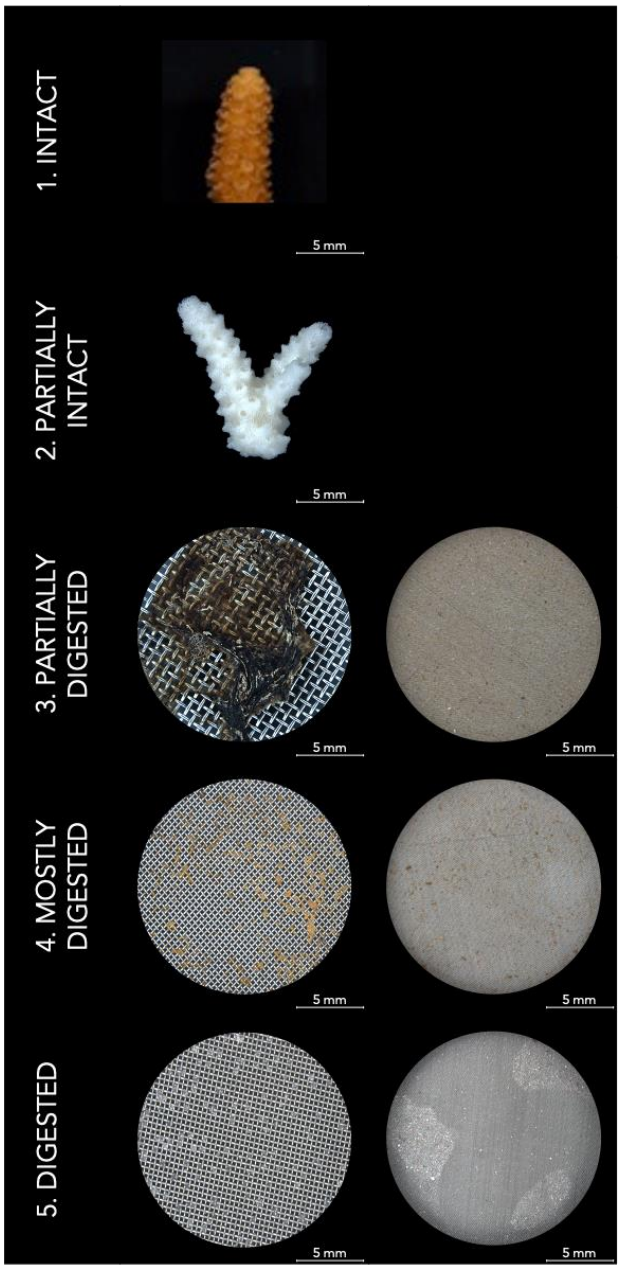

Figure S3: Visual ranking of clarification efficiency (sub-criterion 2), with examples representing each of the five scores. Score 1 (intact) shows a coral fragment, no change (photograph by Andrew Negri). Score 2 (partially intact) shows a coral fragment following alkaline (1M KOH) digestion for 24 h, the organic matter has been digested but the calcium carbonate-based skeleton remains intact. Score 3 (partially digested) shows a dissected sea squirt following alkaline (1M KOH) digestion for 24 h, with the undigested pharynx covering >50% of the surface area of the larger 263 µm mesh and little material present on the smaller 26 µm mesh. Score 4 (mostly digested) shows a sponge following acid (70% HNO_3) digestion for 24 h, in which the retentate occupies <50% of the surface area of both mesh, and does not hamper visual and spectral assessment of microplastics. Score 5 (digested) shows retentate from density flotation of sea cucumber gastro-intestinal tract contents with 1.7 g/cm^3 KI for 24 h, a clear visual and spectral assessment of microplastics is possible.

1.4. Carbonyl Index (CI) calculation and statistical analysis

After exposure to treatments, rayon was the only polymer to return a correlation factor lower than 0.9 (see the results section in the main manuscript for more info). Hence, only rayon spectra were analysed for changes in the carbonyl index (CI). CI was determined for two regions of the rayon spectrum (CI_1 and CI_2). Both regions are noted to be affected by degradation processes[6-8] and were noted to have changed as a result of exposure to treatments. As per Dawson, et al. [9], absorbances at 1420 and 1346 cm^{-1} (1518-1210 cm^{-1} region) and 893 cm^{-1} (917-868 cm^{-1} region) were used to calculate CI_1 ($CI_1 = A_{893}/A_{1420+1346}$). CI_2 was calculated using absorbances at 1640 cm^{-1} (1720-1518 cm^{-1} region) and 893 cm^{-1} (917-868 cm^{-1} region) ($CI_2 = A_{893}/A_{1640}$). Significant changes in CI (p-value < 0.05) were assessed between pre-treated and positive control microplastics, and between pre-treated control and treated microplastics. Data analysis was conducted with R (version 1.2.5042), applying general linear models (glm) with Gamma distribution and pairwise hypothesis testing.

2. Supplementary Results

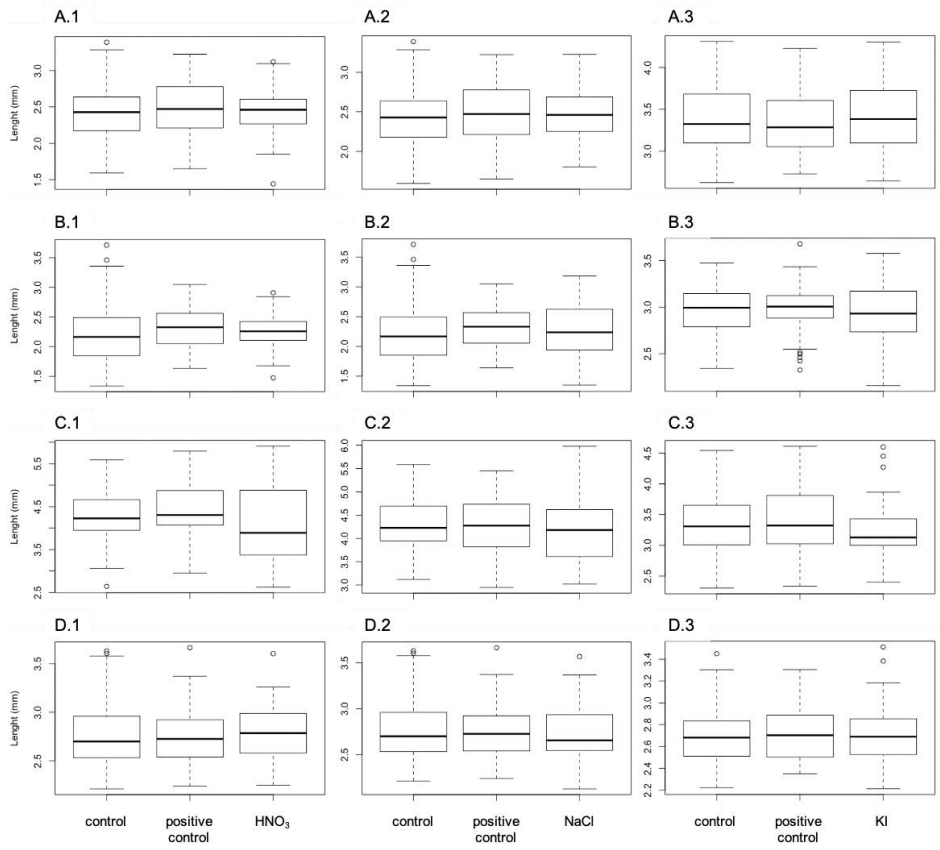

Figure S4: Comparison of maximum length of microplastic fragments (mm, y-axis) before (control) and following 24 h exposure to Milli-Q water (positive control) and separation method (i.e., either 70% HNO_3, 1.2 g cm^{-3} NaCl or 1.7 g cm^{-3} KI, x-axis) (n = 50 microplastics measured per treatment). (a) Polyethylene, (b) polystyrene, (c) polyester, and (d) polyvinylchloride. Each boxplot displays: sample median (bold line within box), interquartile range (box), minimum and maximum lengths with exception of outliers (whiskers), and likely outliers (circles). No significant differences were detected in sizes of microplastics across the control, positive control and separation method.

Table S4: Summary of statistical analyses revealing differences in maximum length of microplastic irregular fragments pre- (control) and post-treatment, including positive control (Milli-Q water), and 24-hour exposure to nitric acid (70% HNO3), 1.2 g/cm3 sodium chloride (NaCl), and 1.7g/cm3 potassium iodide (KI). Control corresponds to the intercept of the model. No significant differences ($p < 0.05$) were found. Polyethylene = PE, polystyrene = PS, polyester = PET, and polyvinylchloride = PVC.

Polymer type and treatment	Statistical analyses					
PE	estimate	std.error	statistic	p.value	conf.low	conf.high
control	2.41	0.02	116.57	$3.52e^{-309}$	2.37	2.45
control vs positive control	0.09	0.06	1.51	0.13	-0.02	0.20
control vs HNO_3	0.02	0.06	0.37	0.71	-0.09	0.13
control vs NaCl	0.04	0.06	0.79	0.43	-0.06	0.15
control vs KI	0.02	0.07	0.26	0.79	-0.12	0.16
PS	estimate	std.error	statistic	p.value	conf.low	conf.high
control	2.20	0.02	90.60	$2.67e^{-267}$	2.15	2.25
control vs positive control	0.12	0.07	1.74	0.08	-0.01	0.25
control vs HNO_3	0.07	0.07	1.10	0.27	-0.05	0.21
control vs NaCl	0.06	0.07	0.84	0.40	-0.07	0.19
control vs KI	-0.02	0.05	-0.41	0.68	-0.11	0.07
PET	estimate	std.error	statistic	p.value	conf.low	conf.high
control	4.28	0.06	69.85	$2.59e^{-148}$	4.16	4.40
control vs positive control	0.13	0.11	1.12	0.26	-0.09	0.35
control vs HNO_3	-0.08	0.11	-0.74	0.46	-0.29	0.14
control vs NaCl	-0.06	0.10	-0.63	0.53	-0.25	0.13
control vs KI	-0.13	0.08	-1.63	0.11	-0.28	0.03
PVC	estimate	std.error	statistic	p.value	conf.low	conf.high
control	2.75	0.02	117.81	$2.27e^{-222}$	2.70	2.80
control vs positive control	-0.00	0.05	-0.07	0.94	-0.09	0.09
control vs HNO_3	0.05	0.05	1.03	0.30	-0.04	0.14
control vs NaCl	-0.01	0.05	-0.29	0.77	-0.11	0.08
control vs KI	0.01	0.04	0.21	0.835	-0.08	0.10

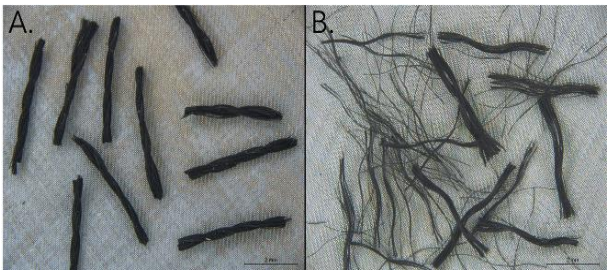

Figure S5: Black rayon fibres prepared from a textile thread and cut into 4 mm lengths, (a) before treatment (control), and (b) after 24 h exposure to Milli-Q water (positive control).

Table S5: Infrared spectral changes detected in rayon after exposure to positive control (i.e., Milli-Q water) for 24 hr, nitric acid (70% HNO3) for 3, 6 or 24 hr, and 1.2 g/cm3 sodium chloride (NaCl) and 1.7 g/cm3 potassium iodide (KI) for 24 hr. * denotes changes observed after acid exposure for 24 hr.

Treatment	Peak wavenumber (cm^{-1})	Bond stretching	Absorbance
Positive Control	3600 – 3000	OH stretching	broadened
	2900 and 2890	CH and/or CH_2 stretching	broadened
70% HNO_3	3600 - 3000*	OH stretching	broadened
	2900 and 2890	CH and/or CH_2 stretching	broadened
	1640 – 1635	HOH bending and/or NO_2 asymmetric stretching	intensified
	1370*	symmetric CH_3 deformation	broadened
	1280	CH bending and/or NO_2 symmetric stretching	intensified
	855	NO_2 bending and/or O-NO_2 stretching	new
	825*	NO_2 bending and/or O-NO_2 stretching	new
	755*	O-NO_2 asymmetric bending	new
	684*	O-NO_2 symmetric bending	broadened
NaCl	3600-3000	OH stretching	broadened
	2900 and 2890 cm^{-1}	CH stretching	broadened
	1370-1260 cm^{-1}	symmetric CH_3 deformation, C-H bending	broadened
KI	3600-3000	OH stretching	broadened
	2900 and 2890 cm^{-1}	CH stretching	broadened

Table S6: Summary of statistical analyses revealing differences in the rayon carbonyl index (CI) pre- and post-exposure to the positive control (i.e., Milli-Q water) for 24 hr, nitric acid (70% HNO3) for 3, 6 or 24 hr, and 1.2 g/cm3 sodium chloride (NaCl) and 1.7 g/cm3 potassium iodide (KI) for 24 hr. Significant differences ($p < 0.05$) are marked in bold.

Rayon	$CI_1 = A_{893}/A_{1420+1346}$						$CI_2 = A_{893}/A_{1640}$					
	estimate	std.error	statistic	p.value	conf.low	conf.high	estimate	std.error	statistic	p.value	conf.low	conf.high
control	5.88	0.64	9.22	$5.54e^{-10}$	4.79	7.33	1.78	0.188	9.51	$2.90e^{-10}$	1.46	7.33
control vs positive control	0.69	0.71	0.97	$3.4e^{-1}$	-0.87	1.98	-0.42	0.20	-2.11	$4.4e^{-2}$	- 0.86	- 0.07
control	5.88	1.37	4.30	$1.87e^{-4}$	3.85	9.63	1.78	0.58	3.10	$4.41e^{-3}$	1.01	3.62
control vs 24 hr-HNO_3	5.76	1.83	3.16	$3.81e^{-3}$	1.01	3.62	1.82	0.78	2.35	$2.62e^{-2}$	-0.17	3.34
control	5.88	0.35	16.9	$3.16e^{-16}$	5.25	6.62	1.78	0.11	15.8	$1.72e^{-15}$	1.58	2.02
control vs 6 hr-HNO_3	-0.84	0.37	-2.24	$3.30e^{-2}$	-1.61	-0.15	0.67	0.13	5.06	$2.35e^{-5}$	0.4	0.92
control	5.88	0.51	11.5	$3.78e^{-12}$	4.98	7.00	1.78	0.12	14.9	$7.29e^{-15}$	1.57	2.04
control vs 3 hr-HNO_3	-0.83	0.55	-1.53	$1.38e^{-1}$	-2.01	0.15	0.52	0.14	3.78	$7.50e^{-4}$	0.24	0.78
control	5.88	0.53	11	$1.10e^{-11}$	4.95	7.06	1.78	0.16	11.4	$4.70e^{-12}$	-0.71	-0.05
control vs NaCl	5.70	0.71	8.01	$1.01e^{-8}$	4.24	7.06	-0.35	0.17	-2.08	$4.71e^{-2}$	-0.705	-0.05
control	5.88	0.34	17.2	$2.16e^{-16}$	5.25	6.60	1.78	0.09	19.7	$6.31e^{-18}$	1.62	1.97
control vs KI	-0.09	0.37	-0.23	$8.17e^{-1}$	-0.87	0.61	-0.14	0.10	-1.44	$1.61e^{-1}$	-0.34	0.04

Table S7: Spectrum similarity (correlation) of control (non-treated) microplastics (n = 3 replicates per microplastic) to those recovered from spiked coral tissues exposed to nitric acid (70% HNO3) for 24 and 3 hr. Correlation threshold is set at 0.9. Correlations in bold indicate they were lower than the threshold. Spectral match (percentage) to the NICDOCOM IR spectral libraries and polymer standard is also reported. Match threshold is set at ≥ 70%.

Replicate and exposure time	Plastic	Replicate	Spectrum similarity	Spectrum search	
Coral #1 24 hr	PE	1	0.98	91.56	PAD0145.SPC POLYETHYLENE PLASTICIZED #2;9002-88-4;(C2H4)N,WWW.IR-SPECTR
		2	0.99	96.28	PAD0141.SPC POLYETHYLENE LOW DENSITY;9002-88-4;(C2H4)N,WWW.IR-SPECTRA.C
		3	0.99	91.15	PAD0145.SPC POLYETHYLENE PLASTICIZED #2;9002-88-4;(C2H4)N,WWW.IR-SPECTR
	PS	1	0.89	77.35	CO0892.SP COPOLYMER SAN TYPE;9003-54-7;(C)NICODOM 2009 IR-SPECTRA.COM
		2	0.99	99.14	CO1111.SP POLY(STYRENE:ETHYLACRYLATE);57516-68-4;(C)NICODOM 2009 IR-SPE
		3	0.90	60.05	PAD0203.SPC POLYSTYRENE HIGH IMPACT #1;9003-70-7,9003-53-6;(C8H8)N,WWW.
	PET	1	0.97	99.41	FB439.SP FB439, FILLWELL, POLYESTER, WELLMAN, COPYRIGHT NICODOM 2007 IR
		2	0.97	99.43	FB439.SP FB439, FILLWELL, POLYESTER, WELLMAN, COPYRIGHT NICODOM 2007 IR
		3	0.92	98.86	FB439.SP FB439, FILLWELL, POLYESTER, WELLMAN, COPYRIGHT NICODOM 2007 IR
	PVC	1	0.81	89.55	FB317.SP FB317, RHOVYL, PVC, RHONE-POULENC, COPYRIGHT NICODOM 2007 IR-S
		2	0.71	82.61	FB317.SP FB317, RHOVYL, PVC, RHONE-POULENC, COPYRIGHT NICODOM 2007 IR-S
		3	0.78	79.85	FB243.SP FB243, PVC BASED FIBER #1, PVC, PEPE, COPYRIGHT NICODOM 2007 I
	Rayon	1	0.69	82.81	FB157.SP FB157, DIAMANTE, 80% RAYON, 20% POLYESTER, KARABELLA, COP. NIC
		2	0.71	80.27	FB413.SP FB413, T-45, RAYON, NORTH AMERICAN RAYON, COPYRIGHT NICODOM 20
		3	0.81	78.74	PAD0441.SPC CELLULOSE MODIFIED, NICODOM
Coral #2 24 hr	PE	1	0.99	97.76	PAD3075.SPC LUWAX AF 32, NICODOM, MICRONIZED POLYETHYLENE WAXES; BASF
		2	0.99	97.74	PAD3075.SPC LUWAX AF 32, NICODOM, MICRONIZED POLYETHYLENE WAXES; BASF
		3	0.99	96.61	PEC0149.SPC LINEAR ALPHA OLEFIN C 24-28, CRUDE OIL OTHER, COPYRIGHT NIC

	PS	1	0.99	91.82	PAD0203.SPC POLYSTYRENE HIGH IMPACT #1;9003-70-7,9003-53-6;(C8H8)N,WWW.
		2	0.99	99.21	CO1111.SP POLY(STYRENE:ETHYLACRYLATE);57516-68-4;(C)NICODOM 2009 IR-SPE
		3	0.99	99.28	CO1111.SP POLY(STYRENE:ETHYLACRYLATE);57516-68-4;(C)NICODOM 2009 IR-SPE
	PET	1	0.92	99.15	FB439.SP FB439, FILLWELL, POLYESTER, WELLMAN, COPYRIGHT NICODOM 2007 IR
		2	0.94	99.01	FB439.SP FB439, FILLWELL, POLYESTER, WELLMAN, COPYRIGHT NICODOM 2007 IR
		3	0.92	99.22	FB439.SP FB439, FILLWELL, POLYESTER, WELLMAN, COPYRIGHT NICODOM 2007 IR
	PVC	1	0.81	92.52	FB317.SP FB317, RHOVYL, PVC, RHONE-POULENC, COPYRIGHT NICODOM 2007 IR-S
		2	0.79	80.52	FB243.SP FB243, PVC BASED FIBER #1, PVC, PEPE, COPYRIGHT NICODOM 2007 I
		3	0.74	84.20	FB317.SP FB317, RHOVYL, PVC, RHONE-POULENC, COPYRIGHT NICODOM 2007 IR-S
	Rayon	1	0.81	66.02	PAD3271.SPC NITRATE LITHIUM;7790-69-4;LINO3,WWW.IR-SPECTRA.COM, COPYRIG
		2	0.95	96.74	FB374.SP FB374, BERMUDA TWEED, MIXED YARN, WONOCO, COPYRIGHT NICODOM 20
		3	0.95	97.44	FB413.SP FB413, T-45, RAYON, NORTH AMERICAN RAYON, COPYRIGHT NICODOM 20
Coral #3 24h	PE	1	0.98	88.07	PAD0145.SPC POLYETHYLENE PLASTICIZED #2;9002-88-4;(C2H4)N,WWW.IR-SPECTR
		2	0.99	90.62	PAD0145.SPC POLYETHYLENE PLASTICIZED #2;9002-88-4;(C2H4)N,WWW.IR-SPECTR
		3	0.98	97.91	PAD0145.SPC POLYETHYLENE PLASTICIZED #2;9002-88-4;(C2H4)N,WWW.IR-SPECTR
	PS	1	0.98	98.12	PAD0278.SPC POLY(STYRENE:ETHYLACRYLATE);57516-68-4;NICODOM,WWW.IR-SPECT
		2	0.99	98.52	CO1111.SP POLY(STYRENE:ETHYLACRYLATE);57516-68-4;(C)NICODOM 2009 IR-SPE
		3	0.98	97.70	PAD0270.SPC POLY(ACRYLONITRILE:ETHYLENE:PROPYLENE:STYRENE) #1, NICODOM
	PET	1	0.95	99.31	FB439.SP FB439, FILLWELL, POLYESTER, WELLMAN, COPYRIGHT NICODOM 2007 IR
		2	0.95	99.24	FB439.SP FB439, FILLWELL, POLYESTER, WELLMAN, COPYRIGHT NICODOM 2007 IR
		3	0.93	98.93	FB439.SP FB439, FILLWELL, POLYESTER, WELLMAN, COPYRIGHT NICODOM 2007 IR
	PVC	1	0.72	83.75	FB317.SP FB317, RHOVYL, PVC, RHONE-POULENC, COPYRIGHT NICODOM 2007 IR-S

		2	0.90	90.87	CO1129.SP POLYVINYLCHLORIDE - HARD;(C)NICODOM 2009 IR-SPECTRA.COM
		3	0.88	92.28	PAD3433.SPC POLYVINYLCHLORIDE - HARD, NICODOM
	Rayon	1	0.72	71.60	PAD3271.SPC NITRATE LITHIUM;7790-69-4;LINO3,WWW.IR-SPECTRA.COM, COPYRIG
		2	0.76	67.45	FB306.SP FB306, EDITA GLAMOUR, COTTON 55%, RAYON 45%, TOPTEX, COP. NICO
		3	0.75	69.82	FB306.SP FB306, EDITA GLAMOUR, COTTON 55%, RAYON 45%, TOPTEX, COP. NICO
Coral #1 3h	Rayon	1	0.82	89.20	FB413.SP FB413, T-45, RAYON, NORTH AMERICAN RAYON, COPYRIGHT NICODOM 20
		2	0.83	89.05	FB374.SP FB374, BERMUDA TWEED, MIXED YARN, WONOCO, COPYRIGHT NICODOM 20
		3	0.83	89.01	FB413.SP FB413, T-45, RAYON, NORTH AMERICAN RAYON, COPYRIGHT NICODOM 20
Coral #2 3h	Rayon	1	0.81	88.31	FB413.SP FB413, T-45, RAYON, NORTH AMERICAN RAYON, COPYRIGHT NICODOM 20
		2	0.70	96.20	PAD0011.SPC CELLULOSE MICROCRYSTALLINE (VIVAPUR 105);9004-34-6;(C6H10O5
		3	0.85	95.43	FB374.SP FB374, BERMUDA TWEED, MIXED YARN, WONOCO, COPYRIGHT NICODOM 20
Coral #3 3h	Rayon	1	0.82	88.66	FB413.SP FB413, T-45, RAYON, NORTH AMERICAN RAYON, COPYRIGHT NICODOM 20
		2	0.81	88.35	FB413.SP FB413, T-45, RAYON, NORTH AMERICAN RAYON, COPYRIGHT NICODOM 20
		3	0.83	88.56	FB413.SP FB413, T-45, RAYON, NORTH AMERICAN RAYON, COPYRIGHT NICODOM 20

Table S8: Spectrum similarity (correlation) of control (non-treated) microplastics (n = 3 replicates per microplastic) to those recovered from spiked sponge tissues exposed to nitric acid (70% HNO3) for 24 and 6 hr. Correlation threshold is set at 0.9. Correlations in bold indicate they were lower than the threshold. Spectral match (percentage) to the NICDOCOM IR spectral libraries and polymer standard is also reported. Match threshold is set at ≥ 70%. (-) indicates data not available because less than 3 items were recovered.

Replicate	Plastic	Replicate	Spectrum similarity	Spectrum search	
Sponge #1 24 hr	PE	1	0.99	95.66	PAD0148.SPC POLYETHYLENE, ENGAGE 8180;9002-88-4;(C2H4)N,WWW.IR-SPECTRA.
		2	0.98	97.17	PAD3075.SPC LUWAX AF 32, NICODOM, MICRONIZED POLYETHYLENE WAXES; BASF
		3	0.99	96.65	PAD2539.SPC DI-N-OCTADECYL DISULFIDE;2500-88-1;C36H74S2,WWW.IR-SPECTRA.
	PS	1	1.00	99.18	CO1111.SP POLY(STYRENE:ETHYLACRYLATE);57516-68-4;(C)NICODOM 2009 IR-SPE
		2	0.99	98.23	PEC0317.SPC POLY(STYRENE:ETHYLACRYLATE), 57516-68-4, COPYRIGHT NICODOM
		3	1.00	99.32	CO1111.SP POLY(STYRENE:ETHYLACRYLATE);57516-68-4;(C)NICODOM 2009 IR-SPE
	PET	1	0.99	99.19	FB439.SP FB439, FILLWELL, POLYESTER, WELLMAN, COPYRIGHT NICODOM 2007 IR
		2	0.98	99.12	FB439.SP FB439, FILLWELL, POLYESTER, WELLMAN, COPYRIGHT NICODOM 2007 IR
		3	0.99	99.19	FB439.SP FB439, FILLWELL, POLYESTER, WELLMAN, COPYRIGHT NICODOM 2007 IR
	PVC	1	0.85	92.24	FB317.SP FB317, RHOVYL, PVC, RHONE-POULENC, COPYRIGHT NICODOM 2007 IR-S
		2	0.84	94.34	FB317.SP FB317, RHOVYL, PVC, RHONE-POULENC, COPYRIGHT NICODOM 2007 IR-S
		3	0.83	95.35	FB317.SP FB317, RHOVYL, PVC, RHONE-POULENC, COPYRIGHT NICODOM 2007 IR-S
	Rayon	1	0.96	82.81	FB402.SP FB402, BEAU GRIP, RAYON, NORTH AMERICAN RAYON, COPYRIGHT NICOD
		2	0.70	80.27	FB306.SP FB306, EDITA GLAMOUR, COTTON 55%, RAYON 45%, TOPTEX, COP. NICO
		3	0.94	78.74	FB374.SP FB374, BERMUDA TWEED, MIXED YARN, WONOCO, COPYRIGHT NICODOM 20
Sponge #2 24 hr	PE	1	0.99	97.12	PAD3075.SPC LUWAX AF 32, NICODOM, MICRONIZED POLYETHYLENE WAXES; BASF
		2	0.99	97.17	PAD3075.SPC LUWAX AF 32, NICODOM, MICRONIZED POLYETHYLENE WAXES; BASF
		3	0.99	87.46	PEC0149.SPC LINEAR ALPHA OLEFIN C 24-28, CRUDE OIL OTHER, COPYRIGHT NIC

	PS	1	0.98	94.73	PAD0203.SPC POLYSTYRENE HIGH IMPACT #1;9003-70-7,9003-53-6;(C8H8)N,WWW.
		2	0.99	98.57	CO1111.SP POLY(STYRENE:ETHYLACRYLATE);57516-68-4;(C)NICODOM 2009 IR-SPE
		3	0.99	99.32	CO1111.SP POLY(STYRENE:ETHYLACRYLATE);57516-68-4;(C)NICODOM 2009 IR-SPE
	PET	1	0.98	99.33	FB439.SP FB439, FILLWELL, POLYESTER, WELLMAN, COPYRIGHT NICODOM 2007 IR
		2	0.98	99.07	FB439.SP FB439, FILLWELL, POLYESTER, WELLMAN, COPYRIGHT NICODOM 2007 IR
		3	0.98	99.21	FB439.SP FB439, FILLWELL, POLYESTER, WELLMAN, COPYRIGHT NICODOM 2007 IR
	PVC	1	0.82	91.96	FB317.SP FB317, RHOVYL, PVC, RHONE-POULENC, COPYRIGHT NICODOM 2007 IR-S
		2	0.84	94.70	FB243.SP FB243, PVC BASED FIBER #1, PVC, PEPE, COPYRIGHT NICODOM 2007 I
		3	0.84	94.53	FB317.SP FB317, RHOVYL, PVC, RHONE-POULENC, COPYRIGHT NICODOM 2007 IR-S
	Rayon	1	0.75	69.24	PAD3271.SPC NITRATE LITHIUM;7790-69-4;LINO3,WWW.IR-SPECTRA.COM, COPYRIG
		2	0.76	81.01	FB374.SP FB374, BERMUDA TWEED, MIXED YARN, WONOCO, COPYRIGHT NICODOM 20
		3	0.72	82.48	FB413.SP FB413, T-45, RAYON, NORTH AMERICAN RAYON, COPYRIGHT NICODOM 20
Sponge #3 24 hr	PE	1	0.98	97.30	PAD2539.SPC DI-N-OCTADECYL DISULFIDE;2500-88-1;C36H74S2,WWW.IR-SPECTRA.
		2	0.99	96.73	PAD2539.SPC DI-N-OCTADECYL DISULFIDE;2500-88-1;C36H74S2,WWW.IR-SPECTRA.
		3	0.99	97.89	PAD0141.SPC POLYETHYLENE LOW DENSITY;9002-88-4;(C2H4)N,WWW.IR-SPECTRA.C
	PS	1	0.99	99.28	CO1111.SP POLY(STYRENE:ETHYLACRYLATE);57516-68-4;(C)NICODOM 2009 IR-SPE
		2	1.00	99.19	CO1111.SP POLY(STYRENE:ETHYLACRYLATE);57516-68-4;(C)NICODOM 2009 IR-SPE
		3	0.99	98.23	PEC0317.SPC POLY(STYRENE:ETHYLACRYLATE), 57516-68-4, COPYRIGHT NICODOM
	PET	1	0.99	99.29	FB439.SP FB439, FILLWELL, POLYESTER, WELLMAN, COPYRIGHT NICODOM 2007 IR
		2	0.99	99.29	FB439.SP FB439, FILLWELL, POLYESTER, WELLMAN, COPYRIGHT NICODOM 2007 IR
		3	0.99	99.17	FB451.SP FB451, DIOLEN, POLYESTER, DIOLEN INDUSTRIAL FIBERS, COP. NICOD
	PVC	1	0.85	92.67	FB317.SP FB317, RHOVYL, PVC, RHONE-POULENC, COPYRIGHT NICODOM 2007 IR-S
		2	0.85	93.28	FB317.SP FB317, RHOVYL, PVC, RHONE-POULENC, COPYRIGHT NICODOM 2007 IR-S

		3	-	-	-
	Rayon	1	0.95	71.60	FB374.SP FB374, BERMUDA TWEED, MIXED YARN, WONOCO, COPYRIGHT NICODOM 20
		2	0.70	67.48	PAD0433.SPC CELLULOSE #1;9004-34-6;(C6H10O5)N,WWW.IR-SPECTRA.COM, COPYR
		3	0.96	69.82	FB374.SP FB374, BERMUDA TWEED, MIXED YARN, WONOCO, COPYRIGHT NICODOM 20
Sponge #1 6hr	Rayon	1	0.68	89.20	FB413.SP FB413, T-45, RAYON, NORTH AMERICAN RAYON, COPYRIGHT NICODOM 20
		2	0.64	89.05	FB413.SP FB413, T-45, RAYON, NORTH AMERICAN RAYON, COPYRIGHT NICODOM 20
		3	0.67	89.01	FB413.SP FB413, T-45, RAYON, NORTH AMERICAN RAYON, COPYRIGHT NICODOM 20
Sponge #2 6 hr	Rayon	1	0.67	85.39	FB413.SP FB413, T-45, RAYON, NORTH AMERICAN RAYON, COPYRIGHT NICODOM 20
		2	0.66	85.45	FB413.SP FB413, T-45, RAYON, NORTH AMERICAN RAYON, COPYRIGHT NICODOM 20
		3	0.64	83.15	FB413.SP FB413, T-45, RAYON, NORTH AMERICAN RAYON, COPYRIGHT NICODOM 20
Sponge #3 6 hr	Rayon	1	0.72	71.13	FB234.SP FB234, COTTON 80%, NATURAL, C&A, COPYRIGHT NICODOM 2007 IR-SPE
		2	0.65	83.94	FB413.SP FB413, T-45, RAYON, NORTH AMERICAN RAYON, COPYRIGHT NICODOM 20
		3	0.65	85.08	FB413.SP FB413, T-45, RAYON, NORTH AMERICAN RAYON, COPYRIGHT NICODOM 20

Table S9: Spectrum similarity (correlation) of control (non-treated) microplastics (n = 3 replicates per microplastic) to those recovered from spiked sea squirt tissues exposed to nitric acid (70% HNO3) for 24 hr. Correlation threshold is set at 0.9. Correlations in bold indicate they were lower than the threshold. Spectral match (percentage) to the NICDOCOM IR spectral libraries and polymer standard is also reported. Match threshold is set at ≥ 70%. (-) indicates data not available because less than 3 items were recovered.

Replicate	Plastic	Replicate	Spectrum similarity	Spectrum search	
Sea squirt #1	PE	1	0.96	98.28	PAD3075.SPC LUWAX AF 32, NICODOM, MICRONIZED POLYETHYLENE WAXES; BASF
		2	0.98	97.95	PAD3075.SPC LUWAX AF 32, NICODOM, MICRONIZED POLYETHYLENE WAXES; BASF
		3	0.95	92.24	PAD0145.SPC POLYETHYLENE PLASTICIZED #2;9002-88-4;(C2H4)N,WWW.IR-SPECTR
	PS	1	0.98	97.46	CO1111.SP POLY(STYRENE:ETHYLACRYLATE);57516-68-4;(C)NICODOM 2009 IR-SPE
		2	0.91	91.60	PAD0204.SPC POLYSTYRENE HIGH IMPACT #2;9003-70-7,9003-53-6;(C8H8)N,WWW.
		3	0.92	91.40	PAD0204.SPC POLYSTYRENE HIGH IMPACT #2;9003-70-7,9003-53-6;(C8H8)N,WWW.
	PET	1	0.99	98.94	FB451.SP FB451, DIOLEN, POLYESTER, DIOLEN INDUSTRIAL FIBERS, COP. NICOD
		2	0.99	98.64	PEC0304.SPC POLY(ETHYLENE TEREPHTHALATE), 25038-59-9, COPYRIGHT NICODOM
		3	0.99	99.04	PAD1516.SPC FABRIC POLY(ETHYLENE TEREPHTHALATE), NICODOM
	PVC	1	0.66	87.51	FB317.SP FB317, RHOVYL, PVC, RHONE-POULENC, COPYRIGHT NICODOM 2007 IR-S
		2	0.58	77.68	FB317.SP FB317, RHOVYL, PVC, RHONE-POULENC, COPYRIGHT NICODOM 2007 IR-S
		3	0.82	89.36	FB317.SP FB317, RHOVYL, PVC, RHONE-POULENC, COPYRIGHT NICODOM 2007 IR-S
	Rayon	1	0.67	82.81	FB413.SP FB413, T-45, RAYON, NORTH AMERICAN RAYON, COPYRIGHT NICODOM 20
		2	0.65	80.27	FB187.SP FB187, FUR OSTRICH, ANIMAL, NA, COPYRIGHT NICODOM 2007 IR-SPEC
		3	-	-	-
Sea squirt #2	PE	1	0.95	94.67	PAD0141.SPC POLYETHYLENE LOW DENSITY;9002-88-4;(C2H4)N,WWW.IR-SPECTRA.C
		2	0.98	97.68	PAD0141.SPC POLYETHYLENE LOW DENSITY;9002-88-4;(C2H4)N,WWW.IR-SPECTRA.C
		3	0.98	98.09	PAD3075.SPC LUWAX AF 32, NICODOM, MICRONIZED POLYETHYLENE WAXES; BASF

	PS	1	0.98	97.72	CO1111.SP POLY(STYRENE:ETHYLACRYLATE);57516-68-4;(C)NICODOM 2009 IR-SPE
		2	0.95	88.31	CO1111.SP POLY(STYRENE:ETHYLACRYLATE);57516-68-4;(C)NICODOM 2009 IR-SPE
		3	0.98	98.42	CO1111.SP POLY(STYRENE:ETHYLACRYLATE);57516-68-4;(C)NICODOM 2009 IR-SPE
	PET	1	0.99	98.80	FB451.SP FB451, DIOLEN, POLYESTER, DIOLEN INDUSTRIAL FIBERS, COP. NICOD
		2	0.99	99.09	FB451.SP FB451, DIOLEN, POLYESTER, DIOLEN INDUSTRIAL FIBERS, COP. NICOD
		3	0.99	98.95	FB451.SP FB451, DIOLEN, POLYESTER, DIOLEN INDUSTRIAL FIBERS, COP. NICOD
	PVC	1	0.72	87.57	FB317.SP FB317, RHOVYL, PVC, RHONE-POULENC, COPYRIGHT NICODOM 2007 IR-S
		2	0.76	92.57	FB317.SP FB317, RHOVYL, PVC, RHONE-POULENC, COPYRIGHT NICODOM 2007 IR-S
		3	0.59	80.80	FB317.SP FB317, RHOVYL, PVC, RHONE-POULENC, COPYRIGHT NICODOM 2007 IR-S
	Rayon	1	0.67	83.48	FB413.SP FB413, T-45, RAYON, NORTH AMERICAN RAYON, COPYRIGHT NICODOM 20
		2	0.64	82.87	FB374.SP FB374, BERMUDA TWEED, MIXED YARN, WONOCO, COPYRIGHT NICODOM 20
		3	0.60	71.59	FB158.SP FB158, SINSATION, 80% RAYON, 20% WOOL, PLYMOUTH BRAND, NICODOM
Sea squirt #3	PE	1	0.96	97.82	PAD3075.SPC LUWAX AF 32, NICODOM, MICRONIZED POLYETHYLENE WAXES; BASF
		2	0.95	97.85	PAD3075.SPC LUWAX AF 32, NICODOM, MICRONIZED POLYETHYLENE WAXES; BASF
		3	0.97	98.50	PAD3075.SPC LUWAX AF 32, NICODOM, MICRONIZED POLYETHYLENE WAXES; BASF
	PS	1	0.97	95.72	PAD0278.SPC POLY(STYRENE:ETHYLACRYLATE);57516-68-4;NICODOM,WWW.IR-SPECT
		2	0.96	89.58	CO1111.SP POLY(STYRENE:ETHYLACRYLATE);57516-68-4;(C)NICODOM 2009 IR-SPE
		3	0.98	95.57	CO1111.SP POLY(STYRENE:ETHYLACRYLATE);57516-68-4;(C)NICODOM 2009 IR-SPE
	PET	1	0.99	99.03	FB451.SP FB451, DIOLEN, POLYESTER, DIOLEN INDUSTRIAL FIBERS, COP. NICOD
		2	0.98	98.74	FB451.SP FB451, DIOLEN, POLYESTER, DIOLEN INDUSTRIAL FIBERS, COP. NICOD
		3	0.99	99.10	FB451.SP FB451, DIOLEN, POLYESTER, DIOLEN INDUSTRIAL FIBERS, COP. NICOD
	PVC	1	0.75	90.71	FB317.SP FB317, RHOVYL, PVC, RHONE-POULENC, COPYRIGHT NICODOM 2007 IR-S
		2	0.61	80.09	FB317.SP FB317, RHOVYL, PVC, RHONE-POULENC, COPYRIGHT NICODOM 2007 IR-S

		3	0.75	89.78	FB317.SP FB317, RHOVYL, PVC, RHONE-POULENC, COPYRIGHT NICODOM 2007 IR-S
	Rayon	1	0.54	69.67	FB367.SP FB367, SILKEN SHETLAND, MIXED YARN, WONOCO, COPYRIGHT NICODOM
		2	0.91	97.10	FB374.SP FB374, BERMUDA TWEED, MIXED YARN, WONOCO, COPYRIGHT NICODOM 20
		3	0.85	95.38	FB374.SP FB374, BERMUDA TWEED, MIXED YARN, WONOCO, COPYRIGHT NICODOM 20

Table S10: Summary of infrared spectral changes observed for polyvinylchloride (PVC) and rayon recovered from spiked coral, sponge and sea squirt tissues exposed to nitric acid (70% HNO3).

Polymer type	Peak wavenumber (cm^{-1})	Bond stretching	Absorbance
PVC	1640 cm^{-1}	CO stretching vibrations or bridging nitrates	new peak
	1462 cm^{-1}	CH_2 bands	new peak
	1355 cm^{-1}	CO_3 formation	new peak
	1278 cm^{-1}	CO formation	new peak
	1184 cm^{-1}	COC stretching vibrations or C–N stretching	new peak
Rayon	1738 cm^{-1}	C=O stretching	new peak
	1370-1260 cm^{-1}	symmetric CH_3 deformation, C-H bending	broadened

Table S11: Spectrum similarity (correlation) of control (non-treated) microplastics (n = 3 replicates per microplastic) to those recovered from spiked sea cucumber GIT content exposed to 1.2 gcm-3 sodium chloride (NaCl) for 24 hr. Correlation threshold is set at 0.9. Correlations in bold indicate they were lower than the threshold. Spectral match (percentage) to the NICDOCOM IR spectral libraries and polymer standard is also reported. Match threshold is set at ≥ 70%. (-) indicates data not available because less than 3 items were recovered.

Replicate	Plastic	Replicate	Spectrum similarity	Spectrum search	
Sea cucumber #1	PE	1	0.98	98.16	PAD3075.SPC LUWAX AF 32, NICODOM, MICRONIZED POLYETHYLENE WAXES; BASF
		2	0.99	98.46	PAD3075.SPC LUWAX AF 32, NICODOM, MICRONIZED POLYETHYLENE WAXES; BASF
		3	0.98	97.82	PAD3075.SPC LUWAX AF 32, NICODOM, MICRONIZED POLYETHYLENE WAXES; BASF
	PS	1	0.99	98.46	CO1111.SP POLY(STYRENE:ETHYLACRYLATE);57516-68-4;(C)NICODOM 2009 IR-SPE
		2	1.00	99.32	CO1111.SP POLY(STYRENE:ETHYLACRYLATE);57516-68-4;(C)NICODOM 2009 IR-SPE
		3	0.99	99.36	CO1111.SP POLY(STYRENE:ETHYLACRYLATE);57516-68-4;(C)NICODOM 2009 IR-SPE
	PET	1	0.99	98.79	PEC0304.SPC POLY(ETHYLENE TEREPHTHALATE), 25038-59-9, COPYRIGHT NICODOM
		2	0.94	97.54	PAD1509.SPC COTTON+POLYESTER (65:35), NICODOM
		3	-	-	-
	PVC	1	0.94	94.30	CO1129.SP POLYVINYLCHLORIDE - HARD;(C)NICODOM 2009 IR-SPECTRA.COM
		2	0.96	90.33	CO1129.SP POLYVINYLCHLORIDE - HARD;(C)NICODOM 2009 IR-SPECTRA.COM
		3	0.97	83.72	CO1129.SP POLYVINYLCHLORIDE - HARD;(C)NICODOM 2009 IR-SPECTRA.COM
	Rayon	1	0.97	97.71	FB158.SP FB158, SINSATION, 80% RAYON, 20% WOOL, PLYMOUTH BRAND, NICODOM
		2	0.97	97.20	FB158.SP FB158, SINSATION, 80% RAYON, 20% WOOL, PLYMOUTH BRAND, NICODOM
		3	0.98	97.98	FB158.SP FB158, SINSATION, 80% RAYON, 20% WOOL, PLYMOUTH BRAND, NICODOM
Sea cucumber # 2	PE	1	0.99	98.60	PAD3075.SPC LUWAX AF 32, NICODOM, MICRONIZED POLYETHYLENE WAXES; BASF
		2	0.99	97.59	PAD3075.SPC LUWAX AF 32, NICODOM, MICRONIZED POLYETHYLENE WAXES; BASF
		3	0.99	97.90	PAD3075.SPC LUWAX AF 32, NICODOM, MICRONIZED POLYETHYLENE WAXES; BASF

	PS	1	1.00	99.41	CO1111.SP POLY(STYRENE:ETHYLACRYLATE);57516-68-4;(C)NICODOM 2009 IR-SPE
		2	0.99	98.57	CO1111.SP POLY(STYRENE:ETHYLACRYLATE);57516-68-4;(C)NICODOM 2009 IR-SPE
		3	0.99	97.09	CO1111.SP POLY(STYRENE:ETHYLACRYLATE);57516-68-4;(C)NICODOM 2009 IR-SPE
	PET	1	1.00	98.90	FB443.SP FB443, AVLIN, POLYESTER, AVTEX, COPYRIGHT NICODOM 2007 IR-SPEC
		2	0.97	97.42	PAD1509.SPC COTTON+POLYESTER (65:35), NICODOM
		3	0.97	98.47	PAD1509.SPC COTTON+POLYESTER (65:35), NICODOM
	PVC	1	0.96	94.45	CO1129.SP POLYVINYLCHLORIDE - HARD;(C)NICODOM 2009 IR-SPECTRA.COM
		2	0.93	91.83	CO1129.SP POLYVINYLCHLORIDE - HARD;(C)NICODOM 2009 IR-SPECTRA.COM
		3	0.95	92.15	CO1129.SP POLYVINYLCHLORIDE - HARD;(C)NICODOM 2009 IR-SPECTRA.COM
	Rayon	1	0.97	95.08	FB158.SP FB158, SINSATION, 80% RAYON, 20% WOOL, PLYMOUTH BRAND, NICODOM
		2	0.97	96.83	FB396.SP FB396, ABSORBIT, RAYON, ENKA, COPYRIGHT NICODOM 2007 IR-SPECTR
		3	0.97	97.79	FB396.SP FB396, ABSORBIT, RAYON, ENKA, COPYRIGHT NICODOM 2007 IR-SPECTR
Sea cucumber #3	PE	1	0.99	97.09	PAD3075.SPC LUWAX AF 32, NICODOM, MICRONIZED POLYETHYLENE WAXES; BASF
		2	0.99	97.93	PAD3075.SPC LUWAX AF 32, NICODOM, MICRONIZED POLYETHYLENE WAXES; BASF
		3	0.99	97.40	PAD3075.SPC LUWAX AF 32, NICODOM, MICRONIZED POLYETHYLENE WAXES; BASF
	PS	1	0.99	97.68	CO1111.SP POLY(STYRENE:ETHYLACRYLATE);57516-68-4;(C)NICODOM 2009 IR-SPE
		2	0.98	89.83	CO1111.SP POLY(STYRENE:ETHYLACRYLATE);57516-68-4;(C)NICODOM 2009 IR-SPE
		3	0.99	99.24	CO1111.SP POLY(STYRENE:ETHYLACRYLATE);57516-68-4;(C)NICODOM 2009 IR-SPE
	PET	1	0.97	98.37	PAD1509.SPC COTTON+POLYESTER (65:35), NICODOM
		2	0.99	98.87	PEC0304.SPC POLY(ETHYLENE TEREPHTHALATE), 25038-59-9, COPYRIGHT NICODOM
		3	-	-	-
	PVC	1	0.92	79.76	PAD3433.SPC POLYVINYLCHLORIDE - HARD, NICODOM
		2	0.94	89.83	PAD3433.SPC POLYVINYLCHLORIDE - HARD, NICODOM

		3	-	-	-
	Rayon	1	0.98	97.17	FB158.SP FB158, SINSATION, 80% RAYON, 20% WOOL, PLYMOUTH BRAND, NICODOM
		2	0.98	97.48	FB158.SP FB158, SINSATION, 80% RAYON, 20% WOOL, PLYMOUTH BRAND, NICODOM
		3	0.98	97.61	FB158.SP FB158, SINSATION, 80% RAYON, 20% WOOL, PLYMOUTH BRAND, NICODOM

Table S12: Spectrum similarity (correlation) of control (non-treated) microplastics (n = 3 replicates per microplastic) to those recovered from spiked sea cucumber GIT content exposed to 1.7 gcm-3 potassium iodide (KI) for 24 hr. Correlation threshold is set at 0.9. Correlations in bold indicate they were lower than the threshold. Spectral match (percentage) to the NICDOCOM IR spectral libraries and polymer standard is also reported. Match threshold is set at ≥ 70%. (-) indicates data not available because less than 3 items were recovered.

Replicate	Plastic	Replicate	Spectrum similarity	Spectrum search	
Sea cucumber 1	PE	1	1.00	98.61	PAD0151.SPC POLYETHYLENE, HOSTALEN GM 7040;9002-88-4;(C2H4)N, NICODOM;
		2	1.00	98.31	PAD0151.SPC POLYETHYLENE, HOSTALEN GM 7040;9002-88-4;(C2H4)N, NICODOM;
		3	1.00	98.04	PAD0151.SPC POLYETHYLENE, HOSTALEN GM 7040;9002-88-4;(C2H4)N, NICODOM;
	PS	1	1.00	98.46	PAD0278.SPC POLY(STYRENE:ETHYLACRYLATE);57516-68-4;NICODOM,WWW.IR-SPECT
		2	1.00	99.32	CO1111.SP POLY(STYRENE:ETHYLACRYLATE);57516-68-4;(C)NICODOM 2009 IR-SPE
		3	1.00	99.36	CO1126.SP POLYSTYRENE;9003-70-7;(C)NICODOM 2009 IR-SPECTRA.COM
	PET	1	1.00	98.99	FB451.SP FB451, DIOLEN, POLYESTER, DIOLEN INDUSTRIAL FIBERS, COP. NICOD
		2	1.00	98.88	FB443.SP FB443, AVLIN, POLYESTER, AVTEX, COPYRIGHT NICODOM 2007 IR-SPEC
		3	0.98	98.53	FB439.SP FB439, FILLWELL, POLYESTER, WELLMAN, COPYRIGHT NICODOM 2007 IR
	PVC	1	0.98	94.30	CO1129.SP POLYVINYLCHLORIDE - HARD;(C)NICODOM 2009 IR-SPECTRA.COM
		2	0.99	90.33	CO1129.SP POLYVINYLCHLORIDE - HARD;(C)NICODOM 2009 IR-SPECTRA.COM
		3	0.98	83.72	CO1129.SP POLYVINYLCHLORIDE - HARD;(C)NICODOM 2009 IR-SPECTRA.COM
	Rayon	1	0.90	96.56	FB286.SP FB286, FIBRO, RAYON, COURTAULDS, COPYRIGHT NICODOM 2007 IR-SPE
		2	0.87	96.12	PAD1514.SPC FABRIC CELLOPHANE BASED, NICODOM

		3	0.85	95.58	FB401.SP FB401, DURVIL RAYON, RAYON, AVTEX, COPYRIGHT NICODOM 2007 IR-S
Sea cucumber 2	PE	1	0.96	96.54	PAD0151.SPC POLYETHYLENE, HOSTALEN GM 7040;9002-88-4;(C2H4)N, NICODOM;
		2	0.99	89.37	PAD3075.SPC LUWAX AF 32, NICODOM, MICRONIZED POLYETHYLENE WAXES; BASF
		3	1.00	98.25	PAD0151.SPC POLYETHYLENE, HOSTALEN GM 7040;9002-88-4;(C2H4)N, NICODOM;
	PS	1	1.00	98.75	CO1126.SP POLYSTYRENE;9003-70-7;(C)NICODOM 2009 IR-SPECTRA.COM
		2	1.00	98.71	PEC0317.SPC POLY(STYRENE:ETHYLACRYLATE), 57516-68-4, COPYRIGHT NICODOM
		3	1.00	98.68	CO1111.SP POLY(STYRENE:ETHYLACRYLATE);57516-68-4;(C)NICODOM 2009 IR-SPE
	PET	1	0.99	98.79	FB439.SP FB439, FILLWELL, POLYESTER, WELLMAN, COPYRIGHT NICODOM 2007 IR
		2	0.99	98.93	FB439.SP FB439, FILLWELL, POLYESTER, WELLMAN, COPYRIGHT NICODOM 2007 IR
		3	0.99	99.09	FB439.SP FB439, FILLWELL, POLYESTER, WELLMAN, COPYRIGHT NICODOM 2007 IR
	PVC	1	0.99	85.87	CO1129.SP POLYVINYLCHLORIDE - HARD;(C)NICODOM 2009 IR-SPECTRA.COM
		2	0.98	85.71	CO1129.SP POLYVINYLCHLORIDE - HARD;(C)NICODOM 2009 IR-SPECTRA.COM
		3	0.99	85.00	CO1129.SP POLYVINYLCHLORIDE - HARD;(C)NICODOM 2009 IR-SPECTRA.COM
	Rayon	1	0.92	96.09	FB252.SP FB252, BAMBOO FIBER, NATURAL, BAMBUS ELEGANG, COPYRIGHT NICODO
		2	0.91	97.19	FB401.SP FB401, DURVIL RAYON, RAYON, AVTEX, COPYRIGHT NICODOM 2007 IR-S
		3	0.88	95.187	PAD1514.SPC FABRIC CELLOPHANE BASED, NICODOM
Sea cucumber 3	PE	1	1.00	98.98	PAD0151.SPC POLYETHYLENE, HOSTALEN GM 7040;9002-88-4;(C2H4)N, NICODOM;
		2	1.00	98.17	PAD0151.SPC POLYETHYLENE, HOSTALEN GM 7040;9002-88-4;(C2H4)N, NICODOM;
		3	1.00	98.83	PAD0151.SPC POLYETHYLENE, HOSTALEN GM 7040;9002-88-4;(C2H4)N, NICODOM;
	PS	1	1.00	98.83	CO1111.SP POLY(STYRENE:ETHYLACRYLATE);57516-68-4;(C)NICODOM 2009 IR-SPE

		2	1.00	98.85	CO1111.SP POLY(STYRENE:ETHYLACRYLATE);57516-68-4;(C)NICODOM 2009 IR-SPE
		3	-	-	
	PET	1	0.99	98.67	FB439.SP FB439, FILLWELL, POLYESTER, WELLMAN, COPYRIGHT NICODOM 2007 IR
		2	0.98	98.41	FB443.SP FB443, AVLIN, POLYESTER, AVTEX, COPYRIGHT NICODOM 2007 IR-SPEC
		3	0.99	98.93	FB439.SP FB439, FILLWELL, POLYESTER, WELLMAN, COPYRIGHT NICODOM 2007 IR
	PVC	1	0.99	85.41	CO1129.SP POLYVINYLCHLORIDE - HARD;(C)NICODOM 2009 IR-SPECTRA.COM
		2	0.98	84.23	CO1129.SP POLYVINYLCHLORIDE - HARD;(C)NICODOM 2009 IR-SPECTRA.COM
		3	0.98	89.36	PAD3433.SPC POLYVINYLCHLORIDE - HARD, NICODOM
	Rayon	1	0.91	95.37	FB252.SP FB252, BAMBOO FIBER, NATURAL, BAMBUS ELEGANG, COPYRIGHT NICODO
		2	0.92	96.76	FB401.SP FB401, DURVIL RAYON, RAYON, AVTEX, COPYRIGHT NICODOM 2007 IR-S
		3	0.90	94.81	FB252.SP FB252, BAMBOO FIBER, NATURAL, BAMBUS ELEGANG, COPYRIGHT NICODO

3. Supplementary References

Comnea-Stancu, I. R.; Wieland, K.; Ramer, G.; Schwaighofer, A.; Lendl, B., On the Identification of Rayon/Viscose as a Major Fraction of Microplastics in the Marine Environment: Discrimination between Natural and Manmade Cellulosic Fibers Using Fourier Transform Infrared Spectroscopy. Appl Spectrosc 2017, 71, (5), 939-950.

Dawson, A. L.; Motti, C. A.; Kroon, F. J., Solving a Sticky Situation: Microplastic Analysis of Lipid-Rich Tissue. Frontiers in Environmental Science 2020, 8.

Fan, M.; Dai, D.; Huang, B., Fourier transform infrared spectroscopy for natural fibres. Fourier transform-materials analysis 2012, 3, 45-68.

Hartmann, N. B.; Huffer, T.; Thompson, R. C.; Hassellov, M.; Verschoor, A.; Daugaard, A. E.; Rist, S.; Karlsson, T.; Brennholt, N.; Cole, M.; Herrling, M. P.; Hess, M. C.; Ivleva, N. P.; Lusher, A. L.; Wagner, M., Are We Speaking the Same Language? Recommendations for a Definition and Categorization Framework for Plastic Debris. Environ Sci Technol 2019, 53, (3), 1039-1047.

Headley Pratt, C. Understanding plastic film: its uses, benefits and waste management options; 1997; p 28.

Khiari, R.; Salon, M. B.; Mhenni, M. F.; Mauret, E.; Belgacem, M. N., Synthesis and characterization of cellulose carbonate using greenchemistry: Surface modification of Avicel. Carbohydr Polym 2017, 163, 254-260.

Rochman, C. M.; Brookson, C.; Bikker, J.; Djuric, N.; Earn, A.; Bucci, K.; Athey, S.; Huntington, A.; McIlwraith, H.; Munno, K.; Frond, H. D.; Kolomijeca, A.; Erdle, L.; Grbic, J.; Bayoumi, M.; Borrelle, S. B.; Wu, T.; Santoro, S.; Werbowski, L. M.; Zhu, X.; Giles, R. K.; Hamilton, B. M.; Thaysen, C.; Kaura, A.; Klasios, N.; Ead, L.; Kim, J.; Sherlock, C.; Ho, A.; Hunga, C., Rethinking Microplastics as a Diverse Contaminant Suite. Environmental Toxicology and Chemistry 2019, 38, 703-711.

Schlawinsky, M. The Intake of Microplastic debris by Marine Organisms on the Great Barrier Reef. Master's Thesis, Oldenburg University, 2020.

Vepraskas, M. J.; Cassel, D. K., Sphericity and Roundness of Sand in Coastal Plain Soils and Relationships with Soil Physical Properties. Soil Science Society of America Journal 1987, 51, (5), 1108-1112.

Appendix B

Supplementary Information for Chapter 3 Distribution and compartmentalisation of microplastic contamination in abiotic and biotic matrices of Lizard Island coral reef, Australia

1. Supplementary Methods

Table S1: Contaminant library details for each abiotic and biotic sample analyzed: (a) surface seawater, (b) mid-column seawater, (c) seafloor sediment, (d) fish gastrointestinal tract (GIT), (e) sea squirt innards, (f) sponge, (g) coral, and (h) sea cucumber GIT contents. Items from the contaminant library are described according to origin, material, shape and colour.

(a) Contaminant library for surface seawater samples

Contaminant item	shape	colour
Blank_putative microplastic_1	transparent	fragment
Blank_putative microplastic_2	transparent	fragment
Blank_putative microplastic_3	transparent	fragment
Blank_putative microplastic_4	white	fibre
Blank_putative microplastic_5	white	fibre
Blank_putative microplastic_6	white	fibre
Blank_putative microplastic_7	black	fragment
Blank_putative microplastic_8	white	fragment
Blank_putative microplastic_9	transparent	fibre
Blank_putative microplastic_10	blue	fibre
Blank_putative microplastic_11	brown	fragment
Blank_putative microplastic_12	white	fibre
Blank_putative microplastic_13	brown	fibre
Blank_putative microplastic_14	black	fibre
Blank_putative microplastic_15	black	fibre
Blank_putative microplastic_16	transparent	fibre
Blank_putative microplastic_17	transparent	fibre
Blank_putative microplastic_18	brown	fibre
Blank_putative microplastic_19	brown	fibre
Blank_putative microplastic_20	brown	fragment
Blank_putative microplastic_21	brown	fibre
Blank_putative microplastic_22	transparent	fibre
Blank_putative microplastic_23	brown	fibre
Blank_putative microplastic_24	transparent	fibre
Field_Charcoal	black	fragment
Field_Coal	black	fragment
Field_Clear_Flask_PP_sample container	transparent	fragment
Field_EtOH_Bottle Lid	blue	fragment
Field_Kapok Fibre	transparent	fibre
Field_Yellow_Lid_PE_sample container	yellow	fragment
Field_Yellow Paint	yellow	fragment
Field_40um Plankton Filter	transparent	fibre
Field_350um Plankton Filter	transparent	fibre
Field_Black Paint	black	fragment
Field_Carpet_Blue	transparent	fibre

Field_Carpet_Grey	transparent	fibre
Field_Filament of yellow and grey rope_grey filament	transparent	fibre
Field_Filament of yellow and grey rope_yellow filament	transparent	fibre
Field_Filament of clear rope	transparent	fibre
General_Green AIMS TShirt	green	fibre
General_Green Chile TShirt	green	fibre
General_Parafilm	transparent	fragment
General_Spray Bottle Lid_Red	red	fragment
General_White TShirt	transparent	fibre
General_Wine Shirt	red	fibre
Lab_BlueSilicone_O-ring	blue	fragment
Lab_Cotton Lab Coat	green	fibre
Lab_Gloves	blue	fragment
Lab_Grill Filter	transparent	fibre
Lab_Red_Stopper	red	fragment
Lab_Spray Bottle Lid_Teflon	white	fragment
Lab_White Stopper	white	fragment

(b) Contaminant library for mid-column seawater samples

Contaminant item	shape	colour
Blank_putative microplastic_1	transparent	fibre
Blank_putative microplastic_2	white	fragment
Blank_putative microplastic_3	white	fragment
Blank_putative microplastic_4	green	fibre
Blank_putative microplastic_5	transparent	fibre
Blank_putative microplastic_6	transparent	fibre
Blank_putative microplastic_7	transparent	fibre
Blank_putative microplastic_8	transparent	fibre
Blank_putative microplastic_9	transparent	fibre
Blank_putative microplastic_10	brown	fibre
Blank_putative microplastic_11	red	fibre
Blank_putative microplastic_12	transparent	fibre
Blank_putative microplastic_13	black	fibre
Blank_putative microplastic_14	yellow	fragment
Blank_putative microplastic_15	brown	fragment
Blank_putative microplastic_16	white	fragment
Blank_putative microplastic_17	blue	fibre
Blank_putative microplastic_18	transparent	fibre
Blank_putative microplastic_19	transparent	fibre
Blank_putative microplastic_20	transparent	fibre
Blank_putative microplastic_21	transparent	fibre
Blank_putative microplastic_22	brown	fibre
Blank_putative microplastic_23	brown	fragment
Blank_putative microplastic_24	brown	fibre
Blank_putative microplastic_25	transparent	fibre
Blank_putative microplastic_26	transparent	fibre
Blank_putative microplastic_27	brown	fibre
Blank_putative microplastic_28	transparent	fibre
Blank_putative microplastic_29	transparent	fibre
Blank_putative microplastic_30	white	fragment
Blank_putative microplastic_31	white	fragment
Blank_putative microplastic_32	white	fragment
Blank_putative microplastic_33	white	fragment
Blank_putative microplastic_34	white	fragment
Blank_putative microplastic_35	white	fragment
Blank_putative microplastic_36	white	fragment
Blank_putative microplastic_37	white	fragment
Blank_putative microplastic_38	white	fragment
Blank_putative microplastic_39	white	fragment
Blank_putative microplastic_40	white	fragment
Blank_putative microplastic_41	white	fragment
Blank_putative microplastic_42	white	fragment

Blank_putative microplastic_43	white	fragment
Blank_putative microplastic_44	white	fragment
Blank_putative microplastic_45	transparent	fibre
Field_Charcoal	black	fragment
Field_Coal	black	fragment
Field_Clear_Flask_PP_sample container	transparent	fragment
Field_EtOH_Bottle Lid	blue	fragment
Field_Kapok Fibre	transparent	fibre
Field_Yellow_Lid_PE_sample container	yellow	fragment
Field_Yellow Paint	yellow	fragment
Field_40um Plankton Filter	transparent	fibre
Field_350um Plankton Filter	transparent	fibre
Field_Black Paint	black	fragment
Field_Carpet_Blue	blue	fibre
Field_Carpet_Grey	white	fibre
Field_Filament of yellow and grey rope_grey filament	white	fibre
Field_Filament of yellow and grey rope_yellow filament	yellow	fibre
Field_Filament of clear rope	transparent	fibre
Field_MPP plankton net canvas 17 03 2016	white	fibre
Field_MPP plankton net codend bottle 17 03 2016	transparent	fragment
Field_MPP plankton net nylon 17 03 2016	transparent	fibre
General_Green AIMS TShirt	green	fibre
General_Green Chile TShirt	green	fibre
General_Parafilm	transparent	fragment
General_Spray Bottle Lid_Red	red	fragment
General_White TShirt	transparent	fibre
General_Wine Shirt	red	fibre
Lab_BlueSilicone_O-ring	blue	fragment
Lab_Cotton Lab Coat	green	fibre
Lab_Gloves	blue	fragment
Lab_Grill Filter	transparent	fibre
Lab_Red_Stopper	red	fragment
Lab_Spray Bottle Lid_Teflon	white	fragment
Lab_White Stopper	white	fragment

(c) Contaminant library for sediment samples

Contaminant item	shape	colour
Blank_putative microplastic_1	white	fragment
Blank_putative microplastic_2	white	fragment
Blank_putative microplastic_3	white	fragment
Blank_putative microplastic_4	white	fragment
Blank_putative microplastic_5	white	fragment
Blank_putative microplastic_6	white	fragment
Blank_putative microplastic_7	white	fragment
Blank_putative microplastic_8	white	fragment
Blank_putative microplastic_9	white	fragment
Blank_putative microplastic_10	white	fragment
Blank_putative microplastic_11	white	fragment
Blank_putative microplastic_12	white	fragment
Blank_putative microplastic_13	transparent	fragment
Blank_putative microplastic_14	white	fibre
Blank_putative microplastic_15	transparent	fragment
Blank_putative microplastic_16	transparent	fibre
Blank_putative microplastic_17	transparent	fibre
Field_Charcoal	black	fragment
Field_Coal	black	fragment
Field_PVC Quadrat	white	fragment
Field_EtOH_Bottle Lid	blue	fragment
Field_Kapok Fibre	transparent	fibre
Field_Sediment Plastic Bag	transparent	fragment
General_Green AIMS TShirt	green	fibre
General_Green Chile TShirt	green	fibre
General_Parafilm	transparent	fragment
General_Spray Bottle Lid_Red	red	fragment
General_White TShirt	transparent	fibre
General_Wine Shirt	red	fibre
Lab_BlueSilicone_O-ring	blue	fragment
Lab_Cotton Lab Coat	green	fibre
Lab_Gloves	blue	fragment
Lab_Grill Filter	transparent	fibre
Lab_Red_Stopper	red	fragment
Lab_Spray Bottle Lid_Teflon	white	fragment
Lab_White Stopper	white	fragment

(d) Contaminant library for fish samples

Contaminant item	shape	colour
Blank_putative microplastic_1	red	fragment
Blank_putative microplastic_2	pink	fragment
Blank_putative microplastic_3	transparent	fibre

Blank_putative microplastic_4	black	fragment
Blank_putative microplastic_5	brown	fibre
Blank_putative microplastic_6	transparent	fibre
Blank_putative microplastic_7	transparent	fibre
Blank_putative microplastic_8	transparent	fibre
Blank_putative microplastic_9	transparent	fragment
Blank_putative microplastic_10	blue	fragment
Blank_putative microplastic_11	transparent	fragment
Blank_putative microplastic_12	transparent	fragment
Blank_putative microplastic_13	transparent	fragment
Blank_putative microplastic_14	orange	fibre
Blank_putative microplastic_15	transparent	fragment
Blank_putative microplastic_16	black	fibre
Field_Charcoal	black	fragment
Field_Coal	black	fragment
Field_Clear_Flask_PP_sample container	transparent	fragment
Field_EtOH_Bottle Lid	blue	fragment
Field_Kapok Fibre	transparent	fibre
Field_Yellow_Lid_PE_sample container	yellow	fragment
Field_Zip Lock bag	transparent	fragment
Field_Fishing Net	green	fibre
General_Green AIMS TShirt	green	fibre
General_Green Chile TShirt	green	fibre
General_Parafilm	transparent	fragment
General_Spray Bottle Lid_Red	red	fragment
General_White TShirt	transparent	fibre
General_Wine Shirt	red	fibre
Lab_BlueSilicone_O-ring	blue	fragment
Lab_Cotton Lab Coat	green	fibre
Lab_Gloves	blue	fragment
Lab_Grill Filter	transparent	fibre
Lab_Red_Stopper	red	fragment
Lab_Spray Bottle Lid_Teflon	white	fragment
Lab_White Stopper	white	fragment
Lab_Glass pipette head	red	fragment

(e) Contaminant library for sea squirt samples

Contaminant item	shape	colour
Blank_putative microplastic_1	transparent	fragment
Blank_putative microplastic_2	transparent	fragment
Blank_putative microplastic_3	transparent	fragment
Blank_putative microplastic_4	white	fibre
Blank_putative microplastic_5	white	fibre
Blank_putative microplastic_6	white	fibre
Blank_putative microplastic_7	black	fragment
Blank_putative microplastic_8	white	fragment
Blank_putative microplastic_9	transparent	fibre
Blank_putative microplastic_10	blue	fibre
Blank_putative microplastic_11	brown	fragment
Blank_putative microplastic_12	white	fibre
Blank_putative microplastic_13	brown	fibre
Blank_putative microplastic_14	black	fibre
Blank_putative microplastic_15	brown	fibre
Field_Charcoal	black	fragment
Field_Coal	black	fragment
Field_Clear_Flask_PP_sample container	transparent	fragment
Field_EtOH_Bottle Lid	blue	fragment
Field_Kapok Fibre	transparent	fibre
Field_Yellow_Lid_PE_sample container	yellow	fragment
Field_Zip Lock bag	transparent	fragment
General_Green AIMS TShirt	green	fibre
General_Green Chile TShirt	green	fibre
General_Parafilm	transparent	fragment
General_Spray Bottle Lid_Red	red	fragment
General_White TShirt	transparent	fibre
General_Wine Shirt	red	fibre
Lab_BlueSilicone_O-ring	blue	fragment
Lab_Cotton Lab Coat	green	fibre
Lab_Gloves	blue	fragment
Lab_Grill Filter	transparent	fibre
Lab_Red_Stopper	red	fragment
Lab_Spray Bottle Lid_Teflon	white	fragment
Lab_White Stopper	white	fragment

(f) Contaminant library for sponge samples

Contaminant item	shape	colour
Blank_putative microplastic_1	transparent	fragment
Blank_putative microplastic_2	transparent	fragment
Blank_putative microplastic_3	white	fragment
Blank_putative microplastic_4	transparent	fragment
Blank_putative microplastic_5	transparent	fibre
Blank_putative microplastic_6	white	fragment
Blank_putative microplastic_7	transparent	fibre
Blank_putative microplastic_8	transparent	fragment
Blank_putative microplastic_9	transparent	fibre
Blank_putative microplastic_10	transparent	fragment
Blank_putative microplastic_11	white	fragment
Blank_putative microplastic_12	transparent	fibre
Blank_putative microplastic_13	black	fragment
Blank_putative microplastic_14	brown	fibre
Blank_putative microplastic_15	transparent	fibre
Blank_putative microplastic_16	transparent	fibre
Blank_putative microplastic_17	transparent	fibre
Blank_putative microplastic_18	transparent	fibre
Blank_putative microplastic_19	transparent	fragment
Blank_putative microplastic_20	transparent	fibre
Blank_putative microplastic_21	transparent	fragment
Blank_putative microplastic_22	black	fibre
Blank_putative microplastic_23	red	fibre
Blank_putative microplastic_24	white	fragment
Blank_putative microplastic_25	white	fragment
Blank_putative microplastic_26	white	fragment
Blank_putative microplastic_27	white	fragment
Blank_putative microplastic_28	white	fragment
Blank_putative microplastic_29	white	fragment
Blank_putative microplastic_30	white	fragment
Blank_putative microplastic_31	white	fragment
Field_Charcoal	black	fragment
Field_Coal	black	fragment
Field_Clear_Flask_PP_sample container	transparent	fragment
Field_EtOH_Bottle Lid	blue	fragment
Field_Kapok Fibre	transparent	fibre
Field_Yellow_Lid_PE_sample container	yellow	fragment
Field_Zip Lock bag	transparent	fragment
General_Green AIMS TShirt	green	fibre
General_Green Chile TShirt	green	fibre
General_Parafilm	transparent	fragment
General_Spray Bottle Lid_Red	red	fragment

General_White TShirt	transparent	fibre
General_Wine Shirt	red	fibre
Lab_BlueSilicone_O-ring	blue	fragment
Lab_Cotton Lab Coat	green	fibre
Lab_Gloves	blue	fragment
Lab_Grill Filter	transparent	fibre
Lab_Red_Stopper	red	fragment
Lab_Spray Bottle Lid_Teflon	white	fragment
Lab_White Stopper	white	fragment

(g) Contaminant library for coral samples

Contaminant item	shape	colour
Blank_putative microplastic_1	transparent	fragment
Blank_putative microplastic_2	transparent	fragment
Blank_putative microplastic_3	white	fragment
Blank_putative microplastic_4	transparent	fragment
Blank_putative microplastic_5	transparent	fibre
Blank_putative microplastic_6	white	fragment
Blank_putative microplastic_7	transparent	fibre
Blank_putative microplastic_8	transparent	fragment
Blank_putative microplastic_9	transparent	fibre
Blank_putative microplastic_10	transparent	fragment
Blank_putative microplastic_11	white	fragment
Blank_putative microplastic_12	transparent	fibre
Blank_putative microplastic_13	black	fragment
Blank_putative microplastic_14	brown	fibre
Blank_putative microplastic_15	transparent	fibre
Blank_putative microplastic_16	transparent	fibre
Blank_putative microplastic_17	transparent	fibre
Blank_putative microplastic_18	white	fragment
Blank_putative microplastic_19	transparent	fibre
Blank_putative microplastic_20	transparent	fibre
Blank_putative microplastic_21	transparent	fibre
Blank_putative microplastic_22	transparent	fibre
Blank_putative microplastic_23	transparent	fibre
Blank_putative microplastic_24	transparent	fibre
Blank_putative microplastic_25	transparent	fibre
Field_Charcoal	black	fragment
Field_Coal	black	fragment
Field_Clear_Flask_PP_sample container	transparent	fragment
Field_EtOH_Bottle Lid	blue	fragment
Field_Kapok Fibre	transparent	fibre
Field_Yellow_Lid_PE_sample container	yellow	fragment
Field_Zip Lock bag	transparent	fragment
General_Green AIMS TShirt	green	fibre
General_Green Chile TShirt	green	fibre
General_Parafilm	transparent	fragment
General_Spray Bottle Lid_Red	red	fragment
General_White TShirt	transparent	fibre
General_Wine Shirt	red	fibre
Lab_BlueSilicone_O-ring	blue	fragment
Lab_Cotton Lab Coat	green	fibre
Lab_Gloves	blue	fragment
Lab_Grill Filter	transparent	fibre

Lab_Red_Stopper	red	fragment
Lab_Spray Bottle Lid_Teflon	white	fragment
Lab_White Stopper	white	fragment

(h) Contaminant library for sea cucumber samples

Contaminant item	shape	colour
Blank_putative microplastic_1	transparent	fibre
Blank_putative microplastic_2	transparent	fragment
Blank_putative microplastic_3	brown	fibre
Blank_putative microplastic_4	red	fibre
Blank_putative microplastic_5	transparent	fibre
Blank_putative microplastic_6	black	fibre
Blank_putative microplastic_7	transparent	fragment
Blank_putative microplastic_8	brown	fragment
Blank_putative microplastic_9	white	fragment
Blank_putative microplastic_10	blue	fibre
Blank_putative microplastic_11	transparent	fibre
Blank_putative microplastic_12	transparent	fibre
Blank_putative microplastic_13	transparent	fibre
Blank_putative microplastic_14	transparent	fibre
Blank_putative microplastic_15	red	fragment
Blank_putative microplastic_16	pink	fragment
Blank_putative microplastic_17	transparent	fragment
Blank_putative microplastic_18	transparent	fragment
Blank_putative microplastic_19	white	fragment
Blank_putative microplastic_20	white	fragment
Blank_putative microplastic_21	transparent	fibre
Field_Charcoal	black	fragment
Field_Coal	black	fragment
Field_Clear_Flask_PP_sample container	transparent	fragment
Field_EtOH_Bottle Lid	blue	fragment
Field_Kapok Fibre	transparent	fibre
Field_Yellow_Lid_PE_sample container	yellow	fragment
Field_Zip Lock bag	transparent	fragment
General_Green AIMS TShirt	green	fibre
General_Green Chile TShirt	green	fibre
General_Parafilm	transparent	fragment
General_Spray Bottle Lid_Red	red	fragment
General_White TShirt	transparent	fibre
General_Wine Shirt	red	fibre
Lab_BlueSilicone_O-ring	blue	fragment
Lab_Cotton Lab Coat	green	fibre
Lab_Gloves	blue	fragment
Lab_Grill Filter	transparent	fibre
Lab_Red_Stopper	red	fragment
Lab_Spray Bottle Lid_Teflon	white	fragment
Lab_White Stopper	white	fragment

1. Supplementary Results

Table S2: Environmental conditions during collection of surface and mid-column seawater samples. (a) Rainfall and temperature parameters retrieved from BOM (Cape Flattery, located 36.5 km from Lizard Island) and wind speed and direction parameters retrieved from AIMS (Lizard Island) weather station datasets and (b) *in situ* observations of wind and sea conditions with specific depth measurements for each sampling event.

(a) *out sourced* observations (BOM and AIMS weather station)

Date (October 2018)	Rainfall (mm)	Temperature (˚C)	Wind speed (kn)	Wind direction (vector)
2	0	29.5	48.33	133.94
3	0	29.4	38.85	128.00
4	0	29.5	28.75	121.73
5	0	30.1	12.20	59.92
6	0	29.0	13.57	55.14
7	0	28.8	18.74	95.63
8	0	29.2	19.82	100.48
9	0	30.3	21.92	108.54
10	0	30.1	21.0003	115.41
11	0	30.1	19.3919	109.80
12	0	31.1	15.1008	116.94

(b) *in situ* observations

Sample type	Sampling site	Sample replicate	Wind speed (kn)	Wind direction	Swell	Depth (start | end for sea surface)
Sea surface	Granite Bluff	1	10 – 15	SE	0 – 0.5	17.8 | 21.2
		2	10 – 15	SE	0 – 0.5	7.7 | 8.8
		3	0 – 5	SE	0 – 0.5	11.7 | 3.4
		4	0 – 5	SE	0 – 0.5	4.2 | 19.2
		5	0 – 5	SE	0 – 0.5	14.2 | 3.8
	Blue Lagoon	1	0	n/a	0	9.3 | 6.8
		2	0	n/a	0	9.8 | 8.6
		3	0	n/a	0	9.5 | 7.6
		4	0	n/a	0	5.7 | 8.6
		5	0	n/a	0	9.5 | 6.9
Water column	Granite Bluff	1	15 – 20	SE	0 – 0.5	8.5
		2	15 – 20	SE	0 – 0.5	6.8
		3	0 – 5	W-NW, O-NO	0 – 0.5	6.1
		4	0 – 5	SE	0 – 0.5	8.8
		5	0 – 5	SE	0 – 0.5	6.3
	Blue Lagoon	1	0	n/a	0	10.8
		2	0	n/a	0	6.6
		3	0	n/a	0	8.2
		4	0 – 5	E	0	8.4
		5	0 – 5	E	0	7.8

Table S3: GPS coordinates (latitude and longitude, Degrees Decimal Minutes - DDM) of surface and mid-column seawater sampling. For surface seawater collections, GPS coordinates include the starting and ending points of the 10 min tow. For mid-column seawater collections, only one GPS coordinate was recorded as this sampling was conducted with the boat anchored.

Sample type	Sampling site	Replicate	Initial (1) or final (2) position (surface seawater only)	Latitude	Longitude
Surface	Granite Bluff	1	1	14°39.222’S	145°26.907’E
			2	14°38.773'S	145°26.980'E
		2	1	14°38.801'S	145°27.031'E
			2	14°39.265'S	145°27.015'E
		3	1	14°38.854'S	145°27.006'E
			2	14°39.327'S	145°27.040'E
		4	1	14°39.352'S	145°27.024'E
			2	14°38.916'S	145°27.004'E
		5	1	14°38.792'S	145°27.026'E
			2	14°39.328'S	145°27.036'E
	Blue Lagoon	1	1	14°41.739'S	145°27.128'E
			2	14°41.420'S	145°27.312'E
		2	1	14°41.401'S	145°27.430'E
			2	14°41.679'S	145°27.241'E
		3	1	14°41.744'S	145°27.130'E
			2	14°41.480'S	145°27.278'E
		4	1	14°41.330'S	145°27.357'E
			2	14°41.680'S	145°27.224'E
		5	1	14°41.730'S	145°27.150'E
			2	14°41.374'S	145°27.373'E
Mid-column	Granite Bluff	1	n/a	14°39.290’S	145°27.029’E
		2	n/a	14°38.907’S	145°27.003’E
		3	n/a	14°39.370’S	145°27.017’E
		4	n/a	14°38.984’S	145°26.994’E
		5	n/a	14°39.136’S	145°27.028’E
	Blue Lagoon	1	n/a	14°41.729’S	145°27.139’E
		2	n/a	14°41.358’S	145°27.366’E
		3	n/a	14°41.519’S	145°27.285’E
		4	n/a	14°41.530’S	145°27.263’E
		5	n/a	14°41.473’S	145°27.285’E

Table S4: Recovery rates (%, mean ± standard deviation [sd]) from spike-recovery tests conducted for each sample matrix and respective separation method. Microplastic polymers used in all spiking experiments were PE, PS and rayon (n = 5 per replicate, n = 3 replicates per spiked-recovery test). Sodium chloride = NaCl, potassium iodide = PI, gastrointestinal tract = GIT, nitric acid = HNO3.

Sample type	Sample processing method	Spiked microplastic type	Recovery rate (%, mean ± sd)
Sea surface	Density separation (1.2 g/cm3 NaCl)	PE	100.00 ± 0.00
		PS	93.33 ± 9.43
		Rayon	73.33 ± 9.43
Water column	Density separation (1.7 g/cm3 KI)	PE	100.00 ± 0.00
		PS	93.33 ± 9.43
		Rayon	93.33 ± 9.43
Sediment	Density separation (1.2 g/cm3 NaCl)	PE	100.00 ± 0.00
		PS	86.67 ± 9.43
		Rayon	93.33 ± 9.43
Fish	GIT visual sort	PE	100.00 ± 0.00
		PS	86.67 ± 9.43
		Rayon	93.33 ± 9.43
Sea squirt	Acid digestion (70% HNO3)	PE	100.00 ± 0.00
		PS	86.67 ± 9.43
		Rayon	73.33 ± 9.43
Sponge	Acid digestion (70% HNO3) + Density separation (1.7 g/cm3 KI)	PE	93.33 ± 9.43
		PS	93.33 ± 9.43
		Rayon	66.67 ± 9.43
Coral	Acid digestion (70% HNO3)	PE	100.00 ± 0.00
		PS	86.67 ± 9.43
		Rayon	80.00 ± 16.33
Sea cucumber	Density separation (1.7 g/cm3 KI)	PE	100.00 ± 0.00
		PS	80.00 ± 16.33
		Rayon	100.00 ± 0.00

Table S5: Total numbers of putative microplastics, excluded items (i.e., items of poor spectra quality, flagged as contaminant, or of natural nature), and final plastic count (i.e., semi-synthetic and synthetic items) per sample matrix per abiotic and biotic compartments, following Kroon et al. (2018).

		Abiotic compartment			Biotic compartment				
		Surface seawater	Mid-column seawater	Sediment	Fish (GIT	Sea squirt (innards)	Sponge	Coral	Sea cucumber (GIT)
Total putative microplastics		335	965	235	169	114	87	80	149
Excluded items:	poor spectra	13	60	5	6	4	3	4	5
	contaminant	34	106	14	16	11	12	7	21
	natural nature	151	445	145	104	74	54	51	91
Micro-plastics:	semi-synthetic	14	97	21	12	6	7	2	10
	synthetic	124	259	50	31	19	11	16	22

Table S6: Microplastics final assignment based on primary composition, including semi-synthetic and synthetic nature.

Synthetic or semi-synthetic nature	Initial assignment	Final assignment/group
synthetic	chlorinated polyolefin	chlorinated polyolefin
	epoxy	epoxy
	alkyd polymer	alkyd polymer
	mineral oil hydrocarbon	mineral oil hydrocarbon
	NFC:acrylonitrile NFC:rayon:acrylonitrile polyacrylonitrile:butadiene polyacrylonitrile:butadiene:styrene	acrylonitrile
	nylon NFC:rayon:nylon:polyurethane NFC:rayon:nylon rayon:nylon NFC:nylon keratin:nylon	nylon
	polyacrylate methyl methacrylate acrylic:alkyd polymer	polyacrylate
	polyalcohol poly(oxyalkylated) alcohol	polyalcohol
	polyamine melamine	polymelamine
	polybutadiene rubber	polybutadiene rubber
	polycarboxylic acid	polycarboxylic acid
	polyethyleneterephthalate polyester:nylon polyester:polyalkyd polyester:polypropylene:acrylic polyester:polyurethane epoxypolyester NFC:polyester rayon:polyester NFC:rayon:polyester NFC:polyester:polypropylene rayon:nylon:polyester keratin:polyester:nylon	PET
	polyethylene	PE
	polyglycol:polyhydrocarbons isothiazolinone:glycol:formaldehyde	polyglycol

	polyoxymethylene	polyoxymethylene
	polypropylene NFC:polypropylene polypropylene:polyethylene ethylene propylene diene	PP
	polysiloxane	polysiloxane
	polystyrene	PS
	polysulfone	polysulfone
	polytetrafluoroethylene	PTFE
	polyurethane polyurethane:polyacrylate polyurethane rubber rayon:polyurethane	polyurethane
	polyvinylchloride polyvinylacetate:vinylchloride polyvinylalcohol polyvinylbenzyl chloride polyvinylacetate:polyethylene	polyvinyl
	soft copolymer	soft copolymer
semi-synthetic items	rayon NFC:rayon rayon:keratin	rayon
	nitrocellulose	nitrocellulose

Table S7: Summary of general linear models (GLM) showing differences in microplastic concentration between (a) abiotic and (b) biotic compartments of Lizard Island, and the influence of sampling site. Abiotic compartments included surface seawater, mid-column seawater and sediment. Biotic compartments included fish gastrointestinal tract (GIT), sea squirt innards, sponge, coral and sea cucumber GIT.

(a) abiotic compartment: Adjusted $R^2 = 0.97$, AIC = 63.83

	estimate	std. error	statistic	p-value
Intercept	6.9350	0.2233	31.059	< 2e-16
water column	-2.9765	0.2735	-10.885	3.53e-11
sea surface	-8.8419	0.2735	-32.333	< 2e-16
blue lagoon	-0.6626	0.2233	-2.968	0.00636

(b) biotic compartment: McFadden's Pseudo $R^2 = 0.68$, AIC = 62.87

term	estimate	std. error	statistic	p.value
Intercept	0.66086065	0.49325838	1.33978595	0.18031494
coral	-25.112503	52322.7567	-4.80E-04	0.99961705
sea cucumber	-25.112503	52322.7567	-4.80E-04	0.99961705
sponge	-25.112503	52322.7567	-4.80E-04	0.99961705
sea squirt	-0.2866708	0.67758608	-0.4230766	0.6722394
blue lagoon	-2.134327	0.85123332	-2.5073349	0.01216454

Table S8: Total number of microplastics per compartment sampled. Columns report numbers by abiotic: seawater surface, seawater column, sediment; and biotic: fish, sea squirt, sponge, coral, and sea cucumber compartments. Rows report total numbers per compartment sampled and per each microplastic characteristic examined in each abiotic compartment: (a) shape, (b) size class, (c) colour, and (d) polymer type. Please note that these are number of items and not concentration.

	water surface	water column	sediment	fish	sea squirt	sponge	coral	sea cucumber
total	139	358	71	43	25	18	18	32
microplastic characteristic								
(a) shape								
fibre	29	190	51	31	13	8	6	19
fragment	110	168	20	12	12	10	12	13
(b) size								
class 1	56	119	33	18	15	13	12	13
class 2	19	34	21	11	4	4	2	8
class 3	44	82	15	14	5	2	1	10
class 4	16	54	2	0	0	1	0	1
class 5	4	69	0	0	1	0	3	0
(c) colour								
black	11	35	7	3	5	1	2	5
blue	37	140	25	12	0	3	0	8
brown	1	17	1	0	1	0	0	2
green	1	12	6	0	0	2	0	0
grey	2	6	0	0	0	0		0
mix	1	2	1	0	0	0	0	0
orange	0	6	0	2	0	0	0	0
pink	35	8	2	1	0	0	0	0
purple	0	6	0	0	0	0	0	0
red	5	27	9	3	0	0	2	4
transparent	16	72	16	19	14	7	7	8
white	27	22	1	1	4	5	8	5
yellow	3	5	3	2	1	0	0	0
(d) polymer								
polyacrylate	20	24	4	0	1	1	0	1
polyacrylonitrile	0	3	5	0	0	0	0	0
alkyd polymer	0	2	0	0	0	0	0	0
chlorinated polyolefin	1	0	0	0	0	0	0	0
epoxy	0	2	2	0	0	0	0	0
polymelamine	0	1	1	0	0	0	1	0
mineral oil hydrocarbon	0	1	0	0	0	0	0	0
nitrocellulose	0	0	1	0	0	0	0	0
nylon	1	10	7	0	0	2	0	0
PE	34	9	3	0	0	0	0	0
PET	12	78	23	27	8	2	2	8
Polyalcohol	3	1	1	0	0	0	0	0

polybutadiene rubber	0	2	1	0	0	0	0	0
polycarboxylic acid	1	2	0	0	0	0	0	0
polyglycol copolymer	0	19	2	2	6	0	2	4
polyoxymethylene	0	1	0	0	0	0	0	0
polysiloxane	2	10	0	2	0	1	0	0
Polysulfone	0	1	0	0	1	1	7	1
polyurethane	0	5	1	1	0	0	0	0
Polyvinyl	1	22	2	0	1	2	0	1
PP	56	94	4	3	2	5	3	2
PS	0	7	0	1	1	0	0	1
PTFE	0	0	0	0	0	0	1	0
rayon	8	62	13	6	5	4	2	5
soft copolymer	0	0	1	1	0	0	0	0

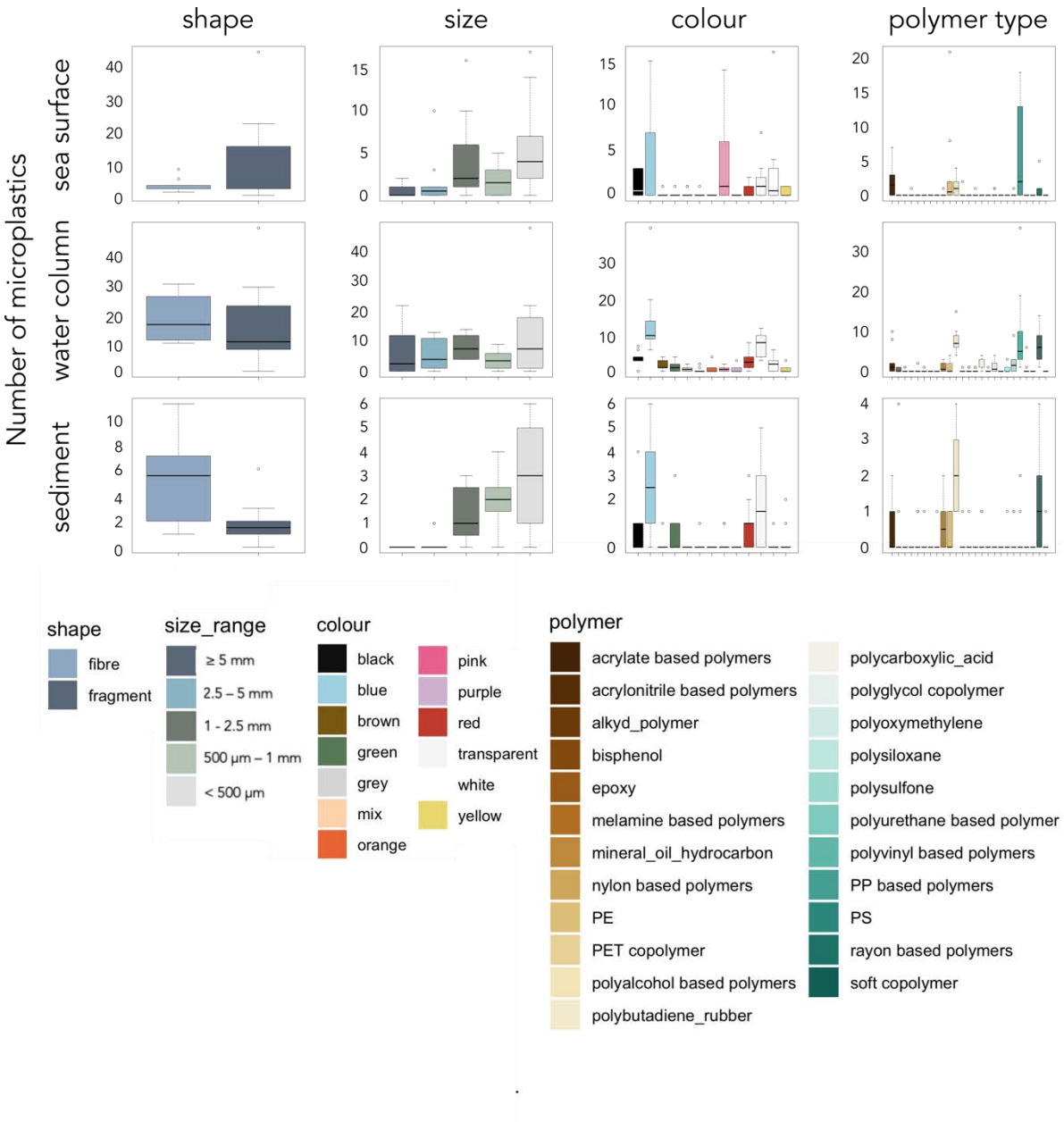

Figure S1: Number of microplastics per shape (1st column), size classes (2nd column), colour (3rd column), and polymer type (4th column) in the surface and mid-column sea water, and sediment (per individual sample). Size class 1: < 500 µm, size class 2: ³ 500 µm and < 1mm, size class 3: ³ 1 and < 2.5 mm, size class 4: ³ 2.5 and < 5 mm, size class 5: ³ 5 mm. Each boxplot displays: sample median (bold line within box), interquartile range (box), minimum and maximum lengths with exception of outliers (whiskers), and likely outliers (circles). No significant differences were detected in sizes of microplastics across the control, positive control and separation method.

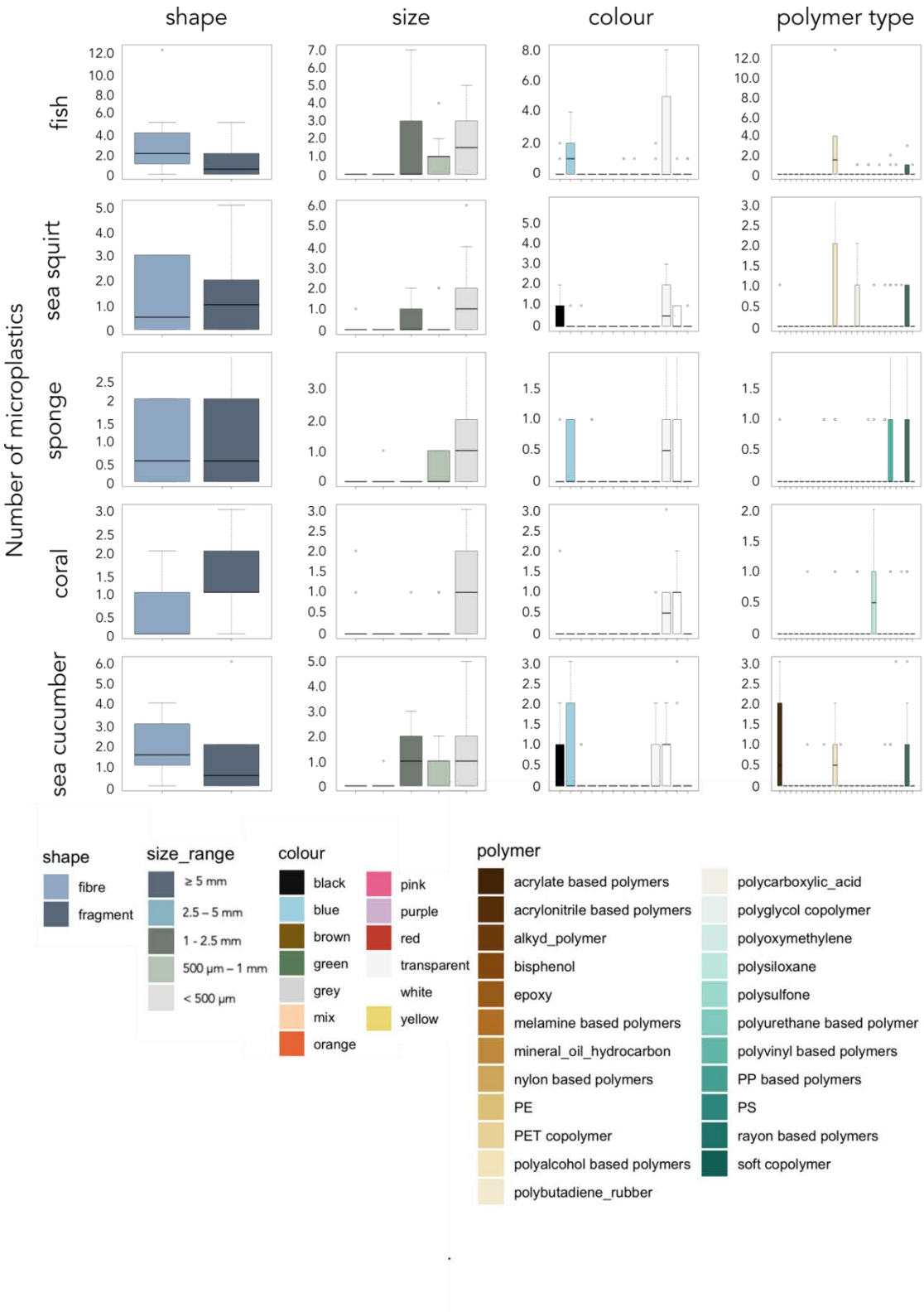

Figure S2: Number of microplastics per shape (1st column), size classes (2nd column), colour (3rd column), and polymer type (4th column) in fish, sea squirt, sponge, coral and sea cucumber (per individual sample). Size class 1: < 500 µm, size class 2: ³ 500 µm and < 1mm, size class 3: ³ 1 and < 2.5 mm, size class 4: ³ 2.5 and < 5 mm, size class 5: ³ 5 mm. Each boxplot displays: sample median (bold line within box), interquartile range (box), minimum and maximum lengths with exception of outliers (whiskers), and likely outliers (circles). No significant differences were detected in sizes of microplastics across the control, positive control and separation method.

Appendix C

Supplementary Information for Chapter 4 Ingestion and depuration of microplastics by a planktivorous coral reef fish, *Pomacentrus amboinensis*

1 Supplementary Methods

1.1. Chemical composition of the two model microplastics

The chemical composition of both PP particles and PET fibers were confirmed using a PerkinElmer Spectrum 100 FTIR spectrometer. Conditions of data acquisition were 1 mm ATR window, pressure gauge = 150, 16 scans at 4 cm^{-1} resolution, wavenumber range between 4000 and 600 cm^{-1}, atmospheric (CO_2/H_2O) suppression, and atmospheric vapor compensation.

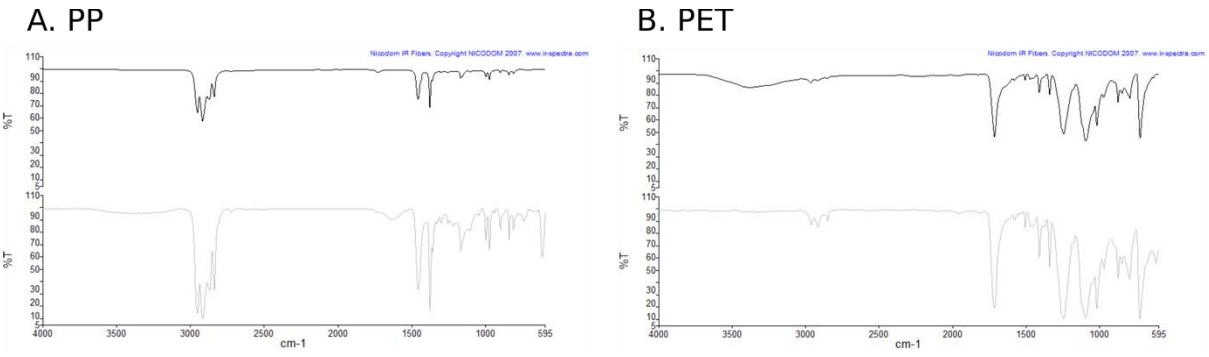

Figure S1: FTIR spectra of microplastic models, namely (a) polypropylene (PP) particles, and (b) polyester (PET) fibers, in comparison to reference spectra from commercially available Nicodom IR spectral libraries (Polymers and Additives, Coatings, Fibers, Dyes and Pigments, Petrochemicals; Nicodom Ltd., Czech Republic). Top spectra are of model microplastics; bottom spectra correspond to polymer references. For both model microplastics similarities with Nicodom spectra were ≥98%.

1.2. Contaminant library

Table S1: Contaminant library details, including item origin (field gear, clothing, experimental equipment, laboratory materials, and sample processing blanks), chemical composition, shape and colour.

Item origin	Materials	Shape	Color
Field gear	Filament of clear rope	fiber	transparent
	Fishing net		black
	Black vessel paint	irregular fragment	black
	Yellow vessel paint		yellow
	Ziplock bag		transparent
	Vessel carpet		blue
	Filament of yellow and grey rope_grey_1	fiber	grey
	Filament of yellow and grey rope_2		yellow
Clothing	TShirt_1	fiber	dark green
	TShirt_2		light green
	TShirt_3		white
	TShirt_4		blue
	Lab coat		green
Experimental equipment	Filter_case_1	fragment	blue
	Fish_tank_1		transparent
	Fish_tank_lid_1		pink
	Fish_tank_lid_2		blue
	Fish_tank_lid_3		green
	Inflow_tubing_fish_tank		transparent
	Outflow_mesh_fish_tank		transparent
	Thread_tape_fittings		white
	Visual_Barrier_1.1	fibre	white
	Visual_Barrier_1.2		brown
	Visual_Barrier_2.1		green
	Visual_Barrier_2.2		black
	Water_pipeline	fragment	black
Laboratory materials	Parafilm	fragment	transparent
	Sample_container		transparent

	Sample_container_lid		white
	Silicone_O-ring		blue
	Nitrile gloves		blue
	Grill Filter	fibre	transparent
	Spray Bottle Lid_Teflon	fragment	white
	White Stopper		white
Sample processing blank	putative_microplastic_1		transparent
	putative_microplastic _2		transparent
	putative_microplastic _3	fibre	transparent
	putative_microplastic _4		transparent
	putative_microplastic _5		transparent
	putative_microplastic _6		transparent
	putative_microplastic _7	fragment	transparent
	putative_microplastic _8	fibre	white
	putative_microplastic _9		blue
	putative_microplastic _10	fragment	green
	putative_microplastic _11	fibre	transparent
	putative_microplastic _12		transparent
	putative_microplastic _13	fragment	transparent
	putative_microplastic _14		transparent
	putative_microplastic _15		transparent
	putative_microplastic _16	fibre	transparent
	putative_microplastic _17		transparent
	putative_microplastic _18	fragment	red
	putative_microplastic _19	fibre	transparent
	putative_microplastic _20		blue
	putative_microplastic _21	fragment	white
	putative_microplastic _22		green
	putative_microplastic _23	fibre	transparent
	putative_microplastic _24		transparent
	putative_microplastic _25		green
	putative_microplastic _26	fragment	white
	putative_microplastic _27		brown
	putative_microplastic _28		white
	putative_microplastic _29	fibre	green
	putative_microplastic _30		transparent
	putative_microplastic _31	fragment	green

putative_microplastic _32		transparent
putative_microplastic _33	fibre	transparent
putative_microplastic _34		transparent

2 Supplementary Results

Table S2. Ingestion and depuration of microplastics by a planktivorous coral reef fish, *Pomacentrus amboinensis*. Fish basic information and microplastic models body burden. Fish basic information includes weight (g), standard and fork lengths (cm), and sex. Microplastic models body burden is reported as absolute numbers of PET fibres and PP particles.

Treatment Information			Fish Basic Information				Microplastic Models Body Burden	
Period of depuration	Concentration of exposure	Replicate No.	Fish weight (g)	Fish Standard Length (cm)	Fish Fork Length (cm)	Fish Sex	PET fibres	PP particle
0	0	1	2.01	3.6	4	male	-	-
0	0	2	9.76	6	6.4	male	-	-
0	0	3	5.37	5.2	5.6	female	-	-
0	0	4	8	5.5	6.5	female	-	-
2	T1	1	2.77	3.9	4.3	imature	1	1
2	T1	2	3.7	4.4	4.9	male	1	1
2	T1	3	2.69	3.9	4.5	male	0	0
2	T1	4	2.67	3.8	4.7	imature	0	1
2	T2	1	2.82	4	4.4	male	5	7
2	T2	2	10.55	6.5	7.2	female	9	8
2	T2	3	8.84	6	7	female	6	5
2	T2	4	1.88	3.3	3.9	male	10	6
2	T3	1	14.4	6.6	7.9	female	86	51
2	T3	2	9.53	5.9	7	female	98	48
2	T3	3	3.4	4.3	5	imature	26	79

2	T3	4	6.14	5.1	5.8	imature	25	54
4	T1	1	15.08	6.9	8.1	imature	1	1
4	T1	2	8.62	5.8	7.2	female	1	1
4	T1	3	5.12	4.8	5.8	male	0	1
4	T1	4	4.24	4.8	5.7	male	1	0
4	T2	1	10.53	6.5	7.8	female	6	5
4	T2	2	5.99	5.2	6.3	female	7	4
4	T2	3	1.79	3.4	4.1	male	7	3
4	T2	4	9.5	6.2	7.4	female	8	5
4	T3	1	10.51	6.4	7.3	female	77	28
4	T3	2	4.45	4.9	5.8	male	70	42
4	T3	3	4.36	4.3	5	male	38	56
4	T3	4	3.26	4.1	5	imature	78	38
8	T1	1	8.55	5.8	6.7	male	0	0
8	T1	2	11.09	6.2	7	male	0	0
8	T1	3	2.75	3.8	4.2	male	0	0
8	T1	4	2.74	3.9	4.2	male	0	0
8	T2	1	3.07	4	4.6	imature	0	0
8	T2	2	2.61	3.7	4.3	male	0	0
8	T2	3	8.44	5.5	6.5	male	0	0
8	T2	4	8.81	6.1	6.8	male	1	0
8	T3	1	5.94	4.9	5.7	female	20	1
8	T3	2	3.46	4.1	4.8	male	1	5

8	T3	3	9.2	5.8	6.5	female	9	0
8	T3	4	3.25	4	4.5	male	12	0
16	T1	1	5.22	5	5.7	imature	0	0
16	T1	2	12.88	6.3	7.8	female	0	0
16	T1	3	6.96	5.1	6	male	0	0
16	T1	4	8.7	5.9	6.6	male	0	0
16	T2	1	1.76	3.3	3.6	imature	0	0
16	T2	2	12.61	6.8	7.9	female	0	0
16	T2	3	2.17	3.8	4.2	imature	0	0
16	T2	4	2.28	3.7	4.2	imature	1	0
16	T3	1	6.67	5.1	6.2	male	1	0
16	T3	2	5.34	5	5.6	imature	5	0
16	T3	3	3.41	4.1	4.4	male	6	0
16	T3	4	2.21	3.7	4.1	imature	2	0
32	T1	1	8.71	6.1	7.3	male	0	0
32	T1	2	2.15	3.5	4.4	male	0	0
32	T1	3	4.56	4.8	5.8	male	0	0
32	T1	4	2.85	4.11	5	male	0	0
32	T2	1	6.55	5.4	6.5	male	0	0
32	T2	2	1	2.9	3.5	imature	0	0
32	T2	3	2.74	4.1	5	male	0	0
32	T2	4	7.75	5.5	6.8	male	0	0
32	T3	1	6.26	5.3	6.4	male	4	0

32	T3	2	7.55	5.6	6.6	male	0	0
32	T3	3	6.9	5.5	6.6	male	0	0
32	T3	4	11.31	6.6	7.9	female	0	0
64	T1	1	5.92	5.4	6.4	female	0	0
64	T1	2	12.17	7	8.2	female	0	0
64	T1	3	11.38	6.7	7.9	female	0	0
64	T1	4	6.41	5.2	6.4	male	0	0
64	T2	1	10.58	6.3	7.7	male	0	0
64	T2	2	5.72	5.3	6.3	male	0	0
64	T2	3	7.3	5.5	6.5	male	0	0
64	T2	4	5.65	5.2	6.2	male	0	0
64	T3	1	9.28	6.1	7.3	male	0	0
64	T3	2	6.45	5.6	6.7	male	9	0
64	T3	3	13.79	7	8.3	female	1	0
64	T3	4	6.19	5.2	6.3	male	0	0
128	T1	1	10.99	6.5	7.9	female	0	0
128	T1	2	9.23	6.2	7.6	male	0	0
128	T1	3	2.55	4	4.8	male	0	0
128	T1	4	3.12	4.2	5.2	male	0	0
128	T1	5	6.28	5.3	6.4	male	0	0
128	T2	2	3.78	4.6	5.5	male	0	0
128	T2	3	9.81	6.1	7.5	female	0	0
128	T2	4	2.77	4.1	5	male	0	0

128	T3	1	7.73	5.7	6.9	male	0	0
128	T3	2	6.04	5.4	6.6	female	2	0
128	T3	3	6.37	5.2	6.5	male	1	0
128	T3	4	6.4	5.3	6.7	female	0	0

Table S3. Dunnett's post hoc test. Multiple comparisons of depuration rates amongst the different model microplastics and concentrations of exposure. Rows marked in grey correspond to comparisons of interest for the study. This table was adapted from the one generated by GraphPad. PP = polypropylene, PET = polyester, ERC = environmentally relevant concentration, 10x = 10 times the ERC, 100x = 100 times the ERC, CI = confidence level

Dunnett's T3 multiple comparisons test	Mean Diff.	95.00% CI of diff.	Summary	Adjusted p-value
PET ERC vs. PP ERC	-0.1887	-0.3483 to -0.02916	**	0.0039
PET ERC vs. PET 10x	0.0385	-0.1071 to 0.1841	ns	0.9989
PET ERC vs. PP 10x	-0.09681	-0.2443 to 0.05063	ns	0.3893
PET ERC vs. PET 100x	0.1988	0.07552 to 0.3220	****	<0.0001
PET ERC vs. PP 100x	0.07641	-0.05523 to 0.2080	ns	0.5623
PP ERC vs. PET 10x	0.2272	0.08247 to 0.3720	****	<0.0001
PP ERC vs. PP 10x	0.09192	-0.05465 to 0.2385	ns	0.4596
PP ERC vs. PET 100x	0.3875	0.2657 to 0.5093	****	<0.0001
PP ERC vs. PP 100x	0.2651	0.1347 to 0.3956	****	<0.0001
PET 10x vs. PP 10x	-0.1353	-0.2659 to -0.004670	*	0.0177
PET 10x vs. PET 100x	0.1603	0.05966 to 0.2609	****	<0.0001
PET 10x vs. PP 100x	0.03791	-0.07346 to 0.1493	ns	0.9849
PP 10x vs. PET 100x	0.2956	0.1922 to 0.3989	****	<0.0001
PP 10x vs. PP 100x	0.1732	0.05933 to 0.2871	***	0.0001
PET 100x vs. PP 100x	-0.1224	-0.1961 to -0.04863	****	<0.0001

Appendix D

Supplementary Information for Chapter 5 Microplastic fibre exposure and seawater warming synergistically affect levels of stress but not fitness parameters of a juvenile coral reef fish (Acanthochromis polyacanthus) under winter conditions

1. Supplementary Methods

1.1. Chemical confirmation of PET fibres

Analysis by Fourier transform infrared spectroscopy (FTIR; PerkinElmer Spectrum 100) confirmed the sewing thread (Gütermann, CA 02776) used as microplastic fibres was polyester (PET), based on > 90% similarity to the PET reference spectrum (Nicodom IR spectral libraries) (Figure S1).

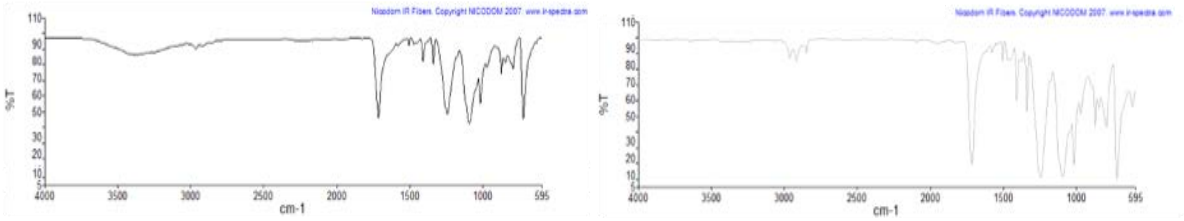

Figure S1: FTIR spectra of (A) Gütermann, CA 02776 polyester (PET) microfibres and (B) PET reference spectrum (Nicodom IR spectral libraries).

1.2. Automated dosing of microplastic fibres

1.2.1. Design and construction of the automated microplastic dosing system

An automated dosing system was designed to deliver a constant known concentration of PET microfibres to the experimental tank system. The dosing system comprised of three main parts: (1) 70 L header tank into which the microplastic stock solution was dosed, (2) primary distribution pipeline, and (3) tank-specific dosing device consisting of a solenoid valve and a secondary pipeline to deliver the microplastic dose into individual experimental tanks (n = 27) (Figure S2). The primary distribution pipeline is a closed system in which the seawater and microplastics mixture is circulated by magnet pump (IWAKI, MX-400CV5E, 50 Hz) throughout experimental room, ultimately returning to the 70 L header tank via (1) an immersed T-shaped outlet located mid-height or (2) an o-ring shower located on the top of 70 L head tank. The T-shaped outlet ensures homogeneity of the stock microplastics solution; the o-ring shower ensures minimal accumulation of microplastics on the walls of the 70 L header tank resulting from water level fluctuations during system use. When a tank-specific solenoid valve is opened that tank is dosed (via the secondary pipeline) for one second with an average of 34.35 mL of stock microplastics solution from the pump-pressurized distribution pipeline.

The secondary pipeline terminates below the water surface to avoid any loss of dosed microplastics due to tank wall adhesion (e.g., splashing).

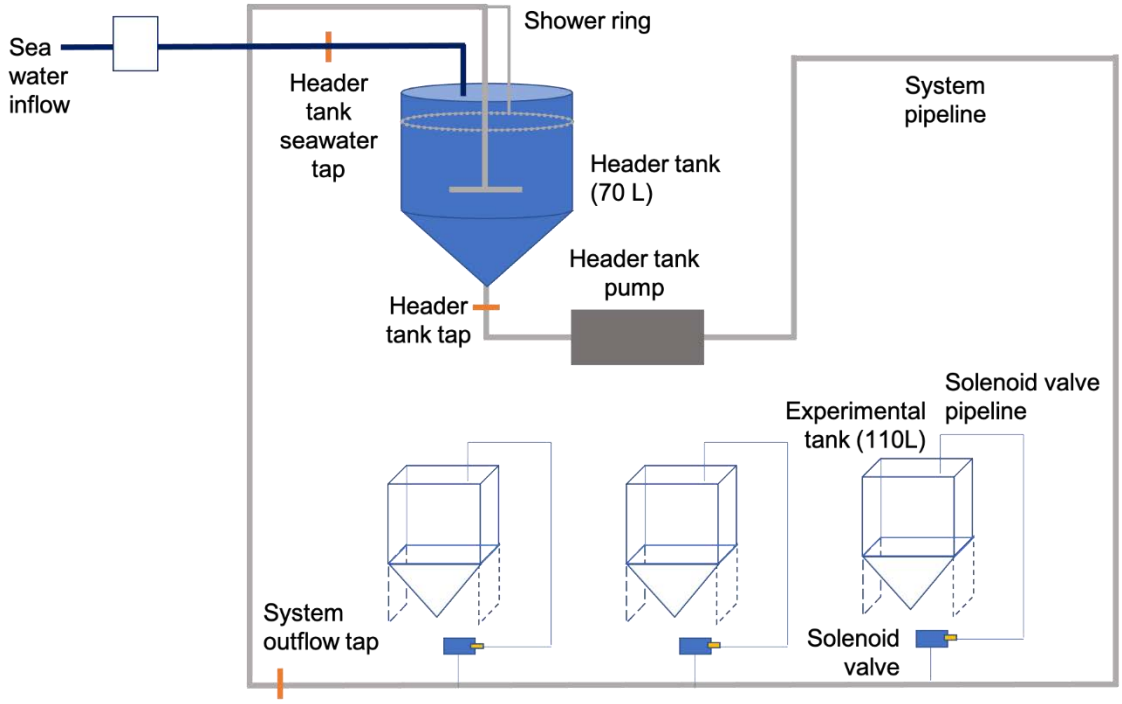

Figure S2: Illustrative scheme of the microplastic automated dosing system and its main parts, including: 70 L header tank, primary distribution pipeline, and 110 L exposure tanks with pecific dosing device (solenoid valve and a secondary pipeline). Seawater inflow is used to fill up header tank with 70 L of seawater. System outflow tap is used to clear the system of old stock solution every time a new stock solution is created.

Due to the high density of PET (1.38 g cm^{-3}) which results in sinking in seawater, the experimental tanks were designed to prevent PET deposit and accumulation at the bottom over time. Each 110 L PVC experimental tank was conical in shape, with the tapered base connected to an independent seawater recirculation system which generated a continuous upwelling thereby ensuring dosed PET fibres are homogeneously mixed (Figure S3). Upwelling was maintained in each experimental tank by individual pumps (SCORPION, MYT 631-2, 50 Hz) with full seawater exchange set at 0.8 L h^{-1}.

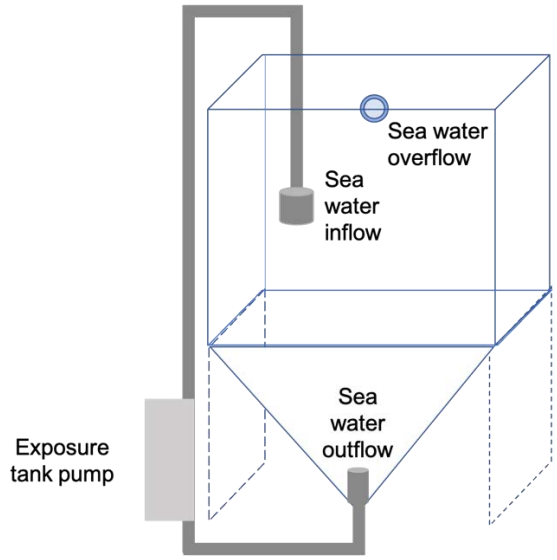

Figure S3: Exposure tank and modelled PET distribution in the tank. Illustrative scheme of the exposure tank and tank circulation system, by which the flow-through water and dosed microplastics get dispersed in the exposure tank.

1.2.2. Automation of the dosing system

The dosing system was controlled through a programmable logic controller (PLC, Siemens SIMANTIC S7-1500), and managed through a supervisory control and data acquisition (SCADA) system. SCADA permitted the adjustment of the duration (seconds) and frequency of solenoid valve opening to accurately regulate the targeted dosing of microplastics into each tank. The dosing system was tested in several pilot trials to optimize the solenoid valve's activation frequency, as the chemical and physical characteristics of the microplastic used (e.g., polymer, size, shape, and biofouling) are known to affect its distribution in seawater (Liu et al., 2020) (see Sections 2.3). In addition to regulating microplastic dosing, the SCADA system also permitted monitoring of the water level in the header tank and the automatic suspension of microplastic dosing if it dropped below a defined threshold Supplementary Figure S2).

1.2.3. Development of the automated dosing system

The automated dosing of microplastics was designed to maintain consistent microplastic concentrations in experimental tanks over time. Consistency depends on interactions between (1) quantity of microplastic dosed into the experimental tank, (2) dosing rate (i.e. number of dosings per unit of time), and (3) elimination rate (i.e., how many microplastics are flushed out with the flow-through water system from the tanks over time). Elimination rate, in turn, is

influenced by four factors: (3.1) how microplastics behave within the automated dosing system (i.e., homogeneous vs heterogeneous dispersal) and the experimental tank (i.e., sinking or floating), (3.2) tank seawater exchange rate, (3.3) microplastics stock solution concentration, and (3.4) duration and frequency of solenoid valve activation.

The elimination rate was determined using a single concentration of stock solution (540 PET microfibres L^{-1}), with seawater flow rate of 7.2 L min^{-1}, and solenoid valves opened for 1 second every 21 seconds (to simulate constant microplastic input). Trials were run over four days. Tanks (n = 1 to 3) were randomly chosen for sampling and assessed up to three times a day. Prior to sampling, the microplastic automated dosing system was operated for at least 2.5 hours (to allow nominal microplastic concentration to stabilize in experimental tanks) and the number of microplastics released by the solenoid valve, the number that were dispersed at the bottom water column, and the number that were dispersed into the upper water column were counted. The number of PET microfibres released by the solenoid valve was analysed by sampling one the stock solution dosed from the end of the secondary pipeline (i.e., at the time of entering into the experimental tank) with 50 mL graduated falcon tubes. The volume of stock solution was recorded and filtered over 0.45 µm membrane filters (HA, Millipore). Retained PET microfibres were counted with stereomicroscopy (Leica MZ6, 4.0x magnification) and PET concentration stablished based on the volume of stock solution dosed. PET concentration and dispersion in experimental tanks was assessed by syphoning water from both bottom and upper water column (15 L each) over a 40 µm plankton sieve (polyamide (PA) mesh, polypropylene (PP) frame), which was backwashed into same type of filters described above. PET count and concentration estimates also followed procedures above. All accessible surfaces of the automated dosing system were visually inspected for potential areas of microplastic accumulation.

Preliminary trials identified microplastic accumulation on the walls of the header tank and experimental tanks, and at the base of the experimental tanks, resulting in modification of the initial design, e.g., t-shaped outlet and o-ring shower added to the header tank and conical base and circulation system added to experimental tanks. The seawater flow rate for the entire system, including in each tank, was adjusted to 15 L min^{-1}; a compromise between keeping the PET microfibres in suspension, maintaining water quality and not disturbing the fish. Based on PET microfibre counts in each tank, the stock solution concentration was adjusted to deliver the required nominal concentration into experimental tanks. The system was tested after every adjustment.

1.2.4. Validation of the automated dosing system

Once operational the dosing system was fully developed, it was validated in a pilot study by adding a known concentration of stock PET microfibre solution (836 or 19286 PET microfibres L^{-1}) to the 70 L header tank and operated in automated mode over 2.5 days, during which experimental tanks (n=3 per microplastic concentration chosen randomly each sampling time point to avoid skewed results due to prior sampling) were sampled twice daily and microplastics (recovered by filtration) counted (the expected nominal dosing being 1.1 microfibre L^{-1} or 11 microfibres L^{-1}). To test for cross contamination the system was also operated in the absence of PET microfibres in the header tank.

Concomitantly, under same animal ethics approval as main experiment, *A. polyacanthus* (sourced from the Marine Aquaculture and Research Facility Unit (MARFU) at James Cook University) were transferred to the Australian Institute of Marine Science's National Sea Simulator, placed in six experimental tanks (n=12 fish per tank, ambient seawater temperature, approx. 23.5°C) and fed live and enriched post-hatched artemia. After two-days acclimation fish in three of the tanks were exposed to the highest supply of microplastics tested for the nominal concentrations (100 PET fibres per fish per tank, equivalent to approx. 11 fibres L^{-1}), the other three tanks acting as controls. After two days exposure, treated and control fish were euthanised, weighed, measured and dissected, and the gills and GIT inspected for microplastic contamination. Refer to the main text for microplastic characterisation methods. The number of contaminating PET microfibres was recorded for each individual fish.

This pilot study confirmed the automated dosing system is capable of providing consistent microplastic exposure at different microplastic concentrations for 2.5 days. No PET microfibres were observed in control tanks ($MP_{control}$), while an average (± SE) of 1.27 ± 0.21 and 10.7 ± 0.89 PET microfibres L^{-1} were found in tanks exposed to low (MP_{low}) and high (MP_{high}) microplastic concentratons. The PET microfibre concentration varied from 0.9 to 1.7 and 9.3 to 12.2 PET microfibres L^{-1} across tanks and sampling times for each microplastic treatment, respectively (Figure S4).

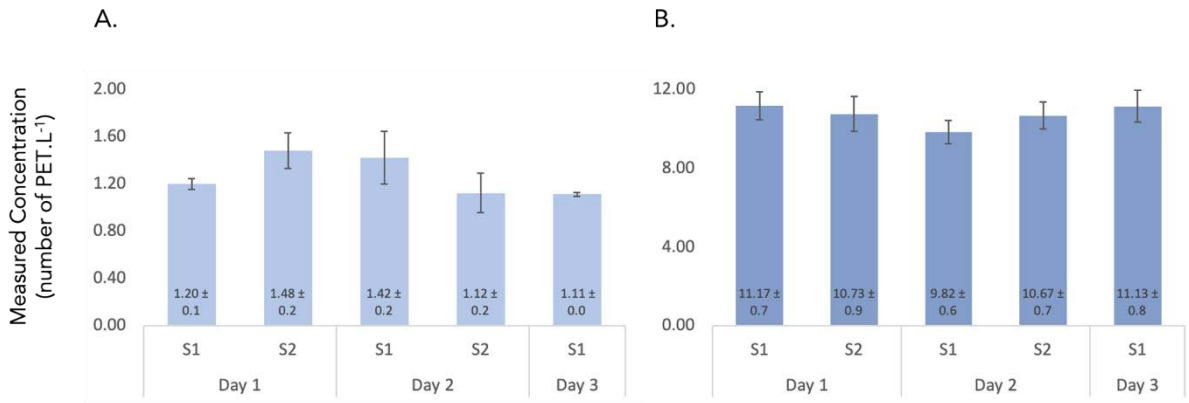

Figure S4: PET microfibre measured concentration (average ± SE) in experimental tanks of (A) MP_{low} and (B) MP_{high} treatments over 2.5 days. S1 and S2 represent sampling one and 2 along the day. Expected nominal concentrations in experimental tanks were 1.1 PET L^{-1} for MP_{low} and 11 PET L^{-1} for MP_{high}.

Inspection of gills and GIT dissected from control fish found no PET microfibres, while GIT from fish exposed to 11 microplastic L^{-1} were found to be contaminated. Gills of exposed fish were PET free. PET concentration in fish GIT varied from 1 to 98 per individual, with an average of 25.26 ± 20.09 PET fibres per fish. Fish size in tanks also varied quite significantly (from 20.95 to 38.46 mm in length, and from 0.21 to 1.61 g in weight), which could have influenced the levels of PET contamination thus, fish size was included as covariant in the glm models utilised in the final study.

1.3. Seawater temperature in fish tanks

Table S1: Seawater temperature (˚C) in experimental tanks, reported per treatment and per day. Ambient temperatures ($T_{23.7}$, 23.7˚C) are based on seawater temperatures logged daily at Davis Reef (Central Great Barrier Reef) and at future predicted 2050 ($T_{25.2}$; ambient +1.5˚C) and 2100 ($T_{26.7}$; ambient +3.0˚C) temperatures (IPCC, 2018).

Date	$T_{23.7}$	$T_{25.2}$	$T_{26.7}$	**Date**	$T_{23.7}$	$T_{25.2}$	$T_{26.7}$	**Date**	$T_{23.7}$	$T_{25.2}$	$T_{26.7}$
8.07	23.6	25.1	26.6	**5.08**	23.3	24.8	26.3	**2.09**	23.8	25.3	26.8
9.07	23.6	25.1	26.6	**6.08**	23.3	24.8	26.3	**3.09**	23.8	25.3	26.8
10.07	23.6	25.1	26.6	**7.08**	23.3	24.8	26.3	**4.09**	23.8	25.3	26.8
11.07	23.5	25.0	26.5	**8.08**	23.3	24.8	26.3	**5.09**	23.9	25.4	26.9
12.07	23.5	25.0	26.5	**9.08**	23.3	24.8	26.3	**6.09**	23.9	25.4	26.9
13.07	23.5	25.0	26.5	**10.08**	23.2	24.7	26.2	**7.09**	24.0	25.5	27.0
14.07	23.5	25.0	26.5	**11.08**	23.2	24.7	26.2	**8.09**	24.0	25.5	27.0
15.07	23.5	25.0	26.5	**12.08**	23.2	24.7	26.2	**9.09**	24.1	25.6	27.1
16.07	23.5	25.0	26.5	**13.08**	23.2	24.7	26.2	**10.09**	24.2	25.7	27.2
17.07	23.4	24.9	26.4	**14.08**	23.2	24.7	26.2	**11.09**	24.2	25.7	27.2
18.07	23.4	24.9	26.4	**15.08**	23.3	24.8	26.3	**12.09**	24.2	25.7	27.2
19.07	23.4	24.9	26.4	**16.08**	23.3	24.8	26.3	**13.09**	24.2	25.7	27.2
20.07	23.4	24.9	26.4	**17.08**	23.4	24.9	26.4	**14.09**	24.2	25.7	27.2
21.07	23.4	24.9	26.4	**18.08**	23.4	24.9	26.4	**15.09**	24.3	25.8	27.3
22.07	23.3	24.8	26.3	**19.08**	23.5	25.0	26.5	**16.09**	24.3	25.8	27.3
23.07	23.3	24.8	26.3	**20.08**	23.5	25.0	26.5	**17.09**	24.3	25.8	27.3
24.07	23.3	24.8	26.3	**21.08**	23.4	24.9	26.4	**18.09**	24.3	25.8	27.3
25.07	23.3	24.8	26.3	**22.08**	23.4	24.9	26.4	**19.09**	24.4	25.9	27.4
26.07	23.3	24.8	26.3	**23.08**	23.5	25.0	26.5	**20.09**	24.4	25.9	27.4
27.07	23.3	24.8	26.3	**24.08**	23.6	25.1	26.6	**21.09**	24.5	26.0	27.5
28.07	23.3	24.8	26.3	**25.08**	23.6	25.1	26.6	**22.09**	24.5	26.0	27.5
29.07	23.3	24.8	26.3	**26.08**	23.6	25.1	26.6	**23.09**	24.5	26.0	27.5
30.07	23.3	24.8	26.3	**27.08**	23.6	25.1	26.6	**24.09**	24.6	26.1	27.6
31.07	23.2	24.7	26.2	**28.08**	23.6	25.1	26.6	**25.09**	24.6	26.1	27.6
1.08	23.2	24.7	26.2	**29.08**	23.6	25.1	26.6	**26.09**	24.6	26.1	27.6
2.08	23.2	24.7	26.2	**30.08**	23.6	25.1	26.6	**27.09**	24.7	26.2	27.7
3.08	23.2	24.7	26.2	**31.08**	23.7	25.2	26.7	**28.09**	24.8	26.3	27.8
4.08	23.3	24.8	26.3	**1.09**	23.7	25.2	26.7				

1.4. Validation of cortisol extraction protocol

Parallelism, accuracy and precision of the cortisol ELISA kit for the extraction method applied was validate following Guest et al. (2016) and (Metcalfe et al., 2018). Parallelism was verified by visual assessment of the slopes of the standard curve and diluted samples (Figure S5). Dilutions tested included 1:0, 1:3, 1:6, 1:12, 1:18, 1:24, 1:30, and 1:36. Dilution factor of 6 was observed at 50% relative maximum binding, with 20–80% B/B_0 relative maximum binding being considered as acceptable (Figure S5a). Method accuracy was assessed by spiking samples with 800 pg cortisol mL^{-1} and assessing recovery (n=3). For each sample, homogenised fish was split into two, and either spiked with cortisol or assay buffer. Samples were then processed following the stablished protocol and cortisol recovery calculated as:

$$\left[\left(\text{cortisol}_{sp}/\text{cortisol}_{ns}\right)/\text{cortisol}_{kn}\right] \text{ x } 100 \qquad \text{(Eq. 1)}$$

where Cortisol_{sp} is the concentration of cortisol in spiked samples, Cortisol_{ns} is the concentration of cortisol in non-spiked samples (buffer added), and Cortisol_{kn} is the known concentration of cortisol spiked in samples (800 pg ml^{-1}).

To calculate final concentration of cortisol in experimental samples, the mean recovery of the spiking test (94.3%, n=3) was used as a correction factor (Figure S5b). Coefficient of variation (CV) within samples was determined to be 10.67 ± 6.45 (mean ± s.d., n=162).

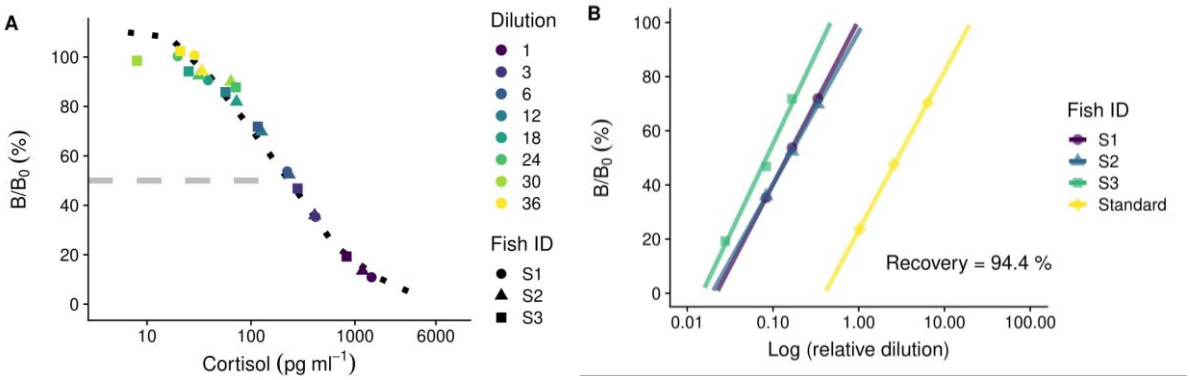

Figure S5: Validation steps for ELISA cortisol analysis of whole-body homogenates of *Acanthochromis polyacanthus*. (A) The optimal sample dilution (50% B/B_0) was determined for three individual fish (S1-3) and compared against the cortisol standard curve (i.e., cortisol without any fish tissue; fine black line). An optimal dilution factor of 6 was determined to be suitable for analysis of fish tissue homogenates based on the concentration of cortisol at which 50% is bound (dashed grey line). (B) Parallelism between fish whole-body homogenates was confirmed by visually assessing the slopes of the standard curve and the diluted samples. Extraction efficiency of cortisol from the fish tissues was 94.4 % (n = 3).

2. Supplementary references

Guest, T.W., Blaylock, R.B., Evans, A.N., 2016. Development of a modified cortisol extraction procedure for intermediately sized fish not amenable to whole-body or plasma extraction methods. Fish Physiol Biochem 42, 1-6.

IPCC, 2018. Global Warming of 1.5°C. An IPCC Special Report on the impacts of global warming of 1.5°C above pre-industrial levels and related global greenhouse gas emission pathways, in the context of strengthening the global response to the threat of climate change, sustainable development, and efforts to eradicate poverty.

Liu, W., Zhao, Y., Shi, Z., Li, Z., Liang, X., 2020. Ecotoxicoproteomic assessment of microplastics and plastic additives in aquatic organisms: A review. Comp Biochem Physiol Part D Genomics Proteomics 36, 100713.

Metcalfe, S.S., Kroon, F.J., Beale, D.J., Miller, G., 2018. Development of a validation protocol of enzyme immunoassay kits used for the analysis of steroid hormones in fish plasma. Journal of Experimental Marine Biology and Ecology 499, 26-34.

Appendix E

Supplementary Information for Chapter 5 Microplastic fibre exposure and seawater warming synergistically affect levels of stress but not fitness parameters of a juvenile coral reef fish (*Acanthochromis polyacanthus*) under winter conditions

1. Supplementary results

1.1. Validation and estimation of microplastic uptake

1.1.1. Microplastic uptake after one week of exposure

Table S1: Microplastic (MP) uptake per treatment (increasing microplastic concentration and seawater temperature) after one week of exposure. Values reported as mean ± SE. Polyethylene terephthalate = PET, control = $MP_{control}$, low PET exposure at 1.1 fibres L^{-1} = MP_{low} and high PET exposure at 11 fibres L^{-1} of filtered seawater = MP_{high}.

Treatment		PET fibres $fish^{-1}$
MP concentration	Temperature ($T_{°C}$)	
$MP_{control}$	$T_{23.7}$	0 ± 0
MP_{low}	$T_{23.7}$	12.50 ± 16.88
MP_{high}	$T_{23.7}$	22.00 ± 18.79
$MP_{control}$	$T_{25.2}$	0 ± 0
MP_{low}	$T_{25.2}$	1.67 ± 1.80
MP_{high}	$T_{25.2}$	51.67 ± 44.14
$MP_{control}$	$T_{26.7}$	0 ± 0
MP_{low}	$T_{26.7}$	3.83 ± 6.36
MP_{high}	$T_{26.7}$	42.0 ± 40.17

1.1.2. Differences in microplastic uptake

Table S2: Influence of microplastic concentration ($MP_{control}$, MP_{low}, and MP_{high}), seawater temperature ($T_{23.7}$ = 23.7°C, $T_{25.2}$ = 25.2˚C and $T_{26.7}$ = 26.7°C on average) and fish size (fork length, cm) on microplastic uptake by *Acanthochromis polyacanthus*. (a) Summary of the regression model, (b) Post-hoc contrasts.

(a) Summary of the regression model used to estimate differences in uptake rates of polyester (PET) microfibres under different exposure conditions and influence on fish fork length (in mm). MP_{high} = 11 PET microfibres $fish^{-1}$, $T_{25.2}$ = 25.2 ˚C and $T_{26.7}$ = 26.7 °C on average. Incidence Rate Ratios, confidence intervals (CI) and p-values (p) are reported, as well as the number of observations and R-squared values. p-values < 0.05 indicate significant differences and are highlighted in **bold**.

	MP count		
Predictors	*Incidence Rate Ratios*	*CI*	*p*
Intercept	8.82	1.19 – 65.14	**0.033**
fork length	0.99	0.95 – 1.03	0.757
MP_{high}	9.56	2.90 – 31.56	**<0.001**
$T_{25.2}$	0.98	0.30 – 3.24	0.980
$T_{26.7}$	1.44	0.44 – 4.72	0.545
MP_{high}: $T_{25.2}$	3.63	0.68 – 19.34	0.130
MP_{high}: $T_{26.7}$	0.80	0.15 – 4.29	0.798
Random Effects			
σ^2	0.79		
$\tau_{00\ tank}$	0.41		
ICC	0.34		
$N_{\ tank}$	18		
Observations	179		
Marginal / Conditional R^2	R^2 / 0.615 / 0.747		

(b) Post-hoc contrasts of uptake rates of polyester (PET) microfibres by fish exposed to different microplastic concentrations (1 PET microfibre fish^{-1} = MP_{low}, and 11 PET microfibres fish^{-1} = MP_{high}) and seawater temperatures ($T_{23.7}$ = 23.7 °C, $T_{25.2}$ = 25.2 ˚C and $T_{26.7}$ = 26.7 °C on average). Estimated ratio, standard error (SE), degrees of freedom (df), t.ratio and p-values are reported. p-values < 0.05 indicate significant differences and are highlighted in **bold**.

Constant	Contrasts	ratio	SE	df	t.ratio	p.value
$T_{23.7}$	MP_{low} / MP_{high}	**0.1046**	**0.0637**	**170**	**-3.708**	**0.0003**
$T_{25.2}$	MP_{low} / MP_{high}	**0.0288**	**0.0174**	**170**	**-5.863**	**<.0001**
$T_{26.7}$	MP_{low} / MP_{high}	**0.1302**	**0.0782**	**170**	**-3.393**	**0.0009**
MP_{low}	$T_{23.7}$ / $T_{25.2}$	1.016	0.618	170	0.026	0.9996
	$T_{23.7}$ / $T_{26.7}$	0.693	0.419	170	-0.606	0.8173
	$T_{25.2}$ / $T_{26.7}$	0.683	0.415	170	-0.628	0.8048
MP_{high}	$T_{23.7}$ / $T_{25.2}$	0.280	0.168	170	-2.127	0.0874
	$T_{23.7l}$ / $T_{26.7}$	0.863	0.522	170	-0.243	0.9679
	$T_{25.2}$ / $T_{26.7}$	3.088	1.841	170	1.891	0.1443

1.2. Fish health and fitness

1.2.1. Differences in cortisol levels

Table S3: Influence of microplastic (MP) concentration ($MP_{control}$, MP_{low}, and MP_{high}), seawater temperature ($T_{23.7}$ = 23.7 °C, $T_{25.2}$ = 25.2 ˚C and $T_{26.7}$ = 26.7 °C on average) and fish size (w.w., g) on cortisol levels in *Acanthochromis polyacanthus*. (a) Summary of the regression model, (b) Post-hoc contrasts.

(a) Summary of the regression model used to estimate differences in levels of bound cortisol as a function of the treatment conditions. Estimates, confidence intervals (CI) and p-values (p) are reported, as well as the number of observations and R-squared values. p-values < 0.05 indicate significant differences and are highlighted in **bold**.

	log(cortisol)		
Predictors	*Estimates*	*CI*	*p*
Intercept	6.67	6.23 – 7.11	**<0.001**
MP_{low}	-0.24	-0.70 – 0.22	0.303
MP_{high}	0.11	-0.35 – 0.57	0.640
$T_{25.2}$	0.03	-0.43 – 0.49	0.900
$T_{26.7}$	0.39	-0.07 – 0.85	0.099
weight	**-0.16**	**-0.25 – -0.07**	**<0.001**
MP_{low} * $T_{25.2}$	0.02	-0.63 – 0.67	0.954
MP_{high} * $T_{25.2}$	-0.02	-0.68 – 0.63	0.942
MP_{low} * $T_{26.7}$	0.10	-0.56 – 0.75	0.773
MP_{high} * $T_{26.7}$	**-0.70**	**-1.35 – -0.05**	**0.036**
Random Effects			
σ^2	0.43		
$\tau_{00\ tank\_n}$	0.01		
ICC	0.03		
N_{tank_n}	27		
Observations	162		
Marginal R^2 / Conditional R^2	0.152 / 0.175		

(b) Post-hoc contrasts of fish cortisol levels as a function of microplastic concentration ($MP_{control}$, MP_{low}, and MP_{high}) and seawater temperature ($T_{23.7}$ = 23.7°C, $T_{25.2}$ = 25.2˚C and $T_{26.7}$ = 26.7°C on average). Estimated ratio, standard error (SE), degrees of freedom (df), t.ratio and p-values are reported. p-values < 0.05 indicate significant differences and are highlighted in **bold**.

contrasts	ratio	SE	df	t.ratio	p.value
Sea water temperature = T1					
$MP_{control}$ / MP_{low}	1.274	0.299	150	1.030	0.5589
$MP_{control}$ / MP_{high}	0.896	0.211	150	-0.467	0.8868
MP_{low} / MP_{high}	0.703	0.165	150	-1.498	0.2950
Sea water temperature = T2					
$MP_{control}$ / MP_{low}	1.250	0.295	150	0.944	0.6131
$MP_{control}$ / MP_{high}	0.918	0.216	150	-0.363	0.9298
MP_{low} / MP_{high}	0.735	0.173	150	-1.309	0.3926
Sea water temperature = T3					
$MP_{control}$ / MP_{low}	1.157	0.272	150	0.622	0.8083
$MP_{control}$ / MP_{high}	**1.799**	**0.423**	**150**	**2.498**	**0.0360**
MP_{low} / MP_{high}	1.554	0.365	150	1.875	0.1494
PET exposure concentration = MP1					
$T_{23.7}$ / $T_{25.2}$	0.971	0.228	150	-0.126	0.9913
$T_{23.7}$ / $T_{26.7}$	0.678	0.159	150	-1.652	0.2275
$T_{25.2}$ / $T_{26.7}$	0.699	0.164	150	-1.525	0.2820
PET exposure concentration = MP2					
$T_{23.7}$ / $T_{25.2}$	0.952	0.225	150	-0.207	0.9766
$T_{23.7}$ / $T_{26.7}$	0.616	0.145	150	-2.060	0.1019
$T_{25.2}$ / $T_{26.7}$	0.647	0.153	150	-1.846	0.1583
PET exposure concentration = MP3					
$T_{23.7}$ / $T_{25.2}$	0.995	0.234	150	-0.022	0.9997
$T_{23.7}$ / $T_{26.7}$	1.362	0.320	150	1.313	0.3901
$T_{25.2}$ / $T_{26.7}$	1.369	0.322	150	1.335	0.3778

1.2.2. Differences in total lipids

Table S4: Influence of microplastic (MP) concentration ($MP_{control}$, MP_{low}, and MP_{high}), seawater temperature ($T_{23.7}$ = 23.7°C, $T_{25.2}$ = 25.2˚C and $T_{26.7}$ = 26.7°C on average) and fish size (w.w., g) on total lipid content in *Acanthochromis polyacanthus*. Estimates, confidence intervals (CI) and p-values (p) are reported, as well as the number of observations and R-squared values. p-values < 0.05 indicate significant differences and are highlighted in **bold**.

	Total Lipids		
Predictors	Estimates	CI	p
Intercept	0.06	0.05 – 0.08	**<0.001**
MP_{low}	0.89	0.71 – 1.12	0.328
MP_{high}	1.06	0.85 – 1.32	0.592
$T_{25.2}$	0.86	0.69 – 1.08	0.189
$T_{26.7}$	0.87	0.70 – 1.08	0.217
weight	**0.93**	**0.87 – 0.99**	**0.029**
Random Effects			
σ^2	0.22		
$\tau_{00\ tank}$	0.02		
ICC	0.07		
$N_{\ tank}$	27		
Observations	162		
Marginal R^2 / Conditional R^2	0.071 / 0.134		

1.2.3. Differences in growth

Table S5: Influence of microplastic (MP) concentration ($MP_{control}$, MP_{low}, and MP_{high}) and seawater temperature ($T_{23.7}$ = 23.7 °C, $T_{25.2}$ = 25.2 ˚C and $T_{26.7}$ = 26.7 °C on average) on growth of *Acanthochromis polyacanthus*. Estimates, confidence intervals (CI) and p-values (p) are reported, as well as the number of observations and R-squared values. p-values < 0.05 indicate significant differences and are highlighted in **bold**.

	Growth		
Predictors	Estimates	CI	p
Intercept	0.66	0.58 – 0.74	**<0.001**
MP_{low}	-0.01	-0.10 – 0.08	0.832
MP_{high}	0.02	-0.06 – 0.11	0.603
$T_{25.2}$	-0.03	-0.12 – 0.06	0.484
$T_{26.7}$	0.04	-0.04 – 0.13	0.332
Random Effects			
σ^2	0.00		
$\tau_{00\ tank}$	0.01		
ICC	0.13		
$N_{\ tank}$	27		
Observations	267		
Marginal R^2 / Conditional R^2	0.027 / 0.157		

1.2.4. Differences in condition factor

Table S6: Influence of microplastic (MP) concentration ($MP_{control}$, MP_{low}, and MP_{high}) and seawater temperature ($T_{23.7}$ = 23.7°C, $T_{25.2}$ = 25.2°C and $T_{26.7}$ = 26.7°C on average) on condition factor of *Acanthochromis polyacanthus*. Estimates, confidence intervals (CI) and p-values (p) are reported, as well as the number of observations and R-squared values. p-values < 0.05 indicate significant differences and are highlighted in **bold**.

	Condition Factor		
Predictors	Estimates	CI	p
Intercept	0.89	0.86 – 0.93	**<0.001**
MP_{low}	-0.00	-0.03 – 0.03	0.943
MP_{high}	0.02	-0.01 – 0.05	0.216
$T_{25.2}$	-0.06	-0.05 – -0.02	**0.422**
$T_{26.7}$	0.01	-0.02 – 0.04	0.626
Random Effects			
σ^2	0.01		
$\tau_{00\ tank}$	0.00		
ICC	0.04		
N_{tank}	27		
Observations	267		
Marginal R^2 / Conditional R^2	0.050 / 0.057		